STUDY OF ORGANIC CATIONS IN THE GAS PHASE BY TANDEM MASS SPECTROMETRY

by Yan An

A thesis submitted to the
School of Graduate Studies and Research

In partial fulfillment of the requirements for the degree of Doctor of Philosophy

In the Ottawa-Carleton Chemistry Institute
Department of Chemistry, University of Ottawa
Ottawa, Ontario, Canada

September, 1995

Candidate	Supervisor
Yan An	Professor John L. Holmes

© Yan An, Ottawa, Canada, 1996

National Library of Canada

Acquisitions and Bibliographic Services Branch

395 Wellington Street
Ottawa, Ontario
K1A 0N4

Bibliothèque nationale du Canada

Direction des acquisitions et des services bibliographiques

395, rue Wellington
Ottawa (Ontario)
K1A 0N4

Your file Votre référence

Our file Notre référence

The author has granted an irrevocable non-exclusive licence allowing the National Library of Canada to reproduce, loan, distribute or sell copies of his/her thesis by any means and in any form or format, making this thesis available to interested persons.

L'auteur a accordé une licence irrévocable et non exclusive permettant à la Bibliothèque nationale du Canada de reproduire, prêter, distribuer ou vendre des copies de sa thèse de quelque manière et sous quelque forme que ce soit pour mettre des exemplaires de cette thèse à la disposition des personnes intéressées.

The author retains ownership of the copyright in his/her thesis. Neither the thesis nor substantial extracts from it may be printed or otherwise reproduced without his/her permission.

L'auteur conserve la propriété du droit d'auteur qui protège sa thèse. Ni la thèse ni des extraits substantiels de celle-ci ne doivent être imprimés ou autrement reproduits sans son autorisation.

ISBN 0-612-15586-2

Canada

UNIVERSITÉ D'OTTAWA
UNIVERSITY OF OTTAWA

ABSTRACT

The structure elucidation of gas-phase isomeric species $C_2H_4X^+$ (X = F, Cl, Br and I), $C_3H_6X^+$ (X = Cl, and Br), $(C_2H_5)_2O^+C_2H_4X$ (X = Cl and Br), and $C_3H_6O_2^{+\bullet}$ has been accomplished by employing tandem mass spectrometric techniques, i.e. metastable ion (MI) mass spectrometry, collision induced dissociation (CID) mass spectrometry, collision induced dissociative ionization (CIDI) mass spectrometry and neutralization reionization (NR) mass spectrometry.

For $C_2H_4X^+$ cations, apart from the α- isomer, CH_3CHX^+, the cyclic ethylenehalonium ions,  are also stable for X = Cl, Br and I (Chapter 3). The two isomers have readily been characterized by CID mass spectrometry and their neutral counterparts have been produced and studied by NR mass spectrometry. It was found that based on an analysis of the heat of formation values of these ions and the electronegativity and polarizibility data of the X atoms, the relative stability of the two isomers is essentially controlled by the C–X bond strength. The relative stability of the cyclic species, however, is also controlled by the polarizibility of the X atom, which indicated that its polarization by the charge-centered carbon involved the outer-electrons in the X atom to form a back-donating bond with the charge-centered carbon.

The isomeric halogen substituted triethyloxonium ions $(C_2H_5)_2O^+C_2H_4X$, (X = Cl and Br) were generated by appropriate gas phase ion molecular reactions between diethylether and appropriate $C_2H_4XBr^{+\bullet}$ via $Br^\bullet$ loss (Chapter 4). The α- substituted isomer, $(C_2H_5)_2O^+CHXCH_3$, and the β- substituted isomer, $(C_2H_5)_2O^+CH_2CH_2X$, are both

stable in the gas-phase and do not interconvert on a time scale of 10^{-5} s.

Three $C_3H_6X^+$ isomers (at least) were found to be stable in the gas-phase (Chapter 5). They are $CH_3-{}^+CX-CH_3$,  and 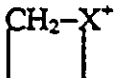 . These ions were characterized by their CID mass spectra and their different behavior in forming oxonium ions — $(C_2H_5)_2O^+C_3H_6X$ — with diethyl ether.

The distonic radical cations $^\bullet CH_2CH_2O^+CHOH$ and $^\bullet CH_2CH_2{}^+C(OH)_2$. have been directly generated and characterized by their MI and CID mass spectra (Chapter 7). Comparing the dissociative process of $^\bullet CH_2CH_2O^+CHOH$ to that of $HCOOCH_2CH_3{}^{+\bullet}$ led to the conclusion that this distonic ion is the key intermediate in the dissociation of the latter. Thus the previous proposal, based only on the dissociation of $HCOOCH_2CH_3{}^{+\bullet}$, was confirmed. The heat of formation of $^\bullet CH_2CH_2O^+CHOH$ was estimated from an appearance energy measurement to be 137 ± 4 kcalmol^{-1}; this is 16 kcalmol^{-1} lower in energy than $HCOOCH_2CH_3{}^{+\bullet}$.

A detailed study of distonic ions is presented in Chapter 6, including a survey of the common methods to generate and characterize these ions. Properties of such ions which were consided were: stability, isomerization, bond cleavage and ring-strain. The results showed that the characteristics of distonic ions which distinguish them from their conventional counterparts result from the specific interaction of charge and radical sites.

Acknowledgement

I wish to express my sincere thanks to my research supervisor, Professor J. L. Holmes, for his direction and guidance throughout the course of this work. I am very appreciative of the time he has spent and the patience he has demonstrated in the course of thesis correction. I was a priviledge and honour for me to work with such a well-known, capable and understanding scientist.

I would like to thank Dr. C. Kazakoff, Dr. J. Krause, Dr. A. A. Mommers, Dr D. Zagorevskii, Dr P. Mayer, Dr. Luo, Dr Sirois, H. Chen,. C. Aubry, D. Harnish, for all their help and advice with the mass spectrometic experiments. Thanks also to Mr. A. Zlotorzynski for his hellp to make a easy computer writing and drawing; to D. Dawson and J. MacDonald, for their pleasant discussions.

Great thanks to my parents for their love and understanding.

Contents

List of Tables

List of Figures

Chapter 1

Introduction

For more than 30 years tandem mass spectrometry, (mass spectrometry / mass spectrometry, MS/MS) has been a valuable physical tool to study gas-phase organic ions, in particular to gain structural information and to elucidate fragmentation mechanisms.

The study of unimolecular or collision induced dissociations of ions is performed by using the first mass spectrometer to select ions with a certain mass. The fragmentation products of these ions are mass analyzed by a second mass spectrometer. In the triple scan technique, using three mass analysers (MS/MS/MS), further structural assignments can be made for individual fragment ions of the originally mass selected species.

The study of the fragmentation behaviour of gas-phase ions has recently led to the recognition of non-classical ion structures, such as DISTONIC IONS;[1] ION-NEUTRAL COMPLEXES;[2] and HYDROGEN-BRIDGED COMPLEXES.[3] The first category refers to radical cations having the formal charge and radical sites separated; The second refers to those ions which consist of an incipient ion co-ordinated to a putative neutral, the two species being bound by ionic forces, rather than a covalent bond; The last type has two partners, a radical and a cation, bonded by a hydrogen atom.

This thesis is mainly concerned with exploring and expanding the use of tandem mass spectrometry to investigate some specific ionic families. They are ions of formula $C_2H_4X^+$ (X = F, Cl, Br and I), $C_3H_6X^+$ (X = Cl and Br), $C_6H_{14}OX^+$ (X = Cl and Br) and $C_3H_6O_2^{+\bullet}$.

The aims of the thesis are:

1. To assign the structures for the above ion groups based on their unimolecular and collision induced dissociations and available thermochemical data;
2. To deepen our understanding of the factors which affect the stability of both classical and non-classical species.

References

1 Details will be discussed in Chapter 6

2 a: P. Longevialle and R. Botter, J. Chem. Soc. Chem. Commun., 823 (1980)

b: T. H. Morton, Org. Mass Spectrom., 27, 353 (1992)

3 M. George, C. A. Kingsmill, D. Suh, J. K. Terlouw and J. L. Holmes, J. Am. Chem. Soc., 116, 7807 (1994)

Chapter 2

Instrumentation and Experimentation

2.1 History

Although the first mass spectrometers of J. J. Thomson and F. W. Aston[1] were built over 80 years ago, the major development leading to the technique of tandem mass spectrometry occurred in 1945 when Hipple and Condon observed and explained the presence of metastable ions in a mass spectrum.[2] A metastable ion is one that is sufficiently stable to leave the ionization chamber, but that decomposes before reaching the collector. This requires a lifetime of 10^{-6} - 10^{-4} sec. Investigation of metastable ions brought fundamental studies on the use of metastable ions as a source of chemical and physical information. This work was the driving force that has led to tandem mass spectrometry as it is practised today.

In the 1960s, the first experiments were performed in which instruments were used in unconventional modes to study the decompositions of metastable ions. These studies were made possible by developments in three different areas. The first development was the introduction of the accelerating-voltage scan on sector instruments by Barber and Elliott.[3] The next major development was the discovery of the enhancement of magnitude and quantity of peaks in a "metastable ion" mass spectrum upon introduction of a collision gas into a localised region of the mass spectrometer.[4] The fragmentation of a polyatomic ion following an energetic collision with a target gas is referred to as collision-induced dissociation (CID). At the time of the initial experiments using CID, the focus of the studies was very narrow and directed primarily toward exploration of the physical aspects

of the phenomenon. Not until a few years later, at the time of publication of the book *Metastable ions*,[5] did tandem mass spectrometry start to gather momentum. Publication of this book marked the beginning of the modern era of tandem mass spectrometry, a period in which instruments would be designed expressly for MS/MS and MS/MS/MS experiments.

More recently the development of the neutralization-reionization technique[6] has made tandem mass spectrometry a valuable tool to generate and study novel neutral species. In a tandem mass spectrometer the neutrals were generated by charge exchange of the fast ions with a permanent gas and further downstream the neutrals (and their fragmentation products) were collisionally ionized. Next, the ions were detected and if a species was observable which had the same m/z ratio as the mass-selected ion, it was concluded that the neutral counterpart was stable. The mass spectrometer used by Tomlinson et al[7] contained a furnace, which made neutralization by metal vapours possible. In the eighties the technique was extended for the investigation of the stability of the neutral counterparts of (well-characterised) poly-atomic, mostly organic ions.[8] Both metal vapours and permanent gases were successfully used for neutralization.

The first MS/MS/MS instrument was constructed in the late seventies.[9] The principal reason for developing triple sector mass spectrometers is to provide high mass resolution mainly for analytical purposes. The advantage of these instruments when used to study gas-phase organic ions is the ability to examine consecutive reactions taking place in sequential field-free regions of the instrument.

2.2 Instrument description

There are a number of instrumental components common to all mass spectrometers. The basic design requires an ion source, where ionization, and some fragmentation take place. The ions then must be separated according to their mass-to-charge ratio in the mass analyser. The detector detects the ions, measuring the relative abundance of each. Usually a data system records, processes, and stores the information. The vacuum system maintains a low pressure in the instrument; the low pressure minimises ion/molecule collisions so that the ions can move through the instrument in a well-defined path. To facilitate sample introduction, an inlet system provides a link between the outside world and the inside of the mass spectrometer.

The VG Analytical ZAB-3F mass spectrometer, a triple sector instrument, was used for the research presented in this thesis. Thus the instrument description will concentrate on the function of the various parts of the VG ZAB-3F mass spectrometer.

2.2.1 The ionization chamber

The ion source in the VG ZAB-3F is a typical electron impact ion source as shown in Figure 2.1.

Electrons are produced from an incandescent helical filament or ribbon usually made from tungsten or rhenium. The electrons are accelerated towards the ionization chamber and enter it through a system of collimating slits. The kinetic energy of the electrons can be varied simply by changing the potential difference between the filament and the ionization chamber.

The region within the ionization chamber is essentially free of electric fields and the electrons traverse it at constant velocity. Electrons which pass through a slit at the far end of the ionization chamber are accelerated towards an electrode at a potential higher than that of the ionization chamber and collected. This electrode is known as the "trap". One or two repeller electrodes are usually located within the ionization chamber. When a small positive voltage is applied to them, positive ions formed by the electrons will be repelled towards the slit A. The ions which leave the ionization chamber under the influence of the repeller electrodes do so with a very small kinetic energy corresponding to about one electron volt. Outside the ionization chamber, however, they come under the action of a strong electric field corresponding to a potential drop of several thousand volts over a distance of the order of a few mm and are accelerated towards a plate containing a slit, known as the source slit.

Figure 2.1 Ion source

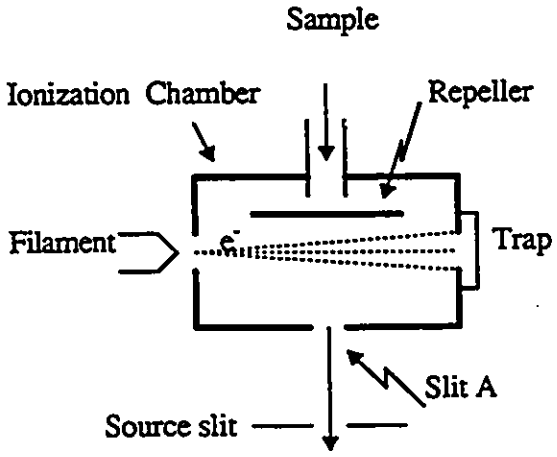

The kinetic energy of an ion of mass m and charge e accelerated through a

potential drop V_{acc} is given by $mv^2/2$ where v is the terminal velocity and

$$1/2\, mv^2 = eV_{acc} \qquad (1)$$

The beam of ions that has a kinetic energy equal to the full accelerating energy is known as the "main ion beam".

2.2.2 The magnetic analyser

The function of a magnetic analyser is shown in Figure 2.2. The use of an electromagnet as a mass analyser is based on the principle that charged particles which pass through a magnetic field, B, perpendicular to their motion, will follow a circular path of radius r_m. The r_m is determined by $mv = Bzr_m$.

Figure 2.2 Focusing action of a sector magnetic analyser

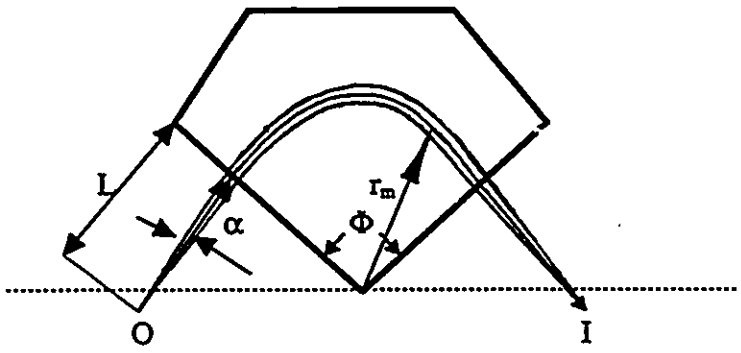

Suppose that ions of mass m and velocity v emerge from the object point O with a half-angular spread in the plane of the paper α (α << 1). An ion with median direction, after traversing the distance L, enters the magnetic field, where it is constrained to follow a circular path of radius r_m. After deflection through the angle Φ, it emerges from the field and proceeds to the image point I at which there is a convergence of the ion beam which

diverged from O. For a certain magnetic analyser, the r_m is fixed. Ions of different m/z ratios are focused by varying the magnetic field strength B, $m/z = Br_m / v$. Since the translational energy of the source generated ions is equal to zV_{acc}. It follows that:

$$B^2 = m/z \cdot 2V_{acc} / r_m^2 \qquad (2)$$

2.2.3 The electrostatic analyser

An electrostatic analyser produces a radial electric field (E) If the outer plate is made positive with respect to the inner plate, and a beam of ions of various energies is injected midway between the plates and perpendicular to the direction of the electric field, there will be some ions which will describe a circular trajectory along the curve of radius r_e which is a line of equipotential. This condition is met when the translation energy (E_T) of these ions, $mv^2 / 2$, is such that the electrostatic force on the ions is exactly balanced by the centrifugal force:

$$mv^2 / r_e = zE \qquad (3)$$

Combining with that $E_T = mv^2 / 2$,

$$E = 2 \cdot E_T / r_e \cdot z \qquad (4)$$

Thus the ESA separates ions according to their translational energy-to-charge ratio. A fragment ion $m_2^{+\cdot}$ formed by dissociation of $m_1^{+\cdot}$ in the FFR-2 will have translational energy (E_{T2}) equal to the ratio of the masses times E_T

$$E_{T2} = m_2/m_1 \cdot E_T \qquad (5)$$

By scanning E, all fragment ions of $m_1^{+\cdot}$ can be recorded. Alternatively by setting E to match E_{tr2}, the fragment ion $m_2^{+\cdot}$ will be transmitted to FFR-3.

Figure 2.3 Focusing action of an electrostatic analyzer

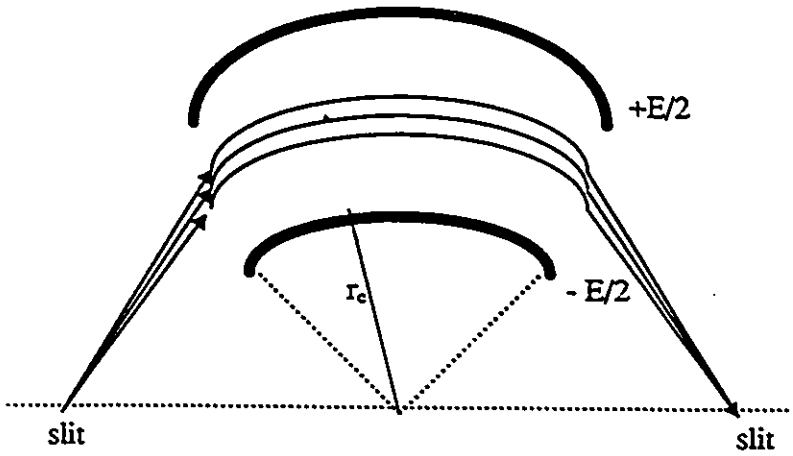

2.2.4 The detector

The detectors in VG ZAB-3F mass spectrometer are off-axis Daly detectors, which employ a scintillator to detect secondary electrons emitted when ions strike a conversion dynode (V_2) , as shown in Figure 2.4. The conversion dynode is at a high negative potential (-20 kV) and attracts the ions that emerge at ground potential from the exit slit of the mass analyzer. The high energy positive ions impinge on the central portion of the conversion dynode and secondary electrons are emitted (about 6 electrons per ion over a wide mass range). The secondary electrons are accelerated by the electric field produced by the conversion dynode potential and strike CaF_2 scintillator. The scintillations produced are detected by an optically coupled photomultiplier

Figure 2.4 Daly detector

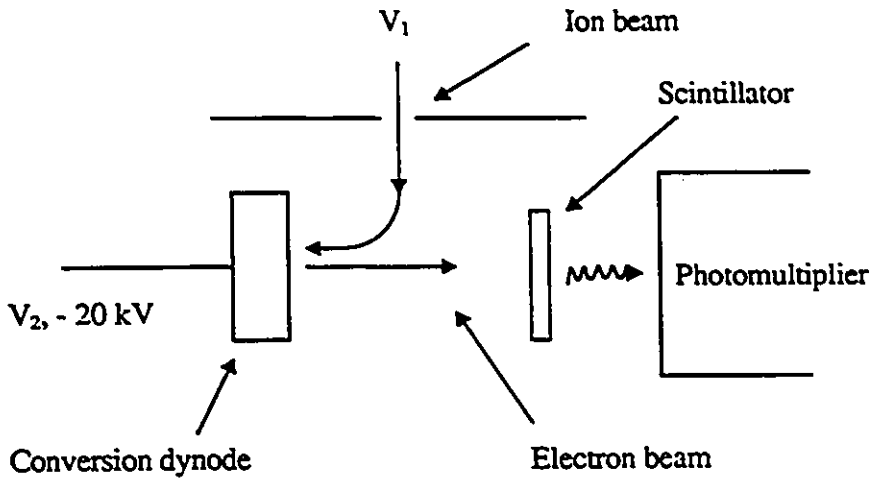

2.2.5 Tandem mass spectrometers used for this thesis

The VG ZAB-3F triple sector mass spectrometer with BEE geometry is schematically shown in Figure 2.5.

Figure 2.5 VG ZAB-3F mass spectrometer

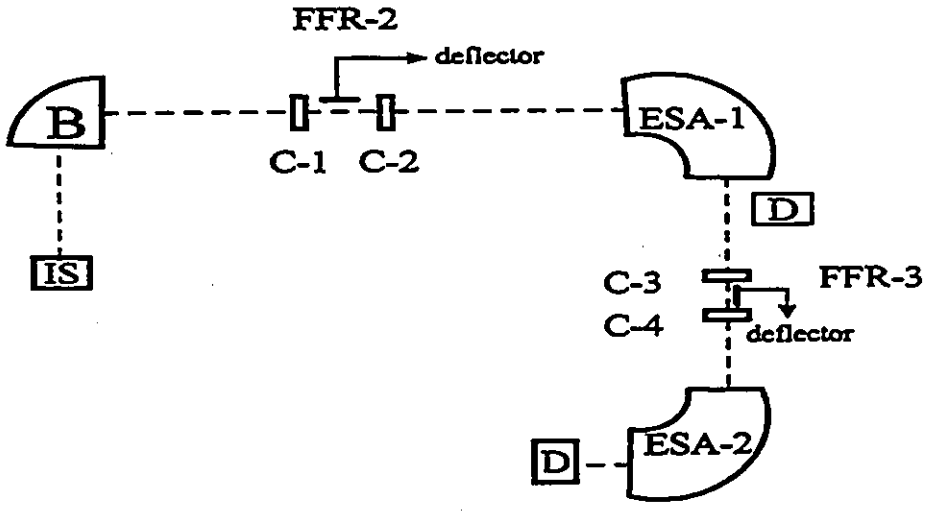

Where,

IS: Ion source
B: Magnetic analyzer
ESA: Electrostatic analyzer
C: Collision cell
FFR: Field-free region
D: Detector

The GEC-AEI MS-902s is also a tandem mass spectrometer with an EB geometry, which was used to measure the appearance energy (AE) of metastably generated ions produced in the first field-free region. Ions were also detected by a Daly Photomultiplier, the advantage of which is that the metastable ion signals may be enhanced relative to source generated species

2.3 Reactions in a tandem mass spectrometer

In general there are four types of reaction involving charged species that can be studied in a tandem mass spectrometer. First of all is *ionization* of an organic molecule in the ion source. There are quite a few ionization techniques applied to tandem mass spectrometry.[13] However, in the region of this thesis only electron impact (EI) ionization will be discussed.

The most commonly observed reaction in a mass spectrometer is a *unimolecular reaction*, which includes unimolecular dissociation and isomerization. The unimolecular dissociation can occur either spontaneously from metastable ions or from initially stable ions rendered unstable by an activating process. The latter is also important, known as *collision activation reactions*, the third type reaction in a tandem mass spectrometer. Not only the collision process activates an ion to fragment, but also it results *charge permutation*, which facilities to study the chemistry of neutrals.

The last type of reaction is an ion-molecule reaction, which can be obtained in the VG ZAB-3F ion source at pressures greater than about 10^{-5} torr.

2.3.1 Ion formation by electron impact (EI) ionization

EI ionization of gaseous molecules is a widely practised ionization technique. Electrons accelerated through a potential of several electron volts have a wavelength of ~ 0.1 nm, which is similar to the molecular dimensions. This results in mutual quantum effects (distortions). The distorted electron wave can be considered to be composed of many different sine waves and some of these waves will be of the "correct" frequency (energy) to interact with a molecular electron, that is, to promote an electron from a lower to a higher orbital (excitation) or - if the electron energy is greater than a critical value (the ionization energy or appearance energy) - to eject an electron from the target, thus producing a positive ion (*cation*).

$$m_1 + e^- \rightarrow [m_1]^{+\bullet} + 2e^- \qquad (6)$$

The minimum energy required to remove an electron from the highest occupied orbital of a molecule is termed the *ionization energy* (IE). A vertical ionization energy (IEv) is determined when ionization process is not involved geometric change (Figure 2.6a), while an adiabatic ionization energy (IEa) is the energy difference between the ion and its precursor when both are at their round states (Figure 2.6b).

Because of the very short time for ionization (~10^{-16} s) compared to vibrational periods (~ 10^{-14} s) EI ionization can be considered largely to be a *vertical* process in the Franck-Condon sense, a process in which inter-nuclear distances remain essentially fixed

at those appropriate for the neutral molecule. A stable ion can be formed by ionization without geometric change (Figure 2.6 a). An ionization process which involves a significant geometric change may produce no stable ion counterpart as shown in Figure 2.6 b.

Figure 2.6 Energy diagram for ionization process

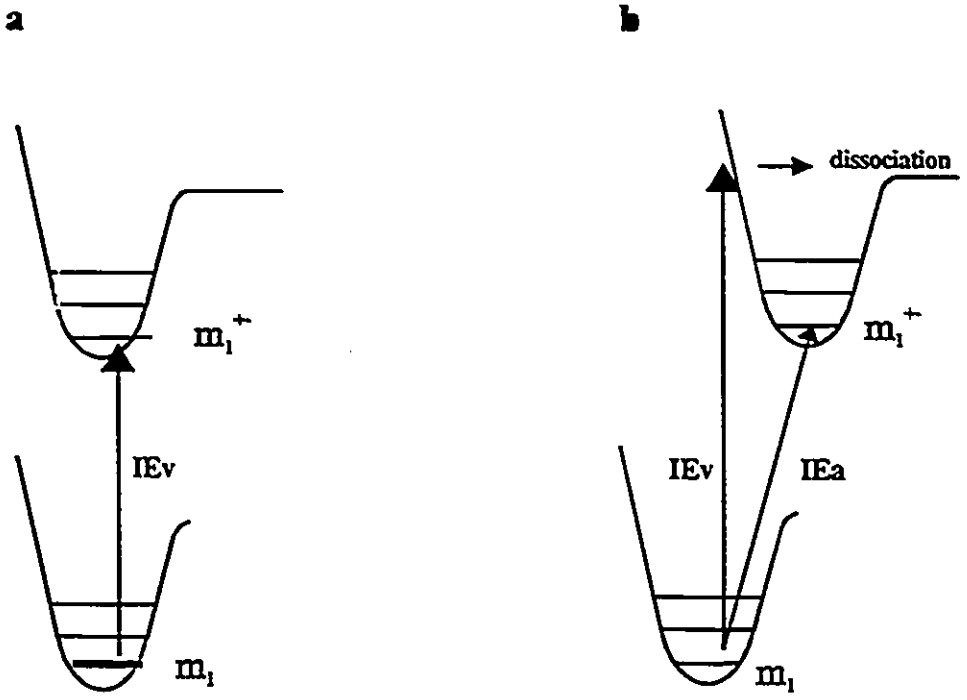

The energy of the electrons is variable, but is usually set at ~ 70 eV at EI ionization, a value much larger than the ionization energy of molecules. Hence, the molecular ions are generated with a large amount of excess internal energy and may dissociate to fragment ions (m_2^+) and neutrals ($m_n^\cdot$):

$$[m_1]^{+\cdot} \rightarrow [m_2]^+ + m_n^\cdot \qquad (7)$$

The minimum energy necessary to form a fragment ion from a given neutral precursor is termed the *appearance energy* (AE). IE and AE values can be measured with good accuracy, ± 0.05 eV, but only with the aid of specialized apparatus such as photoionization mass spectrometers[11] or mass analysers equipped with an energy-selected electron impact ion source.[12]

2.3.2 Unimolecular reactions

The EI mass spectrum is suited to determine the structure of an organic compound if the compound is sufficiently volatile. The molecular ion in such a spectrum contains information about the molecular weight and the elemental composition, while the numerous fragment ions in an ideal case reflect the structure directly. In practice, however, the elucidation of an unknown compound's structure from its EI mass spectrum is complicated not only by the fact that the molecular ion decomposes via rearrangement reactions, but also by multistep dissociations. The unimolecular reaction of organic ions, thus, is crucial to establish a fragmentation map, which is helpful to elucidate the molecular structures. Unimolecular reactions of mass selected ions can readily be studied in a tandem mass spectrometer.

Metastable ions

Ions in a mass spectrometer can be classified rather arbitrarily as stable, unstable, or metastable (Figure 2.7), depending upon when, or if, they fragment during their passage through the instrument.

Figure 2.7 Energy distribution of ions

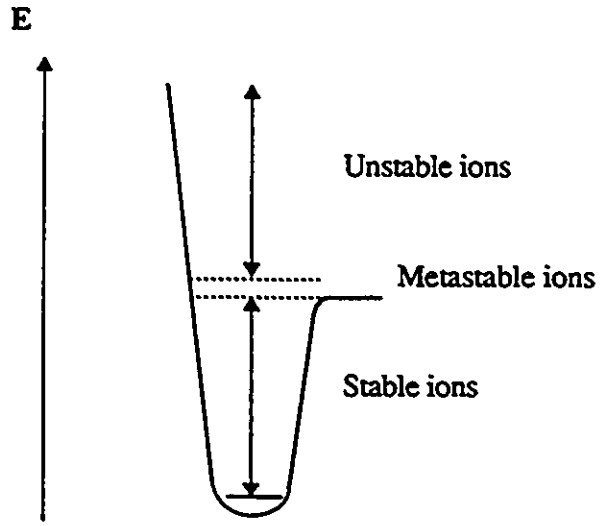

Stable ions are those that have lifetimes longer that the time of passage through the instrument. *Unstable ions* are those that fragment within the ion source, and *metastable ions* dissociate spontaneously outside the ion source but before detection. Ions with high internal energies can fragment with rate constants greater than about 10^6 s^{-1} and therefore do so before leaving the ion source. Metastable ions have intermediate internal energies and therefore dissociate with intermediate rate constants (10^4 - 10^6 sec^{-1}).

The primary use of metastable ions in analysis is to elucidate fragmentation pathways. By using a tandem mass spectrometer with BE geometry, the magnet current is adjusted to select a precursor. A scan of the electrostatic analyzer then records all its fragment ions. The fragmentation pattern thus can be identified. The identification of a particular reaction pathway can provide valuable evidence as to the arrangement of atoms in a molecule. For example, in a hypothetical spectrum the presence of ions corresponding

in mass to AB and ABC could indicate either of the molecular structure possibilities A-B-C-B-A or A-B-B-C-A. However, a metastable decomposition of ABC → AB would be possible, barring rearrangements, only for the structure of A-B-C-B-A.

Detection of metastably generated fragment ions depends upon where, within the instrument, the fragmentation occurs. Fragment ions generated within the magnetic or electric analyzer cannot be detected, the equation of motion, eq. (2) and eq. (4) do not apply to mid-sector changes in mass. Fragmentations occurring after the electric analyzer will also go undetected, since no further energy or momentum analysis is made before detection. Only those fragments due to dissociations in the first or second field-free regions, between the source and magnet and the magnet and electrostatic analyzer respectively, can be independently detected.

By eq. (5) the fragment m_2^+, produced via fragmentation in the second field-free region, will be transmitted through the electric analyzer at an E_v value corresponding to $m_2 / m_1 \bullet V_{acc.}$ Thus the mass of a product ion may be calculated from its kinetic energy. This is not only applicable to fragments of metastable ions, but to all fragments produced (unimolecularly or by collision) in the second field-free region from mass selected precursors.

The ratio of metastable peak intensities was proposed to be related to the structure of a fragmenting ion.[13] The "metastable peak abundance ratio test" was based on the premise that when two (or more) competing fragmentations from the same ion give reasonably intense metastable peaks, then the ratio of the abundances (measured under carefully controlled experimental conditions) may be used as a criterion for ion structure.

Simply, dissociation to give the same m/z peaks, with closely similar intensity ratios, is good circumstantial evidence that the reacting configurations of the two precursor species must be the same. Here we use term of reacting configuration, because all source generated ions, under the EI condition (70 eV), may have enough energy to undergo rearrangement to another structure prior to fragmentation.

Kinetic energy releases

In the dissociation of a singly charged polyatomic ion, represented by eq. (7) some fraction of the internal energy in the reaction co-ordinate in excess of that of the ground-state products is partitioned into the kinetic energy of separation of the fragments. This so-called *kinetic energy release* (KER), symbolized by T, leads to a spread in the kinetic energy of the daughter ions (m_2^+), since the daughter ion is ejected isotropically in the centre-of-mass frame of reference. The excess internal energy can be viewed as consisting of two components, the reverse critical energy (T^r) and the nonfixed energy ($T^‡$). The reverse critical energy is the energy difference between the ground state of the products and the critical energy for the fragmentation. The nonfixed energy is the internal energy in excess of the critical energy required to achieve a dissociation rate consonant with the lifetime of the metastable ion. The observed kinetic energy release includes a fraction of the reverse critical energy ε^r and a fraction of the nonfixed energy $\varepsilon^‡$ such that:

$$T = T^‡ + T^r \qquad (8)$$

where $T^‡$ is the contribution from $\varepsilon^‡$ and T^r is that from ε^r. When ε^r is negligible, the value of T is due to $T^‡$.

When dissociation occurs in the second reaction region of a BE instrument, the ionic products can be analyzed for their kinetic energy by a scan of the electric sector plate voltage. The kinetic energy release, T, will result in a broading of the signal corresponding to the metastable generated ions. T values are commonly reported for the peak widths at their half-height, $T_{0.5}$, irrespective of the shape of the peak.[5]

$$T_{0.5} = (m_1)^2/16m_2m_n \bullet (\Delta E_{0.5})^2/V_{acc} \qquad (9)$$

$$\text{and} \quad (\Delta E_{0.5})^2 = \Delta E(m_2)^2 - \Delta E(m_1)^2$$

where $\Delta E(m_2)$ and $\Delta E(m_1)$ are the peak widths at half-height for m_2^+ and m_1^+, respectively.

Metastable peak shapes, which are recorded under conditions of good energy resolution, fall into one of three categories (Figure 2.8).[14]

Figure 2.8 Metastable peak shapes

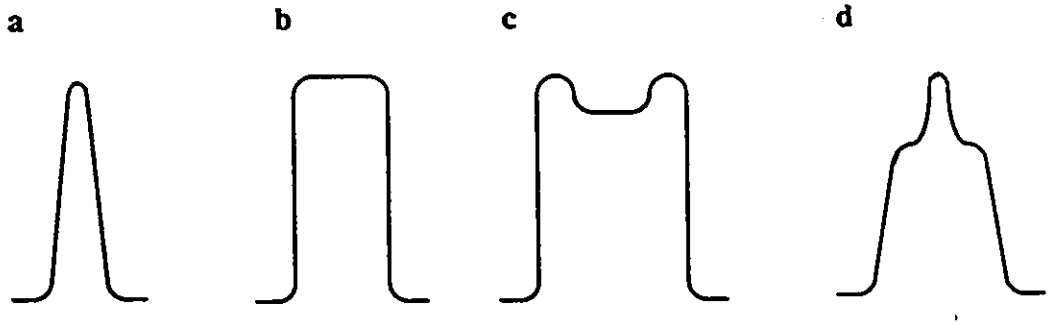

Gaussian type peaks (a) are generally associated with small kinetic energy releases, $T_{0.5}$ typically no more than ~ 80 meV. *Flat-topped* (b) and *Dished* peaks (c) are associated with larger kinetic energy releases due to reverse activation energy, ε^r, although the inverse statement is not necessarily true. The observed dish is produced by Z-axial

discrimination against the ion beam and will be instrument dependent. *Composite* peaks (d) are the result of the combination of two or more metastable peaks. A composite metastable peak indicates the involvement of more than one transition state and/or the production of more than one isomeric fragment ion.

Isomerization

Metastable ions typically have lifetimes of several tens of microseconds and internal energies in excess of the critical energy for the lowest energy dissociation of several tenths of an electron volt. Metastable ions therefore typically produce few product ions in their dissociative reactions, and those product ions that do form result from the lowest energy dissociation mechanisms. These dissociations are characteristic of the so-called reacting configuration of the ion. This configuration may or may not also characterize the structure of stable ions in the mass-selected beam used in MS/MS experiments, because the energized ions are not limited to decomposition alone. A wide range of excess internal energies is transferred on ionization and so it is also possible for the molecular and fragment ions to rearrange to various isomeric structures, of classical or non-classical form. These isomerization reactions can greatly complicate the interpretation of mass spectra and thus some understanding of the parameters involved is necessary. The relative energy barriers for decomposition, E_d, and isomerization, E_i, are the parameters which principally determine whether and to what extent an ion A^+ rearranges to an isomeric ion B^+ at a given internal energy E. Figure 2.9 shows a two-dimensional energy diagram to illustrate this point.

Figure 2.9 Energy diagram for isomerization and dissociation

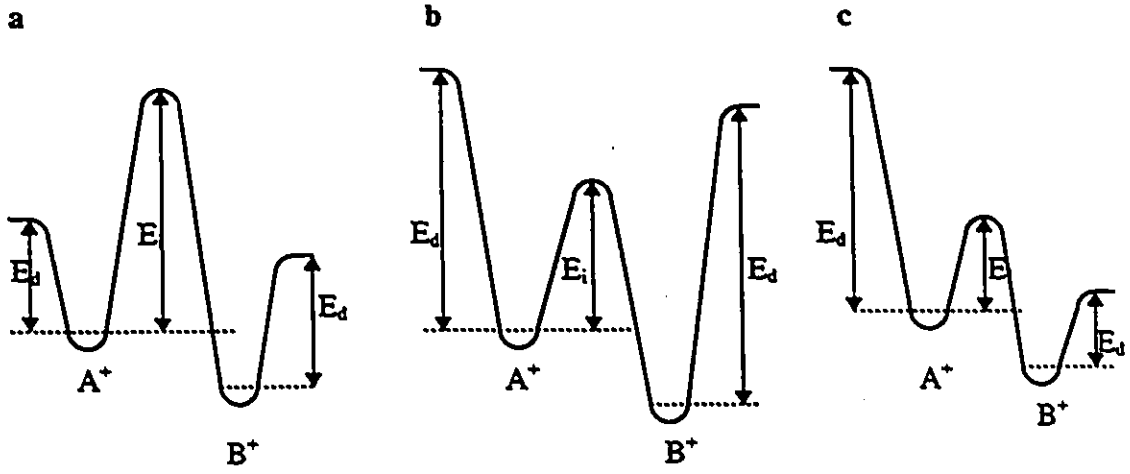

If an isomerization reaction has a critical energy higher than that of energy for a dissociation reaction (Figure 2.9 a), the isomerization cannot occur and so the metastable dissociation may be characteristic of the ionic structure A^+.[15] In the case of (b) where E_i is less than both E_d values, then isomerization is expected. At increased internal energies decomposition becomes possible, however having been preceded by a number of interconversions, the original placement of the atoms with respect to one another may have changed resulting in partial or full randomization of the initial structure. The observed metastable decomposition will depend on the dissociation energy and the density of states of these isomers. If both isomers have similar dissociation energies, the one with a higher density of states is expected predominantly to dissociate. Thus for (b) isomerization will not hide the structural elucidation of A^+ and B^+, whereas for (a) the investigation of the decompositions of these ions will give no information unique to one or the other structure. Situations between these limiting cases are also possible, such as (c)

must isomerize to B^+ prior to fragmenting and thus both A^+ and B^+ will generate similar mass spectral observations.

2.3.3 Activation reactions

Increasing the pressure in a field-free region of a mass spectrometer causes ion-neutral collisions in which some of the ion's kinetic energy is converted into internal energy. The resulting ion decomposition products can be studied using the same techniques developed for unimolecular metastable ion decompositions. The collision of a high-velocity ion with a target gas is the most widely used method to elucidate ionic structures.

The overall mechanism for collision-induced dissociation (CID) in generally accepted as proceeding in two steps.[10,16] The sequence involves collisional activation of the selected ion in the first step and unimolecular dissociation in the second step, i.e.:

$$m_1^+ \xrightarrow{N} m_1^{+*} \rightarrow m_2^+ + m_n \qquad (10)$$

where m_1^{+*} is the activated parent ion. The overall net equation of the CID process, including a mass and energy balance is:

$$q + m_1^+ + N = m_2^+ + m_n + N' + T \qquad (11)$$

where q is the endothermicity of the collision (i.e., the amount of energy converted from the translational energy of the collision partners into internal energy), N' is the target molecule in its postcollision state, and T is the kinetic energy liberated in the unimolecular

dissociation. Provided that no photoemission occurs, the internal energy of $m_1^{+\bullet}$ appears as T and the internal energies of m_2^{+} and m_n.

The most frequently used collision gases are helium and oxygen. Although maximum yields of fragment ions are obtained at pressures corresponding to 40-80% beam reduction, collision gas pressures are usually maintained at a 10% reduction to avoid multi-collisions.[14,17]

The second step of CID, namely unimolecular dissociation, differs from MI dissociation which involves only a narrow range of internal energy (Figure 2.7). The mass-selected ions which suffer collisional activation are ions, originating in the ion source, which have insufficient energy to fragment on the μs time-scale. These non-decomposing ions (m_1^{+}), as shown in Figure 2.7, possess a broad range of internal energies. If it is initially assumed that m_1^{+} ions retain their structure irrespective of their internal energy within this range, then the CID mass spectrum for these ions can tentatively be taken as structure-specific. However, to substantiate this assumption it is necessary to inspect m_1^{+} ions of low internal energy. This can be done in several ways: (I) by transmitting metastably generated m_1^{+} ions with the second mass analyzer in the VG ZAB-3F mass spectrometer; (ii) by lowering the ionizing electron energy to the lowest value compatible with a reasonable signal-to-noise ratio and transmitting the resulting source-generated, low-energy m_1^{+} ions. If the CID mass spectra of ions having broad and narrow internal energy ranges are the same, then it may provisionally be concluded that only a single ion structure is present.[14]

2.3.4 Charge permutation

2.3.4 Charge permutation

Three types of charge permutation reactions can be studied by tandem mass spectrometry.

Charge stripping (CS)

Collisional excitation of fast mass-selected ions ($m_1^{+\bullet}$) may be sufficient to cause the loss of an electron, resulting in a doubly charged species (m_1^{2+}).

$$m_1^{+\bullet} + N \rightarrow m_1^{2+} + N + e^- \qquad (12)$$

The signals resulting from CS may be easily differentiated from those of CID. They are greatly reduced in width, and appear at one half the electric sector voltage for transmission of their singly charged counterparts. Amplification of the CID mass spectrum is usually needed to detect charge stripping peaks because their intensity is in general far less than those from CID. The use of "soft" target gases, particularly O_2, resulting in less energized products, will increase the relative intensities of the CS peaks. As well, these target gases will yield more non-decomposing doubly charged parent ions relative to doubly charged fragments.[14,18]

Collision induced dissociative ionization

The neutral fragment (m_n) from metastable or collision-induced dissociation of a parent ion may be reionized by charge permutation with target gas.

$$m_n + N \rightarrow m_n^+ + N + e^- \qquad (13)$$

This can be done by applying an ion beam deflector set before the collision cell to deflect the ionic species or by applying to the collision cell a positive voltage which is greater than the ion acceleration voltage. Thus all ions were repelled and only neutral species resulting from the unimolecular dissociations of the mass-selected ions entered the cell. The neutral species suffered collisionally induced dissociative ionization in the collision cell and could be identified by the positive ions which were generated. The method proved to be of use in solving problems associated with the structure of the neutral fragment produced in certain ion fragmentations. For example, it was shown that $^{\bullet}CH_2OH$ rather than $^{\bullet}OCH_3$ is lost from ionized methyl acetate.[19]

Neutralization-Reionization (NR)

NR mass spectrometry is used to generate and characterize various transient neutral species.[20] In its simplest form, NR mass spectrometry is carried out as a two-collision experiment in which precursor ions of kilovolt kinetic energies are neutralized by collisions with thermal gaseous atoms or molecules (14), and the neutral species formed are allowed 0.5-5μs to dissociate (15). The surviving neutral intermediates and their dissociation products are reionized by another collision (16) and the ions formed are analyzed and detected.

$$m_1^{+\cdot} \xrightarrow{N} m_1 \qquad (14)$$

$$m_1 \rightarrow m_2 + m_3 \qquad (15)$$

$$m_1 \rightarrow m_1^{+\cdot} \rightarrow m_2^{+\cdot}, m_3^{+}, \bullet\bullet\bullet \qquad (16)$$

Characterization of the intermediate neutral is based on the NR mass spectrum in which the survivor and fragment ion relative abundances reflect the stabilities and dissociations of both the neutral and reionized species.

Because of the very short time-scale for electron transfer neutralization (10^{-16} s), it must be considered as a *vertical* Franck-Condon transition, i.e. the neutral is formed initially in the nuclear configuration of the ion. If the geometries of the ion and corresponding (stable) neutral are closely similar, stable neutrals will be generated upon neutralization of the ion. However if the geometries are markedly different then transition to an unstable part of the potential energy surface of the neutral may take place. If the neutral counterpart of the mass-selected ion is intrinsically unstable, or is stable but is generated with a large amount of internal energy due to exothermic neutralization, the generated neutral will fragment and/or rearrange to a more stable species (m_1').

$$m_1^{+\cdot} \xrightarrow{N} m_1^{*} \rightarrow m_1' \qquad (17)$$

It is also possible that upon neutralization, stable electronic excited states of the neutral are populated.[21] These can undergo spontaneous radiative or radiationless transitions to lower electronic states, which could be stable or dissociative. Thus the absence of a recovery signal, i.e. ions which survive the neutralization-reionization process intact, does not necessarily indicate that the corresponding neutrals are unstable.

The natures of both the neutralization and reionization agent influence the internal energy of the ion obtained after neutralization-reionization. Since collision induced ionization is also *vertical*, it is possible that, although the corresponding ion is stable,

excitation to a repulsive part of the potential energy surface of the ion takes place. Consequently no recovery signal will be present. The convolution of these energies is shown in Scheme 2.1. The excitation energy deposited in the neutral (ΔE) can be passed on to the reionized survivor ion and fragment ions and augmented by reionization (ε) to promote their dissociations. The net result of neutral excitation thus depends on the critical energies for the neutral and ion dissociations.

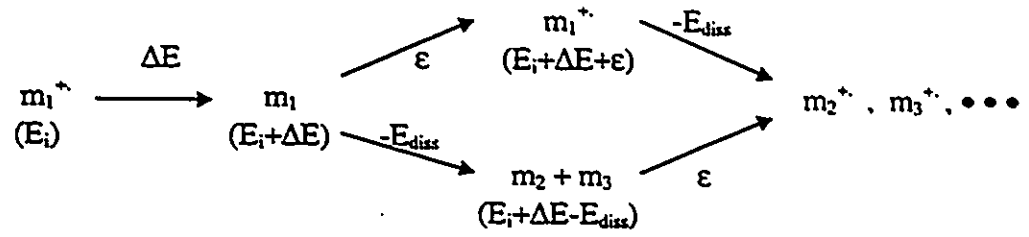

Scheme 2.1

E_i is the internal energy of $m_1^{+\cdot}$ and E_{diss} is the dissociation energy.

Excitation of neutral intermediates that have one or more low-energy dissociation channels will induce neutral dissociation, while excitation of stable neutral species will be passed on the reionized ions and promote their dissociations. Likewise, stable neutral fragments formed by neutral dissociations will pass their internal energy on the reionized species to promote their fragmentations. Collisional energy transfer at kiloelectronvolt kinetic energies is non-specific, resulting in a broad range of internal energies, convolution of neutral and ion fragmentations is an inevitable feature of NR mass spectrometry.

2.3.5 Ion-molecule reactions in the ion source

Most mass spectra are a result of a series of competitive and consecutive unimolecular reactions. However, when a high-pressure ion source is used, such as a chemical ionization source, bimolecular ion/molecule reactions can occur. The most commonly observed ion/molecule reaction is proton transfer, but the formation of *molecular ion/molecule adducts* and *fragment ion/molecule adducts* has also been confirmed with conventional tandem mass spectrometry.[22] Although ion cyclotron resonance (ICR) spectrometers are ideally suited to study many bimolecular reactions, high-pressure ion sources have the advantage of allowing collisional stabilization of the ion-molecule complexes. Thus the intermediates in exothermic reactions may be observed in many cases, while only the ionic products will be detected in an ICR spectrometer.[23]

2.4 Ion thermochemistry

The IE and AE measurements are fundamental to ionic thermochemistry because the heats of formation of organic ions, which are often correlated with ion structure, can be obtained from these values provided that the heats of formation of the corresponding neutrals are known.

$$\Delta_f H^0 (m_2^+) = IE (m_2) + \Delta_f H^0 (m_2) \quad (18)$$

and

$$\Delta_f H^0 (m_2^+) = AE (m_2^+) + \Delta_f H^0 (m_1) - \Delta_f H^0 (m_n) \quad (19)$$

The ionic heat of formation gained from the IE value will be specific for the ion having at least initially the same structure as the neutral molecule. The ion enthalpy

derived from eq. (19) will be the same as that from eq. 18 on the conditions that (i) the fragmentation of m_1^+ has no significant kinetic shift and (ii) the reverse reaction has no energy barrier.[14]

Thousands of $\Delta_f H^0$ values of organic ions have been measured through IE and AE measurements,[24] facilitating ion structure assignment and the understanding of ionic thermochemistry. With these values an empirical relationship between $\Delta_f H^0$ (Ion) and ion size (as represented by the number of atoms, n) in homologous series of organic compounds has been confirmed.[25]

$$\Delta_f H^0 (\text{Ion}) = A - Bn + C/n \qquad (20)$$

Where, A, B and C are constant for a given homologous series and n is the number of atoms in the molecule. An alternative approach is to evaluate the effect of stepwise substitution on a substituted methyl cation[26]:

$$\Delta\, \Delta_f H^0 [\, XCH_3^{+\cdot} / XC(CH_3)_m H_{3-m}\,]$$
$$= \Delta_f H^0 (\, XCH_3^{+\cdot}) - \Delta_f H^0 [\, XC(CH_3)_m H_{3-m}\,] = A + Bm \qquad (21)$$

Where, m represents the number of methyl groups and A and B are the intercept and slope, respectively.

By analyzing the values of A and B, one can not only evaluate the heats of formation of these substituted cations, but also evaluate the capacity of an ionic species to accept the substitution. The latter results from the analysis of B values. A large B value indicates a localized charge and a small B value indicates a delocalized charge.

The discovery of Equation 21 follows the point of view that the stability of a cation is related to the electronegativity of the heteroatom (X) in the cation. The scale of electronegativity suitable for evaluating the stability of organic ions is Vx,[27] which is obtained from the ratio of the number of covalent electrons (n_x) of atom X to the covalent radius (r_x):

$$Vx = n_x / r_x \qquad (22)$$

2.5 Ion structure assignment

With tandem mass spectrometry the ion structure is assigned specifically as to how the atoms are joined together and the probable (formal) locations of radical and/or charge sites. Details of geometry, such as bond lengths, bond angles and charge distribution are not yet accessible to experiment for polyatomic ions. Considerable progress has, however, been made in these areas by means of *ab initio* molecular orbital calculations, performed at a sufficiently high level of theory.[28]

The two chief experimental methods involving conventional tandem mass spectrometers currently available are: (i) Ion thermochemistry, i.e. IE and AE measurements; (ii) Ion dissociation characteristics, including MI, CID, CS and NR mass spectrometries.[14,29] Each of these now is commonly assisted by employing isotopic labelling experiments. High level ab initio calculations have also contributed greatly to the solution of the ion structure problem especially for those with unusual structures.[30]

A good example to illustrate the combination of these technique to assign ionic structures in the gas phase is the study of isomeric [C, H_3, N, O]$^+$ ions.[31]

$[H_2NC(H)O]^{+\bullet}$ (1) was generated by electron ionization of neutral $H_2NC(H)O$; $[H_2NCOH]^{+\bullet}$ (2) was generated by fragmentation of $[H_2NC(O)CH_2CH_3]^{+\bullet}$ via C_2H_4 loss; $[H_3CNO]^{+\bullet}$ (3) was generated by fragmentation of $[H_3CNO_2]^{+\bullet}$ via O loss; and $[H_2CNOH]^{+\bullet}$ (4) was generated by thermolysis of trimetric formaldoxime hydrochloride. The heats of formation of the four isomers were either experimentally measured or calculated by ab initio MO theory. The values were 189.0, 190.7, 231.1 and 230.9 kcalmol^{-1} for ions **1**, **2**, **3**, **4**, respectively.

The four isomers were identified by MI mass spectrometry, as shown in the following.

			$T_{0.5}$ (meV)
$[H_2NC(H)O]^{+\bullet}$ (1)	→	$[H_2NCO]^+ + H^\bullet$	33
$[H_2NCOH]^{+\bullet}$ (2)	→	$[H_2NCO]^+ + H^\bullet$	10
	→	$[H_3N]^{+\bullet} + CO$	43
$[H_3CNO]^{+\bullet}$ (3)	→	$[NO]^+ + CH_3^\bullet$	0.5
$[H_2CNOH]^{+\bullet}$ (4)	→	$[NO]^+ + CH_3^\bullet$	35
	→	$[H_2NCO]^+ + H^\bullet$	63

The CID mass spectra of these isomers provided further evidence. The signals at m/z 14 $(CH_2)^{+\bullet}$, 18 $(H_2O)^{+\bullet}$, and 31 $(NOH)^{+\bullet}$ in the CID mass spectrum of ion (4) confirmed its structure with a terminal CH_2 group. Moreover, some identical dissociation channels for ions **1** and **2** , i.e. CO loss and $NH_2^\bullet$ loss, indicated that the isomerization energy barrier for **1** ↔ **2** is lower than these dissociation barriers. The calculated isomerization energy value supported this proposal.

2.6 References

1. F. W. Aston, Proc. Chem. Phil. Soc., 19, 317 (1919)

2. J. A. Hipple and E. U. Condon, Phys. Rev., 68, 54 (1945)

3. M. Barber and R. M. Elliot, Presented at the ASTM E-14 Conference on Mass Spectrometry, Montreal, June 1964

4. W. F. Haddon and F. W. McLafferty, J. Am. Chem. Soc., 90, 4745 (1968)

5. a: R. G. Cooks, J. H. Beynon, R. M. Caprioli and G. R. Lester, *Metastable ions*, Elsevier: Amsterdam, 1973

   b: J. C. Traeger and A. A. Mommers, Org. Mass Spectrom., 22, 592 (1987)

6. J. L. Holmes, Mass Spectrom. Rev., 8, 513 (1989)

7. a: J. Gray and R. H. Tomlinson, Chem. Phys. Lett., 3, 523 (1969);

   b: J. Gray and R. H. Tomlinson, Chem. Phys. Lett., 4, 251 (1969)

   c: J. Gray and R. H. Tomlinson, Int. J. Mass Spectrom. Ion Phys., 15, 121 (1974)

8. a: C. Wesdemiotis and F. W. McLafferty, Chem. Rev., 87, 485 (1987)

   b: J. K. Terlouw and H. Schwarz, Angew. Chem. Int. Ed. Engl., 26, 805 (1987)

9. a: F. W. McLafferty, Acc. Chem. Res., 13, 33 (1980)

   b: F. W. McLafferty, P. J. Todd, D. C. McGilvery and M. A. Baldwin, J. Am. Chem. Soc., 102, 3360 (1980)

   c: D. H. Riddell, D. H. Smith, R. J. Warmack and L. K. Bertram, Int. J. Mass Spectrom. Ion Phys., 35, 381 (1980)

10. K. L. Busch, G. L. Glish and S. A. McLuckey, *Mass spectrometry/Mass spectrometry* VCH Publishers, NY, 1988

11. J. C. Traeger and R. G. McLoughlin, Int. J. Mass Spectrom. Ion Phys., 27, 319 (1978)

12. a: F. P. Lossing and J. C. Traeger, Int. J. Mass Spectrom. Ion Phys., 19, 9 (1976)

b: J. L. Holmes and F. P. Lossing, J. Am. Chem. Soc., 110, 7343 (1988)

c: K. Maeda, G. P. Semeluk and F. P. Lossing, Int. J. Mass Spectrom. Ion Phys., 1, 395 (1968)

13. a: T. S. Shannon and F. W. McLafferty, J. Am. Chem. Soc., 88, 5021 (1966);

b: H. M. Rosenstock, V. H. Dibeler and F. N. Harllee, J. Chem. Phys., 40, 591 (1964)

14 J. L. Holmes, Org. Mass Spectrom., 20, 169 (1985)

15 J. L. Holmes and J. K. Terlouw, Org. Mass Spectrom., 15, 383 (1980)

16 D. J. Douglas, J. Phys. Chem., 86, 185 (1982)

17 M. S. Kim, Int. J. Mass Spectrom. Ion Phys., 50, 189 (1983)

18 J. L. Holmes, Int. J. Mass Spectrom. Ion Phys., 118/119, 381 (1992)

19 a: P. C. Burgers, J. L. Holmes, A. A. Mommers, J. E. Szulejko and J. K. Terlouw, Org. Mass Spectrom., 19, 442 (1984);

b: R. Clair, J. L. Holmes, A. A. Mommers, and P. C. Burgers, Org. Mass Spectrom., 20, 207 (1985)

20. a: F. W. McLafferty, Int. J. Mass Spectrom. Ion Phys., 118/119, 221 (1992)

b: J. L. Holmes, Adv. Mass Spectrom., 11, 53 (1989)

21 a: G. I. Gellene, D. A. Cleary, R. F. Porter, C. E. Burkhardt and J. J. Leventhal, J. Chem. Phys., 77, 1354 (1982)

b: S. F. Selgren, D. E. Hipp and G. I. Gellene, J. Chem. Phys., 88, 3116 (1988)

22 D. L. Miller and M. L. Gross, J. Am. Chem. Soc 105, 3783 (1983)

23 M. L. Gross, D. H. Russell, R. J. Aerni and S. A. Bronczyk, J. Am. Chem. Soc 99, 3603 (1977)

24 S. G. Lias, J. E. Bartmess, J. F. Liebman, J. L. Holmes, R. D. Levin and W. G. Mallard, J. Phys. Chem. Ref. Data, 17, No. 1 (1988)

25 a: J. L. Holmes and F. P. Lossing, Org. Mass Spectrom., 26, 537 (1991)

b: J. L. Holmes, M. Fingas and F. P. Lossing, Can. J. Chem., 59, 80 (1981)

c: J. L. Holmes and F. P. Lossing, Can. J. Chem., 60, 2365 (1982)

26 Y-R. Luo, Y. An and J. L. Holmes, Org. Mass Spectrom., 29, 579 (1994)

27 a: Y. R. Luo and S. W. Benson, Acc. Chem. Rev., 25, 375 (1992)

b: Y. R. Luo and J. L. Holmes, J. Phys. Chem., 98, 303 (1994)

28 *Ab initio Molecular orbital theory*, W. J. Hehre, L. Radom, P. v.R. Schleyer and J. A. Pople , John Wiley & Sons, Inc., 1986

29 a: J. H. Beynon and R. G. Cooks, Adv. Mass Spectrom., 6, 835 (1974)

b: C. J. Porter, J. H. Beynon and T. Ast., Org. Mass Spectrom., 16, 101 (1981)

30 M. George, C. A. Kingsmill, D. Suh, J. K. Terlouw and J. L. Holmes, J. Am. Chem. Soc., 116, 7807 (1994)

31 C. A. Hop, H. Chen, P. J. A. Ruttink and J. L. Holmes, Org. Mass Spectrom., 26, 679(1991)

Chapter 3

C_2H_4X cations and neutrals

3.1 Introduction

The structure and energetics of halogen substituted cations have generated widespread interest since their involvement in the bromination of alkenes was first proposed by Roberts and Kimball[1]. Several decades later, the direct observation of an isolated cyclic halonium ion in the condensed phase came from Olah and Bolinger[2] by proton magnetic resonance spectroscopy of the tetramethylethylene halonium ions, formed via ionization of 2,3-dihalo-2,3-dimethylbutanes in superacidic media [$(CH_3)_2CXCX(CH_3)_2$, with X = Cl, Br and I).

This observation of the non-classical $C_2H_4X^+$ cation in the condensed phase sparked the theoretical calculations aimed to evaluate the relative energies of these cations and their isomers and related transition states. According to calculation there are two stable isomers of $C_2H_4X^+$ for X = Cl and Br. They are the α-substituted haloethyl cation, CH_3CHX^+ (I), and the cyclic- ethylenehalonium cation, $\overline{CH_2X^+CH_2}$ (II). For $C_2H_4F^+$, isomer II is about 30 kcalmol^{-1} higher in energy than isomer I. The β-substituted structures, $XCH_2CH_2^+$ (III), were calculated to be transition states between isomers I and II, and do not exist as minima on the potential energy surfaces. No calculations on $C_2H_4I^+$ have been reported. The results of the calculations are summarized in Table 3.1. Although the calculated values are scattered, the differences between F-, Cl- and Br- substituted ethyl cations are clear from the average values. The cyclic-$\overline{CH_2F^+CH_2}$ ion is ~ 30 kcalmol^{-1} higher

in energy than CH_3CHF^+ and about as high as $FCH_2CH_2^+$. It is noteworthy that the energy of the transition state for hydrogen bridging,  , is about the same as that for fluorine bridging. Thus the CH_3CHF^+ ion is unlikely to isomerize to the cyclic -$\overline{CH_2F^+CH_2}$. In the case of $C_2H_4X^+$ (X = Cl and Br), the cyclic-$\overline{CH_2X^+CH_2}$ ion is similar in energy to CH_3CHX^+. However, the acyclic ion $XCH_2CH_2^+$ is much higher in energy. Thus isomers **I** and **II** have a similar stability but are separated by a high energy barrier.

The theoretical calculations strongly support experimental values for the heats of formation of $C_2H_4X^+$. The measured heats of formation of $C_2H_4X^+$, for X = F, Cl, Br and I, are shown in Table 3.2, along with a brief description of the experimental method. The experimentally derived values for Δ_fH^0 $C_2H_4X^+$ (X = Cl, Br) and CH_3CHF^+ from different measurements are very close to each other. The heat of formation of cyclic-$\overline{CH_2F^+CH_2}$ was only obtained by estimation using the method of equivalent cores, which assumes that "The energy of the process in which an electron is transfered from a core level of an atom to the nucleus of the atom is independent of the chemical environment of the atom".[17a]

In the gas phase, the unimolecular and bimolecular reactions of both CH_3CHX^+ and cyclic-$\overline{CH_2X^+CH_2}$, for X = Cl and Br, have been reported by several groups using tandem mass spectrometry[18-20] and ion cyclotron resonance mass spectrometry[21-23]. However for $C_2H_4F^+$, the cyclic ethylenefluorinium ion has only been observed as a proposed intermediate species in the gas phase during the electron impact-induced decomposition of 2-phenoxyethyl fluoride.[17,24] The gas-phase reactions of $C_2H_4I^+$ cations

have not been reported.

The results reported in this Chapter are from detailed studies of the gas-phase unimolecular reactions of the $C_2H_4X^+$ cations, the chief aim of which was to identify the isomers. The Neutralization-Reionization mass spectra of $C_2H_4X^+$ cations are reported here for the first time. Compared with $C_2H_4X^+$, fewer studies have been reported on the corresponding C_2H_4X radicals.[25-37]

The heats of formation of C_2H_4X radicals (X = F, Cl and Br) have been measured[25-29] via kinetic studies and by appearance energy measurements. The values are summarized in Table 3.3.

Most of the theoretical studies of C_2H_4X radicals were performed in regard to bridging in the β-haloethyl radical, $\overset{\frown}{CH_2XCH_2}^{\bullet}$.[30-34] Engels and Peyrimhoff calculated the energy difference between the minimum asymmetric structure $XCH_2CH_2^{\bullet}$ (X = F, Cl and Br) and the optimal symmetric structure $CH_2X^{\bullet}CH_2$, using MRD-CI calculations.[30-32] The differences were 33, 8 and 1 kcalmol^{-1} for X = F, Cl and Br, respectively. Thus $C_2H_4F^{\bullet}$ is certainly expected to behave as a classical unbridged radical[31]. Guerra's calculation agreed that the symmetric bridged structure is less stable than the classical structure for $C_2H_4X^{\bullet}$ (X = F and Cl). The energy differences between the two structures were 36.0 kcalmol^{-1} for X = F and 13.3 kcalmol^{-1} for X = Cl, respectively.[33] The symmetric structure was found to be stable with respect to dissociation.[31] Robinson et al, calculated that the dissociation of $C_2H_4F^{\bullet}$ to $C_2H_4 + F^{\bullet}$ was endothermic by 46 kcalmol^{-1} and the energy barrier to $C_2H_3F + H^{\bullet}$ was about 44 kcalmol^{-1}.[35] The C-F dissociation energy in $C_2H_4F^{\bullet}$ was calculated to be 37 kcalmol^{-1}.[30] However, the C-Cl dissociation of

$C_2H_4Cl^{\bullet}$ was only 17 kcalmol.[36] The lower stability of $ClC_2H_4^{\bullet}$ (with respect to $Cl\text{-}C_2H_4$ separation) can be traced to the different strengths of the fluorine-carbon and chlorine-carbon bonds.[32]

Barat et al, studied the reaction of hydrogen atoms with vinyl chloride.[37] At low-pressure, room temperature conditions, the consumption of C_2H_3Cl by reaction with $H^{\bullet}$ occurs primarily by n-ipso attack by H on the $=CH_2$ group to form $(CH_3CHCl)^*$. This energized complex then undergoes a H-shift to form $(CH_2CH_2Cl)^*$, which decomposes to form $Cl + C_2H_4$.

The decomposition behaviour of $C_2H_4X^{\bullet}$ radicals may also be examined by NR mass spectrometry; results will be shown in this chapter.

3.2 Experimental

All metastable ion (MI), collision induced dissociation (CID) and neutralization reionization (NR) mass spectra were performed with a VG-ZAB-3F mass spectrometer. The ionization energy was 70 eV and the ion translational energy (accelerating voltage) 8 keV, unless, otherwise indicated. The correction of the CID mass spectra for MI contributions was done by setting a potential of -1000 V on the collision cell. The NR mass spectrum was performed using a potential of -1000 V on the ion beam deflector electrode between the neutralization and reionization cells. The distances between the two cells were 10 cm and 2 cm in the 2ffr and 3ffr, respectively. Appearance energy (AE) measurements were performed either using the MS-9 mass spectrometer or an electron monochromator. For greater detail of the experimental procedues, see Chapter 2.

3.3 Results

3.3.1 Formation of the $C_2H_4X^+$ isomers

In general C-X (X = Br or I) bond dissociations in molecular ions proceed with a negligible reverse energy barrier. Thus a good way to produce a desired cation is to use an appropriate halogen containing precursor. To produce the $C_2H_4X^+$ cation, the selected precursor was C_2H_4XY (X = F, Cl, Br and I; Y = Br and I).

CH_3CHX^+ (I) is produced from $CH_3CHXY^{+\cdot}$ by Y loss.

$$CH_3CHXY^{+\cdot} \rightarrow CH_3CHX^+ \text{ (I)} + Y \qquad (1)$$

$\overline{CH_2X^+CH_2}$ (II) is produced from $CH_2XCH_2Y^{+\cdot}$ by loss of Y.

$$CH_2XCH_2Y^{+\cdot} \rightarrow \overline{CH_2X^+CH_2} \text{ (II)} + Y \qquad (2)$$

The $C_2H_4X^+$ cations are numbered as shown below:

X	CH_3CHX^+	$\overline{CH_2X^+CH_2}$
F	**Ia**	**IIa**
Cl	**Ib**	**IIb**
Br	**Ic**	**IIc**
I	**Id**	**IId**

3.3.2 Unimolecular dissociation of $C_2H_4X^+$ isomers

The metastable ion (MI) dissociations of $C_2H_4X^+$ (X = F, Cl and Br) were dominated by HX loss with a large kinetic energy release (KER) for X = F and a very small kinetic energy release for X = Cl and Br. The KER values are shown in Table 3.4. No fragmentation was observed in the MI mass spectrum of $C_2H_4I^+$.

In CID mass spectra, as shown in Table 3.5, the eight cations, **Ia-d**, **IIa-d**, show structure distinguishing dissociations. The dissociation energies of $C_2H_4X^+$ ions are summarized in Table 3.6. The comparison of CID mass spectra of CH_3CHF^+ at different translational energies is shown in Table 3.7.

3.3.3 Neutralization-Reionization (NR) mass spectra of $C_2H_4X^+$

The NR mass spectra of $C_2H_4X^+$ (X = F, Cl Br and I) are shown in Figure 3.1 - 3.7. The neutralization target was dimethylamine (DMA). Xe was also used as neutralization target and it showed results similar to those with DMA. O_2 was used as the reionization target. The NR mass spectra of each $C_2H_4X^+$ were obtained both in the 2ffr (the distance between two cells is 10 cm) and in the 3ffr (distance is 2 cm). No recovery signal was observed in the NR mass spectrum of $C_2H_4I^+$ (Figures 3.6 and 3.7). The NR mass spectrum of $C_2H_4I^+$ was dominated by I^+. The energy values related to the dissociations of $C_2H_4X^+$ radicals are shown in Table 3.8.

3.3.4 Deuterium-labelling of cyclic-$\overline{CH_2X^+CD_2}$ (X = Cl, Br).

The MI mass spectra and CID mass spectra of $XCD_2CH_2^+$ ($XCD_2CH_2Y^{+\cdot}$ - Y, X = Cl, Br; Y = Br, Cl) and $XCH_2CD_2^+$ ($XCH_2CD_2Y^{+\cdot}$ - Y, X = Cl, Br; Y = Br, Cl) are identical. Both metastable $C_2H_2D_2Cl^+$ isomers showed the same ratio of DCl loss to HCl loss as 1:16. The ratio sharply increased to 1:1.6 in the CID mass spectra. Both metastable $C_2H_2D_2Br^+$ isomers showed the same ratio of DBr loss to HBr loss, namely 1:14. The ratio increased to 1:1.06 in the CID mass spectra. Table 3.9 shows the partial CID mass spectra of $C_2H_2D_2X^+$ (X = Cl, Br).

3.4 Discussion

3.4.1 $C_2H_4F^+$ isomers

The $C_2H_4F^+$ cations produced either from CH_3CHF_2 or from CH_2FCH_2Br showed similar dissociations in their CID mass spectra, as shown in Table 3.5. The appearance energy (AE) measured for the process of $CH_2FCH_2Br \rightarrow C_2H_4F^+ + Br^\cdot$ is 10.94±0.05 eV (252 kcalmol^{-1}), corresponding to a heat of formation for $C_2H_4F^+$ of 165.6 kcalmol^{-1} [taking ΔH_f° (CH_2FCH_2Br) = -60 kcalmol^{-1}, ΔH_f° (Br) = 26.7 kcalmol^{-1}][38]. This value is the same as the heat of formation of CH_3CHF^+ (165 kcalmol^{-1})[15,16]. Thus the $C_2H_4F^+$, produced from $CH_2FCH_2Br^{+\cdot}$, appears to be CH_3CHF^+ (Ia). Moreover, since the threshold for production of $C_2H_4F^+$ is the same as the calculated enthalpy change of the reaction [AE = ΔH_f° (CH_3CHF^+) + ΔH_f° (Br) - ΔH_f° (CH_2FCH_2Br)] and this dissociation has little reverse energy barrier ($T_{0.5}$ = 0.76 kcalmol^{-1}), indicating the threshold product ion cannot

be CH_2-CH_2 (ΔH_f = 183 kcalmol^{-1}). So the hydrogen shift may happen before the Br cleavage, i.e.

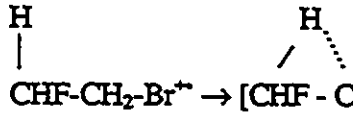

$$CHF\text{-}CH_2\text{-}Br^{+\cdot} \rightarrow [CHF - CH_2...Br]^{+\cdot} \rightarrow CH_3CHF^+ + Br^\cdot \qquad (3)$$

Morton et al, showed that the cleavage of the O-C bond in $PhO\text{-}CH_2CH_2F^{+\cdot}$ involves an ion-neutral complex, $[PhO^\cdot\ {}^+CH_2CH_2F]$. In the complex, the cyclic-$\overline{CH_2F^+CH_2}$ (IIa) was proposed to be an intermediate in competition with H-bridged $\overline{CH_2H^+CHF}$. In contrast, the free $C_2H_4F^+$ ions have the structure of CH_3CHF^+. However, in the case of

the cleavage of the Br-C bond in $CH_2FCH_2Br^{+\bullet}$, the cyclic-$\overline{CH_2F^+CH_2}$ cannot have been an intermediate, otherwise, the AE value should have been at least 17 kcalmol^{-1} higher than that observed.

$$\begin{array}{lccccc} & CH_2FCH_2Br & \rightarrow & \overline{CH_2F^+CH_2} + Br^\bullet & \rightarrow & CH_3CHF^+ + Br^\bullet \\ \Delta H_r\ (kcalmol^{-1}) & & & 269 & & 252 \end{array} \qquad (4)$$

In the 2ffr CID mass spectrum the dissociation of $C_2H_4F^+$ was dominated by HF loss. However in 3ffr CID mass spectrum the major dissociations were H and H_2 losses, as shown in Table 3.7. The parent ions in the 3ffr have a slightly lower average internal energy than those in the 2ffr. The CID mass spectrum of $C_2H_4F^+$, generated from metastable $BrCH_2CH_2F^{+\bullet}$ ions also showed a more intense peak for $C_2H_3F^{+\bullet}$ (H loss) than for $C_2H_3^+$ (HF loss). Thus the fragmentation of CH_3CHF^+ is very sensitive to its internal energy. The dissociation of $C_2H_4F^+$ ions having lower internal energy is dominated by H and H_2 losses and the dissociation at slightly higher internal energy is dominated by HF loss. It is proposed that the HF loss channel may involve an isomerization into a stable isomer, CH_2CHFH^+. The isomerization barrier for $CH_3CHF^+ \rightarrow CH_2CHFH^+$ is less than the energy required to dissociate the ion into $C_2H_2F^+$ (ΔH_f° = 227 kcalmol^{-1}) + H_2.

The absence of $C_2H_4^{+\bullet}$ in the CID mass spectra of $C_2H_4F^+$, although it is less endothermic than some observed fragmentations (see Table 3.6), shows that the energy barrier for the F loss is at least as high as 63 kcalmol^{-1} (compare with the energy required for dissociation to $C_2HF^{+\bullet} + H_2 + H$), as shown in Table 3.6.

In Figure 3.1, it can be seen that the NR mass spectra of $C_2H_4F^+$ are similar to the corresponding CID mass spectra, even though the total ion current after NR with

DMA/O_2 was judged to be approximately a factor of 10^4 lower than the current of the mass selected ions entering the collision cells, indicative of a small overall cross-section for the process.[39] The NR mass spectra performed in the 2ffr (Figure 3.1 b) showed the fragments F^+, $HF^{+\cdot}$ and $C_2H_4^{+\cdot}$, which are not observed in the corresponding CID mass spectrum. These fragments must arise from decomposition of the neutral $C_2H_4F^{\cdot}$. In the NR mass spectrum of $C_2H_4F^+$ performed in the 3ffr (Figure 3.1 c), the recovery signal increased and neutral fragments decreased. In the 3ffr the distance between the two collision cell is 2 cm, significantly shorter than that in the 2ffr (10 cm) where the neutral C_2H_4F spends a longer time before reionization, and so in the 3ffr the neutrals showed less dissociation. In the NR mass spectrum of $C_2H_4F^+$ performed in the 2ffr (Figure 3.1 b), the more intense $C_2H_2^{+\cdot}$, $C_2H_3^+$ and CF^+, $CHF^{+\cdot}$, CH_2F^+ ions compared to those in the 3ffr (Figure 3.1 c), indicated that the $C_2H_4F^{\cdot}$ radicals may have some dissociation channels similar to that of the ion. Note that $C_2H_4F^{\cdot}$ may dissociate to C_2H_3 + HF, the reaction of the lowest energy among its dissociations, see Table 3.8.

3.4.2 $C_2H_4Cl^+$ isomers

The identical MI and CID mass spectra (see Table 3.9) of D-labelled $C_2H_2D_2Cl^+$ ions (**IIb**) confirmed the cyclic structure of $\overline{\lceil \cdot \rceil}CH_2Cl^+CH_2$.

The CID mass spectra of the $C_2H_4Cl^+$ isomers (Table 3.5) indicate that the two isomers, CH_3CHCl^+ (**Ib**) and cyclic - $\overline{\lceil \rceil}CH_2Cl^+CH_2$ (**IIb**) are readily distinguishable. Isomer **Ib** fragments to CH_3^+ + CHCl and $CHCl^+$ + CH_3; However, isomer **IIb** fragments to $CH_2^{+\cdot}$ + CH_2Cl and CH_2Cl^+ + CH_2. The small fragment at m/z 49 (CH_2Cl^+) from **Ib** indicates some H shift from the CH_3 group to the CHCl group. Thus this H-shift is energetically

accessible by collision activition.

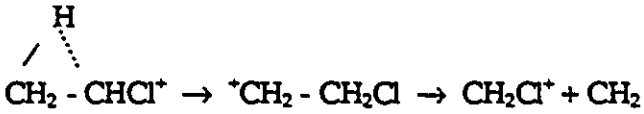

$$CH_2 - CHCl^+ \rightarrow {}^+CH_2 - CH_2Cl \rightarrow CH_2Cl^+ + CH_2 \qquad (5)$$

The CID mass spectra of D-labelled **IIb** showed neither a fragment at m/z 50 ($CHDCl^+$) nor one at m/z 17 (CHD_2^+), indicating the reactions in Scheme 3.1 did not occur. This reveals that the energy barrier for H-shift (reaction i) or cyclic-opening (reaction ii) is relatively high.

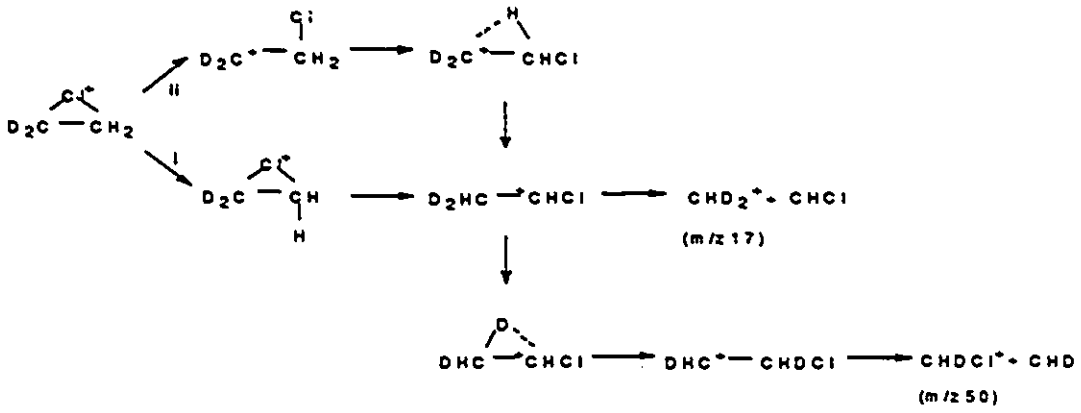

Scheme 3.1

In the MI mass spectra both isomers dissociated to $C_2H_3^+ + HCl$, with a very small KER value ($T_{0.5}$ = 1.4 meV). The appearance energy (AE) values for this dissociation are 12.5±0.2 eV for **Ib** and 12.7±0.2 eV for **IIb**. The results indicated no reverse energy barrier for the dissociation processes. The D-labelling experiments showed a strong isotope effect for HCl:DCl losses (MI, 16; CID, 1.6). Furthermore, the observation of H_2Cl^+ in the CID mass spectra of the two isomers and the presence of $HDCl^+$, D_2Cl^+ in the

CID mass spectrum of cyclic-$\overline{CH_2Cl^+CD_2}$ (see Table 3.9) confirms that the fragmentation may well involve another isomer, either CH_2CHClH^+ (like CH_2CHFH^+) or an ion-neutral complex [$C_2H_3^+$ ClH], which will be discussed later. Theoretical calculations have set the complex 4.5 kcalmol^{-1} below the product energies[11].

The NR mass spectra of both isomers **Ib** and **IIb** showed a small recovery signal (Figures 3.2 and 3.3). However the fragmentations of the two isomers were still distinguishable, indicating little or no interconvertion between the two $C_2H_4Cl^\bullet$ radicals. It is noteworthy that as the distance between the neutralization cell and reionization cell is increased (in 2ffr, Figures 3.2 b and 3.3 b), the recovery intensity is lower due to the decomposition of the neutral $C_2H_4Cl^\bullet$. However the intensity of $C_2H_3^+$, supposed to be produced from the reionized neutral, is not lower. This phenomenon reveals that the decomposition of the neutral may also produce $C_2H_3^\bullet$ + HCl, as in the case of C_2H_4F. The energy required for this dissociation is about the same as that of dissociation to C_2H_4 + $Cl^\bullet$, see Table 3.8.

Comparing the NR mass spectra of CH_3CHCl^+ (Figure 3.2) and $\overline{CH_2Cl^+CH_2}$ (Figure 3.3) the former showed the more intense recovery signal. The latter showed more intense peaks for Cl^+ and $HCl^{+\bullet}$. These results indicate that neutral $CH_3CHCl^\bullet$ is more stable than $CH_2Cl\ CH_2^\bullet$; $\Delta H_f^\circ(CH_3CHCl^\bullet) \sim 18$ kcalmol^{-1} whereas $\Delta H_f^\circ(CH_2ClCH_2^\bullet)$ is ca 22 kcalmol^{-1}.[27,28]

The  produced from neutralization of  (**IIb**) would be the transition state between $ClCH_2CH_2^\bullet$ and $^\bullet CH_2CH_2Cl$. This transition state has been

calculated to be 6 - 13 kcalmol^{-1} higher in energy than $ClCH_2CH_2^{\bullet}$.[31-33] It is therefore possible that  may isomerize to $ClCH_2CH_2^{\bullet}$ before reionization. The different peak ratio of CCl^+ to CH_2Cl^+ in the NR mass spectrum of **IIb** compared to that in the CID mass spectrum of **IIb** indicates that the reionized $C_2H_4Cl^+$ ions are not pure **IIb** ions.

3.4.3 $C_2H_4Br^+$ isomers

The identical MI and CID mass spectra of D-labelled **IIc** ions confirm the structure as cyclic-$\overline{CH_2Br^+CH_2}$. The CID mass spectra (Table 3.5), indicated that the two isomers, CH_3CHBr^+ (**Ic**) and cyclic-$\overline{CH_2Br^+CH_2}$ (**IIc**) are distinguishable. Isomer **Ic** fragmented to $CHBr^+ + CH_3$, whereas, isomer **IIc** fragmented to $CH_2Br^+ + CH_2$. The CID mass spectra of D-labelled **IIc** showed no fragment at m/z 92 ($CHDBr^+$), indicating no H-shift between the two carbons, as in the case of $C_2H_2D_2Cl^+$.

In the MI mass spectra both isomers showed the fragment $C_2H_3^+$, with the same extremely small KER value ($T_{0.5}$ = 0.1-0.2 meV). The D-labelling experiments again showed a strong isotope effect (MI, 14; CID, 1.06). Furthermore, the observation of H_2Br^+ in the CID mass spectra of the two isomers confirmed the proposal that the fragmentation may involve another isomer, either CH_2CHBrH^+ or an ion-neutral complex [$C_2H_3^+$ BrH] which also will be discussed later. The binding energy in this complex is probably less than that in the complex [$C_2H_3^+$ ClH] (4.5 kcalmol^{-1})[11].

The NR mass spectra of both isomers **Ic** and **IIc** (Figures 3.4 and 3.5) showed a small recovery signal. However, the fragmentation of the two isomers was still distinguishable in the region CBr^+, $CHBr^{+\bullet}$ and CH_2Br^+, indicating no interconvertion

between the two C_2H_4Br radicals. In Figure 3. 4, a large recovery signal was observed in the 3ffr NR mass spectrum of CH_3CHBr^+, indicating less dissociation of neutral $CH_3CHBr^•$. The very small recovery signal in Figure 3.5 indicates $CH_2BrCH_2^•$ is less stable than $CH_3CHBr^•$ under these experimental conditions.

3.4.4 $C_2H_4I^•$ isomers

In the MI mass spectra of $C_2H_4I^+$, no dissociation by HI loss was observed, indicating presumably that $C_2H_3IH^+$ ions are not formed. Unlike the other $C_2H_4X^+$ cations, the CID mass spectra of $C_2H_4I^+$ ions are not dominated by HI loss, but by C_2H_4 loss instead, see Table 3.5 and Figures 3.6 and 3.7, even though the energy for $C_2H_3^+ + HI$ is about 6 kcalmol^{-1} lower than that of $I^+ + C_2H_4$, see Table 3.6. Thus the HI loss process must have a higher activation energy than that for C_2H_4 loss. The CID mass spectra of CH_3CHI^+ (**Id**) and cyclic-$CH_2\ I^+CH_2$ (**IId**) are distinguishable via the diagnostic $CHI^{+•}$ and CH_2I^+ peaks, see Table 3.5. The complete absence of CH_2I^+ in the CID mass spectrum of CH_3CHI^+ shows that any H-shift is inaccessible by collision activation.

The NR mass spectra of the $C_2H_4I^+$ isomers were dominated by I^+ (~ 90%, Figures 3.6 and 3.7). No recovery signals were observed. If I^+ was produced by the reionization of $I^•$ which may result from the dissociation of neutral $C_2H_4I^•$, the $C_2H_4^+$ ion should be also observed, as the ionization energy of C_2H_4 (10.51 eV) is close to that of I (10.45 eV). Thus the I^+ is most likely produced from the dissociation of the reionized $C_2H_4I^+$, which may be formed in an excited state during neutralization-reionization process. This excited $C_2H_4I^+$ ion dissociates completely to $I^+ + C_2H_4$.

3.4.5 Some features of $C_2H_4X^+$ ions

3.4.5.1 $C_2H_3XH^+$ and $[C_2H_3^+ XH]$ species

The very small KER values in the MI dissociations of $C_2H_4X^+$ (X = Cl, Br) indicate the possible existence of an ion-neutral complex $[C_2H_3^+ \ XH]$[40].

$$C_2H_4X^+ \rightarrow C_2H_3XH^+ \rightarrow [C_2H_3^+ XH] \qquad (7)$$

The observed H_2X^+ in the CID mass spectra of $C_2H_4X^+$ (X = Cl, Br) supports this proposal. In such complexes, proton (or hydrogen) transfer is common[40]. Furthermore, the formation of $[C_2H_3^+ \ XH]$ involves an H-shift from carbon to halogen (reaction 7) and so there should be a strong isotope effect. This was indeed observed for the D-labelled $\overline{CD_2X^+CH_2}$ (X = Cl, Br) ions which showed very strong isotope effects of 1:16, for X = Cl, and 1:14, for X = Br in favour of HX loss.

The strong isotope effect was also observed in the HCl loss from $C_2H_5Cl^{+\bullet}$ ions.[41] According to ab initio calculations this dissociation involves an ion-neutral complex $[C_2H_4^{+\bullet} \ HCl]$.[42] Thus the HX losses in the dissociations of $C_2H_4X^+$ and $C_2H_5X^{+\bullet}$ ions show similar features.

In the case of $C_2H_4F^+$, the HF loss was the chief high energy dissociation, but lost its importance among low energy ions. Thus a stable isomer may be produced if the precursor ion contains enough energy to pass over the isomerization barrier. This isomer is proposed to be $C_2H_3FH^+$. The difficulty in the formation of $C_2H_3FH^+$ (compared to $C_2H_3ClH^+$ and $C_2H_3BrH^+$) could be explained by the lower proton affinity (PA) of fluorine,

compared to the PA of other small halogenated molecules, see Table 3.10.

However the PA of RI is the highest among RX (R = H, CH_2, CH_3, C_2H_3, C_2H_4, C_2H_5), and HI loss was not observed in the MI dissociation of $C_2H_4I^+$. In the CID mass spectra of $C_2H_4I^+$, the HI loss was overwhelmed by the C_2H_4 loss channel. The geometry of $C_2H_4I^+$ has not been calculated. The C-I bond in $C_2H_4I^+$ is expected to be longer than the C-X bond in $C_2H_4X^+$ (X = F, Cl, Br) and so the energy barrier for the H-shift in $C_2H_4I^+$ should be higher than that for the direct C-I bond cleavage.

3.4.5.2 H-shift in CH_3CHX^+

An H-shift in CH_3CHX^+ is required to account for the observation of CH_2X^+ in the CID mass spectra of CH_3CHX^+ ions.

$$\underset{\text{(I)}}{CH_2(H) - CHX^+} \rightarrow \underset{\text{(III)}}{{}^+CH_2 - CH_2X} \rightarrow CH_2X^+ + CH_2 \qquad (7)$$

According to some high level theoretical calculations, see Table 3.1, the average energy difference between I and III is ~ 31 kcalmol^{-1} for X = F[8,9] and ~ 21 kcalmol^{-1} for X = Cl[11] and Br[14]. However the energy barrier for CH_3CHCl^+ isomerizing to $ClCH_2CH_2^+$ is ~ 32 kcalmol^{-1} [11] which is higher than that for CH_3CHBr^+ (21.8 kcalmol^{-1} [14]). Thus the H-shift from the CH_3 group to the CHX group requires an energy ranging from 22 - 32 kcalmol^{-1}. Note that for the classical ethyl cation, the carbon to carbon H-shift requires no energy[43].

3.4.5.3 Relative stabilities of $C_2H_4X^+$

The heats of formation of CH_3CHX^+ increased in going from X = F to X = I, (see Table 3.2) and they can be related to the electronegativity (EN) of the halogens. Indeed, the ΔH_f° values for CH_3CHX^+, X = F, Cl, Br, showed a linear relationship with Vx, see line 1 in Figure 3.8. The Vx is a new scale of EN,[44] and has been shown quantitatively to relate to the bond dissociation energies (BDE) of many common organic compounds.[45] The linear relationship between ΔH_f (CH_3CHX^+) and Vx reveals that the BDE C-X in CH_3CHX^+ determines the stability of CH_3CHX^+. From the slope of line 1, the heat of formation of CH_3CHI^+ can be estimated to be ~ 219 kcalmol^{-1}.

The heats of formation of the cyclic ions $\overline{CH_2X^+CH_2}$ (X = Cl, Br, I) also showed a linear relationship with Vx, see line 2 in Figure 3.8. The slope of line 2 is smaller than that of line 1. This reveals that the stability of cyclic-$\overline{CH_2X^+CH_2}$ is not only affected by the EN of the halogens. Another factor affecting the stability of these latter ions is the polarizability of the halogen atoms, as shown in Figure 3.9, where the $\Delta\Delta_fH^0 = \Delta_fH^0$ (CH_3CHX^+) - Δ_fH^0 ($\overline{CH_2X^+CH_2}$). The higher polarizible atom (such as I) is showing that the cyclic species is more stable ($\Delta\Delta_fH^0 > 0$), because the halogen atom in $\overline{CH_2X^+CH_2}$ will be polarized by the charge on $C_2H_4^{+\cdot}$. Thus, in the case of $\overline{CH_2X^+CH_2}$ (X = Br, I), the polarizability of X stabilizes the cation by a back electron donation. In contrast, the polarizability of X (X = F, Cl) destabilizes the cation by decreasing the BDE of C-X.

3.5 References

1. I. Robert and G. E. Kimball, J. Am. Chem. Soc., 59, 947 (1937)
2. a: G. A. Olah and J. M. Bollinger, J. Am. Chem. Soc., 89, 4744 (1967);
   b: G. A. Olah and J. M. Bollinger, J. Am. Chem. Soc., 90, 947 (1967);
   c: G. A. Olah, J. M. Bollinger and J. Brinich, J. Am. Chem. Soc., 90, 2587 (1967)
3. M. J. S. Dewar and G. P. Ford, J. Am. Chem. Soc., 101, 783 (1979)
4. W. J. Hehre and P. C. Hiberty, J. Am. Chem. Soc., 96, 2665 (1974)
5. D. T. Clark and D. M. Lilley, Tetrahedron, 29, 845 (1973)
6. K. Raghavachari, R. C. Haddon and W. H. Starnes, Jr, J. Am. Chem. Soc., 104, 5054 (1982)
7. H. Lischka and H-J Köhler, J. Am. Chem. Soc., 100, 5297 (1978)
8. G. P. Ford and K. S. Raghuveer, Tetrahedron, 44, 7489 (1988)
9. C. H. Reynolds, J. Chem. Soc. Chem. Commun., 1990, 1533
10. A. C. Hopkinson, M. H. Lien and K. Yates, I. G. Csizmadia. Theoret. Chim. Acta, 44, 385 (1977)
11. C. F. Rodriquez, D. K. Böhme and A. C. Hopkinson, J. Am. Chem. Soc., 115, 3263 (1993)
12. R. A. Poirier, G. R. Demaré, K. Yates and I. G. Csizmadia, J. Mol. Struct., 94, 137 (1983)
13. B. Galland, E. M. Evleth and M. Ruasse, J. Chem. Soc. Chem. Comm., 898 (1990)
14. T. P. Hamilton and H. F. Schaefer, III, J. Am. Chem. Soc., 112, 8260 (1990)

15. A. D. Williamson, P. R. LeBreton and J. L. Beauchamp, J. Am. Chem. Soc., 98, 2705 (1976)

16. D. P. Ridge, J. Am. Chem. Soc., 97, 5670 (1975)

17. a: D. A. Stams, T. D. Thomas, D. C. MacLaren, D. Ji and T. H. Morton, J. Am. Chem. Soc., 112, 1427 (1992);

b: T. A. Shaler and T. H. Morton, J. Am. Chem. Soc., 113, 6771 (1991)

18. J. L. Holmes, F. P. Lossing and R. A. McFarlane, Int. J. Mass Spectrom. Ion Proc., 86, 209 (1988)

19. J. Monstrey and C. C. Van de Sande, J. Chem. Soc. Chem. Commun., 1978, 796

20. B. Ciommer and H. Schwarz, Z. Naturforsch., 38b, 635 (1983)

21. D. W. Berman, V. Anicich and J. L. Beauchamp, J. Am. Chem. Soc., 101, 1239 (1979)

22. A. J. R. Heck, L. J. de Koning and N. M. M. Nibbering, Org. Mass Spectrom., 28, 245 (1993)

23. A. J. R. Heck, L. J. de Koning and N. M. M. Nibbering, Org. Mass Spectrom., 28, 235 (1993)

24. V. Nguyen, X. Cheng and T. H. Morton, J. Am. Chem. Soc., 114, 7127 (1992)

25. E. Tschuikow-Roux, D. R. Salomon and S. Paddish, J. Phys. Chem., 91, 699 (1987)

26. Y. Chen, A. Rauk and E. Tschuikow-Roux, J. Chem. Phys., 93, 1187 (1990)

27. J. L. Holmes and F. P. Lossing, J. Am. Chem. Soc., 110, 7343 (1988)

28. E. Tschuikow-Roux, D. R. Salomon and S. Paddison, J. Phys. Chem., 91, 3037 (1987)

29. K. Miyokawa and E. Tschuikow-Roux, J. Phys. Chem., 94, 715 (1990)

30. B. Engels and S. D. Peyerimhoff, J. Mol. Structure, 138, 59 (1986)

31. B. Engels and S. D. Peyerimhoff, J. Phys. Chem., 93, 4462 (1989)

32. B. Engels, S. D. Peyerimhoff and P. S. Skell, J. Phys. Chem., 94, 1267 (1990)

33. M. Guerra, J. Am. Chem. Soc., 114, 2077 (1992)

34. T. Hoz, M. Sprecher and H. Basch, J. Phys. Chem., 89, 1664 (1985)

35. G. N. Robinson, R. E. Continetti and Y. T. Lee, J. Chem. Phys., 92, 275 (1990)

36. H. B. Schlegel and C. Sosa, J. Phys. Chem., 88, 1141 (1984)

37. R. B. Barat and J. W. Bozzelli, J. Phys. Chem., 96, 2494 (1992)

38. S. G. Lias, J. E. Bartmess, J. F. Liebman, J. L. Holmes, R. D. Levin and W. G. Mallard, J. Phys. Chem. Ref. Data, 17, Suppl. 1 (1988)

39. H. W. Zappey, T. Drewello, S. Ingemann and N. M. M. Nibbering, Int. J. Mass Spectrom. Ion Proc., 115, 193 (1992)

40. D. J. McAdoo, Mass Spectrom. Rev., 7, 363 (1988)

41. a: J. L. Holmes, P. C. Burgers, J. K. Terlouw, H. Schwarz, B. Ciommer and H. Halim, Org. Mass Spectrom., 18, 208 (1983)

b: M. C. Blanchette, J. L. Holmes and F. P. Lossing, Org. Mass Spectrom., 22, 701 (1987)

42. a: J. C. Morrow and T. Baer, J. Phys. Chem., 92, 6567 (1988)

b: J. A. Booze, K-M. Weitzel and T. Baer, J. Phys. Chem., 94 3649 (1991)

43. a: M-W. Wong, J. Baker, R. H. Nobes and L. Radom, J. Am. Chem. Soc., 109, 2245 (1987)

b: B. Ruscic, J. Berkowitz. L. A. Curtiss and J. A. Pople, J. Chem. Phys., 91, 114 (1989)

c: G. Trinquier, J. Am. Chem. Soc., 114, 6807 (1992)

44. Y. R. Luo and S. W. Benson, Acc. Chem. Res., 25, 375 (1992)

45. Y. R. Luo and J. L. Holmes, J. Phy. Chem., 98, 303 (1994)

46. Y. R. Luo and S. W. Benson, J. Phys. Chem., 92, 5255 (1988)

47. R. C. Weast, CRC Handbook of Chemistry & Physics, CRC press, Inc., Florida, 1987

Table 3.1 The theoretically calculated relative energies (kcalmol^{-1}) of the $C_2H_4X^+$ cations

	CH_3CHX^+ (I)	$CH_2X^+CH_2$ (II)	$XCH_2CH_2^+$ (III)	TS[1]	CH_2CHXH^+	Methods	Ref.
X = F							
	0	41.3	22.6			MNDO	3
	0		18			6-31G**	4
	0	35.8	39.4			SCF	5
		0	3.8			MP3/6-31G**	6
	0	33.5	23.3			SCF	7
	0	24.7	31.2	27.9[2], 42.6[3]		MP2/6-31G**	8
	0	24.7	31.3			MP2/6-31G**	9
X = Cl							
	0		14	12[2]		4-31G	4
	0	4.3	9.9			MNDO	3
	0	3.8	20.3			SCF	7
		0	25.8			MP3/6-31G**	6
	0	13.4	29.2			SCF	5
		0	9.4			4-31G	10
	0	4.0	31.2			MP2/6-31G**	9
	0	4.3		32.1[2]		MP4/6-31G(2df,p)	11
	0	7.5		22.5[2]		HF/6-31G(d,p) 11	
	0	3.3		33.3[2]	20.0, 44.5[4]	MP2/6-311G(d,p)	11
	0		21.0			SCF/6-31G(d,p)	11
X = Br							
	0.3	0	15			STO-3G	12
		0	12			MNDO	13
	1.5	0	21.9	21.8[2]		DZ+d,SCF	14

1. Transition state of either H-bridged for $CH_3CHX^+ \rightarrow XCH_2CH_2^+$ or X-bridged for $XCH_2CH_2^+ \rightarrow {}^+CH_2CH_2X$.
2. Transition state of H-bridged for $CH_3CHX^+ \rightarrow XCH_2CH_2^+$.
3. Transition state of X-bridged for $XCH_2CH_2^+ \rightarrow {}^+CH_2CH_2X$.
4. An ion-neutral complex [$C_2H_3^+$ ClH].

Table 3.2 Experimental heats of formation of $C_2H_4X^+$ (kcalmol^{-1})

	CH_3CHX^+	$\overset{\frown}{CH_2X^+CH_2}$	Methods	Ref.
X = F	165.9	-	PIMS-AE[1]	15
	164.5	-	ICR-PA[2]	16
	164.9	181.6	Estimation[3]	17a,b
X = Cl	198	200	EREEM-AE[4]	18
	198.8	204.4	PIMS-AE[1]	21
X = Br	208	206.5	EREEM-AE[4]	18
	207.9	206.5	PIMS-AE[1]	21
X = I	-	212.5	EREEM-AE[4]	18

1. PIMS-AE: Photoionization mass spectrometry-Appearance energy measurements
2. ICR-PA: Ion cyclotron resonance mass spectrometry-Proton affinity measurements
3. Estimation by the method of equivalent cores
4. EREEM-AE: Energy resolved electrostatic electron monochromator-Appearence energy measurements

Table 3.3 Heats of formation of C_2H_4X radicals ($kcalmol^{-1}$)

	CH_3CHX	CH_2XCH_2	Methods	Ref.
X = F	-17.7	-	Kinetic	25
	-17.2	-	HF/6-31G*	26
X = Cl	19.3	22.8	EREEM-AE[1]	27
	17.6	21.8	Kinetic	28
X = Br	27.3	32.3	EREEM-AE[1]	27
	29.6	-	Kinetic	29

1. EREEM-AE: Energy resolved electrostatic electron monochromator-Appearence endrgy measurements

Table 3.4 Kinetic energy release values ($T_{0.5}$, meV) of $C_2H_4X^+$ cations

X =	F	Cl	Br
I $\rightarrow C_2H_3^+ + HX$	445	1.4	0.1
II $\rightarrow C_2H_3^+ + HX$	461	1.4	0.2

Structure I = CH_3CHX^+, II = $\overline{CH_2X^+CH_2}$

Table 3.5 CID mass spectra of $C_2H_4X^+$ *

	CH_3CHF^+ (Ia)	$[CH_2F^+CH_2]$ (IIa)	CH_3CHCl^+ (Ib)	$[CH_2Cl^+CH_2]$ (IIb)	CH_3CHBr^+ (Ic)	$[CH_2Br^+CH_2]$ (IIc)	CH_3CHI^+ (Id)	$[CH_2I^+CH_2]$ (IId)
$CH_2^{+\bullet}$	5.5	2.9	0.5	1.1	-	-	-	-
CH_3^+	7.6	3.9	1.1	-	-	-	-	-
C_2H^+	14	8.8	7.8	5.9	4.3	3.5	-	-
$C_2H_2^{+\bullet}$	51	33	35	25	20	11	1.8	1.6
$C_2H_3^+$	100 (48)	100 (43)	100 (78)	100 (52)	100 (72)	100 (31)	27	19
$C_2H_4^{+\bullet}$	-	-	20	12	20	7.7	3.6	3.2
$C_2H_4X^{2+}$	-	-	1.1	1.1	8.0	3.0	2.5	1.3
X^+	-	-	7.6	9.6	10	6.0	100	100
$HX^{+\bullet}$	-	-	4.4	5.0	4.9	3.0	-	-
H_2X^+	-	-	1.1	0.8	1.7	1.2	-	-
CX^+	31	22	14	9.0	6.2	3.4	11	9.3
$CHX^{+\bullet}$	17	15	18	8.4	8.0	3.0	20	10
CH_2X^+	4.2	5.4	2.2	18	0.9	4.3	4.2	19
C_2X^+	0.7	0.6	1.6	0.3	-	-	-	-
$C_2HX^{+\bullet}$	14	10	7.6	2.0	1.2	0.8	0.9	1.0
$C_2H_2X^+$	33	25	21	3.1	4.6	1.0	2.2	2.2
$C_2H_3X^{+\bullet}$	21	24	27	8.4	10	3.7	9.0	7.7

* He, 90% transmission; Values in parenthesis have been corrected for contributions from the MI mass spectrum.

Table 3.6 The energies[1] of the dissociation products of $C_2H_4X^+$

	$C_2H_4F^+$	$C_2H_4Cl^+$	$C_2H_4Br^+$	$C_2H_4I^+$
$C_2H_3^+$+HX	201	244	257	272
$C_2H_4^{+\bullet}$+$X^\bullet$	274[2]	284	282	281[2]
X^++C_2H_4	433[2]	340	311	278
$HX^{+\bullet}$+$C_2H_3^\bullet$	368[2]	335	323	309[2]
H_2X^++C_2H_2	238[2]	261	272	279[2]
CX^++CH_4	253	279	344	-
$CHX^{+\bullet}$+$CH_3^\bullet$	303	333	320	-
CH_2X^++CH_2	292	322	317	-
$C_2HX^{+\bullet}$+H_2+$H^\bullet$	337	357	349	-
$C_2H_2X^+$+H_2	227	-	-	-
$C_2H_3X^{+\bullet}$+$H^\bullet$	258	288	297	298

1. All values from reference 38 in kcalmol^{-1}. Some heats of formation of the cations are not available.
2. The fragment is not observed in CID mass spectrum of $C_2H_4X^+$.

Table 3.7 CID mass spectra of CH_3CHF^+ at different energies[1]

	Second field-free region		Third field-free region	
	8 kV[2]	5 kV[2]	8 kV	5 kV[3]
CH_3^+	3.5	0.5	0.8	-
$C_2H_2^{+\bullet}$	36	10	12	8.3
$C_2H_3^+$	100	48	43	9.3
CF^+	21	9.7	12	5.3
$CHF^{+\bullet}$	20	14	15	8.0
CH_2F^+	8.3	6.7	8.8	3.0
C_2F^+	0.4	0.7	0.7	0.7
$C_2HF^{+\bullet}$	9.7	19	18	11
$C_2H_2F^+$	25	64	62	49
$C_2H_3F^{+\bullet}$	32	100	100	100

1. The $C_2H_4F^+$ is produced from $BrCH_2CH_2F^{+\bullet}$ and the collision gas is O_2 with 90% transmission of the ion current.
2. The translational energy.
3. The CID mass spectrum of $C_2H_4F^+$, generated from MI of $BrCH_2CH_2F^{+\bullet}$.

Table 3.8 The energies of the dissociation products of C_2H_4X[1]

	C_2H_4F	C_2H_4Cl	C_2H_4Br	C_2H_4I
CH_2+CH_2X	85	124	135	-
CH_3+CHX	61	106	-	-
C_2H_3+HX	-2	41	54	69
C_2H_4+X	32	42	40	39
C_2H_3X+H	19	57	71	83

1. All values from reference 38 in kcalmol^{-1}. Some heats of formation of the neutrals are not available.

Table 3.9 Partial CID mass spectra of $C_2H_2D_2X^+$ (X = Cl, Br)

	Relative Abundances			
Fragment ion	$ClCH_2CD_2^+$	$ClCD_2CH_2^+$	$BrCH_2CD_2^+$	$BrCD_2CH_2^+$
CX^+	23	23	33	32
$CHX^{+\bullet}$	14	14	-	-
CH_2X^+,$CDX^{+\bullet}$	33	33	42	45
CD_2X^+	30	30	25	23

Table 3.10 The Proton Affinity (PA) values of some small molecules and radicals, kcalmol^{-1}

X =	F	Cl	Br	I
CH_2X	141	151	171	-
CH_3X	145	163	166	171
C_2H_3X	168	172	179	185
C_2H_5X	165	169	171	176

1. The values are taken from Reference 38.

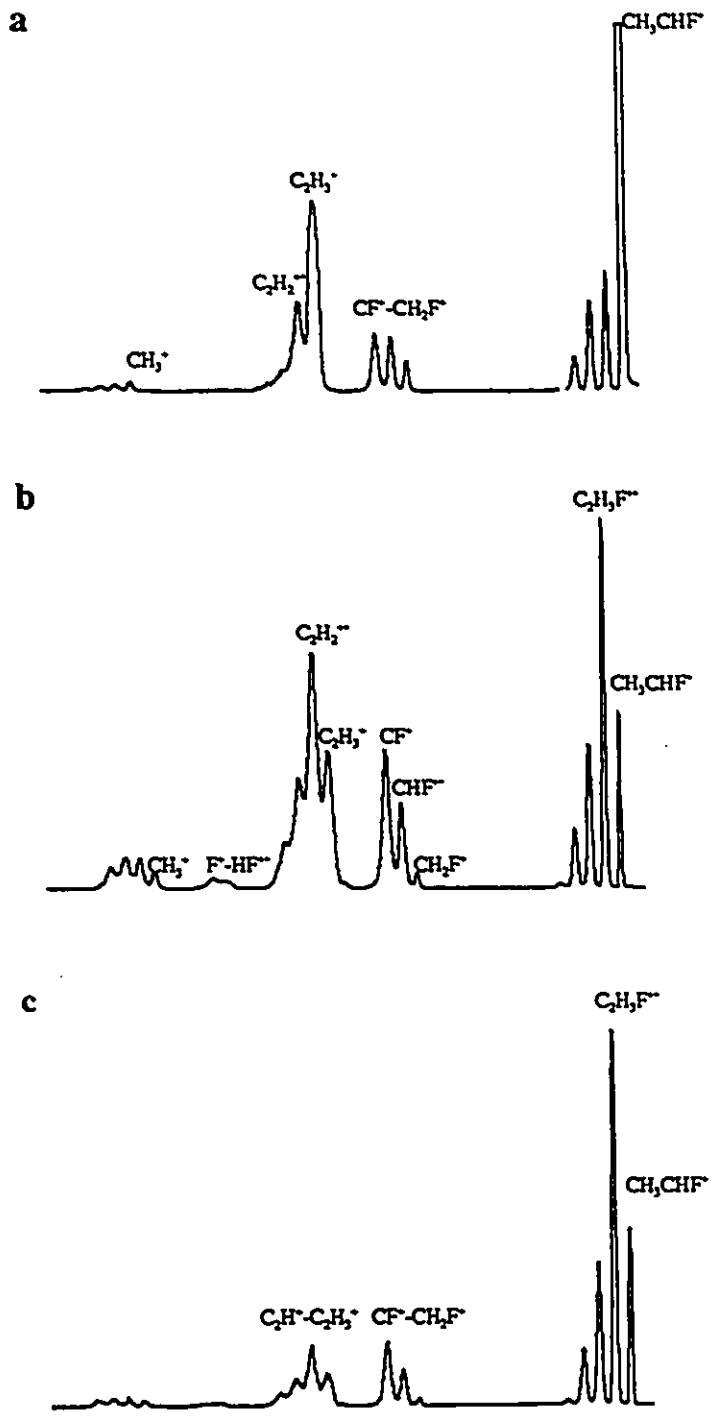

Figure 3.1 **The CID and NR mass spectra of CH_3CHF^+**

a. The CID mass spectrum of CH_3CHF^+, O_2

b. The NR mass spectrum of CH_3CHF^+ in 2ffr, DMA/O_2

c. The NR mass spectrum of CH_3CHF^+ in 3ffr, DMA/O_2

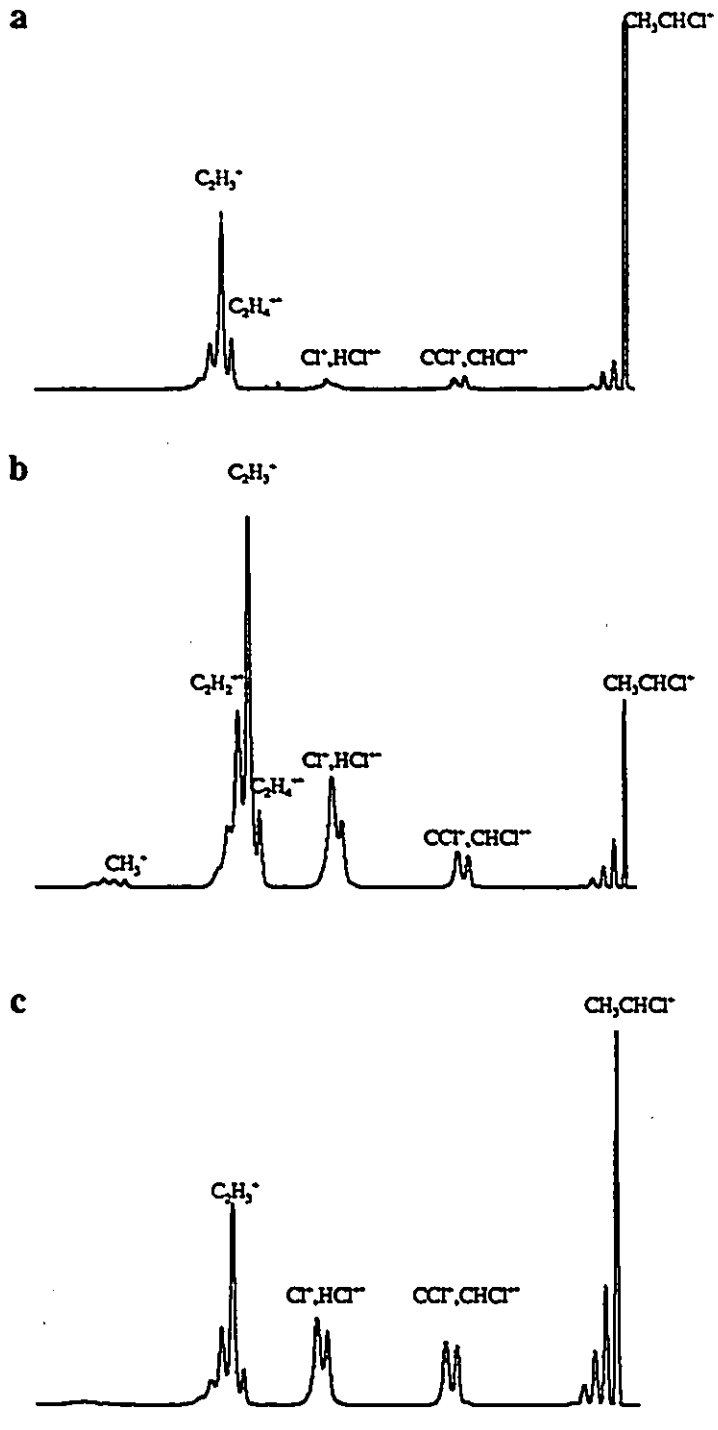

Figure 3.2 **The CID and NR mass spectra of CH_3CHCl^+**

a. The CID mass spectrum of CH_3CHCl^+, O_2

b. The NR mass spectrum of CH_3CHCl^+ in 2ffr, DMA/O_2

c. The NR mass spectrum of CH_3CHCl^+ in 3ffr, DMA/O_2

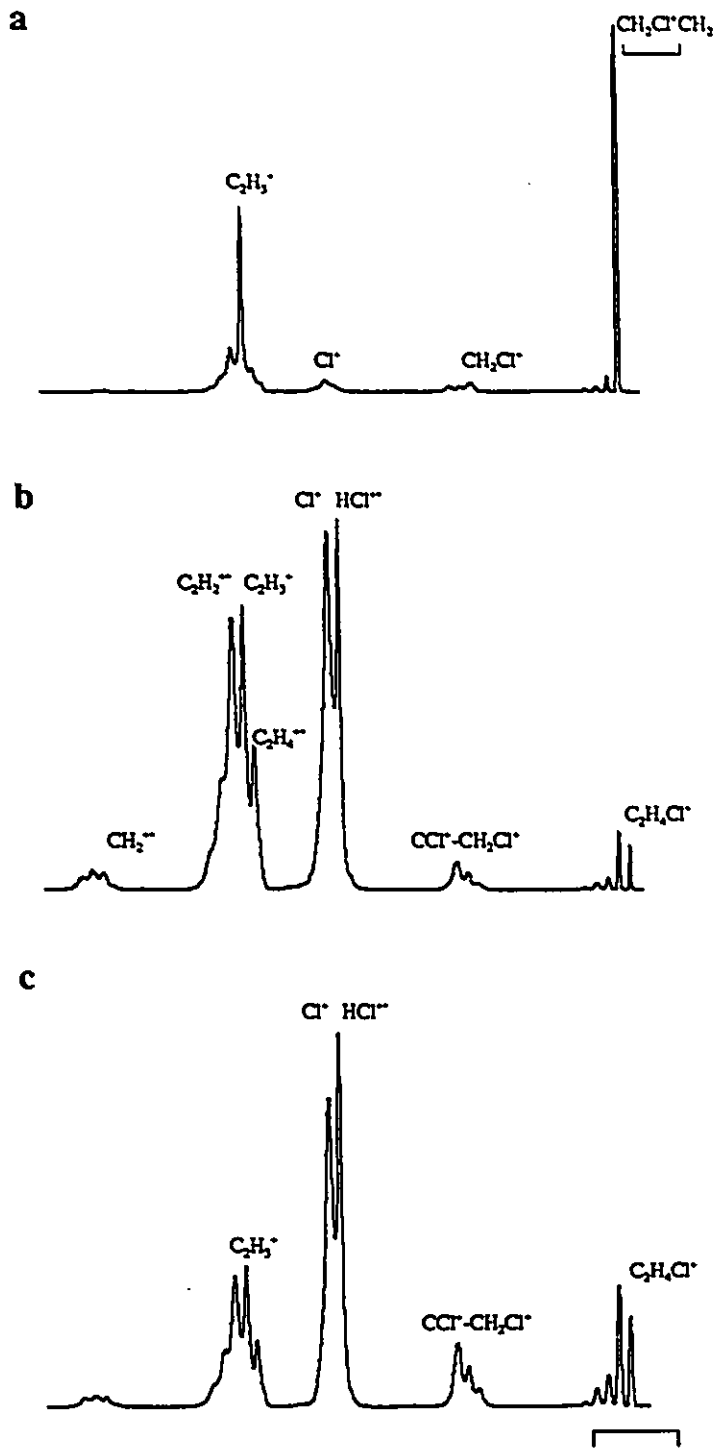

Figure 3.3 **The CID and NR mass spectra of $CH_2Cl^{\bullet}CH_2$ (IIb)**

a. The CID mass spectrum of **IIb**, O_2

b. The NR mass spectrum of **IIb** in 2ffr, DMA/O_2

c. The NR mass spectrum of **IIb** in 3ffr, DMA/O_2

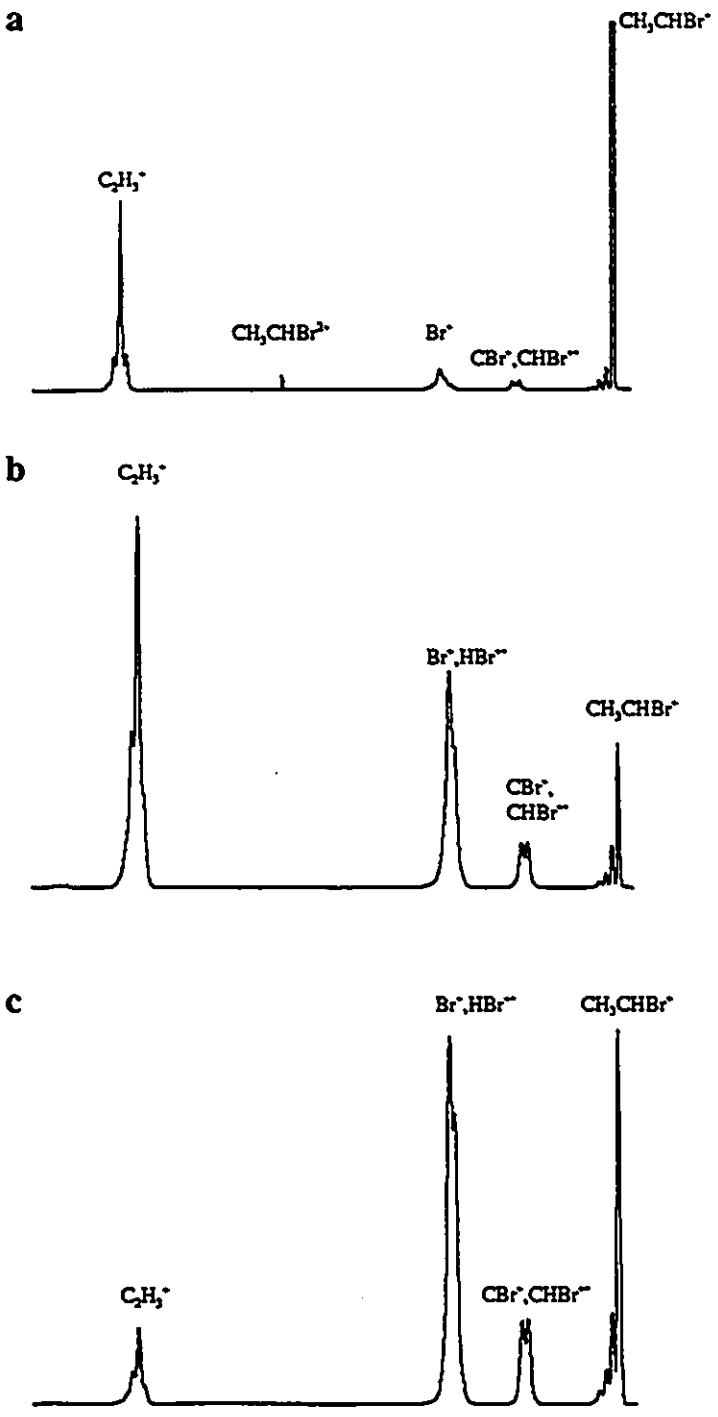

Figure 3.4 **The CID and NR mass spectra of CH_3CHBr^+**

a. The CID mass spectrum of CH_3CHBr^+, O_2

b. The NR mass spectrum of CH_3CHBr^+ in 2ffr, DMA/O_2

c. The NR mass spectrum of CH_3CHBr^+ in 3ffr, DMA/O_2

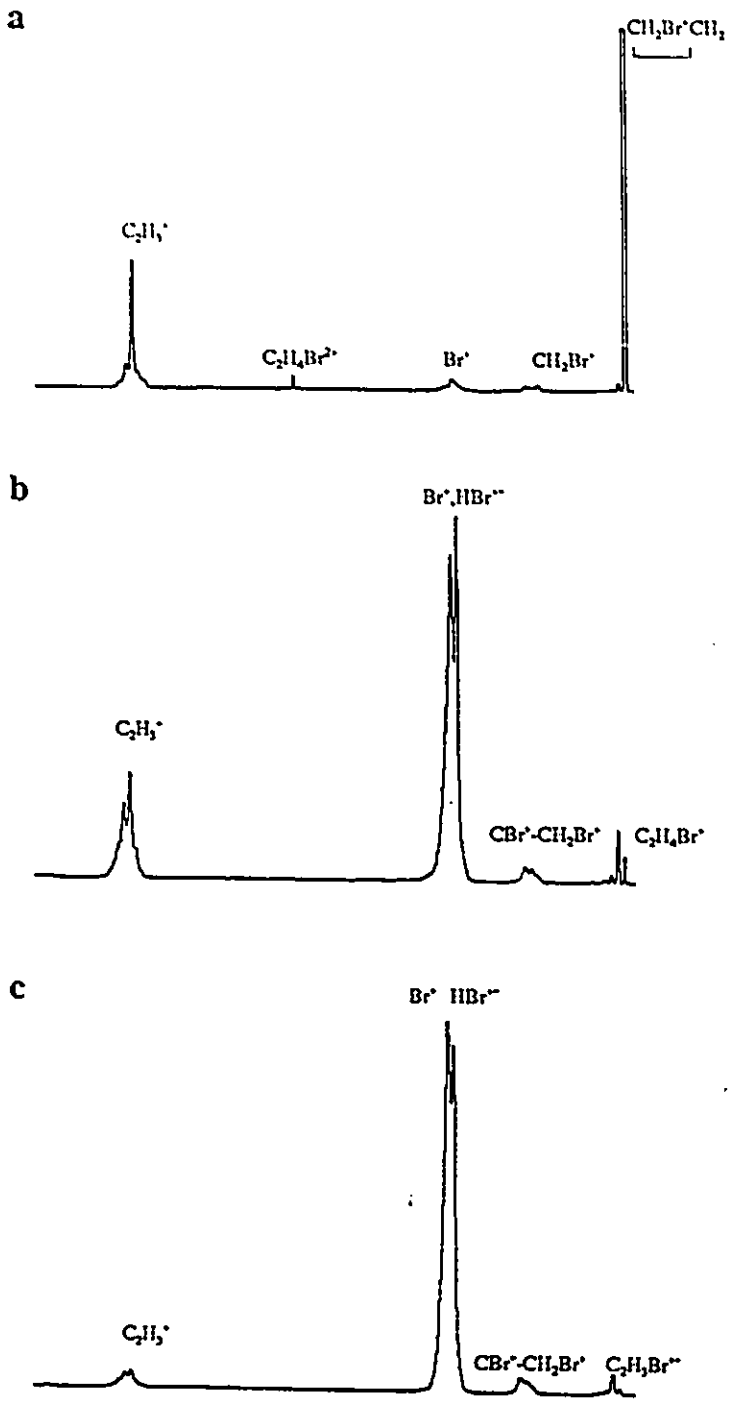

Figure 3.5 **The CID and NR mass spectra of $\overline{CH_2Br^+CH_2}$ (IIc)**

a. The CID mass spectrum of **IIc**, O_2

b. The NR mass spectrum of **IIc** in 2ffr, DMA/O_2

c. The NR mass spectrum of **IIc** in 3ffr, DMA/O_2

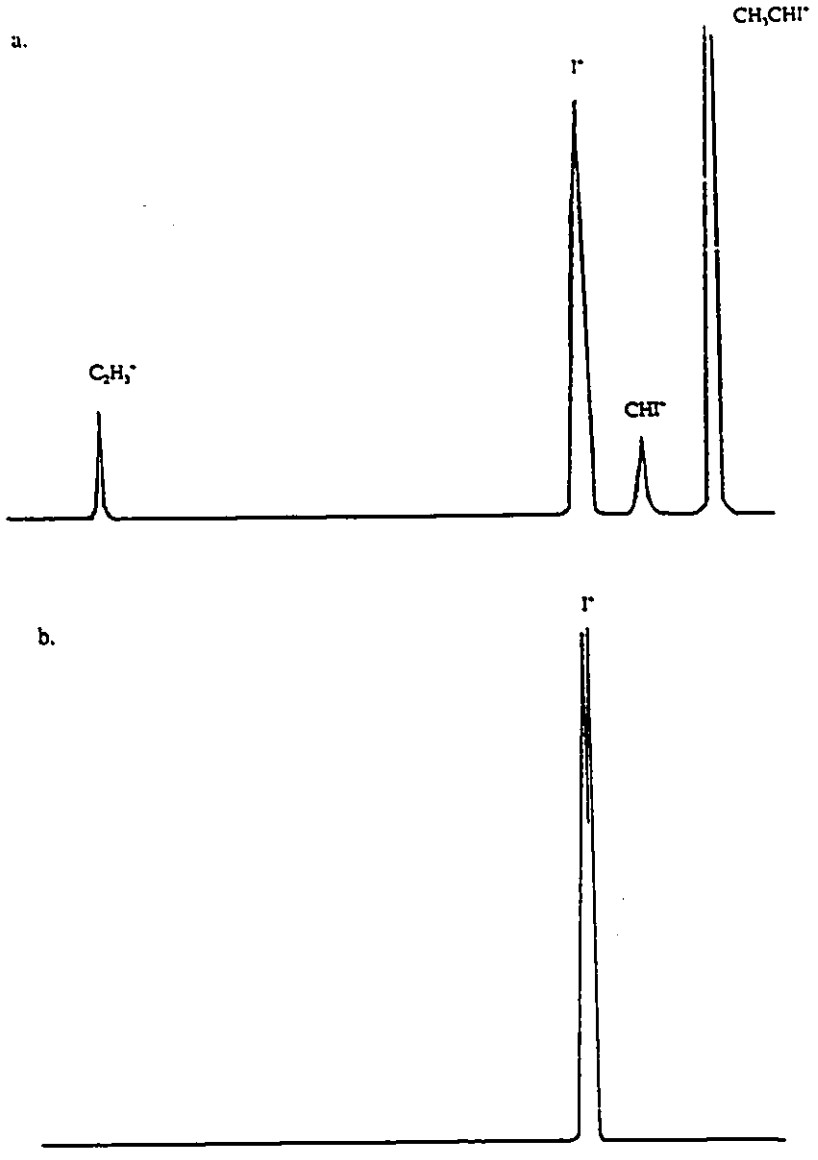

Figure 3.6 The CID and NR mass spectra of CH_3CHI^+ (Id)
a. The CID mass spectrum of Id, He
b. The NR mass spectrum of Id, Xe/O_2

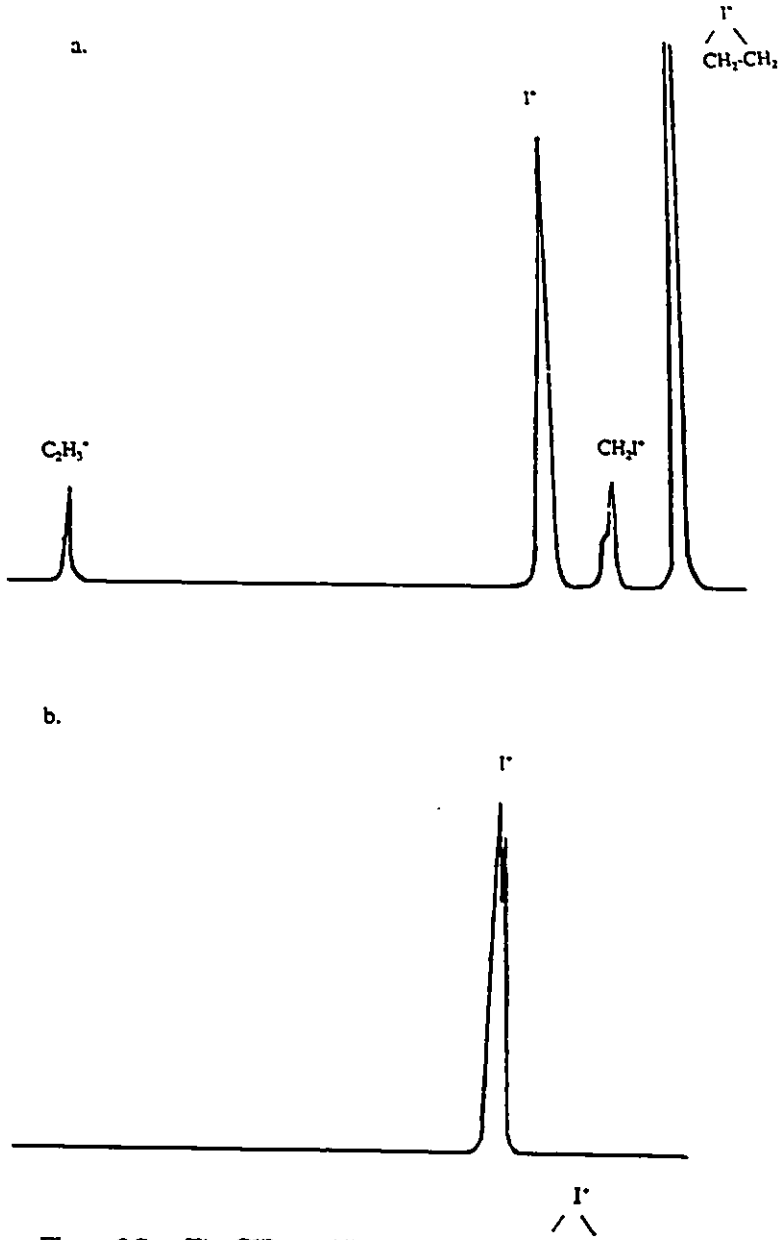

Figure 3.7 The CID and NR mass spectra of CH_2-CH_2 (IId)
a. The CID mass spectrum of IId, He
b. The NR mass spectrum of IId, Xe/O_2

Figure 3.8 $\Delta_f H^0$ of C_2H_5X vs Vx

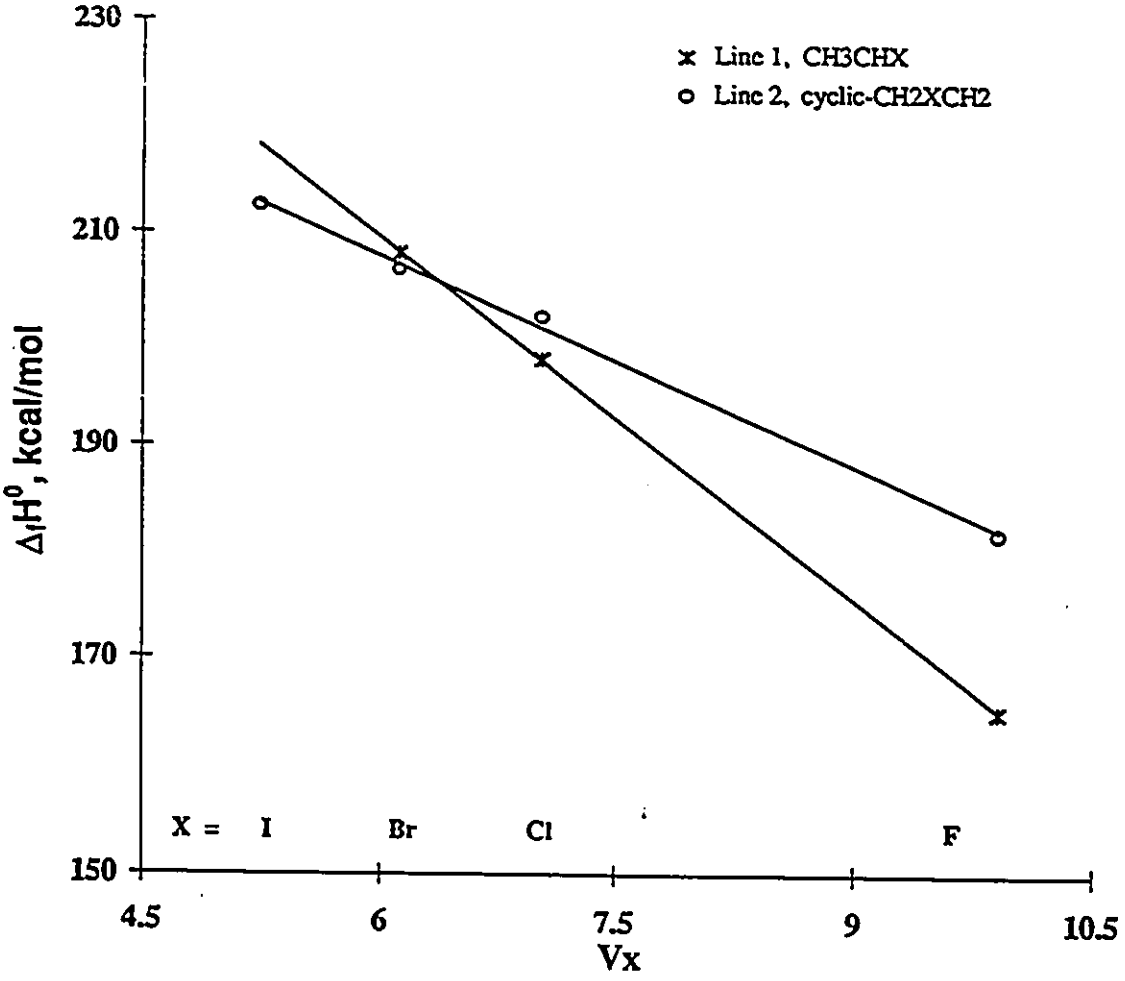

Figure 3.9 $\Delta\Delta H_f$ vs. log α

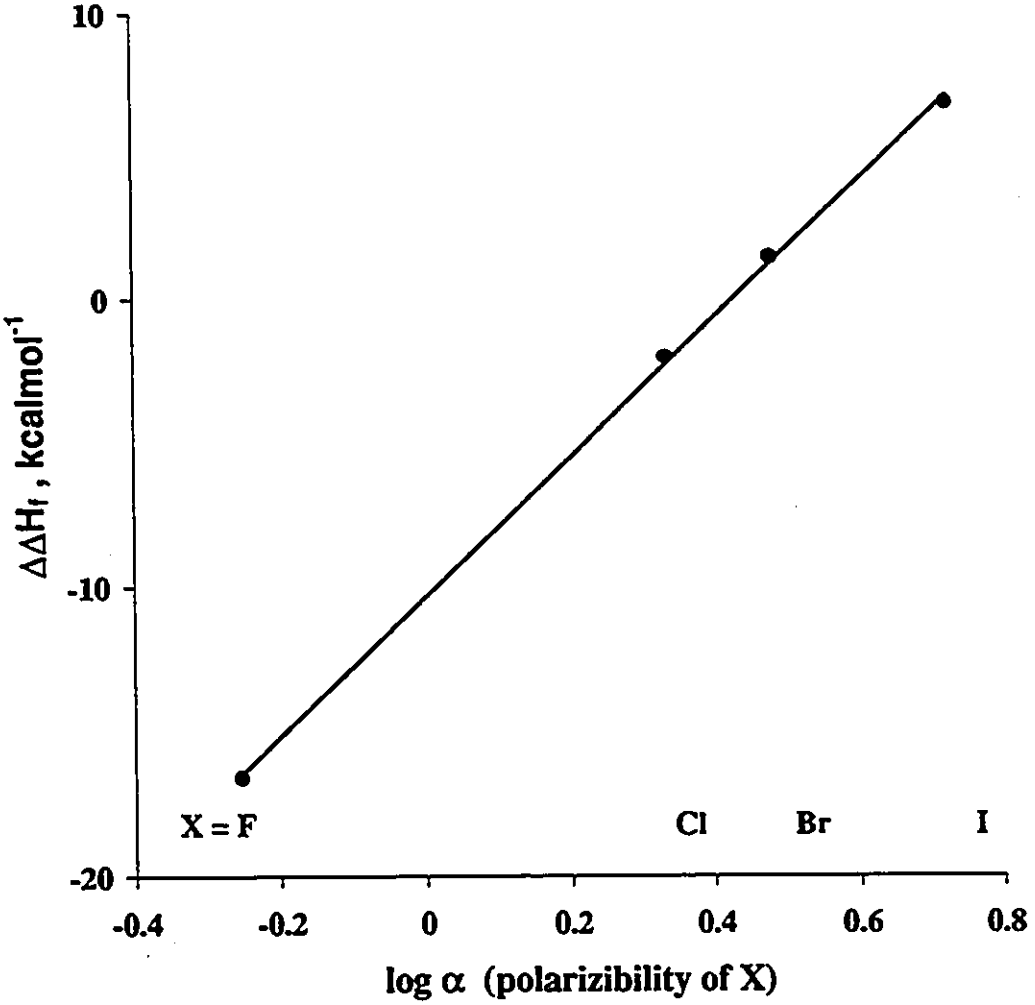

Chapter 4

Halogen substituted triethyloxonium ions

4.1 Introduction

The triethyloxonium ion is a well known ethylating agent in the liquid phase. It is easily attacked by a nucleophile, which can be either an anion or a neutral, as shown in the following Reactions.[1]

$$(C_2H_5)_3O^+ + Y^- \rightarrow C_2H_5Y + (C_2H_5)_2O \quad (1)$$

$$(C_2H_5)_3O^+ + :Y \rightarrow C_2H_5Y^+ + (C_2H_5)_2O \quad (2)$$

With both field desorption (FD) and fast atom bombardment (FAB) mass spectrometries $(C_2H_5)_3O^+$, (Et_3O^+) was observed as an intact cation from the salt $(C_2H_5)_3O^+Sb_5Cl_6^-$.[2] Whereas in a FD mass spectrometer the dissociation products of $(C_2H_5)_3O^+SbCl_6^-$ are $(C_2H_5)_3O^+$ (100%), $(C_2H_5)_2O^{+\bullet}$ (33%) and $C_2H_5Cl^{+\bullet}$ (23%), in a FAB mass spectrometer the products are $(C_2H_5)_3O^+$ (100%), $(C_2H_5)_2OH^+$ (C_2H_4 loss, 52%), $C_4H_9O^+$ (C_2H_6 loss, 55%), $C_2H_5OH_2^+$ (68%), $C_2H_5O^+$ (85%) and $C_2H_5^+$ (95%). The authors[2] indicated that the $C_4H_9O^+$ was produced by C_2H_6 loss from the cation. However recent studies on the triethyloxonium ion in a ZAB-3F mass spectrometer[3] showed that in the metastable timeframe only C_2H_4 loss was observed. The $(C_2H_5)_3O^+$ was derived from the ion-molecule reactions 3 and 4 in the ion source of the ZAB-3F mass spectrometer.

$$(C_2H_5)_2O^{+\bullet} + C_2H_5I \rightarrow (C_2H_5)_3O^+ + I^\bullet \quad (3)$$

$$C_2H_5I^{+\bullet} + (C_2H_5)_2O \rightarrow (C_2H_5)_3O^+ + I^\bullet \quad (4)$$

Although the C_2H_6 loss (reaction 6) has a lower endothermicity than C_2H_4 loss (reaction 5), it was not observed in the MI mass spectrum of $(C_2H_5)_3O^+$ and was only a very weak peak in its CID mass spectrum.

$(C_2H_5)_3O^+$	$\rightarrow$	$(C_2H_5)_2OH^+$	+	C_2H_4	(5)
ΔH_f°		105		13	kcalmol^{-1}
$(C_2H_5)_3O^+$	$\rightarrow$	$C_4H_9O^+$	+	C_2H_6	(6)
ΔH_f°		125		-20	kcalmol^{-1}

Based on the MI and CID mass spectra of various deuterium labelled precursors the authors[3] proposed that the loss involves a simple β-H^+ transfer from ethyl to oxygen followed by the C_2H_4 loss from a protonated diethylether-ethene ion-molecule complex. Therefore the $(C_2H_5)_3O^+$ ion produced from Reactions 3 and 4 has structure **a** in which the C_2H_5 groups have classical configuration.

$(C_2H_5)_2O^+CH_2CH_3$ **a**

$(C_2H_5)_2O\cdots H^+\cdots \begin{matrix} CH_2 \\ \| \\ CH_2 \end{matrix}$ **b**

It was also proposed that the $(C_2H_5)_3O^+$ ion formed from reaction of protonated diethyl ether and C_2H_5I (reaction 7) has structure **b** in which one C_2H_5 group has a proton-bridged non-classical configuration. The observation of H/D mixing, which is the evidence for a non-classical structure ethyl group[4], supports the proposal of structure **b**.

$$(C_2H_5)_2OH^+ + C_2H_5I \rightarrow (C_2H_5)_2O^+(C_2H_5) + HI \qquad (7)$$

Whereas the C_2H_6 loss from $(C_2H_5)_3O^+$ is only a very minor reaction,[3] it was a major MI reaction of the diethylhalonium ions, $(C_2H_5)_2X^+$ (X = Cl and Br), as shown in the following.[5]

		Intensities (%)		
	X =	Cl	Br	
$(C_2H_5)_2X^+ \rightarrow CH_3CHX^+ + C_2H_6$		74	39	(8)
$(C_2H_5)_2X^+ \rightarrow CH_3CH_2X^{+\cdot} + C_2H_4$		0.7	58	(9)

As shown above $(C_2H_5)_2Cl^+$ and $(C_2H_5)_2Br^+$ exhibited different behaviours in the C_2H_4 loss (reaction 9). The C_2H_4 loss was a minor peak in the MI mass spectrum of $(C_2H_5)_2Cl^+$, whereas it was a major peak in the MI mass spectrum of $(C_2H_5)_2Br^+$.

The diverse reactivity of the ethyl group in triethyloxonium ions and diethylhalonium ions challenged us to investigate onium ions which contain both an oxygen atom and a halogen atom, e.g. $(C_2H_5)_2O^+C_2H_4X$ and $C_2H_5OC_2H_4X^+C_2H_5$ ions.

4.2 Experimental

Electron impact (ionizing electron energy - 70 eV), metastable ion (MI), collision induced dissociation (CID) and collision induced dissociative ionization (CIDI) mass spectra were recorded[6a] using a modified VG Analytical ZAB-2F mass spectrometer with BEE geometry. Oxygen and helium were used for the collisional activation of ions. Oxygen was also used for the ionization of neutrals originating from metastable and collisionally activated ions. In all cases the target gases pressure reduced the main beam by 15%. In the MS/MS/MS experiments, ions formed in the second field-free region (2-FFR) by the metastable or collision induced dissociation of mass selected precursor ions, were transmitted into the 3-FFR and then collisionally activated. Recording the MI, CID and

CIDI mass spectra was carried out using the ZABCAT program.[60b] Kinetic energy release (KER) measurements have been performed on the same mass spectrometer at sufficient energy resolution to reduce the main ion beam width at half height to 3-5 V. The reproducibility of $T_{0.5}$ values was better than 10%.

To produce the onium ions, precursor molecules were introduced into the ion source in about a 1:1 mixture. The total ion source pressure was set at 1-3 x 10^{-5} mbar.

4.3 Results and discussion

4.3.1 Observation of the halogen substituted triethyloxonium ions

The halogen substituted triethyloxonium ion $(C_2H_5)_2O^+C_2H_4X$ was observed in the normal mass spectra of mixtures of C_2H_4XY + $(C_2H_5)_2O$ (X, Y = Cl, Br) at m/z 137 (for X = Cl) and m/z 181 (for X = Br), as shown in Figure 4.1. No molecular adduct $(C_2H_5)_2O{\bullet}C_2H_4XY^{+\bullet}$ was detected. The oxonium ions formed from different C_2H_4XY precursors have different dissociation characteristics as shown in Table 4.1. Thus the ion formed from XCH_2CH_2Y + $(C_2H_5)_2O$ is of type **I** and the ion formed from $XYCHCH_3$ + $(C_2H_5)_2O$ is of type **II**. The subscripts **a** and **b** refer to X = Cl and X = Br, respectively.

$(C_2H_5)_2O^+CH_2CH_2X$		$(C_2H_5)_2O^+CHXCH_3$	
Ia	(X = Cl)	**IIa**	(X = Cl)
Ib	(X = Br)	**IIb**	(X = Br)

4.3.2 Formation of ions I and II

Ions **I** and **II** may be produced from the following reactions in the ion source:

$$C_2H_4XY^{+\bullet}\ (X{=}Cl, Y) + (C_2H_5)_2O \rightarrow [(C_2H_5)_2OC_2H_4XY]^{+\bullet} \rightarrow (C_2H_5)_2OC_2H_4X^+ + Y^{\bullet} \quad (10)$$

$$C_2H_4XY + (C_2H_5)_2O^{+\bullet} \rightarrow [(C_2H_5)_2OC_2H_4XY]^{+\bullet} \rightarrow (C_2H_5)_2OC_2H_4X^+ + Y^{\bullet} \quad (11)$$

$$C_2H_4XY^{+\bullet} + (C_2H_5)_2O \rightarrow C_2H_4X^+ + Y^\bullet + (C_2H_5)_2O \rightarrow (C_2H_5)_2OC_2H_4X^+ + Y^\bullet \quad (12)$$

Although no molecular adduct was observed in the normal mass spectra, reactions 10 and 11 cannot be excluded if the lifetime of the adduct is $< 10^{-6}$ s. However, reaction 11 is unlikely to produce the oxonium ions **I** and **II**, since if the charge were located on the oxygen the halogen would be attracted to the charged oxygen, which is not a favorable geometry to form the oxonium ions. It is also shown in Table 4.2 that when the proportion of $(C_2H_5)_2O$ is high ($ClCH_2CH_2Br$ / $(C_2H_5)_2O$ = 1:3) the yield of the oxonium ions is the lowest. This indicates that the high $(C_2H_5)_2O^{+\bullet}$ concentration does not favor the formation of **I**.

Reaction 12 is also unlikely. If it were the case, the yield of the oxonium ion would be only proportional to the intensity of $C_2H_4X^+$ no matter what kind of precursor was used. However, when the precursor is $ClCH_2CH_2Br$ the ratio of **Ib** to $C_2H_4Br^+$ is 0.11 and when the precursor is $BrCH_2CH_2Br$ the ratio of **Ib** to $C_2H_4Br^+$ is 0.02. Reaction 10 is the most plausible. The overall reaction is an addition-elimination process, as shown in Scheme 4.1.

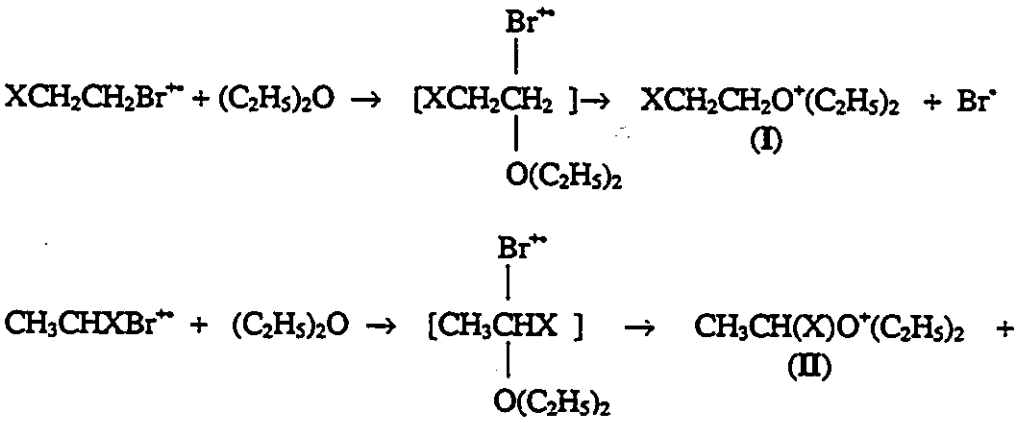

Scheme 4.1

Three observations support this mechanism:

(i) It is shown in Table 4.2 that when the ratio of $ClCH_2CH_2Br$ (or $BrCH_2CH_2Br$) : $(C_2H_5)_2O$ is 1:1 the yield of $(C_2H_5)_2O^+CH_2CH_2Cl$ (Ia) or $(C_2H_5)_2O^+CH_2CH_2Br$ (**Ib**) is greater than that at ratios 1:3 and 3:1. Both low concentrations of $XCH_2CH_2Y^{+\cdot}$ and low concentrations of $(C_2H_5)_2O$ will lower the yield of **I**.

(ii) It is also shown in Table 4.2 that the yield of **Ib** is higher when the precursor is $BrCH_2CH_2Br$ than that when the precursor is $BrCH_2CH_2Cl$. This is expected by the Scheme 4.1 since Br is a better leaving atom (i.e. more weakly bonded) than Cl.

(iii) The much lower yield of $(C_2H_5)_2O^+CHXCH_3$ (**III**) than that of **I** may be accounted for by both the shielding effect and steric effect of the X atom on the α-position.

In Scheme 4.1 the oxonium ions **I** and **II** are formed by the covalent binding of O-C as $(C_2H_5)_2O^+C_2H_4X$ isomers. Ion **I** has the halogen on the β-position and ion **II** has the halogen on the α-position. It is shown in Table 4.3 that the dissociation of **I** is not affected by the composition in the ion source, indicating **I** is a thermochemically stable species. As a halogen substituted triethyloxonium ion both **I** and **II** should have some reactions in common with $(C_2H_5)_3O^+$, which shows the major dissociation by C_2H_4 loss. In addition **I** and **II** may have some specific reaction related to the halogen atom. Moreover since **I** and **II** have the halogen atom in different positions (β- and α-), the isomers should display different dissociation characteristics.

4.3.3 Fragmentation of $(C_2H_5)_2O^+CH_2CH_2X$ (I)

From the MI and CID mass spectra of **Ia** and **Ib** (Table 4.1) and the CIDI mass spectra of **Ia** and **Ib** (Figure 4.2) their dissociations can be characterized by C_2H_4, C_2H_5X,

and $(C_2H_5)_2O$ losses as shown in reactions 13-15.

		Product Enthalpies, kcalmol^{-1}		
	X =	Cl	Br	
$(C_2H_5)_2O^+CH_2CH_2X \rightarrow C_4H_{10}OX^+ + C_2H_4$		117	128	(13)
$\rightarrow C_4H_9O^+ + C_2H_5X$		124	136	(14)
$\rightarrow C_2H_4X^+ + (C_2H_5)_2O$		142±2	146±1	(15)

The product enthalpies were obtained either from Reference 7 or from the estimations which will be discussed in 4.3.6. The above values show that the C_2H_4 loss has the lowest endothermicity and the $(C_2H_5)_2O$ loss has the highest endothermicity among these three MI dissociations. The energy differences between the two processes are 25 kcalmol^{-1} and 18 kcalmol^{-1} for **Ia** and **Ib**, respectively. Reactions 13 and 14 were not sensitive to collisional activation indicating the involvement of other intermediates or isomers. However, reaction 15 was sensitive to collision indicating it is a direct bond cleavage without involving other intermediates. The different kinetic energy release (KER) values for the $(C_2H_5)_2O$ loss (**Ia**, 109 meV; **Ib**, 33 meV) indicate different reverse energy barriers. In the MI mass spectrum of **Ib** the $(C_2H_5)_2O$ loss (48%) was competitive with C_2H_4 loss (100%), even though it is 18 kcalmol^{-1} more endothermic, indicating that C_2H_4 loss involved an energy barrier of this magnitude for either dissociation or isomerization. The latter is pronounced since this process was insensitive to collisional activation and the KER values were relatively small (**Ia**, 38 meV; **Ib**, 26 meV).

The weak signal of $C_2H_4Cl^+$ in the MI mass spectrum of **Ia** may be accounted for by collision induced dissociation by residual gas in the field-free region. Thus the energy barrier for **Ia** to dissociate via $(C_2H_5)_2O$ loss is much higher than that for **Ib** to dissociate

via $(C_2H_5)_2O$ loss. This explains why the KER value for $(C_2H_5)_2O$ loss from **Ia** is greater than that from **Ib**.

Another common fragmentation in the MI mass spectra of **Ia** and **Ib** is C_2H_5X loss. In the MI mass spectrum of **Ia** the relative intensity of C_2H_5Cl loss was ~ 13% of that for C_2H_4 loss and it was not sensitive to collision activation, indicating that another isomer may be involved, This will be discussed later in detail (4.3.5). The energy barrier for C_2H_5Cl loss is approximately 5-10 kcalmol^{-1} higher than the energy barrier for C_2H_4 loss. In the MI mass spectrum of **Ib** the relative intensity of C_2H_5Br loss was ~ 6% of that of C_2H_4 loss and it was collision sensitive. Thus the energy barrier for C_2H_5Br loss is approximately_≥10 kcalmol^{-1} higher than the energy barrier for C_2H_4 loss. The discuss ion of the above thermochemistry will be presented in 4.3.6.

4.3.3.1 C_2H_4 loss

The MI and CID mass spectra of both **Ia** and **Ib** (Table 4.1) are dominated by C_2H_4 loss. The ionic product is $C_4H_{10}OX^+$, which was examined by recording its CID mass spectra (Table 4.4) and found be $C_2H_5O^+(H)CH_2CH_2X$. This reaction resembles the C_2H_4 loss from $(C_2H_5)_3O^+$ which produced $C_2H_5O^+(H)C_2H_5$[3]. The deuterium labelling experiments showed that the C_2H_4 lost from **Ia** and **Ib** originates only from the diethyl ether and that the hydrogen transfered to the oxygen originated in the methyl group of the diethyl ether (Table 4.5).

$$(C_2H_5)_2O^+CD_2CD_2X \rightarrow C_2H_5O^+(H)C_2D_4X + C_2H_4 \quad (16)$$

$$CD_3CH_2O^+(C_2H_5)C_2H_4X \rightarrow C_2H_5O^+(D)C_2H_4X + C_2H_2D_2\ ; \quad \rightarrow CD_3CH_2O^+(H)C_2H_4X + C_2H_4 \quad (17)$$

The isotope effect for this process was obtained from the ratio of $C_4H_7D_3OX^+$ / $C_4H_9DOX^+$ (Table 4.5) in the MI mass spectrum of $CD_3CH_2O(C_2H_5)\bullet C_2H_4X^+$. The values are 100/49 and 100/51 for X = Cl and Br, respectively. This result indicates the existence of a transition state **TS** (Scheme 4.2) involving direct transfer of H or D in a rate determining step. It is generally observed that a transition state involving a direct hydrogen transfer will result in a significant isotope effect.[8] Compared to the dissociation of $(C_2H_5)_3O^+$ [3] an ion-neutral complex $[C_2H_5O(C_2H_4X)H^+\bullet\bullet\bullet C_2H_4]$, **C1** (Scheme 4.2) may be involved in this process, although the KER values ($T_{0.5}$ = 26-38 meV, Table 1) are not small enough to support such a proposal.

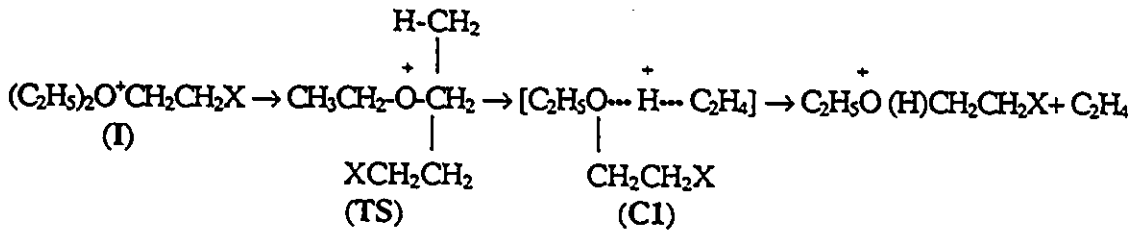

Scheme 4.2

It is also noticible that no H/D exchange was observed in this process. Harrison suggested[9] that when the ΔPA of the two partners is > 12 kcalmol^{-1} there would be no H/D exchange. Since the PA of $C_2H_5OCH_2CH_2X$ is ~ 200 kcalmol^{-1} (assumed to be the same as $C_2H_5OC_2H_5$[7] and the PA of C_2H_4 is 163 kcalmol^{-1} [7] the ΔPA is larger than the suggested limit. Therefore the observation of no H/D exchange is reasonable. However the absence of H/D exchange in the dissociation of D-labelled **Ia** and **Ib** indicates that their ethyl groups must likely have the classical configuration.[3]

4.3.3.2 C_2H_5X loss

In the MI and CID mass spectra of **Ia** and **Ib** (Table 4.1) the second most important fragment is $C_4H_9O^+$, corresponding to a C_2H_5X loss. The intensity of $C_4H_9O^+$ in the MI mass spectra of **Ia** and **Ib** is 6 - 13 % of the major peak $C_4H_{10}OX^+$. The CIDI mass spectra of **Ia** and **Ib** (Figure 4.2) further confirmed the lost neutrals to be C_2H_5X. The deuterium labelling experiments showed that the C_2H_5 in the C_2H_5X lost originates from the diethylether (Table 4.5).

$$(C_2H_5)_2O^+CD_2CD_2X \rightarrow C_2H_5OC_2D_4^+ + C_2H_5X \quad (18)$$

$$CD_3CH_2O^+(C_2H_5)C_2H_4X \rightarrow CD_3CH_2OC_2H_4^+ + C_2H_5X\ ; \quad C_2H_5OC_2H_4^+ + C_2H_2D_3X \quad (19)$$

Two possible mechanisms which account for this C_2H_5X loss (Scheme 4.3) are a concerted reaction (1,3-elimination) or one involving an intermediate halonium ion $C_2H_5OC_2H_4X^+C_2H_5$ (**III**).

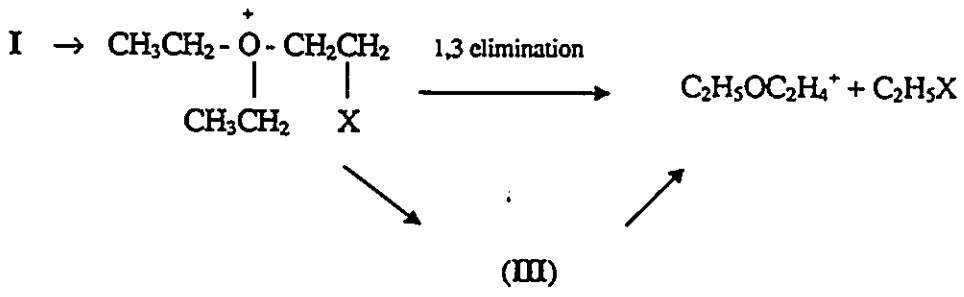

Scheme 4.3

It is shown in the energy diagram (Figure 4.11) that the isomers **IIIa** (Δ_fH° 114 kcalmol^{-1}) and **IIIb** (Δ_fH° 123 kcalmol^{-1}) lie below the dissociation limit for reaction (18), even though they are higher in energy than isomers **Ia** (Δ_fH° 93 kcalmol^{-1}) and **Ib** (Δ_fH°

104 kcalmol^{-1}). The smaller KER value of **IIIa** ($T_{0.5}$, 22 meV, Table 4.7) in the MI dissociation via C_2H_5Cl loss, compared to that of **Ia** ($T_{0.5}$, 34 meV) illustrated that the isomerization barrier from **Ia** to **IIIa** is higher than the product enthalpies, thus only the **Ia** ions containing higher internal energy can isomerize to **IIIa** and release more kinetic energy in dissociation via C_2H_5Cl loss than stable **IIIa** ions.

That **I** having isomerized to **III** showed C_2H_5Cl loss could explain the absence of C_2H_6 loss from $(C_2H_5)_3O^+$ ions[3] which cannot form isomers such as **III**. Moreover, the proposed C_2H_6 loss in the dissociations of $(C_2H_5)_3O^+ \cdot SbCl_6^-$ in FAB mass spectrometry[2] could possibly be C_2H_5Cl loss instead.

The structure of the ionic product $C_4H_9O^+$ in the dissociation of **I** via C_2H_5X loss is most likely $C_2H_5O^+CHCH_3$[10] (Figure 4.3). However the instantly formed species could be $C_2H_5OCH_2CH_2^+$, which rapidly isomerized to the more stable isomer $C_3H_2O^+CHCH_3$ on the time scale of $< 10^{-5}$ s.

In the CID mass spectra of **Ia** and **Ib** (Table 4.1), the fragments $C_2H_6OX^+$ and $C_2H_5O^+$ are the results of two consecutive neutral losses, as shown in reactions 20 and 21. The structure of $C_2H_5O^+$ was shown by its CID mass spectrum to be CH_3CHOH^+ (Figure 4.4 a) and the structure of $C_2H_6OX^+$ was found similarly to be $H_2OC_2H_4X^+$ (Figure 4.4 b).

$$(C_2H_5)_2O^+CH_2CH_2X \xrightarrow{-C_2H_4} C_2H_5O^+(H)CH_2CH_2X \xrightarrow{-C_2H_4} H_2O^+CH_2CH_2X \qquad (20)$$

$$(C_2H_5)_2O^+CH_2CH_2X \xrightarrow{-C_2H_5X} C_2H_5OC_2H_4^+ \xrightarrow{-C_2H_4} CH_3CHOH^+ \qquad (21)$$

4.3.3.3 $(C_2H_5)_2O$ loss

The loss of $(C_2H_5)_2O$ is a major fragment in the MI dissociation of **Ib**, but is only a minor peak in the MI mass spectrum of **Ia** (Table 4.1). A deuterium labelling experiment (Table 4.5) confirmed that the dissociation is an O–C bond cleavage.

$$(C_2H_5)_2\overset{+}{O}CD_2CD_2X \longrightarrow C_2D_4X^+ + (C_2H_5)_2O \qquad (22)$$

The CID mass spectra of $C_2H_4X^+$ ions produced from **I** are similar to the CID mass spectra of $\overset{\frown}{CH_2X^+}\,CH_2$ produced from $CH_2XCH_2Y^{+\cdot}$ via $Y^\cdot$ loss (Y = Cl or Br, Figure 4.5), indicating that the cyclic structure $\overset{\frown}{CH_2X^+}\,CH_2$ was formed from the $(C_2H_5)_2O$ loss. The high reverse energy barrier ($T_{0.5}$ = 109 meV) in the formation of $\overset{\frown}{CH_2Cl^+}CH_2$ from **Ia** may be indicative of the O-C bond cleavage being followed by isomerization of $ClCH_2CH_2^+$ to a more stable $\overset{\frown}{CH_2Cl^+}CH_2$. In the dissociation of **Ib** the relatively smaller KER value ($T_{0.5}$ = 33 meV) may be accounted for by the concerted formation of the cyclic $\overset{\frown}{CH_2Br^+}CH_2$ at the same time as the O-C bond cleavage. In MI dissociations of **Ib** the $(C_2H_5)_2O$ loss (48%) was competitive with C_2H_4 loss (100%) indicating that the two processes have similar activation energies. In contrast, the dissociation of **Ia** by $(C_2H_5)_2O$ loss (3%) has a significantly higher activation energy than C_2H_4 loss (100%).

In summary, $(C_2H_5)_2O^+CH_2CH_2X$ (X = Cl and Br), formed from $BrCH_2CH_2X^{+\cdot}$ + $(C_2H_5)_2O$ - Br, is a covalently bound species. The C_2H_4 loss from **I** is a similar process to that from $(C_2H_5)_3O^+$. The C_2H_5X loss indicates the involvement of an isomer **III**, which is the dissociation configuration for C_2H_5X loss. This result leads to the conclusion that

when the halogen is substituted at the β-position, it will show strong tendency to form a C-X bond. According to the fragment intensities in the MI mass spectra of **Ia** and **Ib** the activition energy for O-C bond cleavage of **I** increases in the following series:

$$C_2H_5O^+(C_2H_4X)\text{-}CH_2CH_3 \quad < \quad (C_2H_5)_2O^+\text{-}CH_2CH_2Br \quad < (C_2H_5)_2O^+\text{-}CH_2CH_2Cl$$

4.3.4 Fragmentation of $(C_2H_5)_2O^+CHXCH_3$ (**II**)

The MI and CID mass spectra of $(C_2H_5)_2O^+CHXCH_3$ (**IIa**, X = Cl; **IIb**, X = Br) formed from the reaction of $XYCHCH_3^{+\bullet}$ + $(C_2H_5)_2O$ - Y are given in Table 4.1. The CIDI mass spectra of **IIa** and **IIb** are shown in Figure 4.6. The MI dissociations of ions **Ia** and **Ib** are characterized by C_2H_3X, C_2H_4, and $(C_2H_5)_2O$ losses.

		Relative intensity (%)		
	X =	Cl	Br	
$(C_2H_5)_2O^+CHXCH_3 \rightarrow C_4H_{11}O^+ + C_2H_3X$		100	100	(23)
$\rightarrow C_4H_{10}OX^+ + C_2H_4$		2	3	(24)
$\rightarrow C_2H_4X^+ + (C_2H_5)_2O$		-	7	(25)

Unlike the MI dissociations of **I**, which showed C_2H_4 loss as the major process, the MI dissociations of **II** showed C_2H_3X loss as the dominant fragmentation. Even though C_2H_4 loss has approximately the same endothermicity as C_2H_3X loss, its intensity was only 2-3% of that of C_2H_3X loss. The different intensities may indicate the different energy barriers for the hydrogen shift, since the two processes involve a hydrogen shift from the C_2H_4X group or the C_2H_5 group to the oxygen.

4.3.4.1 C_2H_3X loss

The dissociations of **IIa** and **IIb** are dominated by C_2H_3X loss, (reaction 23). The CID mass spectrum of the product $C_4H_{11}O^+$ ions (Figure 4.7) is identical to that of protonated diethyl ether $(CH_3CH_2)_2OH^+$. The deuterium labelled ion $(C_2D_5)_2O^+CH(Cl)CH_3$ dissociated to $(C_2D_5)_2OH^+ + C_2H_3Cl$ without H/D exchange, which confirmed that this reaction involves a hydrogen transfer from haloethyl to the diethyl ether, as shown in Scheme 4.4.

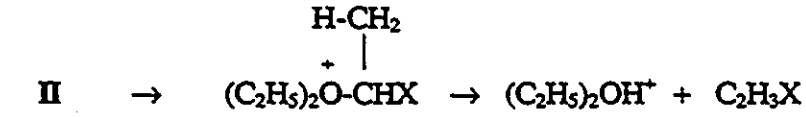

Scheme 4.4

Heck et al[11] investigated the reactions between CH_3^+CHX and D_2O by ICR-MS. It was shown that the total population of the ions rapidly exchanges up to three hydrogen atoms for deuterium atoms. It was proposed that the three chemically identical methyl hydrogen atoms can be involved in the reaction with water. No fourth hydrogen atom exchange was observed because the exchange of the α-hydrogen atom was energetically inaccessible. From this point of view, the proton in adduct **IIa** and **IIb** likely originated from the methyl hydrogens in the CH_3CHX^+ ion.

The major C_2H_3X loss from **II** indicates that the $(C_2H_5)_2O^+$ - $CHXCH_3$ bond must be weaker than the $(C_2H_5)_2O^+$-CH_2CH_2X and $C_2H_5O^+(C_2H_4X)$-CH_2CH_3 bonds.

4.3.4.2 C_2H_4 loss

Ethene loss, which is predominant in the dissociations of ion **I**, is only a minor process in the dissociations of ion **II**. The ionic fragment $C_4H_{10}OX^+$, produced in reaction 24, is different from that produced in reaction 13. It is shown in Figure 4.7 that the major fragment in the former ion's CID mass spectra is $C_2H_7O^+$, corresponding to C_2H_3X loss. The $C_4H_{10}OX$+ ions produced from C_2H_4 loss from **I**, however, prefer lose C_2H_4 (Table 4.4). This result reveals that the C_2H_4X groups in the two $C_4H_{10}OX^+$ isomers (**I** - C_2H_4 and **II** - C_2H_4) are indeed completely different (Scheme 4.5) and so confirms that the $(C_2H_5)_2O^+C_2H_4X$ isomers (**I** and **II**) are in no way interconvertible.

$$\mathbf{I} \xrightarrow{-C_2H_4} C_2H_5O^+(H)CH_2CH_2X \longrightarrow H_2O^+CH_2CH_2X + C_2H_4$$

$$\mathbf{II} \xrightarrow{-C_2H_4} C_2H_5O^+(H)CH(X)CH_3 \longrightarrow H_2O^+C_2H_5 + C_2H_3X$$

Scheme 4.5

The C_2H_3X loss in the CID mass spectrum of $C_4H_{10}OX^+$ (**II** - C_2H_4) indicated that the X is still at the α-position, i.e. the ion is $C_2H_5O^+(H)CHXCH_3$. An ion-neutral complex, $[C_2H_5O(CHXCH_3)H^+\bullet\bullet\bullet C_2H_4]$ (C2) could be involved in the dissociation of **II** via C_2H_4 loss.

The different behaviours of **II** and **I** shows that when X is on the_α-position (**II**), it promoted the hydrogen transfer from the neighbouring methyl group (C_2H_3X loss) and the hydrogen transfer from the ethyl group (C_2H_4 loss) was less competitive. When X sits at the β-position (**I**), the hydrogen transfer originated only from the ethyl group. A

comparison of all the hydrogen transfers in I and II showed that the activity of hydrogen decreases in the following series:

$$(C_2H_5)_2OCHXCH_2 - H > XC_2H_4O(C_2H_5)CH_2CH_2 - H > (C_2H_5)_2OCH_2CHX - H$$

(II) (I) & (II) (I)

4.3.4.3 $(C_2H_5)_2O$ loss

The loss of $(C_2H_5)_2O$ is a major fragmentation in the MI dissociation of **IIb**, but is not observed in the MI mass spectrum of **IIa** (Table 4.1). The CID mass spectrum of the daughter ion $C_2H_4Br^+$ confirmed its structure as CH_3CHBr^+. Thus the dissociation is a simple bond cleavage producing $CH_3CHBr^+ + (C_2H_5)_2O$. This shows that there is no hydrogen shift between the two carbons in the haloethyl group, and again the isomers I and II are not interconvertible with each other.

4.3.5 Reaction of $C_2H_5I^{+\bullet} + ClCH_2CH_2OC_2H_5$

The gas-phase diethylhalonium ions have been throughly studied.[5,12] To search for the possible formation of $CH_3CH_2OCH_2CH_2X^+CH_2CH_3$ (III), an ethoxy diethylhalonium ion, we investigated the reaction between $CH_3CH_2OCH_2CH_2Cl$ and $C_2H_5I^{+\bullet}$. Unlike the system of $C_2H_5OC_2H_5 + C_2H_4ClBr^{+\bullet}$, which showed no molecular adducts, the molecular adduct ion of $ClCH_2CH_2OCH_2CH_3 \bullet C_2H_5I^{+\bullet}$ (A, m/z 264) was observed in the normal mass spectrum of $C_2H_5I^{+\bullet} + ClCH_2CH_2OCH_2CH_3$ (Figure 4.8). The MI and CID mass spectra of A (Table 4.6) showed a major fragment $C_6H_{14}OCl^+$ (IIIa, m/z 137), corresponding to I loss. The MI and CID mass spectra of IIIa are given in Table 4.7, and they showed the same fragments as Ia but with a different ratio of $C_4H_9O^+$ / $C_4H_{10}ClO^+$

(Table 4.1). Figure 4.9 shows the same structure of $C_2H_5O^+(H)CH_2CH_2Cl$ from **IIIa** - C_2H_4 as produced from **Ia** - C_2H_4 (Table 4.4). Two possible $C_6H_{14}OCl^+$ isomers could be formed and may be interconvertable, as shown in Scheme 4.6.

A comparison of deuterium labelled **IIIa** and **Ia** is given in Table 4.8, which showed that ion **IIIa** from { $ClCH_2CH_2OCH_2CH_3$ + $CH_3CD_2I^{+\bullet}$ (or $CD_3CH_2I^{+\bullet}$) } - I$^\bullet$ lost more CH_3CD_2Cl (or CD_3CH_2Cl) than CH_3CH_2Cl. The CID mass spectrum of metastably generated **IIIa** showed an even higher ratio of $C_4H_9O^+/C_4H_{10}ClO^+$. Furthermore the CIDI mass spectrum of **IIIa** (Figure 4.10) barely showed $(C_2H_5)_2O^{+\bullet}$, but only $C_2H_5Cl^{+\bullet}$. Those results support the proposal that the structure of **IIIa** is $CH_3CH_2OCH_2CH_2Cl^+CH_2CH_3$. Thus the adduct A produces ion **IIIa** by I loss. Ion IIIa dissociates competitively to C_2H_5Cl loss and C_2H_4 loss.

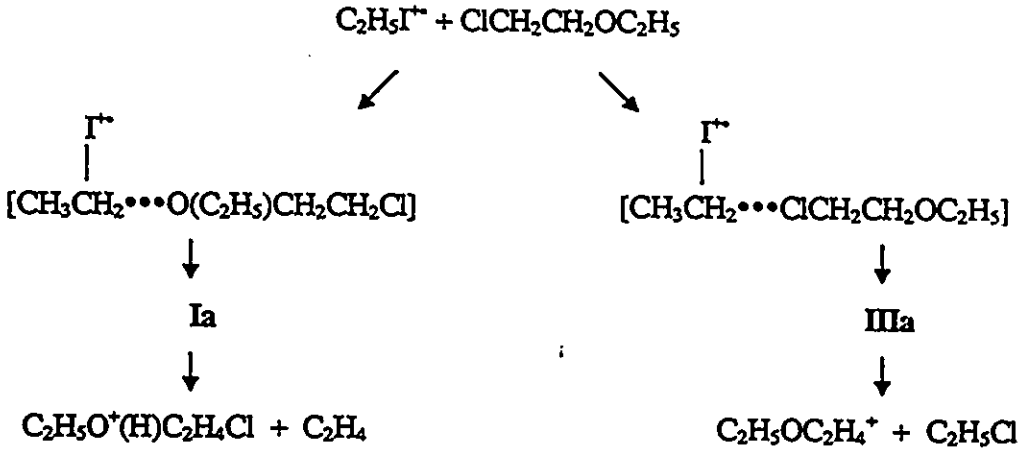

Scheme 4.6

4.3.6 Thermochemical evaluations

To thoroughly understand the dissociation processes of **I**, **II** and **III** a knowledge of their energetics is needed, including the heats of formation of **I**, **II**, **III**, their fragmentation

products, the energy barriers for both isomerization and dissociation, and also the energies of the possible intermediates such as ion-neutral complex C_1. All estimated heat of formation values are summarized in Table 4.9 and the energetics of configurations involved in the dissociation processes are illustrated in Figure 4.11.

4.3.6.1 Heats of formation of **I** and **III**

The heats of formation of **I**, **II** and **III** are not available from experiment. However the heats of formation of onium ions can be obtained by estimation using the ethyl cation affinity (ECA) of the molecules based on Eq. 1.[5]

$$C_2H_5OCH_2CH_2X + C_2H_5^+ \xrightarrow{\Delta Hr} \underset{\textbf{Ia \& Ib}}{(C_2H_5)_2O^+CH_2CH_2X} \qquad (18)$$

$$ECA(C_2H_5OCH_2CH_2X) = -\Delta Hr = \Delta H_f^\circ(C_2H_5OCH_2CH_2X) + \Delta H_f^\circ(C_2H_5^+) - \Delta H_f^\circ[(C_2H_5)_2O^+CH_2CH_2X] \quad Eq.1$$

The heat of formation of $C_2H_5^+$ is readily obtained from Reference 7 to be 216 kcalmol^{-1} and the heat of formation of $C_2H_5OC_2H_4X$ can be obtained using the additivity rule[13].

	$C_2H_5OCH_2CH_2Cl$	$C_2H_5OCH_2CH_2Br$	$C_2H_5OCHClCH_3$
ΔH_f° (kcalmol^{-1})	-66.6	-54.2	-73.6

The key step to get the heats of formation of **Ia** and **Ib** is to estimate the ECA values. First we need to estimate the ECA of $C_2H_5OC_2H_5$, and then find the correction term for substitution of the β-halogen. It has been found that for some homologous

molecules the difference between the MCA (methyl cation affinity) and the ECA is approximately constant[5, 14], as shown below.

	MCA	ECA	Δ = MCA -ECA (kcalmol^{-1})
H_2O	67	37	30
CH_3OH	83	50	33
C_2H_5OH	87	55	32
		Average	32±2

Thus it is reasonable to assume that the difference between MCA ($C_2H_5OC_2H_5$) and ECA ($C_2H_5OC_2H_5$) is also about 32 kcalmol^{-1}. The measured MCA of $(CH_3)_2O$ was 92±5 kcalmol^{-1}[15], which may be close to the MCA of $(C_2H_5)_2O$. Thus the ECA of diethyl ether is estimated to be 92±5 -32 = 60±5 kcalmol^{-1}. The correction term for the presence of the β-halogen is estimated from the differences between the proton affinity (PA) values of C_2H_5OH (188 kcalmol^{-1}), $ClCH_2CH_2OH$ (184 kcalmol^{-1}) and $BrCH_2CH_2OH$ (185 kcalmol^{-1})[11]. The β-position effect of halogens is thus taken as 3 ± 1 kcalmol^{-1} and so the ECA($C_2H_5OCH_2CH_2X$) is taken as ECA($C_2H_5OC_2H_5$) - 3 = 57±5 kcalmol^{-1}. Thus from Equation 1 the heats of formation of **Ia** and **Ib** are obtained to be 93 kcalmol^{-1} and 104 kcalmol^{-1}, respectively, with an uncertainty of ±5 kcalmol^{-1}.

The heat of formation of **III** was estimated from the ECA of C_2H_5X (36 kcalmol^{-1} for X = Cl and 38 kcalmol^{-1} for X = Br[5]). The estimated values are 114 kcalmol^{-1} and 123 kcalmol^{-1} for **IIIa** and **IIIb**, respectively.

The heat of formation of **II** cannot be evaluated since the halogen effect at an α-position ($C_2H_5OCHXCH_3$) is not available.

4.3.6.2 Heats of formation of the product ions

The heats of formation of $C_2H_5O^+(H)CH_2CH_2X$ were estimated from PA ($C_2H_5OCH_2CH_2X$), which can be obtained from PA($C_2H_5OC_2H_5$) - 3 kcalmol^{-1} (a correction term for the halogen in the neutral ether). The results are given in Table 4.9.

The heat of formation of $C_2H_5OCH_2CH_2^+$ was estimated by comparing $\Delta H_f^\circ(HO^+CHCH_3)$ (139 kcalmol^{-1}) and ΔH_f° ($HOCH_2CH_2^+$) (165 kcalmol^{-1}). The stable isomer is 26 kcalmol^{-1} lower in energy. By the same consideration it is resonable that $\Delta H_f^\circ(C_2H_5OCH_2CH_2^+) > \Delta H_f^\circ$ ($C_2H_5O^+CHCH_3$) + 26 kcalmol^{-1} = 125 kcalmol^{-1}[7] + 26 kcalmol^{-1} = 151 kcalmol^{-1}.

4.3.6.3 The energy of intermediate C_1

An ion-neutral complex [$XCH_2CH_2O(C_2H_5)H^+ \bullet\bullet\bullet C_2H_4$] ($C_1$) has been proposed as an intermediate in the dissociation of **I** via C_2H_4 loss. The energy of C_1 could be estimated through the stabilization energy (SE) in the complex. The SE values in some analogous ion-neutral complexes have been calculated. For instance, the SE of [$H_3O^+ \bullet\bullet\bullet C_2H_4$] has been calculated to be 21.5 kcalmol^{-1}[16] or 19.6 kcalmol^{-1}[17] and the SE of [$CH_3OH_2^+ \bullet\bullet\bullet C_3H_6$] to be 12 kcalmol^{-1}[18].

The SE decrease from [$H_3O^+ \bullet\bullet\bullet C_2H_4$] to [$CH_3OH_2^+ \bullet\bullet\bullet C_3H_6$] is expected since the charge density decreases from H_3O^+ to $CH_3OH_2^+$. Consequently the SE of [$XCH_2CH_2O(C_2H_5)H^+ \bullet\bullet\bullet C_2H_4$] should likely be less than 12 kcalmol^{-1}. We will assume an SE of ca. 10 kcalmol^{-1}, and so the energy of C_1 is estimated to be about 107 kcalmol^{-1} and 118 kcalmol^{-1} for X = Cl and Br, respectively.

4.3.6.4 Energetics of dissociations

It is known that metastable ions contain a narrow range of internal energies. In other words, for dissociations detected in an MI spectrum, their energy requirements will be similar (covering an energy range of ca ≤ 10 kcalmol^{-1}). In the case of the MI dissociations of **Ib** the C_2H_4 loss and $(C_2H_5)_2O$ loss are competitive, so both processes may involve a similar energy barrier. Dissociation via $(C_2H_5)_2O$ loss has been shown to be a direct O–C bond cleavage without isomerization. So the activation energy barrier could be set above the product energies [ΔH_f° ($C_2H_4Br^+$) = 206 kcalmol^{-1} and ΔH_f° ($C_2H_5OC_2H_5$) = -60 kcalmol^{-1}]. The KER value ($T_{0.5}$, 33 meV) for this process is a little higher than a simple bond cleavage and so a small reverse barrier should be considered. Thus the activation energy barrier is estimated to be > 206 - 60 - 116 (ΔH_f° of **Ib**) = 30 kcalmol^{-1}, ca. 32 kcalmol^{-1}, which is the same as the activation energy barrier for dissociation via C_2H_4 loss (Figure 4.11). Radom et al[15], calculated the energy of the transition state for hydrogen transfer in $CH_3CH_2OH_2^+$ followed by C_2H_4 loss. The transition state is 23 kcalmol^{-1} above $C_2H_5OH_2^+$. In the case of $(C_2H_5)_2O^+CH_2CH_2X$ (I) the difficulty for hydrogen transfer can arise for two reasons: the steric and the inductive effects of the C_2H_4X and C_2H_5 groups. By the same arguments the activation energy barrier for **Ia** to dissociate via C_2H_4 loss was also set 32 kcalmol^{-1} above **Ia**.

4.4. Conclusion

The isomeric $(C_2H_5)_2O^+C_2H_4X$ ions (I and II) are not interconvertable. Only the hydrogen in a methyl group will transfer to oxygen. The halogen substituted at the β position has a strong tendency to form a C-X bond with an ethyl group, however, in the α position the halogen promotes $O\text{-}C_2H_4X$ bond cleavage.The dissociation energy of the O-C bond increases in the following series:

$$(C_2H_5)_2O^+\text{-}CHXCH_3 < C_2H_5O^+(C_2H_4X)\text{-}CH_2CH_3 < (C_2H_5)_2O^+\text{-}CH_2CH_2X .$$

4.5 References

1. a: D. N. Kevill and E. K. Fujimoto, J. Chem. Research, Symposia, 408 (1988);
   b. D. N. Kevill, S. W. Anderson, N. H. Ismail and E. K. Fujimoto, Studies in Organic Chemistry (Amsterdam), 31, 311 (1987)
2. K. Laali, D. L. Fishel, R. P. Lattimer and J. E. Hunt, Org. Mass Spectrom., 23, 705, (1988)
3. a: M. Sirois, Ph.D. thesis, University of Ottawa, 1993
   b: D. V. Zagoreskii and J. L. Holmes, in preparation
4. a: D. Harnish and J. L. Holmes, J. Am. Chem. Soc., 103, 9729 (1991);
   b: M. Sirois, M. George and J. L. Holmes, Org. Mass Spectrom., 29, 11 (1994);
   c: C. Wesdemiotis, A. Fura and F. W. Mclafferty, J. Am. Soc. Mass Spectrom., 2, 459 (1991);
   d: A. G. Harrison, Org. Mass Spectrom., 22, 637 (1987);
   e: K. Hiraoka, T. Mori and Y. J. Hopilliard, Chem. Phys. Lett., 207, 178 (1993)
5. a: D. V. Zagorevskii, S. P. Palii and J. L. Holmes, J. Am. Chem. Soc. Mass Spectrom., 5, 814 (1994)
6. a: P. C. Burgers, J. L. Holmes, J. E. Szulejko, A. A. Mommers and J. K. Terlouw, Org. Mass Spectrom., 18, 254 (1983)
   b: J. C. Traeger and A. A. Mommers, Org. Mass Spectrom., 22, 592 (1987)
7. S. G. Lias, J. E. Bartmess, J. F. Liebman, J. L. Holmes, R. D. Levin and W. G. Mallard, J. Phys. Chem. Ref. Data, Vol. 17, Suppl. 1, (1988)
8. a: L. Melander and W. H. Saunders, Jr, Reaction rates of isotopic molecules.,

Wiley, New York (1980);

b: P. J. Derrick, Mass Spectrom. Rev., 2, 285 (1983);

c: R. G. Cooks, J. H. Beynon, R. M. Caprioli and G. R. Lester, Metastable Ions, Elsevier, Amsterdam (1973)

9. A. G. Harrison, Org. Mass Spectrom., 22, 637 (1987)

10. T. J. Mead and D. H. Williams, J. Chem. Soc. Perkin II, 867 (1972)

11. A. J. R. Heck, L. J. de Koning and N. M. M. Nibbering, Org. Mass Spectrom., 28, 245 (1993)

12. D. V. Zagorevskii and J. L. Holmes, Org. Mass Spectrom., 29, 594 (1994)

13. S. W. Benson, Thermochemical Kinetics, 2nd. ed., John Wiley and Sons, New York, 1976

14. T. B. McMahon, T. Heinis, G. Nicol, J. K. Hovey and P. Kebarle, J. Am. Chem. Soc., 110, 7591 (1988)

15. D. Wang, R. R. Squires and D. Farcasiu, Int. J. Mass Spectrom. Ion Proc., 107, R7 (1991)

16. D. J. Swanton, D. C. J. Marsden and L. Radom, Org. Mass Spectrom., 26, 227 (1991)

17. G. Bouchoux and Y. Hoppilliard, J. Am. Chem. Soc., 112, 9110 (1990)

18. H. E. Audier, C. Monteiro, D. Berthomieu and J. Tortajada, Int. J. Mass Spectrom. Ion Processes, 104, 145 (1991)

Table 4.1 MI and CID[1] mass spectra of I and II[2]

	Ia		Ib		IIa		IIb	
Fragments	MI	CID	MI	CID	MI	CID	MI	CID
$C_4H_{10}OX^+ + C_2H_4$	100(38)	100	100(26)	90	2(34)	3	3(27)	3
$H_2OC_2H_4X + 2\ C_2H_4$	-	5	-	-	-	-	-	-
$C_4H_{11}O^+ + C_2H_3X$	-	-	-	-	100(33)	100	100(21)	100
$C_4H_9O^+ + C_2H_5X$	13(34)	15	6(29)	11	-	4	-	5
$C_2H_4X^+ + (C_2H_5)_2O$	3(109)	6	48(33)	100	-	2	7(29)	13
$C_2H_7O^+ + C_2H_4 + C_2H_3X$	-	-	-	-	-	4	-	7
$C_2H_5O^+ + C_2H_4 + C_2H_5X$	2	4	<1	6	-	-	-	-

1. Oxygen is the target gas with 90% transmission of the mass selected ion current.
2. KER values ($T_{0.5}$, meV) are given in parentheses.

Table 4.2 The effect of the composition of C_2H_4XY and $(C_2H_5)_2O$ on the yield of Ia and Ib

Precursor ratio	Intensity Ratio	
$BrCH_2CH_2Cl / (C_2H_5)_2O$	$Ia / BrCH_2CH_2Cl^{+\cdot}$	$Ib / BrCH_2CH_2Cl^{+\cdot}$
3 / 1	0.20	0.07
1 / 1	0.22	0.11
1 / 3	0.10	0.06
$BrCH_2CH_2Br / (C_2H_5)_2O$		$Ib / BrCH_2CH_2Br^{+\cdot}$
3 / 1		0.62
1 / 1		1.18
1 / 3		0.23

Table 4.3 The effect of composition of $BrCH_2CH_2Cl$ and $(C_2H_5)_2O$ mixtures on the dissociation of Ia

$ClCH_2CH_2Br$ / $(C_2H_5)_2O$	1 / 3		1 / 1		3 / 1	
Fragment	MI	CID	MI	CID	MI	CID
$C_4H_{10}OCl^+$	100	100	100	100	100	100
$C_2H_6OCl^+$	-	5	-	5	-	6
$C_4H_9O^+$	13	14	13	15	13	14
$C_2H_4Cl^+$	3	7	3	6	3	7
$C_2H_5O^+$	3	4	2	4	2	5

Oxygen is the target gas with 90% transmission of the mass selected ion beam.

Table 4.4 CID mass spectra of $C_4H_{10}OCl^+$ ions

	Precursors		
Fragments	**Ia - C_2H_4**	**$C_2H_5O^+(H)CH_2CH_2Cl$**	**Ib - C_2H_4**
$H_2O^+C_2H_4X+C_2H_4$	100	100	51
$C_2H_4X^+ + C_2H_5OH$	29	27	100
$HOC_2H_4^+ + C_2H_5Cl$	14	16	14

Table 4.5 MI and CID mass spectra of deuterium-labelled Ia and Ib

Precursors	$C_2H_2D_2Cl^+\bullet(C_2H_5)_2O$		$C_2H_2D_2Br^+\bullet(C_2H_5)_2O$		$C_2H_4Cl^+\bullet CD_3CH_2OC_2H_5$		$C_2H_4Br^+\bullet CD_3CH_2OC_2H_5$	
Fragments	MI	CID	MI	CID	MI	CID	MI	CID
$CD_3H_2O^+(H)C_2H_4X+C_2H_4$					100	100	100	66
$C_2H_5O^+(H)C_2H_2D_2X+C_2H_4$	100	100	100	100				
$C_2H_5O^+(D)C_2H_4X+C_2H_2D_2$					49	52	51	34
$CD_3CH_2OC_2H_4^+ + C_2H_5X$					9	10	7	6
$C_2H_5OC_2D_2H_2^+ + C_2H_5X$	9	10	7	8				
$C_2H_5OC_2H_4^+ + C_2H_2D_3X$					6	7	4	4
$C_2H_2D_2X^+ + (C_2H_5)_2O$	1	4	49	92				
$C_2H_4X^+ + CD_3CH_2OC_2H_5$					1	5	94	100
$HOC_2H_2D_2^+ + C_2H_5X + C_2H_4$	1	3	<1	3				
$DOC_2H_4^+ + C_2H_5X + C_2H_2D_2$					1	4	<1	4
$HOC_2H_4^+ + C_2H_2D_3X + C_2H_4$					1	5	<1	3

Table 4.6 MI and CID mass spectra of the adduct ion $C_2H_5I^{+\cdot}$ $ClCH_2CH_2OC_2H_5$

Fragments	MI	CID
$ClCH_2CH_2O^+(H)C_2H_5 + C_2H_4I$	33	37
$C_2H_5OCH_2CH_2Cl^+C_2H_5 + I$	100	100
$C_2H_5I^{+\cdot} + C_2H_5OCH_2CH_2Cl$	14	34

Table 4.7 MI and CID[1] mass spectra of IIIa[2]

Fragments	MI	CID	CID[3]
$C_4H_{10}ClO^+ + C_2H_4$	100 (31)	100	67
$C_4H_9O^+ + C_2H_5Cl$	79 (22)	80	100
$C_2H_4Cl^+ + (C_2H_5)_2O$	1	25	17
$C_2H_5O^+ + C_2H_5Cl + C_2H_4$	2	24	17

1. O_2 is the target gas with 90% transmittance of the mass selected ion.
2. KER values ($T_{0.5}$, meV) are shown in brackets.
3. Metastably generated IIIa in 2ffr.

Table 4.8 MI and CID mass spectra of deuterium labelled Ia and IIIa

	Precursors						
	$CD_3CH_2I^{+\cdot}$ + $ClC_2H_4OC_2H_5$		$C_2H_4ClBr^{+\cdot}$ + $CD_3CH_2OC_2H_5$		$CH_3CD_2I^{+\cdot}$ + $ClC_2H_4OC_2H_5$		$C_2H_4ClBr^{+\cdot}$ + $CH_3CD_2OC_2H_5$
Fragments	MI	CID	MI	CID	MI	CID	MI
$C_4H_9O^+$	76	75	40	41	82	75	44
$C_4H_6D_3O^+$	24	25	60	59			
$C_4H_7D_2O^+$					18	25	56
			**********				
$C_4H_9DClO^+$	37	32	33	34			
$C_4H_7D_3ClO^+$	63	68	67	66			
$C_4H_{10}ClO^+$					52	51	50
$C_4H_8D_2ClO^+$					48	49	50

Table 4.9 Estimated heats of formation, in kcalmol^{-1}.

	ΔH_f		ΔH_f
$C_2H_5OCH_2CH_2Cl$	-66±1	$C_2H_5OCH_2CH_2Br$	-55±1
$C_2H_5O^+(H)CH_2CH_2Cl$	103±3	$C_2H_5O^+(H)CH_2CH_2Br$	114±3
$(C_2H_5)_2O^+CH_2CH_2Cl$ (Ia)	93±5	$(C_2H_5)_2O^+CH_2CH_2Br$ (Ib)	104±5
$C_2H_5Cl^+CH_2CH_2OC_2H_5$ (IIIa)	114±3	$C_2H_5Br^+CH_2CH_2OC_2H_5$ (IIIb)	123±3
$C_2H_5OCH_2CH_2^+$	≥151±3		

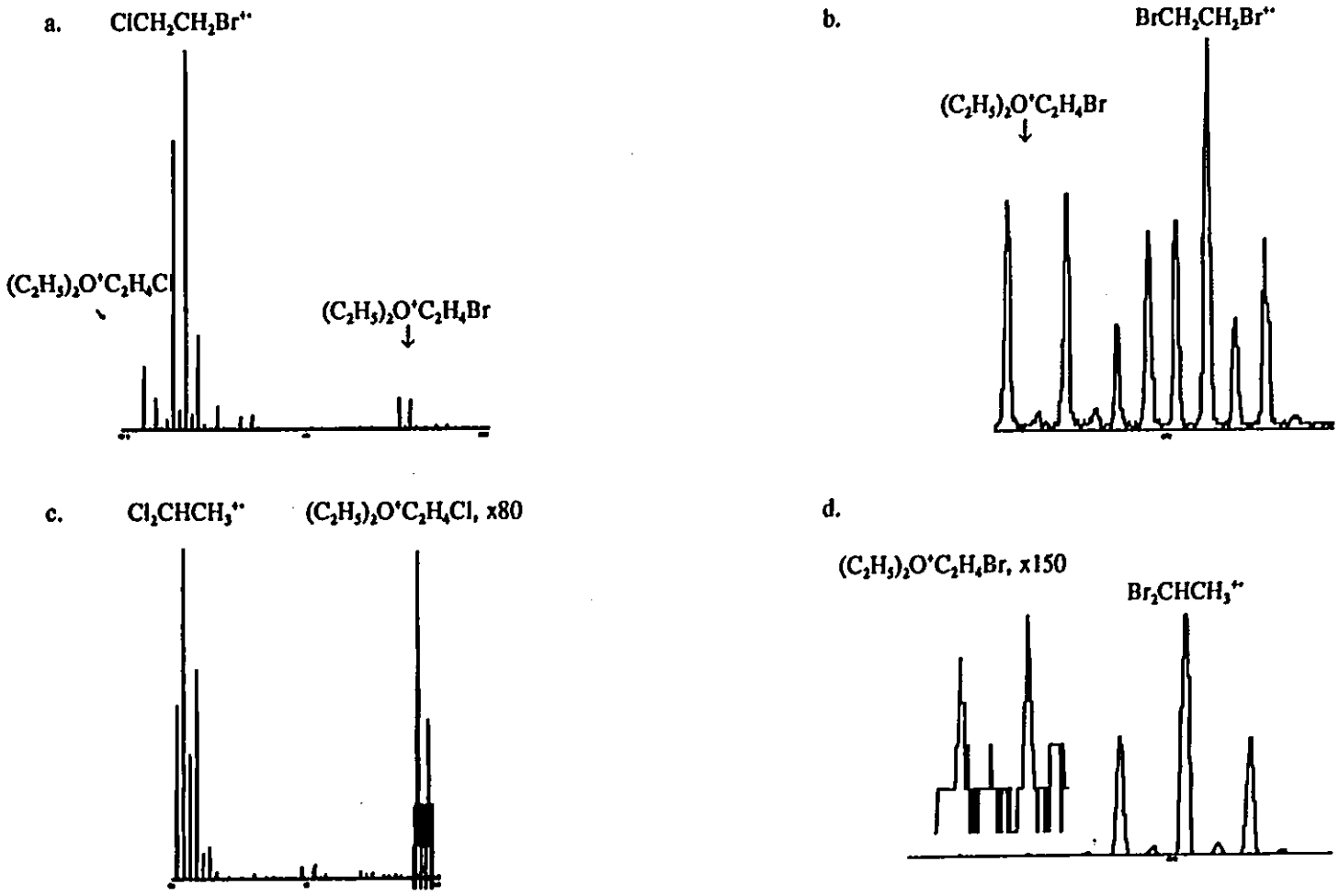

Figure 4.1 Normal mass spectra of $C_2H_4XY^{+\cdot}O(C_2H_5)_2$

a. $BrCH_2CH_2Cl + O(C_2H_5)_2$

b. $BrCH_2CH_2Cl + O(C_2H_5)_2$

c. $Cl_2CHCH_3 + O(C_2H_5)_2$

c. $Br_2CHCH_3 + O(C_2H_5)_2$

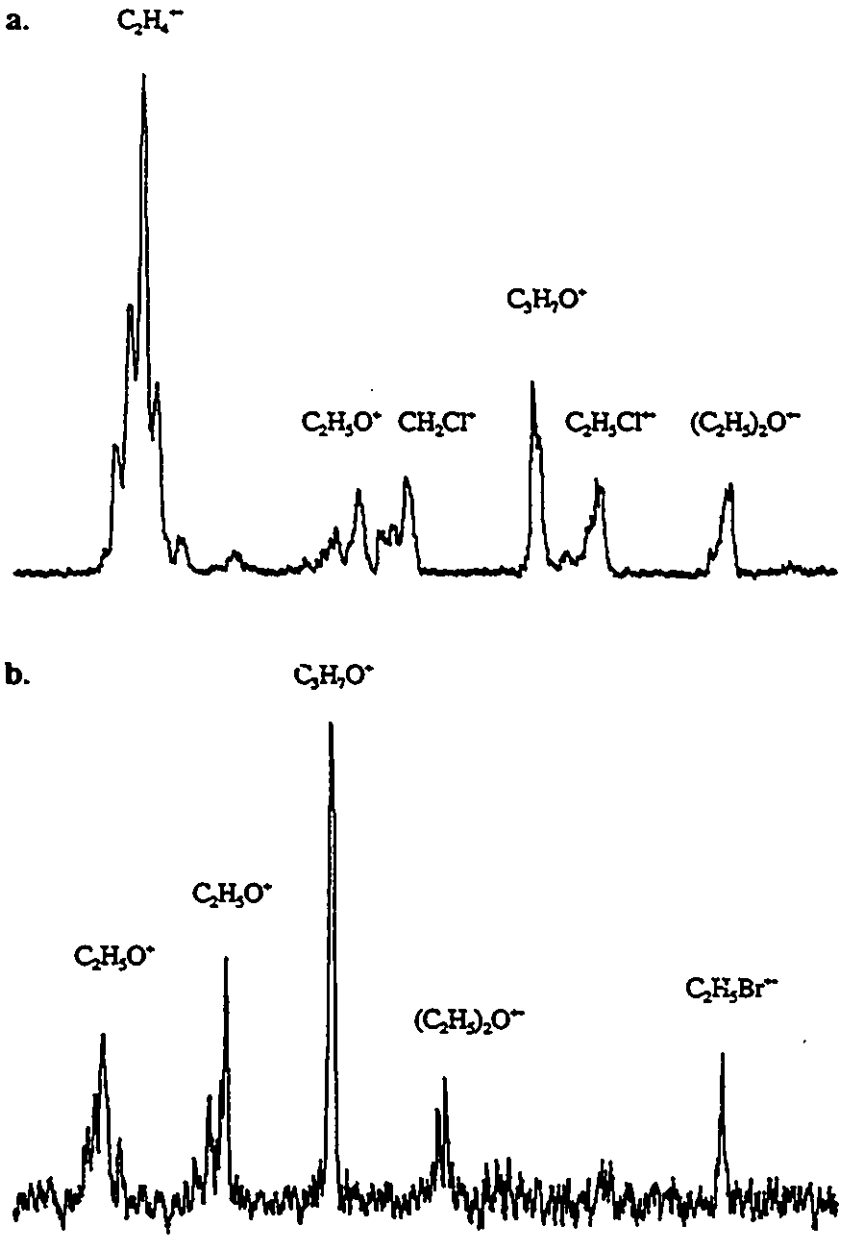

Figure 4.2 **CIDI mass spectra of $(C_2H_5)_2O^+CH_2CH_2X$**
a. X = Cl
b. X = Br

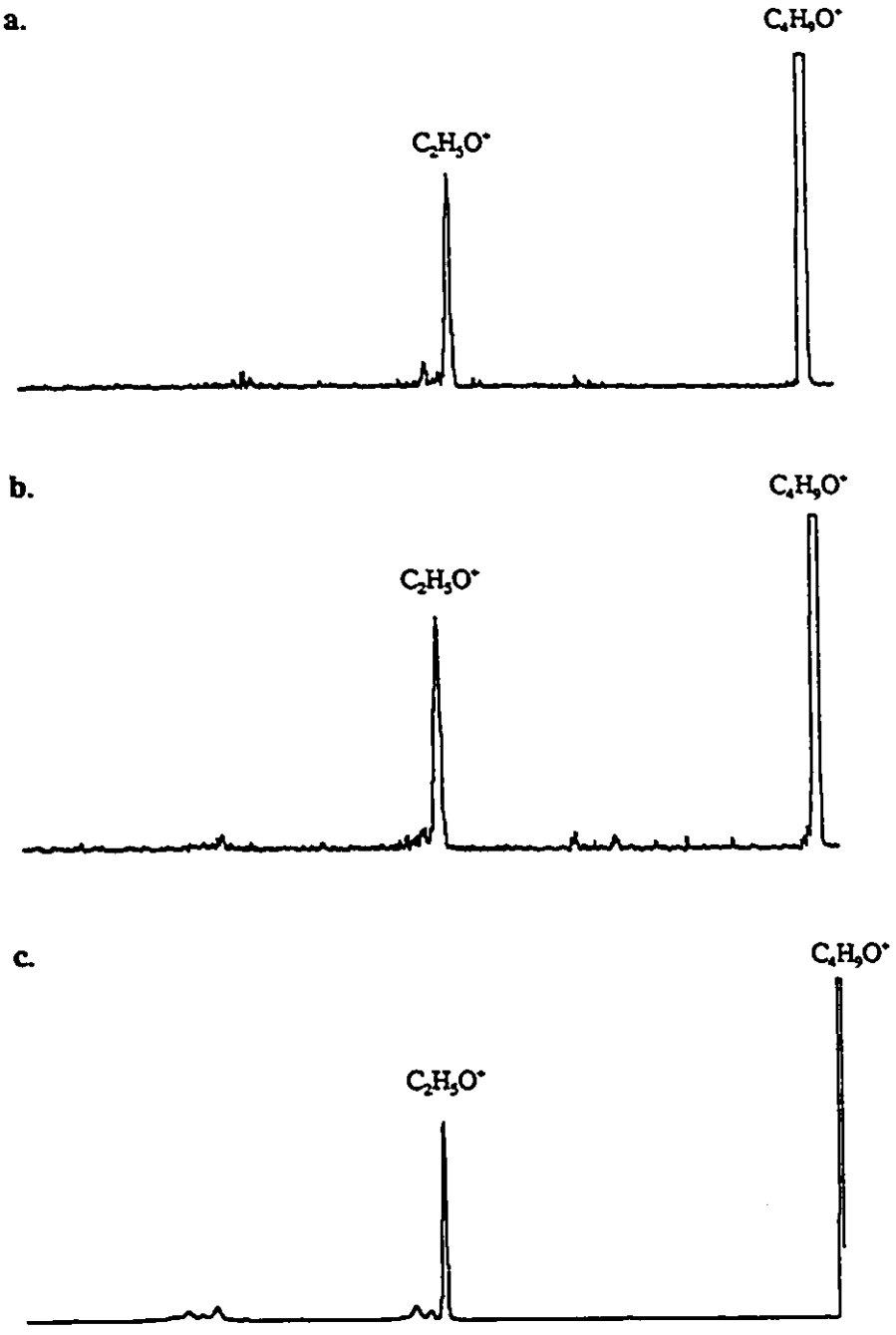

Figure 4.3 **CID mass spectra of $C_4H_9O^+$ ions**

a. $(C_2H_5)_2O^+CH_2CH_2Cl$ - C_2H_5Cl
b. $(C_2H_5)_2O^+CH_2CH_2Br$ - C_2H_5Br
c. $(C_2H_5O)_2CHCH_3^{+\bullet}$ - $C_2H_5O^\bullet$

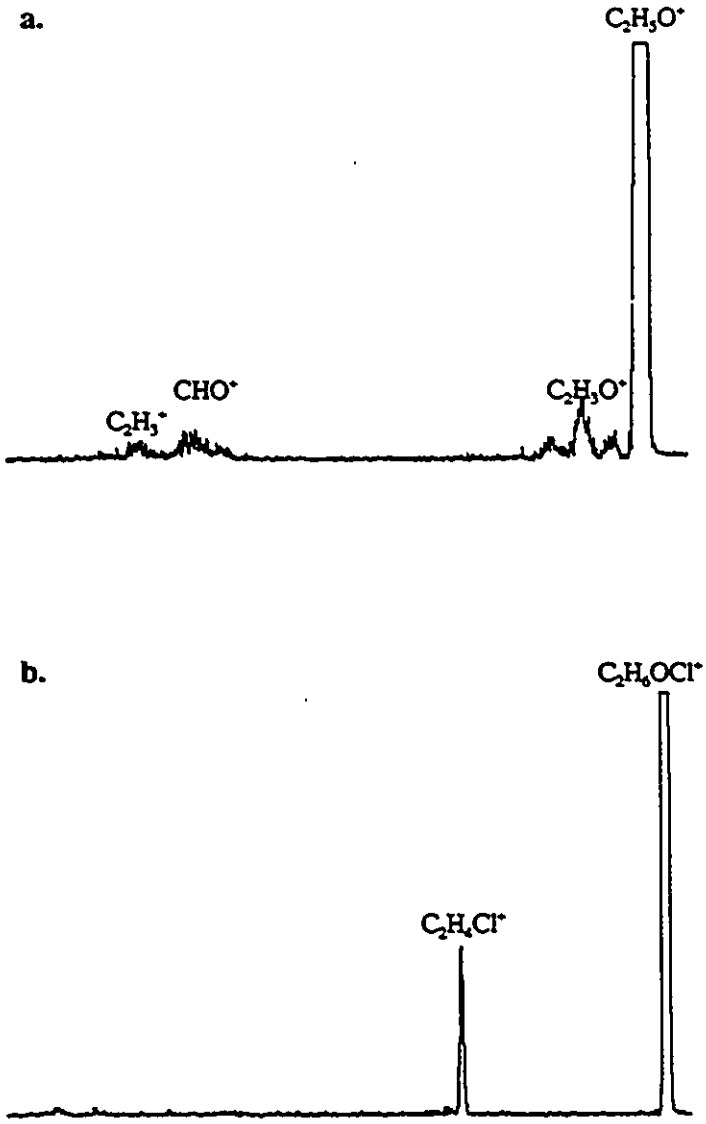

Figure 4.4 **CID mass spectra of the fragments from $(C_2H_5)_2O^+CH_2CH_2Cl$**

a. $(C_2H_5)_2O^+CH_2CH_2Cl$ - C_2H_4 - C_2H_5Cl

b. $(C_2H_5)_2O^+CH_2CH_2Cl$ - 2 C_2H_4

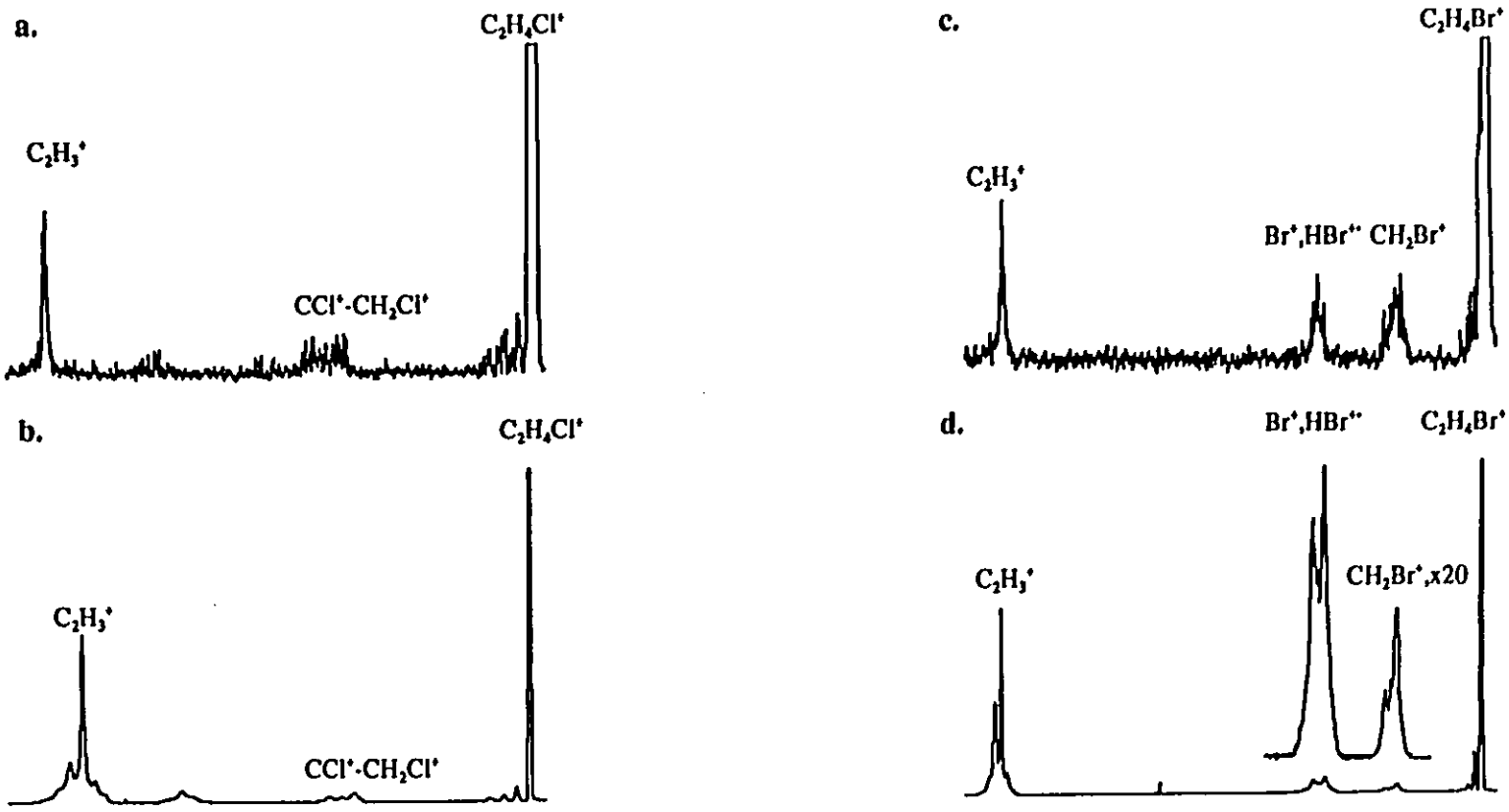

Figure 4.5 CID mass spectra of $C_2H_4X^+$ ions from I - $(C_2H_5)_2O$ and from $ClCH_2CH_2Br^{+\bullet}$ - $Br^\bullet$ (or $Cl^\bullet$)

a. Ia - $(C_2H_5)_2O$
b. $ClCH_2CH_2Br^{+\bullet}$ - $Br^\bullet$
c. Ib - $(C_2H_5)_2O$
d. $ClCH_2CH_2Br^{+\bullet}$ - $Cl^\bullet$

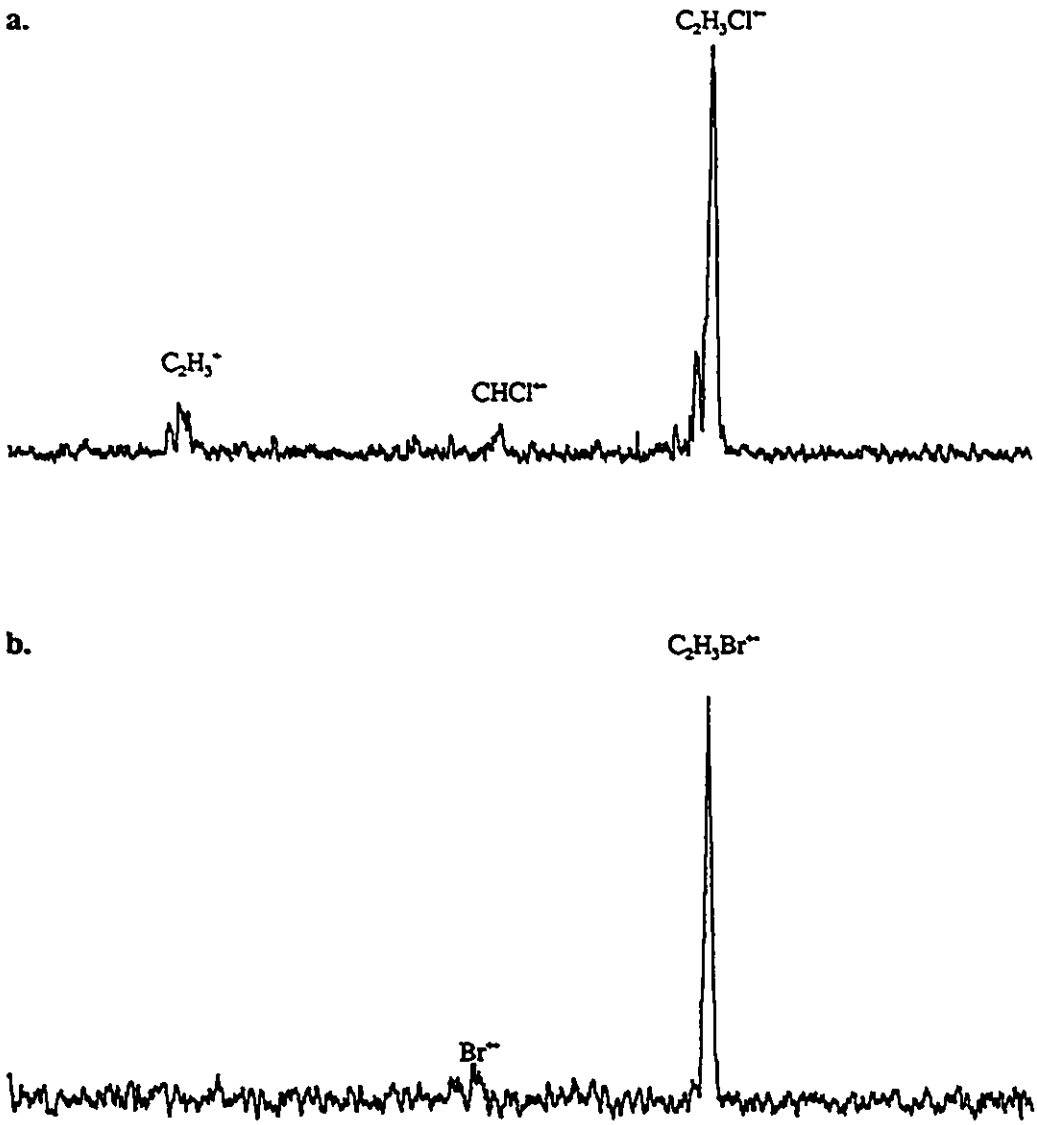

Figure 4.6 **CIDI mass spectra of $(C_2H_5)_2O^+CH(X)CH_3$**
a. X = Cl
b. X = Br

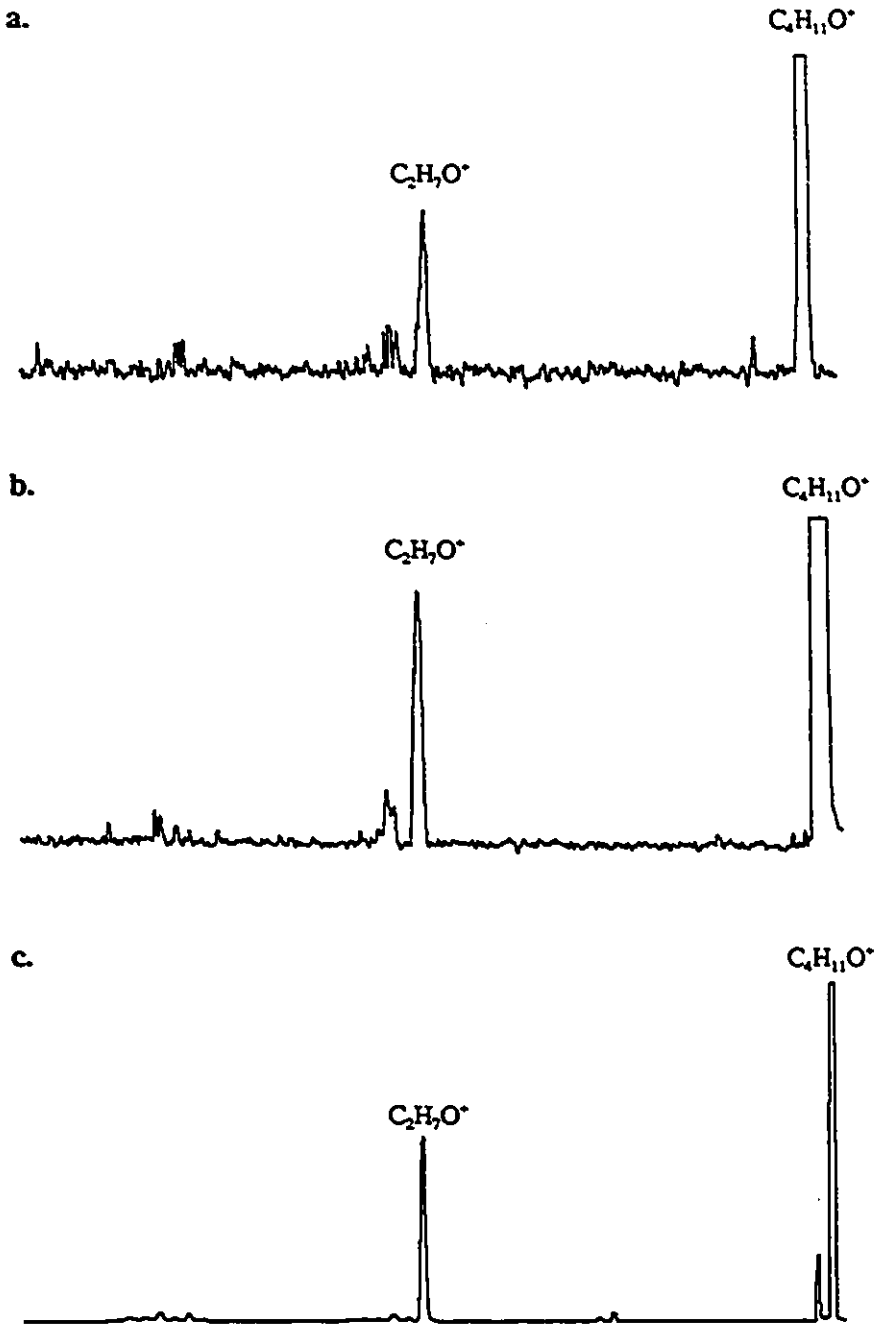

Figure 4.7 **CID mass spectra of $C_4H_{11}O^+$ ions**
a. $(C_2H_5)_2O^+CH(Cl)CH_3$ - C_2H_3Cl
b. $(C_2H_5)_2O^+CH(Br)CH_3$ - C_2H_3Br
c. $(C_2H_5)_2O + H^+$

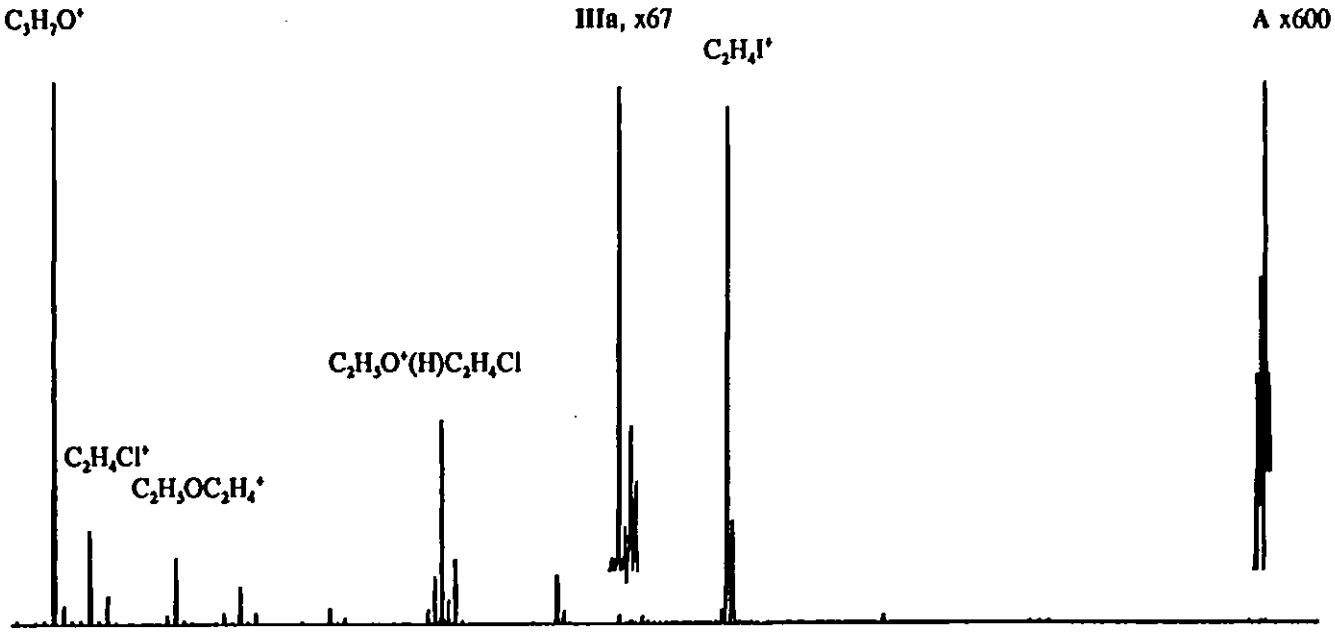

Figure 4.8 Normal mass spectrum of $ClCH_2CH_2OC_2H_5$ + C_2H_5I

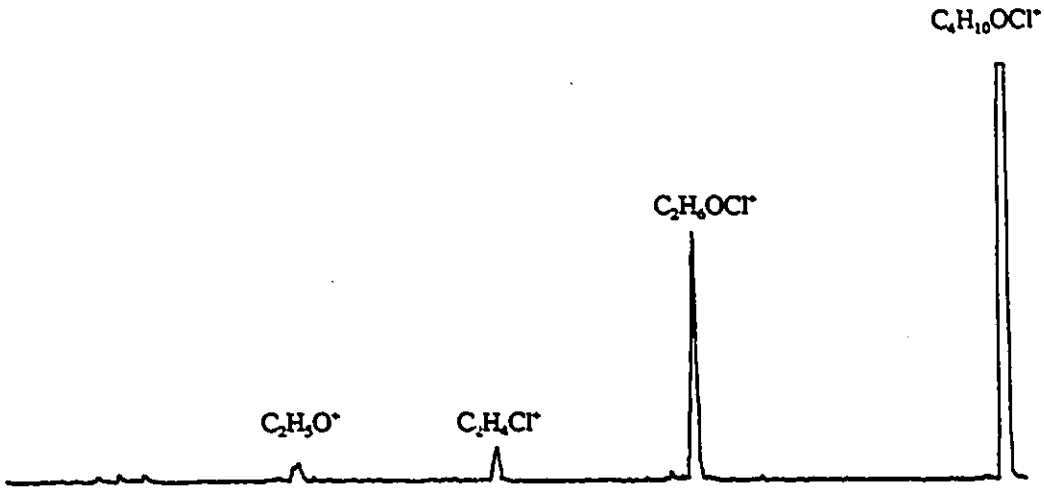

Figure 4.9 CID mass spectrum of $C_4H_{10}OCl^+$ from III - C_2H_4

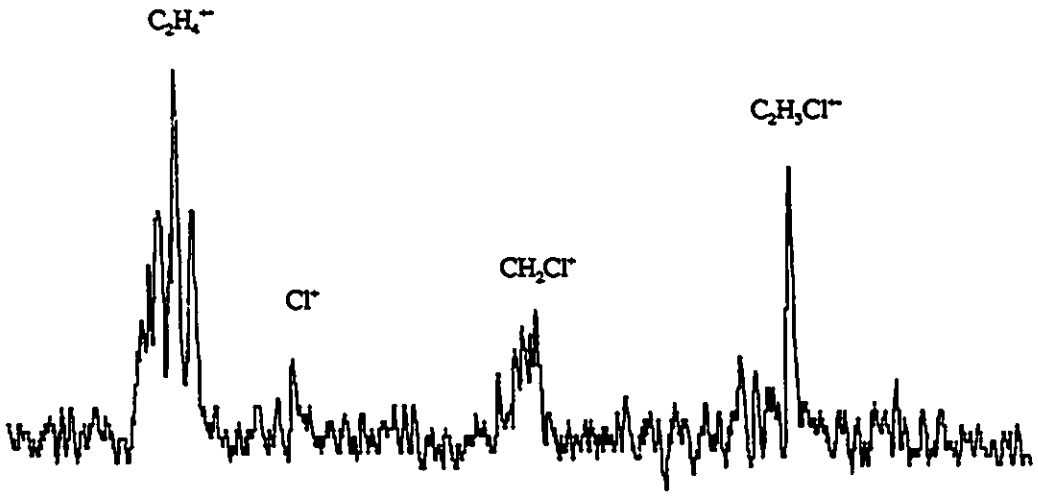

Figure 4.10 CIDI mass spectrum of III

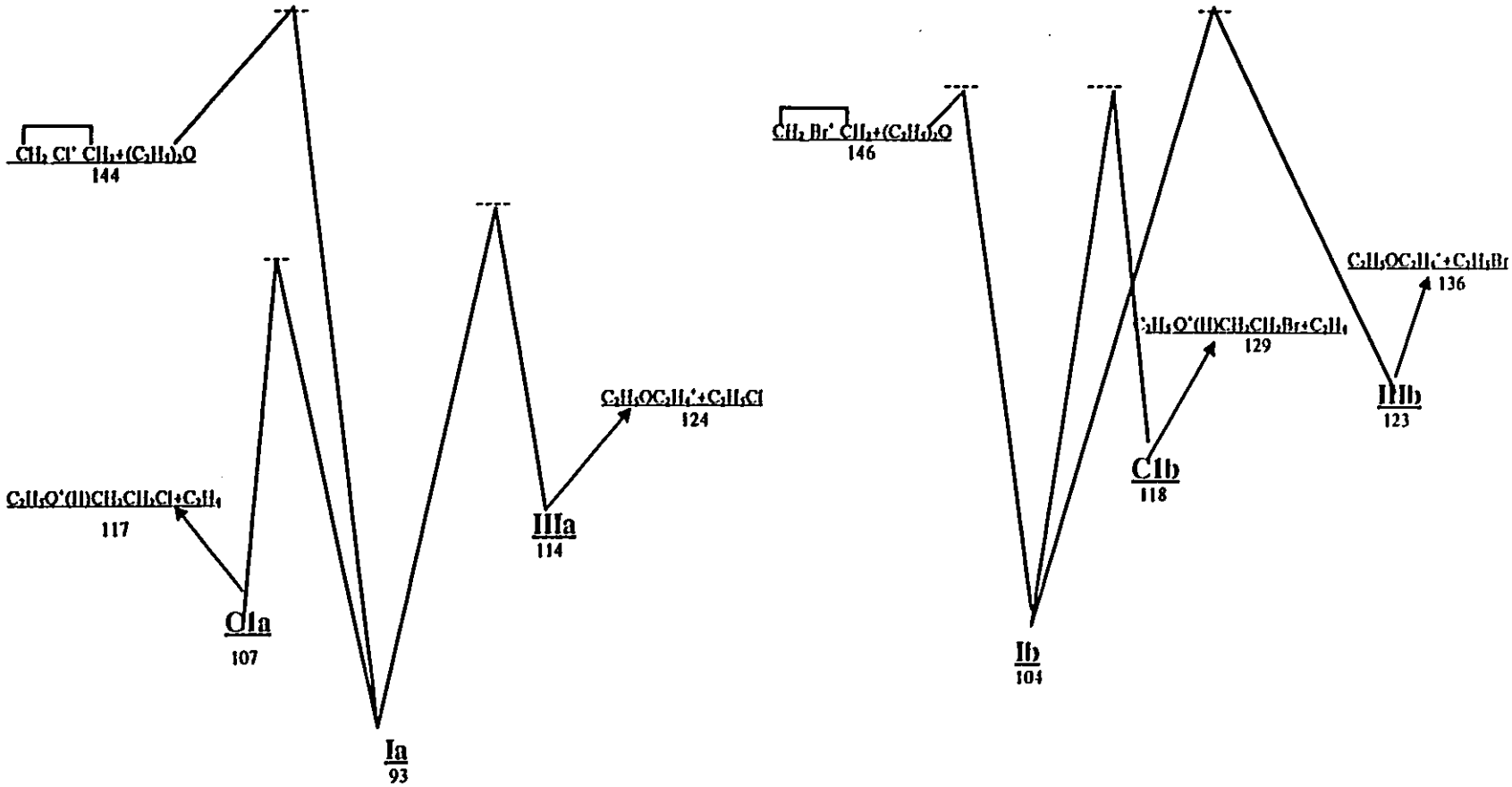

Figure 4.11 The Energy diagram for dissociations of Ia and Ib, in kcalmol^{-1}

Ia	$(C_2H_5)_2O^+CH_2CH_2Cl$	**Ib**	$(C_2H_5)_2O^+CH_2CH_2Br$
IIIa	$C_2H_5Cl^+CH_2CH_2OC_2H_5$	**IIIb**	$C_2H_5Br^+CH_2CH_2OC_2H_5$
C1a	$[C_2H_5O(C_2H_4Cl)H^+\bullet\bullet\bullet C_2H_4]$	**C1b**	$[C_2H_5O(C_2H_4Br)H^+\bullet\bullet\bullet C_2H_4]$

Chapter 5

$C_3H_6X^+$ Cations

5.1 Introduction

In Chapter 3 the $C_2H_4X^+$ isomers have been described in detail. Studies of the analogous $C_3H_6X^+$ ions (X = Cl and Br) will be presented in this chapter.

The possible structures for $C_3H_6X^+$ are given in Scheme 5.1. **IV** to **VIII** are so-called open halogen cations; **IX** is a four-membered cyclic halonium ion. Of special interest is the effect of methyl substitution on the $C_2H_4X^+$ isomers. $CH_3{}^+CXCH_3$ (**IV**) and $CH_3CH_2{}^+CHX$ (**VIII**) result from methyl substitution on $CH_3{}^+CHX$; $CH_3CHX^+CH_2$ (**V**) and $CH_3{}^+CHCH_2X$ (**VI**) result from methyl substitution on $XCH_2CH_2{}^+$; propenehalonium ions (**X**) result from methyl substitution on the cyclic ethylenehalonium ions. $XCH_2CH_2CH_2{}^+$ (**VII**) and its cyclic isomer, the trimethylene halonium ions (**IX**) are also important, being analogous to $XCH_2CH_2{}^+$ and $\overset{\frown}{CH_2\ X^+\ CH_2}$.

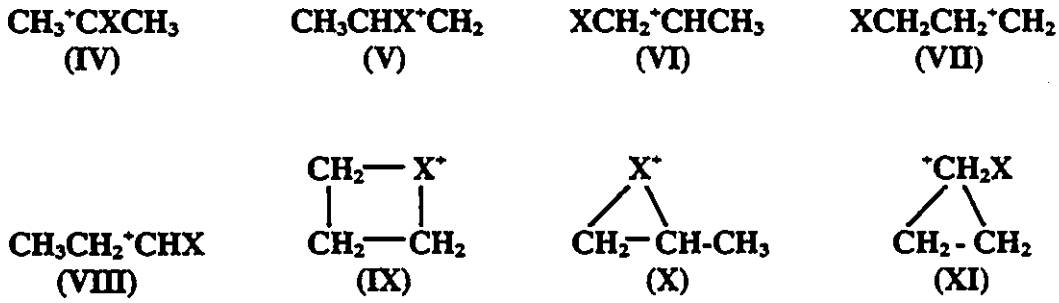

Scheme 5.1

When substituted 1,3-dihalo-propanes were dissolved in superacid media,[1-3] four

-membered ring halonium ions IX were observed, based on the observation of a 1,3-halogen shift. The participation of the 1,3-shift decreased in the sequence I > Br > Cl.[3] According to theoretical calculations, the four-membered cyclic chloronium ion (IXb) is ~18 kcalmol^{-1}[4] (or ~21 kcalmol^{-1}[5]) lower in energy than the open structured 3-chloro-propenyl ion (**VIIb**). For bromo analogues, the cyclic structure is also ~20 kcalmol^{-1} more stable than the opened form.[4]

Lambert et al suggested that the possible intermediates in the electrophilic opening of cyclopropane attacked by X^+ also involve another bridged species, CH_2-CH_2 ($^+CH_2X$) (**XIb**).[6] The 1-chloro-cyclopropanyl ion (**XIb**) was calculated to be 6 kcalmol^{-1} more stable than the 3-chloro-propenyl ion (**VIIb**).[7]

Olah et al[8] found that when 1,3-dihalo-propanes were treated with SbF_5-SO_2 at -78°C, the propenehalonium ion (X) was formed. Ion X could be formed through the trimethylenehalonium ion (IX) but this latter was not observed as an intermediate. The isomerization to X must therefore be fast. In addition, they found that 1,1-, 1,2- and 1,3-dichloropropanes exhibited identical pmr spectra and behaviour when dissolved in SbF_5-SO_2ClF solution.

$$\begin{matrix} CH_3CH_2CHCl_2 \text{ or} \\ CH_3CHClCH_2Cl \text{ or} \\ ClCH_2CH_2CH_2Cl \end{matrix} \xrightarrow[-60^{oc}]{SbF_5SO_2ClF} \underset{\textbf{VIIIb}}{CH_3CH_2{}^+CHCl} \longleftrightarrow \underset{\textbf{VIb}}{CH_3{}^+CHCH_2Cl} \longleftrightarrow \underset{\textbf{Xb}}{\overset{Cl^+}{\diagup\diagdown}\ CH_2\ CH\text{-}CH_3} \quad (1)$$

These observations suggest the formation of rapidly equilibrating ions **VIIIb**, **VIb** and **Xb**. The experiment also showed that the methyl hydrogens are not involved in any

exchange with the other three hydrogens. Finally the authors suggested that the chlorine atom, instead of stabilizing the charge by forming a σ bond, **Xb**, or via chlorine back donation, **VIIIb**, destabilizes ion **VIb** by its inductive effect.

Hehre and Hiberty[9] calculated the methyl substituent effects on CH_3CHX^+ and $XCH_2CH_2^+$ (X = F, Cl) from the energies (E) of the isodesmic reactions (reaction 2) using theoretical calculations at the STO-3G level.

$$C_3H_6X^+ + CH_4 \rightarrow C_2H_4X^+ + C_2H_6 \qquad (2)$$

The results showed that when the methyl group was substituted on the α-carbon (charge site), i.e. $CH_3CHX^+ \rightarrow CH_3^+CXCH_3$ or $XCH_2CH_2^+ \rightarrow XCH_2^+CHCH_3$, the ion will be stabilized by about 22 - 26 kcalmol^{-1}, however, when substituted on the β-carbon, i.e. $XCH_2CH_2^+ \rightarrow CH_3CHXCH_2^+$, the ion is only stabilized by about 6 kcalmol^{-1} (Table 5.1).

The gas phase $C_3H_6Br^+$ isomers have been produced from ionized dibromopropane molecular ions followed by Br loss.[10-12] The heats of formation of $CH_3^+CBrCH_3$ (**IVc**) and $CH_3^+CHCH_2Br$ (**VIc**) have been measured using an electron monochromator.[10] The heat of formation of **IVc** is 178 kcalmol^{-1} and that of **VIc** is 195 kcalmol^{-1}. This shows that the ion with the Br on the α-position is more stable than that with Br on the β-position. Compared to the heats of formation of $C_2H_4Br^+$ ions (Table 3.2), it can be seen that the methyl group is a more effective stabilizer at the α-carbon of an acyclic isomer than at a ring carbon of the cyclic isomer, as shown in Scheme 5.2.

$$\underset{(\Delta H_f^\circ = 208\ \text{kcalmol}^{-1})}{CH_3^+CHBr} \xrightarrow{CH_3,\ -H} \underset{(\Delta H_f^\circ = 178\ \text{kcalmol}^{-1})}{CH_3^+CBrCH_3}$$

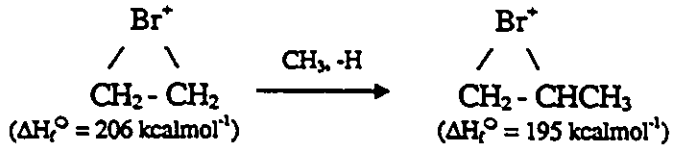

Scheme 5.2

Moreover, when methyl substitution is made on the ring carbon of the cyclic bromonium structure, the calculated angle of C(Br) – C increased from 70.6° to 90.7°.[13] In the analogous chloronium ion, the angle of C(Cl) – C increased from 69.6° to 86.8°.[14] These results indicate that the stabilization by the methyl group replaces the electron-donation of the halogen.

Recently, Heck and Nibbering studied the bimolecular reactions of $C_3H_6Br^+$ isomers by FT-ICR mass spectrometry. Three stable isomers IVc, IXc and Xc were identified.[12] Isomer IVc reacted with substrate molecules predominantly via proton transfer whereas isomer IXc predominantly reacted via adduct formation. Since the $C_3H_6Br^+$ ion, produced from $BrCH_2CHBrCH_3^{+\bullet}$ by $Br^\bullet$ loss, did not easily transfer a proton to a suitable substrate, the structure Xc was proposed for it.

The $C_3H_6Br^+$ isomers will be further distinguished and the $C_3H_6Cl^+$ isomers will be characterized in this chapter.

5.2 Experimental

All metastable ion (MI), collision induced dissociation (CID) and neutralization reionization (NR) mass spectra were performed with a VG-ZAB-3F mass spectrometer. The conditions are same as described in Chapter 2. Collision induced dissociative

ionization (CIDI) mass spectra were recorded using a potential of -1000 V on the ion beam deflector electrode in the 2ffr; the ionization target was oxygen. The CID mass spectra of the daughter ions were obtained by transmiting them to the 3ffr, where the target gas was O_2. Appearance energies (AE) were measured using an electron monochromator.

To examine the reactions of $C_3H_6X^+$ ions with diethylether, appropriate halogenated precursor molecules were admitted to the ion source such that the ratio of the ether to the precursor was 1:1. The total ion source pressure was set at 2-4 x 10^{-5} mbar.

The $C_3H_6X^+$ ions were produced by loss of Y from the ionized dihalo-propane $C_3H_6XY^{+\cdot}$ (X and Y = Cl and Br). The dihalo-propanes were commercially available. Table 5.2 shows the formation of $C_3H_6X^+$ ions, the structures of which required further examination.

5.3 Results and discussion

5.3.1 Unimolecular dissociations

The MI mass spectra of $C_3H_6X^+$ ions were dominated by HX loss ($C_3H_6X^+ \rightarrow C_3H_5^+ + HX$). The metastable peak for this process was composite. The distribution of released energies, n(T) vs the released energy, T (meV) was obtained by the method described in Reference 62. A representive plot of n(T) vs T (meV) from the metastable peak of $CH_3C^+ClCH_3$ is shown in Figure 5.1. The metastable peak components of $C_3H_6Cl^+$ isomers were thus separated into a narrow peak with the KER value ($T_{0.5}$) ranging from 6 to 16 meV and a wide peak with $T_{0.5}$ ranging from 79 to 225 meV. The results are given in Table 5.3.

A detailed CID mass spectrometric study of the $C_3H_5^+$ daughter ion was attempted by transmitting $C_3H_5^+$ ions at the center (4260 eV) of the metastable peak from $CH_3^+CClCH_3$ to the 3ffr, where the $C_3H_5^+$ ions were collisionally activated by target gas. The ratio of m/z 26 to m/z 27 in the CID mass spectrum thus produced was close to 1.0. It has been demonstrated[15] that at a translational energy of 4200 eV the ratio of m/z 26 to m/z 27 is 2 and 0.67 for $CH_3^+CCH_2$ and $CH_2CHCH_2^+$, respectively. Hence the ratio of 1.0 indicated that the MI dissociation process produced mainly the allyl cation. An attempt to separate the two isomers by transmitting the $C_3H_5^+$ ions at the edge (4306 eV) of the metastable $CH_3^+CClCH_3$ peak to the 3ffr failed, because the ratio of m/z 26 to m/z 27 in the CID mass spectrum remained close to 1.0. Possibly some of the $C_3H_5^+$ ions transmitted from the edge of the peak were collision induced in the 2ffr. Moreover, the components of the metastable peak were not easily separable given the resolution of the mass spectrometer.

Further study by increasing the collision gas pressure in the 2ffr showed that the ratio of m/z 26 to m/z 27 in the CID mass spectrum of the $C_3H_5^+$ daughter ion did not change, indicating that the two isomers of $C_3H_5^+$ ions were produced with the same energy barrier. The production of the allyl cation will give a higher kinetic energy release value than the production of $CH_3CCH_2^+$ since the heat of formation of $CH_2CHCH_2^+$ is 226 $kcalmol^{-1}$[38], being 5 $kcalmol^{-1}$ lower in energy than isomer $CH_3CCH_2^+$. Thus the broad component, which is also the greater component in the MI composite peaks of $C_3H_6Cl^+$ isomers likely arises from the allyl cation. The cogeneration of $CH_3CCH_2^+$ with $CH_2CHCH_2^+$ resulted in the observed composite metastable peak but with $CH_3C^+CH_2$

giving rise to the small, narrow component. Moreover the dissociation energy barrier for $CH_3CCl^+CH_3$ ions to dissociate to $C_3H_5^+$ via HCl loss was estimated to be above 209 kcalmol^{-1} [$\Delta_fH^\circ(CH_3CCH_2^+)$ + $\Delta_fH^\circ(HCl)$ = 231 - 22 = 209 kcalmol^{-1}). The other $C_3H_6Cl^+$ isomers also showed a product mixture of $C_3H_5^+$ isomers (Table 5.4) and similar kinetic release energy ($T_{0.5}$) values in their MI mass spectra (Table 5.3), indicating they have a similar dissociation energy barrier for HCl loss.

The CID mass spectra of the $C_3H_6X^+$ ions are still dominated by the HX loss (Tables 5.5 and 5.6), which is the dissociation of lowest energy requirement. The next fragmentation process is C_2H_4 loss, which requires 38 kcalmol^{-1} (X = Cl) or 20 kcalmol^{-1} (X = Br) more energy than HX loss.

						Product enthalpies (kcalmol^{-1})		
					X =	Cl	Br	
$C_3H_6X^+$	→	$C_3H_5^+$	+	HX		204	217	(3)
$C_3H_6X^+$	→	CH_2X^+	+	C_2H_4		242	236.5	(4)

5.3.1.1 The $C_3H_6Cl^+$ isomers

The CID mass spectrum of $CH_3^+CClCH_3$ is distinguishable from the other $C_3H_6Cl^+$ ions by the production of $C_3H_6^{+\cdot}$ (Table 5.5), indicating an easy hydrogen shift from a methyl group to the center carbon. In radical ions hydrogen tends to act as an electrophile.[17] The center carbon atom may have some electron density which could be obtained by electron-donation from the halogen atom. A mechanism is shown in Scheme 5.3.

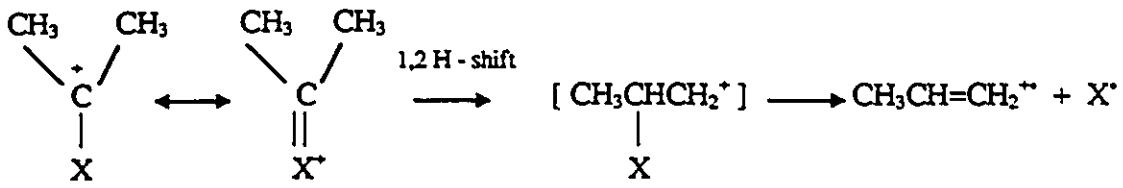

Scheme 5.3

The ions of formal structure $CH_3^+CHCH_2Cl$ **(VIb)**, $CH_3CH_2^+CHCl$ **(VIIIb)** and $ClCH_2CH_2CH_2^+$ **(VIIb)** are indistinguishable (Table 5.5). A more detailed CID mass spectrometric study on the region of $C_2HX^{+\bullet}$ to $C_2H_3X^{+\bullet}$ (Figure 5.2) also failed to clearly distinguish these isomers. This indicates that the hydrogen atoms may be able to transfer freely between carbons.

VIb is approximately 20 kcalmol^{-1} lower in energy than **VIIb**, analogous to that of $CH_3^+CHCH_3$ (ΔH_f° = 191 kcalmol^{-1}) and $CH_3CH_2CH_2^+$ (ΔH_f° = 211 kcalmol^{-1}). **VIIIb** may be similar in energy to **VIb**, but the latter can also form a more stable isomer **Xb** involving a Cl bridge. Thus a sequence of hydrogen shifts may be proposed, as shown in Scheme 5.4. The estimation of the heats of formation of these isomers will be discussed later.

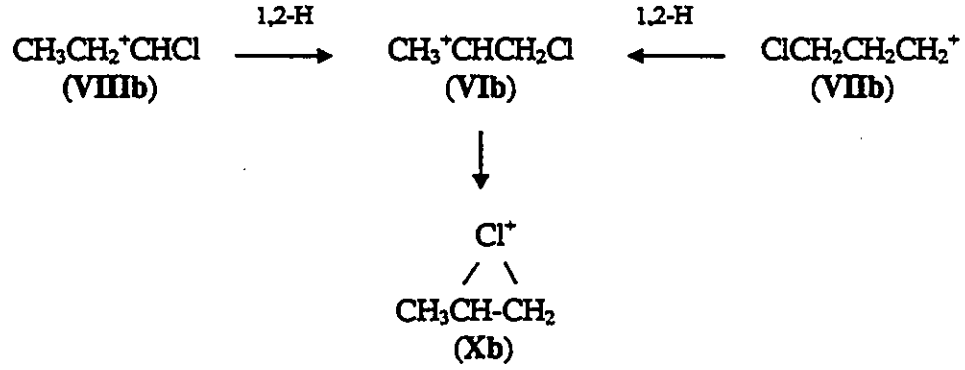

Scheme 5.4

As the CID mass spectrum of **VIIb** was identical with that of **VIb** and **VIIIb**, the four-membered isomer **IXb** could not be identified by CID mass spectrometry.

The NR mass spectrum of $CH_3^+CClCH_3$ (Figure 5.3) showed an intense recovery signal of $C_3H_6Cl^+$, indicating that stable neutral $C_3H_6Cl^\cdot$ survived the neutralization process. Moreover, the NR mass spectrum of $CH_3^+CClCH_3$ is generally similar to its CID mass spectrum, indicating no geometric change in the neutralization process. The observed Cl^+ and $HCl^{+\cdot}$ in the NR mass spectrum of $CH_3^+CClCH_3$ likely results from the collision induced dissociation of $CH_3^+CClCH_3$ accompanying the neutralization process with dimethylamine (DMA), as shown by reaction 4. The dissociations of $CH_3^+CClCH_3$ via Cl and HCl losses are reactions of low energy requirement, the latter producing the pase peak in the CID mass spectrum. The dissociation of neutral $CH_3C^\cdot ClCH_3$ (reaction 6) may contribute to the flux of neutral $Cl^\cdot$ and HCl. Note that the ionization energies (IE) of $Cl^\cdot$ and $HCl^{+\cdot}$ (13.0 eV and 12.7 eV) are much higher than those of $C_3H_5^+$ and $C_3H_6^{+\cdot}$ (8.13 eV and 9.73 eV).

$$\begin{array}{lcl} & \xrightarrow{\text{DMA}} & \\ CH_3^+CClCH_3 & \rightarrow & \begin{array}{l} C_3H_5^+ + HCl \xrightarrow{\text{deflector}} HCl \xrightarrow{O_2} HCl^{+\cdot}, Cl^+ \\ C_3H_6^{+\cdot} + Cl \rightarrow Cl \rightarrow Cl^+ \end{array} \end{array} \qquad (4)$$

$$\begin{array}{lcl} & \xrightarrow{\text{DMA}} & \xrightarrow{O_2} \\ CH_3^+CClCH_3 & \rightarrow & CH_3^\cdot CClCH_3 \rightarrow CH_3^+CClCH_3 \rightarrow \begin{array}{l} C_3H_5^+ + HCl \\ C_3H_6^{+\cdot} + Cl^\cdot \end{array} \end{array} \qquad (5)$$

$$\begin{array}{lcl} & \xrightarrow{\text{DMA}} & \xrightarrow{O_2} \\ CH_3^+CClCH_3 & \rightarrow & CH_3^\cdot CClCH_3 \rightarrow \begin{array}{l} C_3H_5^\cdot + HCl \rightarrow C_3H_5^+ + HCl^{+\cdot} \\ C_3H_6 + Cl^\cdot \rightarrow C_3H_6^{+\cdot} + Cl^+ \end{array} \end{array} \qquad (6)$$

The NR mass spectra of the other isomers **VIb**, **VIIb** and **VIIIb** showed very weak recovery signals (Figures 5.4 - 5.6), suggesting either a low neutralization probability or production of unstable neutral $C_3H_6Cl^{\bullet}$, which rapidly dissociates to fragments such as $C_3H_5^{\bullet}$ + HCl or C_3H_6 + $Cl^{\bullet}$ (reaction 7). Note that for these isomers, $HCl^{+\bullet}$ and Cl^+ are relatively much more important than for $CH_3C^+ClCH_3$ ions. Since little $C_3H_6^{+\bullet}$ is observed in the CID mass spectra of these $C_3H_6Cl^+$ isomers, the observation of Cl^+ in their NR mass spectra may result from the dissociation of $HCl^{+\bullet}$.

$$C_3H_6Cl^+ \xrightarrow{DMA} CH_3{}^{\bullet}CClCH_3 \rightarrow \begin{matrix} C_3H_5^{\bullet} + HCl \xrightarrow{O_2} C_3H_5^+ + HCl^{+\bullet} \\ C_3H_6 + Cl^{\bullet} \rightarrow C_3H_6^{+\bullet} + Cl^+ \end{matrix} \qquad (7)$$

$$C_3H_6Cl^+ \xrightarrow{DMA} C_3H_5^+ + HCl \xrightarrow{deflector} Hcl \xrightarrow{O_2} HCl^{+\bullet}, Cl^+ \qquad (8)$$

The intense peak at $C_2H_3Cl^{+\bullet}$ in the NR mass spectra of **VIb**, **VIIb** and **VIIIb** indicated that neutral $C_3H_6Cl^{\bullet}$ preferably dissociated via $CH_3^{\bullet}$ loss, which is rarely observed in their CID mass spectra. Thus the structure of neutral $C_3H_6X^{\bullet}$ is likely to be $CH_3CHClCH_2^{\bullet}$, which may easily lose $CH_3^{\bullet}$ compared to the other isomers.

5.3.1.2 The $C_3H_6Br^+$ isomers

By CID mass spectrometry $CH_3{}^+CBrCH_3$ (**IVc**) and $BrCH_2CH_2CH_2^+$ (**VIIc**) are distinguishable from $CH_3CHBrCH_2^+$ (**Vc**) and $CH_3{}^+CHCH_2Br$ (**VIc**), see Table 5.6 and Figure 5.7.

The formation of the four-membered isomer $\begin{matrix} CH_2 - Br^+ \\ | \quad | \\ CH_2 - CH_2 \end{matrix}$ (**IXc**) from **VIIc** has been

observed by FT-ICR mass spectrometry[12]. Since the ion **IXc** is calculated to be about 20 kcalmol^{-1} more stable than **VIIc**[4], the isomer produced from $BrCH_2CH_2CH_2Br^{+\bullet}$ is indeed likely to be **IXc**. This indicates that the bromonium ion has a stronger tendency to form the four-membered ring than the analogous chloronium ion, a result consistent with the observations in the condensed phase.[1-3] The identical CID mass spectra of **Vc** and **VIc** (Table 5.6 and Figure 5.7) suggests that both ions likely form the propenebromonium ion CH_3-$\overline{CHBr^{+}CH_2}$ (**Xc**). The three isomers, **IVc**, **Xc** and **XIc** can be identified by CID mass spectrometry indicating that hydrogen transfer is not competing with brominium ion transfer (or bridging), as shown in Scheme 5.5.

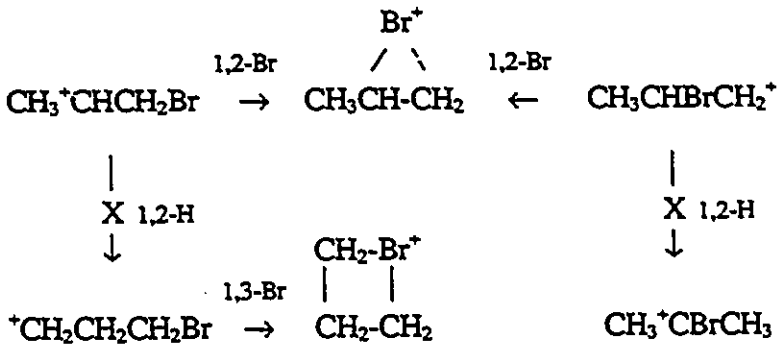

Scheme 5.5

The NR mass spectra of $C_3H_6Br^+$ isomers were dominated by neutral dissociations, as shown in Figures 5.8 - 5.10. The most intense peaks of $HBr^{+\bullet}$ and Br^+ may result from the collision process shown in reaction 9, which is the lowest energy requirement process in the dissociations of $C_3H_6Br^+$, see Table 5.9.

$$C_3H_6Br^+ \xrightarrow{DMA} C_3H_5^+ + HBr \xrightarrow{deflector} HBr \xrightarrow{O_2} Br^{+\bullet}, Br^+ \qquad (9)$$

$$C_3H_6Br^+ \xrightarrow{DMA} C_3H_6Br^\bullet \rightarrow \begin{matrix} C_3H_6 + Br^\bullet \\ C_3H_5^\bullet + HBr \end{matrix} \xrightarrow{O_2} \begin{matrix} C_3H_6^{+\bullet} + Br^+ \\ C_3H_5^+ + HBr^{+\bullet} \end{matrix} \qquad (10)$$

The intense Br^+ peak may also result from the radical dissociation to $Br^\bullet$ shown in reaction 8. The C-Br bond in $C_3H_6Br^\bullet$ neutrals will be much weaker than that in $C_3H_6Br^+$ and those in $C_3H_6Br^\bullet$ and $C_3H_6Br^+$ could be analogous to those in $C_2H_4Br^\bullet$ and $C_2H_4Br^+$, i.e.

					Bond energy
	$BrCH_2CH_2^\bullet$	$\rightarrow$	C_2H_4 +	$Br^\bullet$	(kcalmol^{-1})
ΔH_f°(kcalmol^{-1})	32		12.5	27	7.5
	$CH_2Br^+CH_2$	$\rightarrow$	$C_2H_4^{+\bullet}$ +	$Br^\bullet$	
ΔH_f°(kcalmol^{-1})	206		255	27	76

However, as in the case of $C_3H_6Cl^+$, the ionization energies of $Br^\bullet$ and HBr (11.8 eV and 11.7 eV) are higher than those of $C_3H_5^\bullet$ and C_3H_6, reaction 10 may only produce minor Br^+ and $HBr^{+\bullet}$. Thus in the NR mass spectra of $BrCH_2CH_2CH_2^+$ and $BrCH_2{}^+CHCH_3$ (Figures 5.9 and 5.10) the major process is the collision induced dissociation of $C_3H_6Br^+$ in the neutralization process. This is consistent with the fact that no recovery signal was observed. In the NR mass spectrum of $CH_3{}^+CBrCH_3$ the observation of a recovery signal and the similarity to its CID mass spectrum indicated that the neutral $CH_3C^\bullet BrCH_3$ is stable and survived the reionization process.

$$CH_3{}^+CBrCH_3 \xrightarrow{DMA} CH_3{}^\bullet CHBrCH_3 \xrightarrow{O_2} CH_3{}^+CBrCH_3 \rightarrow \begin{matrix} C_3H_5^+ + HBr \\ C_3H_6^{+\bullet} + Br^\bullet \end{matrix} \qquad (11)$$

5.3.2 Reaction with diethyl ether

When dihalopropanes (except $CH_3CX_2CH_3$) were reacted with diethylether in the ion source, oxonium ions $(C_2H_5)_2O^+C_3H_6X$ were observed in the normal mass spectra at m/z 151 (X = Cl) and m/z 195 (X = Br). The formation of the oxonium ions is discussed in Chapter 7 where it is proposed that the oxonium ions were formed from molecular adducts by a halogen loss.

$$XCH_2CH_2CH_2Br^{+\bullet} + (C_2H_5)_2O \rightarrow XCH_2CH_2CH_2Br^{+\bullet}\bullet(C_2H_5)_2O$$

$$\downarrow$$

$$(C_2H_5)_2O^+C_3H_6X + Br^\bullet$$

The oxonium ions $(C_2H_5)_2O^+C_3H_6X$ showed competing dissociations by C_2H_4, $(C_2H_5)_2O$, C_2H_5X and C_3H_5X losses in their CID mass spectra (Tables 5.7 and 5.8). The neutral structures were confirmed by their CIDI mass spectra (Figures 5.11 and 5.12).

$$\begin{array}{lcccl} (C_2H_5)_2O^+C_3H_6X & \rightarrow & C_5H_{12}OX^+ & + & C_2H_4 \\ & \rightarrow & C_5H_{11}O^+ & + & C_2H_5X \\ & \rightarrow & C_3H_6X^+ & + & (C_2H_5)_2O \\ & \rightarrow & (C_2H_5)_2OH^+ & + & C_3H_5X \end{array} \qquad (12)$$

The first three dissociation channels resemble the dissociations of $(C_2H_5)_2O^+CH_2CH_2X$, however the last resembles the dissociation of $(C_2H_5)_2O^+CHXCH_3$ (Chapter 4). The CID mass spectrum of the daughter ions from $[(C_2H_5)_2O\bullet CH_2CH_2CH_2X]^+$ showed that the structure of $C_5H_{12}OX^+$ (from C_2H_4 loss) is likely to be $C_2H_5O^+(H)CH_2CH_2CH_2X$ (Figures 5.13a and 5.14a), an ion which dissociated by C_2H_4, C_2H_5OH, C_2H_3X and C_3H_5X losses. The structure of $C_5H_{11}O^+$, (the daughter ion

from C_2H_5X loss) was $C_2H_5OC_3H_6^+$ which in turn dissociated predominantly by C_2H_4 loss (Figure 5.13 b). The $(C_2H_5)_2O$ loss from $[(C_2H_5)_2O{\bullet}CH_2CH_2CH_2X]^+$ produces a $C_3H_6X^+$ ion as shown in Figures 5.13c and 5.14b. The structure of the daughter ion $C_4H_{11}O^+$ (C_3H_5X loss) was shown to be $(C_2H_5)_2OH^+$ which also dissociated predominantly by C_2H_4 loss (Figure 5.13d). Analogous to the dissociations of $(C_2H_5)_2O^+CH_2CH_2X$, the structure of $[(C_2H_5)_2O{\bullet}CH_2CH_2CH_2X]^+$ is most likely $(C_2H_5)_2O^+CH_2CH_2CH_2X$, with a covalent O-C bond. The C_3H_5X loss indicates a hydrogen transfer from the C_3H_6X group to oxygen. Note that the β-H shift was not observed in the MI and CID mass spectra of $(C_2H_5)_2O^+CH_2CH_2Cl$ (Chapter 4). Thus the hydrogen in the group $CH_2CH_2CH_2X$ is more active than that in the CH_2CH_2X group, indicating that the C-H bond was strengthened by the α-halogen in the CH_2CH_2X group. Since $XCH_2CH_2CH_2^+$ has a similar reactivity to diethylether as that of $CH_2X^+CH_2$ (Chapter 4), the identity of the four-membered ring isomer **IX** is thus further confirmed.

The oxonium ions $(C_2H_5)_2O^+C_3H_6X$, formed from the reaction of $CH_3CHBrCH_2X$ (X = Cl or Br) with $(C_2H_5)_2O$ followed by Br loss, dissociated largely by loss of C_3H_5X as shown in their CID and CIDI mass spectra (Tables 5.7 and 5.8, Figures 5.11 and 5.12) indicative of the active hydrogen in the methyl group.

$$[(C_2H_5)_2O{\bullet}CH(CH_2X)CH_2]^+ \rightarrow C_4H_{10}OH^+ + C_3H_5X \qquad (13)$$

In the normal mass spectrum of $CH_3CX_2CH_3$ + $(C_2H_5)_2O$ no oxonium ions were found. It was shown in Chapter 4 that the possibility of forming $(C_2H_5)_2O^+CHXCH_3$ ions is much lower than that to form $(C_2H_5)_2O^+CH_2CH_2X$. The formation of these oxonium ions is proposed as an elimination-addition process, i.e. the diethyl ether molecule replaces Y (the leaving atom being Cl or Br). The methyl group may have strong steric effect and thus in the case of $CH_3CX_2CH_3$, the two methyl groups will certainly hinder the formation of $[(C_2H_5)_2OC_3H_6X]^+$.

5.3.3 Energetic evaluations

5.3.3.1 Methyl substituent effects on CH_3CHX^+ and heats of formation of $CH_3^+CXCH_3$

Referring to the reaction 2 $(C_3H_6X^+ + CH_4 \rightarrow C_2H_4X^+ + C_2H_6)$[9] the methyl substitution effect on CH_3CHF^+ (ΔH_f°, 166 kcalmol^{-1} [18] can be estimated from the heat of formation of $CH_3^+CFCH_3$ (138 - 143 kcalmol^{-1} [18,19]) to be - 24±3 kcalmol^{-1} and the methyl substitution effect on CH_3CHBr^+ (ΔH_f°, 208 kcalmol^{-1} [10]), estimated from the heat of formation of $CH_3^+CBrCH_3$ (178 kcalmol^{-1} [10]) to be - 28 kcalmol^{-1} [taking ΔH_f° (CH_4) = - 18 kcalmol^{-1} [16] and ΔH_f° (C_2H_6) = -20 kcalmol^{-1} [16]]. Thus if the methyl sustituent effect on CH_3CHCl^+ is within - 24-28 kcalmol^{-1}, then the heat of formation of $CH_3^+CClCH_3$ can be estimated to be 170 ± 3 kcalmol^{-1}, using ΔH_f° (CH_3CHCl^+) = 198 kcalmol^{-1} [10].

A plot of Δ_fH° (CH_3CHX^+) vs Vx (a scale of electronegativity[20]) values gave an equation for Δ_fH° (CH_3CHX^+) = 276 - 11.1 Vx (kcalmol^{-1}), see Chapter 3. The heats of formation of CH_3CHX^+ are 166 kcalmol^{-1}, 198 kcalmol^{-1} and 208 kcalmol^{-1} for X = F, Cl and Br, respectively, and the Vx value are 9.915, 7.04 and 6.13 for X = F, Cl and Br, respectively.[20] A plot of Δ_fH° ($CH_3C^+XCH_3$) against Vx can be described by the

equation $\Delta_f H^\circ$ ($CH_3C^+XCH_3$) = 239 - 9.85 Vx (kcalmol^{-1}). The heats of formation of $CH_3C^+ClCH_3$ are 141 kcalmol^{-1}, 170 kcalmol^{-1} and 178 kcalmol^{-1} for X = F, Cl and Br, respectively. The stability of $CH_3^+CXCH_3$ ions is controlled by the C-X bond energy, like that of CH_3CHX^+. However, the slightly lower slope for $CH_3^+CXCH_3$ (-9.85) compared to that of CH_3CHX^+ (-11.1) may indicate another minor effect. This could be a contribution from the electron-donation of the heavier halogen atom to form $CH_3\overset{X^+}{\overset{\|}{C}}CH_3$.

5.3.3.2 Heats of formation of $C_3H_6Cl^+$

The heats of formation of $C_3H_6Cl^+$ isomers are not available, however they can be estimated from the calculated methyl substituent effect (Table 5.1), see the estimation of ΔH_f° ($CH_3^+CClCH_3$) shown above. By high level ab initio calculations[21] $ClCH_2CH_2^+$ is 21 kcalmol^{-1} higher in energy than CH_3CHCl^+ (ΔH_f° 198 kcalmol[10]), thus the heat of formation of $ClCH_2CH_2^+$ is ~ 219 kcalmol^{-1}. The methyl substitution effect on its α-position (charged carbon) is - 25 kcalmol^{-1}, thus the heat of formation of $CH_3^+CHCH_2Cl$ (**VIb**) is estimated to be 192 kcalmol^{-1}. Methyl substitution on its β-position (next to charged carbon) is only - 6 kcalmol^{-1}, and so the heat of formation of $CH_3CHClCH_2^+$ (**Vb**) is estimated to be 211 kcalmol^{-1}. The isomers **IVb** and **VIb** with the charge on the center carbon are more stable than isomer **Vb** with the charge on the terminal carbon. Moreover **IVb** with Cl at the α-position is more stable than **VIb** with Cl on the β–carbon.

If the methyl substitution effect at the β-carbon of CH_3CHCl^+ is also - 6 kcalmol^{-1}, then the heat of formation of $CH_3CH_2CHCl^+$ may be estimated to be 191 kcalmol^{-1}. Note that $CH_3CH_2CHCl^+$ is about 20 kcalmol^{-1} lower in energy than $CH_3CHClCH_2^+$, indicating

that the $C_3H_6Cl^+$ isomer with the halogen atom setting at the charged carbon is more stable than that with the halogen atom setting at the other carbons.

$\overline{CH_2Cl^+CH_2}$ (Δ_fH^0 = 200 kcalmol^{-1}, see Chapter 3) is ~ 19 kcalmol^{-1} lower in energy than $ClCH_2CH_2^+$; while it is also estimated to be 19 kalmol^{-1} lower in energy than $CH_3^+CHCH_2Cl$. Since the energy difference between $\overline{CH_2Cl^+CH_2}$ and $ClCH_2CH_2^+$ results from the cyclic structure and the linear structure, the energy defference between $CH_3CHCl^+CH_2$ and $CH_3^+CHCH_2Cl$ may result from a cyclic structure and a linear structure as well. The $CH_3CHCl^+CH_2$ ion is therefore most likely a cyclic species

$CH_3CH - CH_2$ .However the methyl group has both inductive and steric effects, which will reduce the efficiency of the electron - donation from Cl. The calculated angle in

$CH_3^+CH\text{-}CH_2$ is 86.8°, higher than that in $^+CH_2\text{-}CH_2$ (69.6°),[14] indicating an incomplete back-bonding. The heat of formation of $C_3H_6Cl^+$ (Table 5.9) increases in the following series:

$$CH_3^+CClCH_3 < \overline{CH_3CHCl^+CH_2} < CH_3CH_2\dot{C}H{=}Cl^+ \sim CH_3^+CHCH_2Cl < CH_3CHClCH_2^+$$

ΔH_f°	170 ± 3	191	192	211

5.3.3.3 Heats of formation of $C_3H_6Br^+$

The heats of formation of IVc and VIc have been measured[10] to be 178 kcalmol^{-1} and 195 kcalmol^{-1}, respectively. The ΔH_f°(IXc) was estimated to be 172 kcalmol^{-1} by the appearance energy value (9.37 eV) for the process $BrCH_2CH_2CH_2Br$ (DBP) → $C_3H_6Br^+$

(XIc) + $Br^{\bullet}$ [taking ΔH_f° (DBP) = - 17 kcalmol^{-1} , ΔH_f° ($Br^{\bullet}$) = 26.7 kcalmol^{-1}]. As shown before this ion is most likely a four-membered ring isomer $\overline{CH_2CH_2CH_2}\,Br^+$ (IXc). From the values shown above IXc has the lowest energy among the three isomers.

Comparing the heats of formation of $C_3H_6Br^+$ (Table 5.9) gives the following series:

	$\overline{CH_2CH_2CH_2Br}^+$	<	$CH_3{}^+CBrCH_3$	<	$CH_3CHBr^+CH_2$
ΔH_f°(kcalmol^{-1})	172		178		195

5.3.3.4 Comparison of methyl substituent effects on $C_2H_4Cl^+$ and $C_2H_4Cl^{\bullet}$

The heat of formation of $CH_3{}^{\bullet}CClCH_3$ can estimated from BDE (bond dissociation energy) values. The BDE of the secondary C-Cl in $CH_3CHClCH_3$ is 86 kcalmol^{-1}, 2 kcalmol^{-1} higher than the BDE for the primary C-Cl in CH_3CH_2Cl (84 kcalmol^{-1}); if it is assumed that the BDE of C-Cl in $CH_3CCl_2CH_3$ will be 2 kcalmol^{-1} higher than the BDE of the primary C-Cl in CH_3CHCl_2 (78 kcalmol^{-1}). Then ΔH_f° ($CH_3{}^{\bullet}CClCH_3$) is 9 kcalmol^{-1} [taking ΔH_f° ($CH_3CCl_2CH_3$) = - 42 kcalmol^{-1} (additivity rule[9]) and ΔH_f° ($Cl^{\bullet}$) = 29 kcalmol^{-1}]. This is a reasonable value, typical of the result of replacing $H^{\bullet}$ by $Cl^{\bullet}$.

Analogous to Eq. 2 the methyl sustituent effect on $CH_3CHCl^{\bullet}$ is - 7 kcalmol^{-1}, which is smaller than the methyl substituent effect on CH_3CHCl^+, namely - 23-28 kcalmol^{-1}. Hence the stabilizing effect of the methyl substituent is greater at the charge center than on the radical center.

5.4 Conclusions

Three isomers of $C_3H_6X^+$ (X = Cl and Br) have been characterized by their CID, CIDI and NR mass spectra and by the formation of isomeric $(C_2H_5)_2O^+C_3H_6X$ ions. By MI and CID mass spectrometry $CH_3{}^+CXCH_3$ has been distinguished from $CH_3{}^+CHCH_2X$ or $XCH_2CH_2CH_2{}^+$. The latter two isomers have been distinguished by the formation of $(C_2H_5)_2O^+C_3H_6X$ isomers which showed different dissociation characteristics in their MI and CID mass spectra. By NR mass spectrometry it has been shown that the radical $CH_3{}^{\cdot}CClCH_3$ is more stable than the radical $CH_3{}^{\cdot}CBrCH_3$.

Methyl substitution on the charge center of CH_3CHX^+ and $XCH_2CH_2{}^+$ produces two $C_3H_6X^+$ isomers, $CH_3{}^+CXCH_3$ and $CH_3{}^+CHCH_2X$. The former is significantly lower in energy than the latter. As with CH_3CHX^+, the stability of $CH_3{}^+CXCH_3$ is predominantly controlled by the C-X bond strength, in particular the partial formation of a double bond by electron-donation from the halogen. The C-X bond strength is not a major factor controlling the stability of $CH_3{}^+CHCH_2X$ ions because its ΔH_f° value is closer to that of $CH_3{}^+CHCH_3$ (191 kcalmol^{-1} [16]), i.e. the effect of halogen in the ion is similar to that in the corresponding neutral radical.

5.5 References

1. J. H. Exner, L. D. Kershner and T. E. Evans, J. Chem. Soc. Chem. Comm., 361 (1973)
2. P. E. Peterson and W. F. Boron, J. Am. Chem. Soc., 93, 4076 (1971)
3. C. E. Reineke and J. R. McCarthy, Jr, J. Am. Chem. Soc., 92, 6376 (1970)
4. S. Yamabe, T. Minato, M. Seki and Inagaki, J. Am. Chem. Soc., 110, 6047 (1988)
5. K. Raghavachari, R. C. Haddon and W. H. Starnes, Jr, J. Am. Chem. Soc., 104, 5054 (1982)
6. J. B. Lambert and W. J. Schulz, Jr, J. Am. Chem. Soc., 106, 792 (1984)
7. G. Frenking, Tetrahedron., 40, 377 (1984)
8. G. A. Olah, J. M. Bollinger, Y. K. Mo and J. M. Brinich, J. Am. Chem. Soc., 94, 1164 (1972)
9. W. J. Hehre and P. C. Hiberty, J. Am. Chem. Soc., 96, 2665 (1974)
10. J. H. Holmes, F. P. Lossing and R. A. McFarlane, Int. J. Mass Spectrom. Ion. Processes., 86, 209 (1988)
11. R. H. Staley, R. D. Wieting and J. L. Beauchamp, J. Am. Chem. Soc., 99, 5964 (1977)
12. A. J. R. Heck and M. M. Nibbering, J. Am. Soc. Mass Spectrom., 6, 11 (1995)
13. S. Yamabe and T. Minato, Bull. Chem. Soc. Japan., 66, 3339 (1993)
14. S. Yamabe and T. Tsuji, Chem. Phys. Lett., 146, 236 (1988)
15. P. C. Burgers, J. L. Holmes, A. A. Mommers and J. E. Szulejko, Org. Mass Spectrom., 18, 596 (1983)

16. S. G. Lias, J. E. Bartmess, J. F. Liebman, J. L. Holmes, R. D. Levin, and W. G. Mallard, J. Phys. Chem. Ref. Data, 17, No 1, 1988

17. F. W. McLafferty, *Interpretation of Mass Spectra*, 2Ed., The Benjamin/Cummings Publishing Co., Massachusetts, 1973

18. A. D. Williamson, P. R. LeBreton and J. L. Beauchamp, J. Am. Chem. Soc., 98, 2705 (1976)

19. J. Y. Park and J. L. Beauchamp, J. Phys. Chem., 80, 575 (1976)

20. T. Hoz, M. Sprecher and H. Basch, J. Phys. Chem., 89, 1664 (1985)

21. C. F. Rodriquez, D. K. Bohme and A. C. Hopkinson, J. Am. Chem. Soc., 115, 3263 (1993)

Table 5.1 Calculations for methyl substitution on $C_2H_4X^+$ (STO-3G)[9]

$C_3H_6X^+$	$C_2H_4X^+$	E(kcalmol^{-1})*
$CH_3^+CFCH_3$	CH_3CHF^+	23.2
$CH_3^+CClCH_3$	CH_3CHCl^+	21.6
$CH_3^+CHCH_2F$	$FCH_2CH_2^+$	25.7
$CH_3CHFCH_2^+$	$FCH_2CH_2^+$	6.8
$CH_3^+CHCH_2Cl$	$ClCH_2CH_2^+$	24.9
$CH_3CHClCH_2^+$	$ClCH_2CH_2^+$	5.7

* The energies of the isodesmic reaction

$$C_3H_6X^+ + CH_4 \rightarrow C_2H_4X^+ + C_2H_6$$

Table 5.2 Formation of $C_3H_6X^+$ ions

Precursor	Neutral loss	$C_3H_6X^+$	No.
$CH_3CCl_2CH_3^{+\bullet}$	Cl	$CH_3^+CClCH_3$	**IVb**
$CH_3CHBrCH_2Cl^{+\bullet}$	Br	$CH_3^+CHCH_2Cl$	**VIb**
$ClCH_2CH_2CH_2Br^{+\bullet}$	Br	$ClCH_2CH_2CH_2^+$	**VIIb**
$CH_3CH_2CHCl_2^{+\bullet}$	Cl	$CH_3CH_2^+CHCl$	**VIIIb**
$CH_3CBr_2CH_3^{+\bullet}$	Br	$CH_3^+CBrCH_3$	**IVc**
$CH_3CHBrCH_2Cl^{+\bullet}$	Cl	$CH_3CHBrCH_2^+$	**Vc**
$CH_3CHBrCH_2Br^{+\bullet}$	Br	$CH_3^+CHCH_2Br$	**VIc**
$BrCH_2CH_2CH_2Br^{+\bullet}$	Br	$BrCH_2CH_2CH_2^+$	**VIIc**

Table 5.3 Kinetic energy release (KER) values of metastable $C_3H_6X^+$ ions losing HX to give a composite peak

$C_3H_6X^+$	$T_{0.5}$ (meV)*		
	Peak 1	Peak 2	Composite peak
$CH_3^+CClCH_3$	16	225	156
$CH_3^+CHCH_2Cl$	16	145	93
$ClCH_2CH_2CH_2^+$	16	165	109
$CH_3CH_2^+CHCl$	16	145	100
$CH_3^+CBrCH_3$	8.8	133	86
$CH_3^+CHCH_2Br$	12	89	45
$BrCH_2CH_2CH_2^+$	8.0	81	32
$CH_3CHBrCH_2^+$	6.4	79	37

* Deviation: ± 5 meV.

Table 5.4 Partial CID mass spectra of C_3H_5 ions.

Parent ions	Ratio of m/z 26/27
$CH_3^+CClCH_3$	1.1
$CH_3CH_2^+CHCl$	0.93
$CH_3^+CHCH_2Cl$	1.0
$ClCH_2CH_2CH_2^+$	0.75
$CH_3^+CBrCH_3$	1.05
$CH_3^+CHCH_2Br$	0.89
$BrCH_2CH_2CH_2^+$	0.85
$CH_2CHCH_2I^{+\bullet}$	0.53[15]
$CH_3ClCH_2^{+\bullet}$	2.05[15]

Table 5.5 CID mass spectra of $C_3H_6Cl^+$ isomers*

Fragment	$CH_3{}^+CClCH_3$	$ClCH_2{}^+CHCH_3$	$ClCH_2CH_2CH_2{}^+$	$CH_3CH_2{}^+CHCl$
$CH_2^{+\cdot}$	1	< 1	< 1	< 1
CH_3^+	2	2	2	2
$C_2H_2^{+\cdot}$	10	10	7	8
$C_2H_3^+$	12	14	13	13
$C_2H_4^{+\cdot}$	-	4	3	2
$C_2H_5^+$	-	< 1	< 1	2
C_3H^+	3	4	5	3
$C_3H_2^{+\cdot}$	10	8	10	6
$C_3H_3^+$	50	38	32	39
$C_3H_5^+$	100	100	100	100
$C_3H_6^{+\cdot}$	22	-	-	-
CCl^+	3	4	4	4
$CHCl^{+\cdot}$	2	4	4	4
CH_2Cl^+	14	20	20	23
$C_2HCl^{+\cdot}$	2	< 1	< 1	< 1
$C_2H_2Cl^+$	7	3	3	3
$C_2H_3Cl^{+\cdot}$	7	3	3	3
$C_3H_4Cl^+$	1	1	1	2
$C_3H_5Cl^{+\cdot}$	10	2	1	2

* He, 90% transmission of ion beam

Table 5.6 CID mass spectra of $C_3H_6Br^+$ isomers*

Fragment	*$CH_3{}^+CBrCH_3$*	*$BrCH_2{}^+CHCH_3$*	*$BrCH_2CH_2CH_2{}^+$*	*$CH_3CHBrCH_2{}^+$*
$C_2H_2^{+\cdot}$	2.5	1.5	1	3
$C_2H_3^+$	3.5	3.5	2	5
$C_2H_4^{+\cdot}$	-	-	1	-
$C_3H_3^+$	32	17	14	15
$C_3H_5^+$	100	100	100	100
$C_3H_6^{+\cdot}$	43	-	-	-
Br^+	9	4	8	4
$CBr^{+\cdot}$	2	5	5	2
CH_2Br^+	10	18	22	6
$C_2HBr^{+\cdot}$	2	< 1	-	< 1
$C_2H_2Br^+$	4	2	2	1
$C_2H_3Br^{+\cdot}$	4	2	< 1	1
$C_2H_4Br^+$	-	< 1	< 1	< 1
$C_3H_5Br^+$	6	-	-	-

* He, 90 % transmission of ion beam; including the MI contributions

Table 5.7 Metastable ion (MI) and partial CID mass spectra of $(C_2H_5)_2O^+C_3H_6Cl$

	Precursors					
	$CH_3CHBrCH_2Cl\bullet(C_2H_5)_2O]^{+\bullet}$-$Br^\bullet$		$[ClCH_2CH_2CH_2Br\bullet(C_2H_5)_2O]^{+\bullet}$-$Br^\bullet$		$[CH_3CH_2CHCl_2\bullet(C_2H_5)_2O]^{+\bullet}$-$Cl^\bullet$	
Fragments	MI	CID*	MI	CID*	MI	CID*
$C_5H_{11}ClO^+$+C_2H_4	-	<1	74	55	1	1
$C_5H_{11}O^+$+C_2H_5Cl	-	-	12	11	-	<1
$C_3H_6Cl^+$+$(C_2H_5)_2O$	3	7	18	29	3	12
$(C_2H_5)_2OH^+$+C_3H_5Cl	100	100	100	100	100	100
$C_4H_9O^+$+C_3H_7Cl	-	1	-	-	-	3

* Including MI contributions

Table 5.8 MI and partial CID mass spectra of $(C_2H_5)_2O^+C_3H_6Br$

Precursors	$[CH_2CHBrCH_2Br \bullet (C_2H_5)_2O]^{+\cdot}$-$Br^{\cdot}$		$[BrCH_2CH_2CH_2Br \bullet (C_2H_5)_2O]^{+\cdot}$-$Br^{\cdot}$	
Fragments	MI	CID*	MI	CID*
$C_5H_{11}BrO^+ + C_2H_4$	2	1.5	21	17
$C_3H_6Br^+ + (C_2H_5)_2O$	8	40	100	100
$C_5H_{11}O^+ + C_2H_5Br$	-	-	3	4
$(C_2H_5)_2OH^+ + C_3H_5Br$	100	100	22	22
$C_4H_9O^+ + C_3H_7Br$	-	5	-	-

* Including MI contributions.

Table 5.9 Heats of formation of $C_3H_6X^+$ ions and related species, kcalmol^{-1}.[1]

Ions		Δ_fH^0	Species	Δ_fH^0
$CH_3^+CFCH_3$	IVa	141±3[2]	$C_3H_5^\bullet$	39
			$C_3H_5^+$	226
$CH_3^+CClCH_3$	IVb	170±3[3]	C_3H_6	20
$CH_3^+CHCH_2Cl$	VIb	192±1[3]	$C_3H_6^{+\bullet}$	229
$CH_3CHClCH_2^+$	Vb	211±1[3]	$Cl^\bullet$	29
$CH_3CH_2^+CHCl$	VIIIb	191±1[3]	Cl^+	328
			$Br^\bullet$	27
$CH_3^+CBrCH_3$	IVc	178[4]	Br^+	299
			HCl	-22
$CH_3CHBr^+CH_2$	VIc	195[4]	$HCl^{+\bullet}$	272
			HBr	-9
$CH_2CH_2CH_2Br^+$	IXc	172[5]	$HBr^{+\bullet}$	260
			$C_2H_3Cl^{+\bullet}$	236
$CH_3^\bullet CClCH_3$	IVb	9[3]	$C_2H_3Br^{+\bullet}$	245
			$CH_3^\bullet$	35

1. Data are from Reference 38 except indicated.
2 From References 15 and 64. Estimations, see text.
4. From Reference 18.
5. Estimation from the appearance 3. energy measurement.

Figure 5.1 The distribution of released energies (T) in the MI dissociation of $CH_3C^+ClCH_3$ via HCl loss

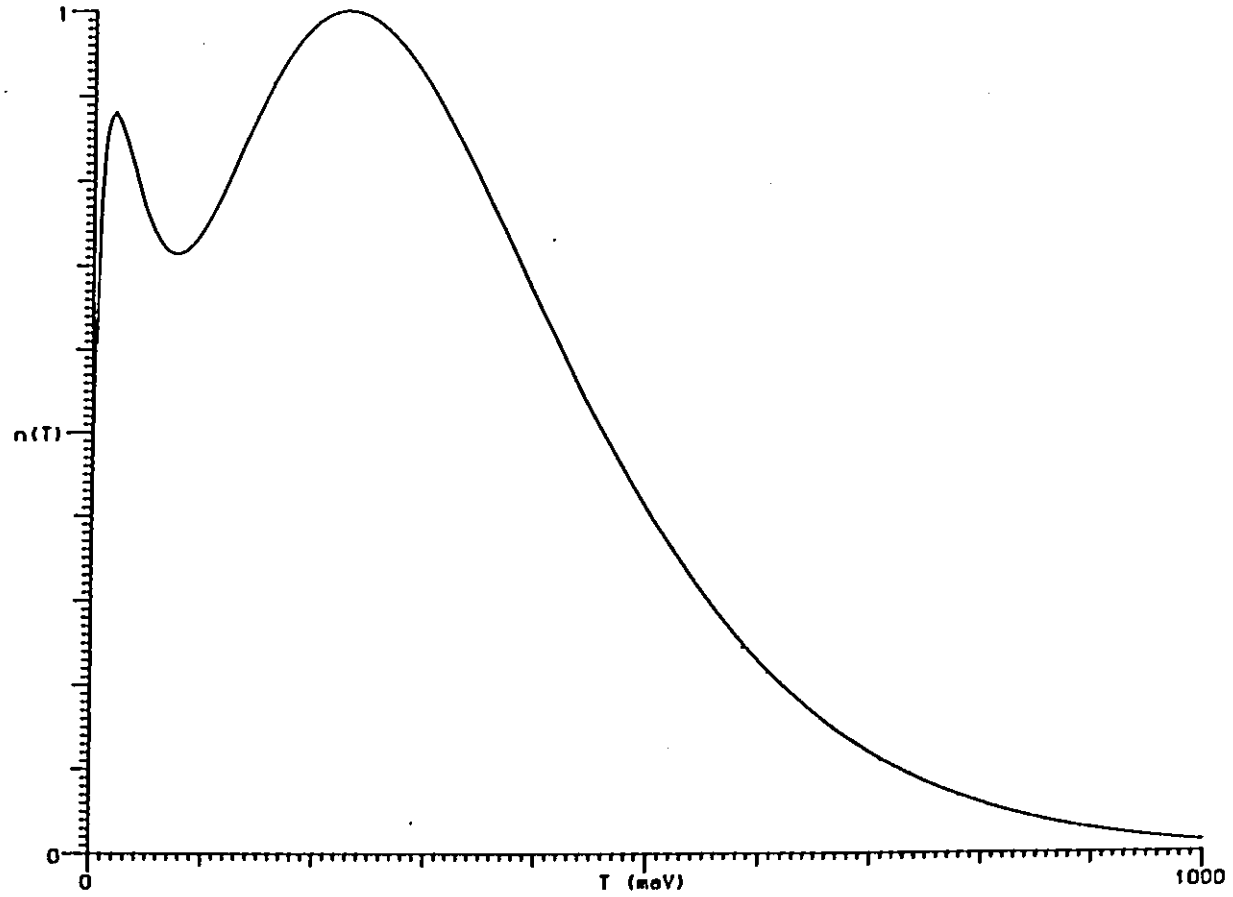

n(T): the distribution of released energies

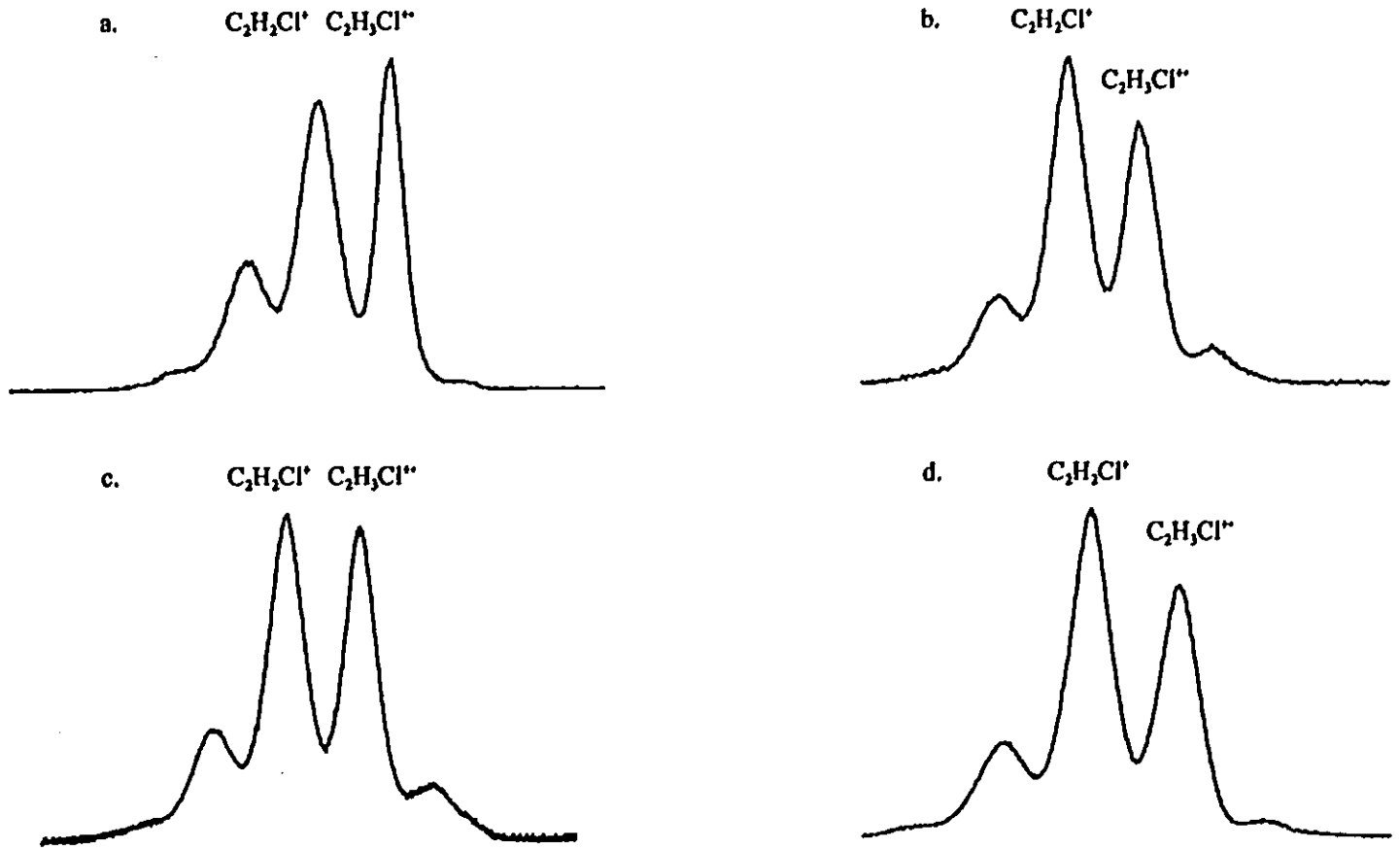

Figure 5.2 Partial CID mass spectra of $C_3H_6Cl^+$ isomers.

Parent ions: a. $CH_3{}^+CClCH_3$ b. $ClCH_2CH_2CH_2{}^+$ c. $CH_3{}^+CHCH_2Cl$ d. $CH_3CH_2{}^+CHCl$

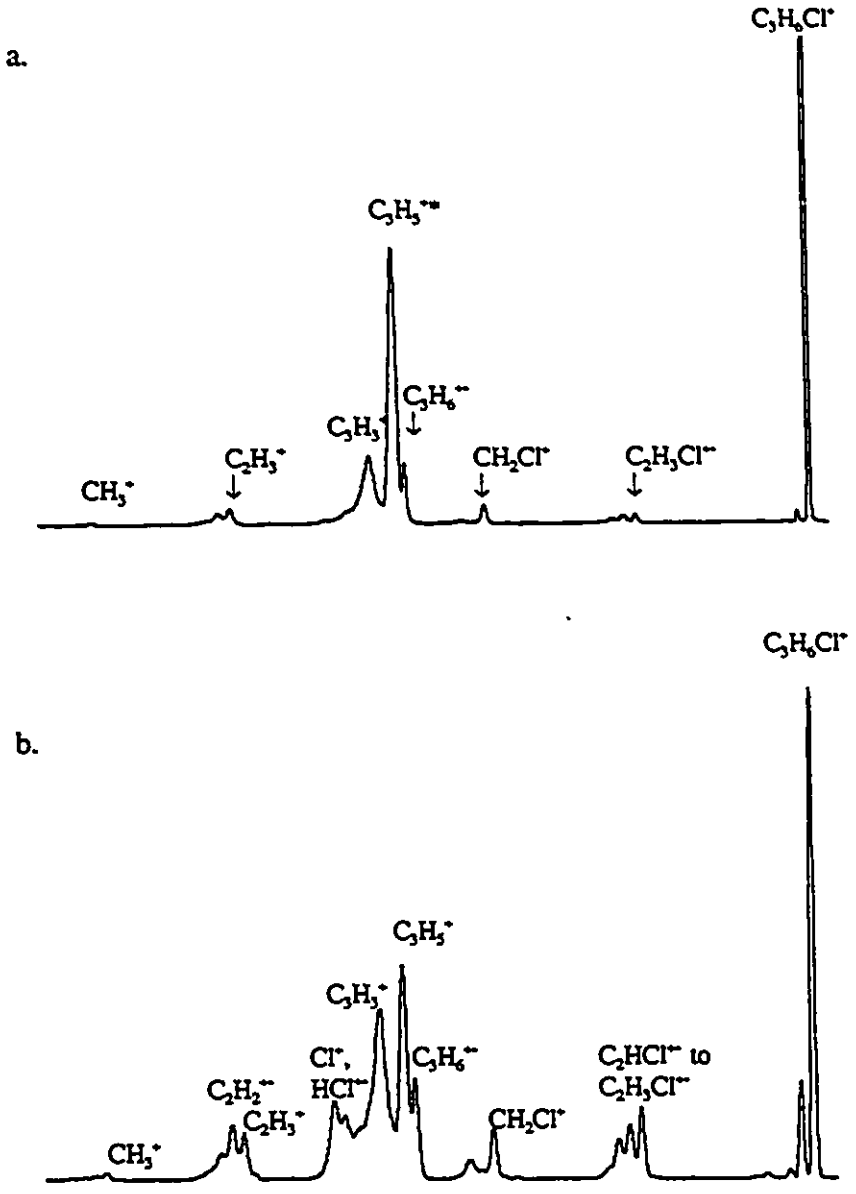

Figure 5.3 The CID and NR mass spectra of $CH_3^+CClCH_3$

a: CID mass spectrum

b: NR mass spectrum

* Including the MI contributions

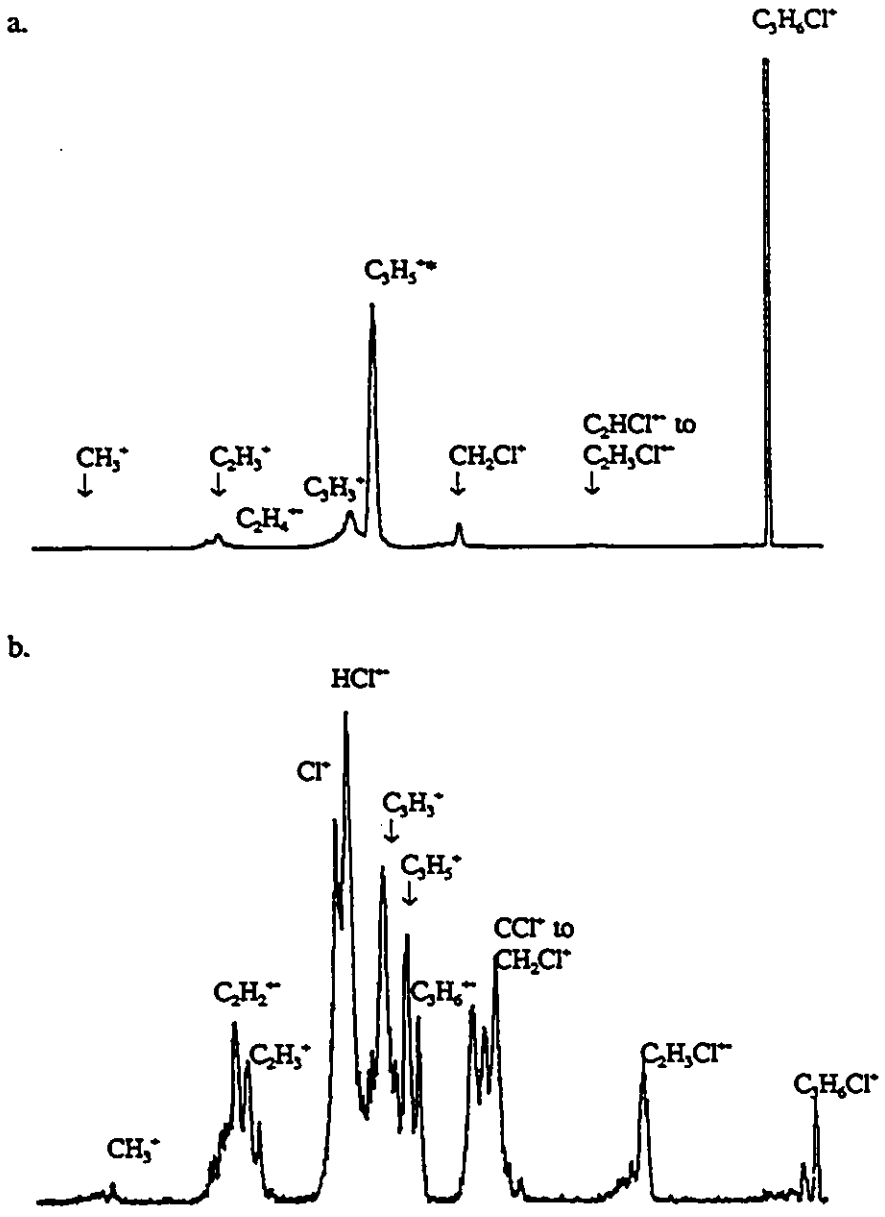

Figure 5.4 **The CID and NR mass spectra of $ClCH_2CH_2CH_2^+$**
a: CID mass spectrum
b: NR mass spectrum
* Including the MI contributions

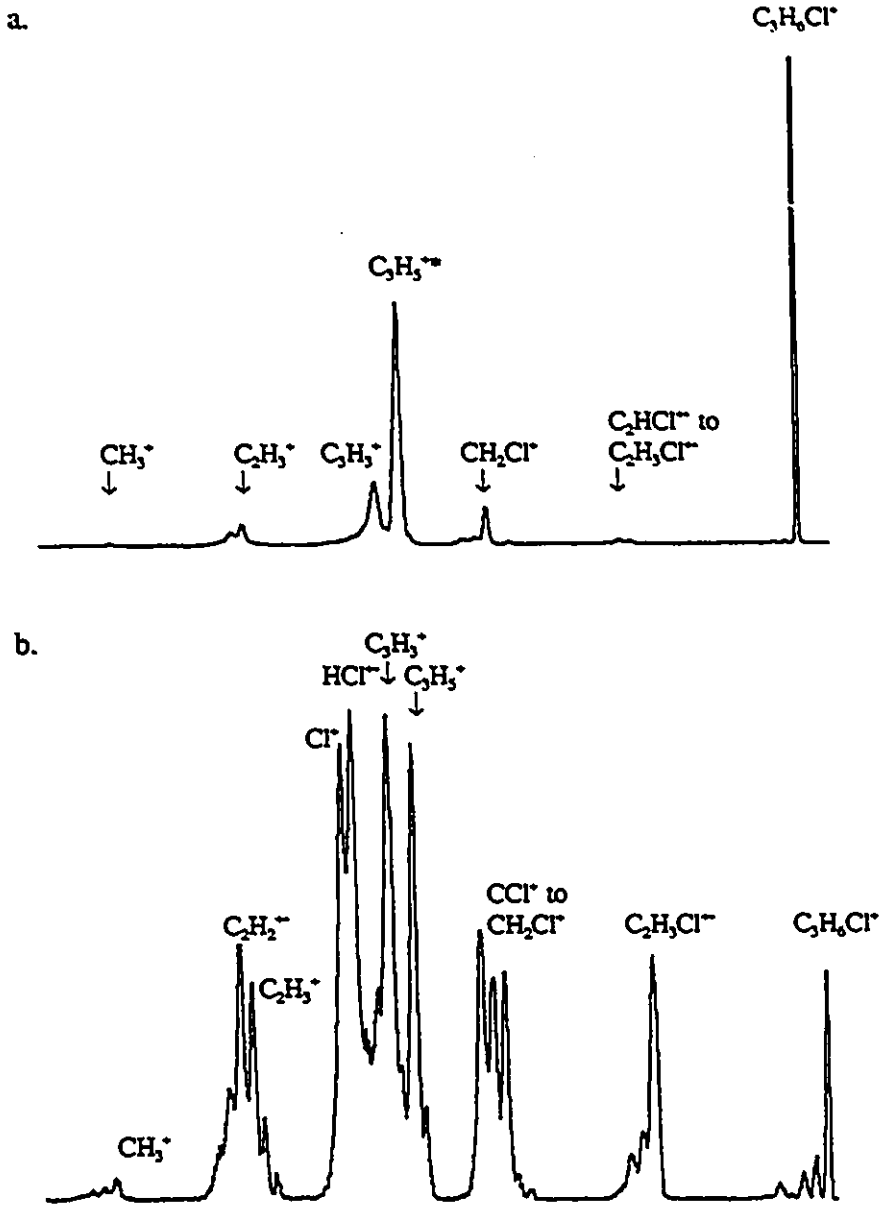

Figure 5.5 **The CID and NR mass spectra of $CH_3CH_2^+CHCl$**
a: CID mass spectrum
b: NR mass spectrum
* Including the MI contributions

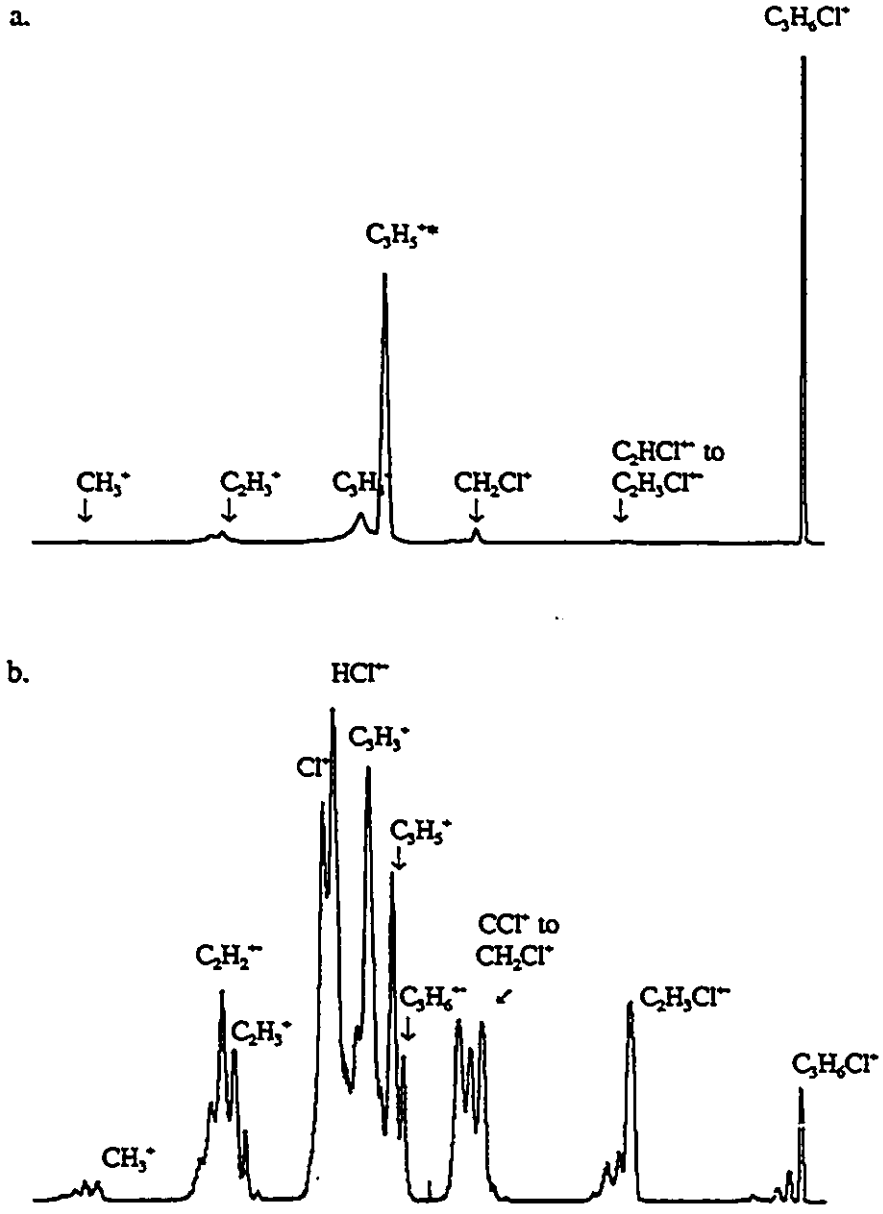

Figure 5.6 **The CID and NR mass spectra of $CH_3^+CHCH_2Cl$**
a: CID mass spectrum
b: NR mass spectrum
* Including the MI contributions

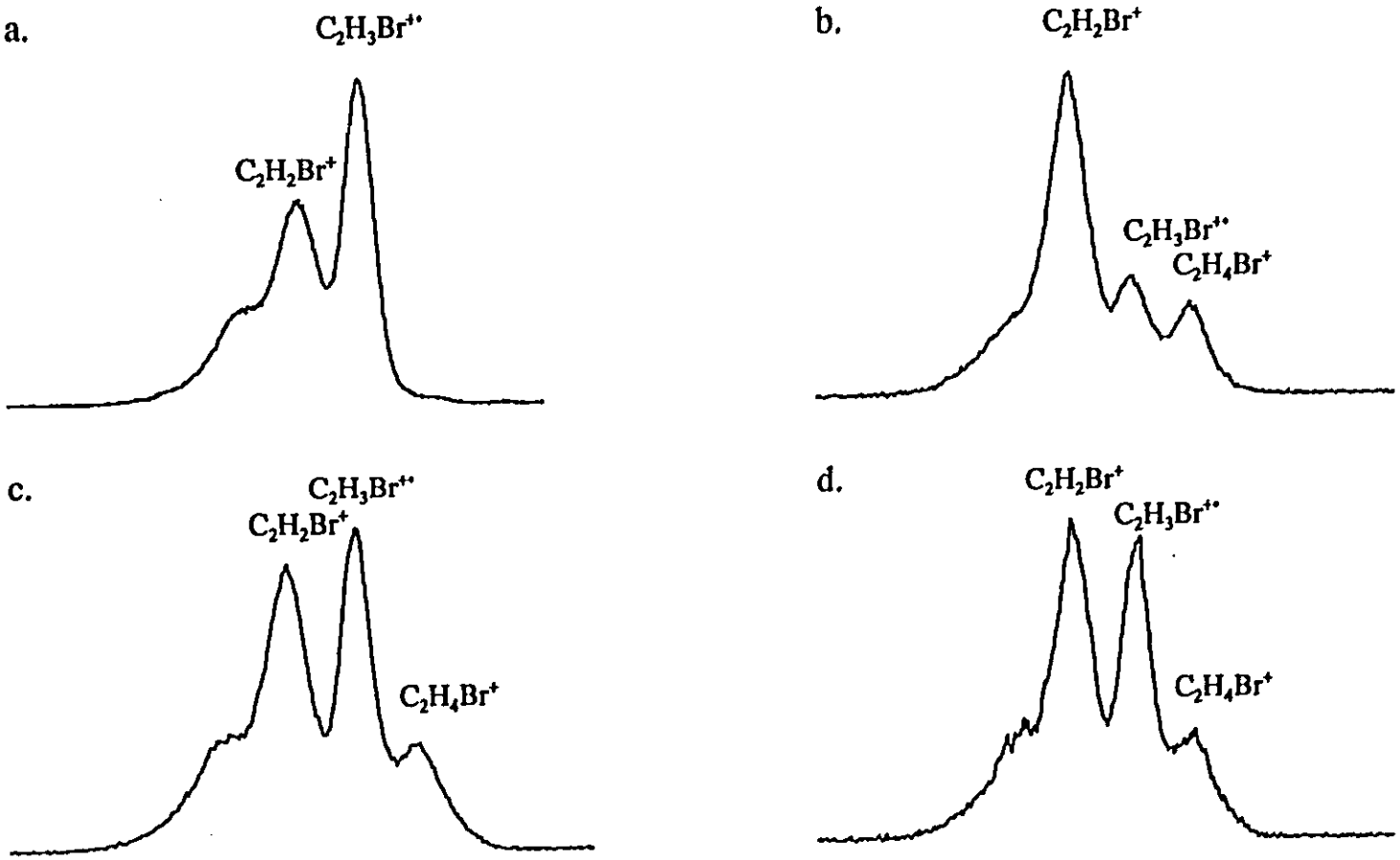

Figure 5.7 **Partial CID mass spectra of $C_3H_6Br^+$ isomers.**
Parent ions: a. $CH_3{}^+CBrCH_3$ b. $BrCH_2CH_2CH_2{}^+$ c. $CH_3{}^+CHCH_2Br$ d. $CH_3CHBr^+CH_2$

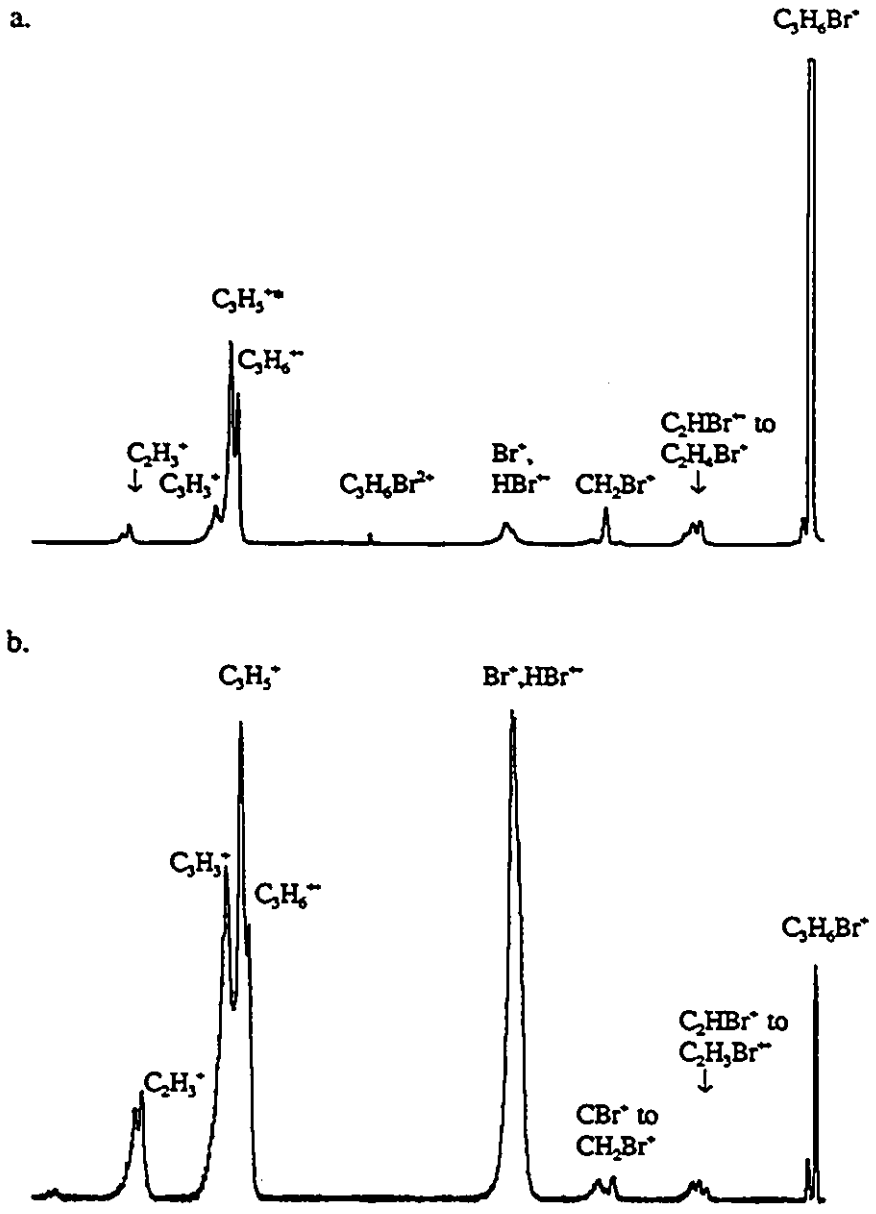

Figure 5.8 **The CID and NR mass spectra of $CH_3^+CBrCH_3$**
a: CID mass spectrum
b: NR mass spectrum
* Including the MI contributions.

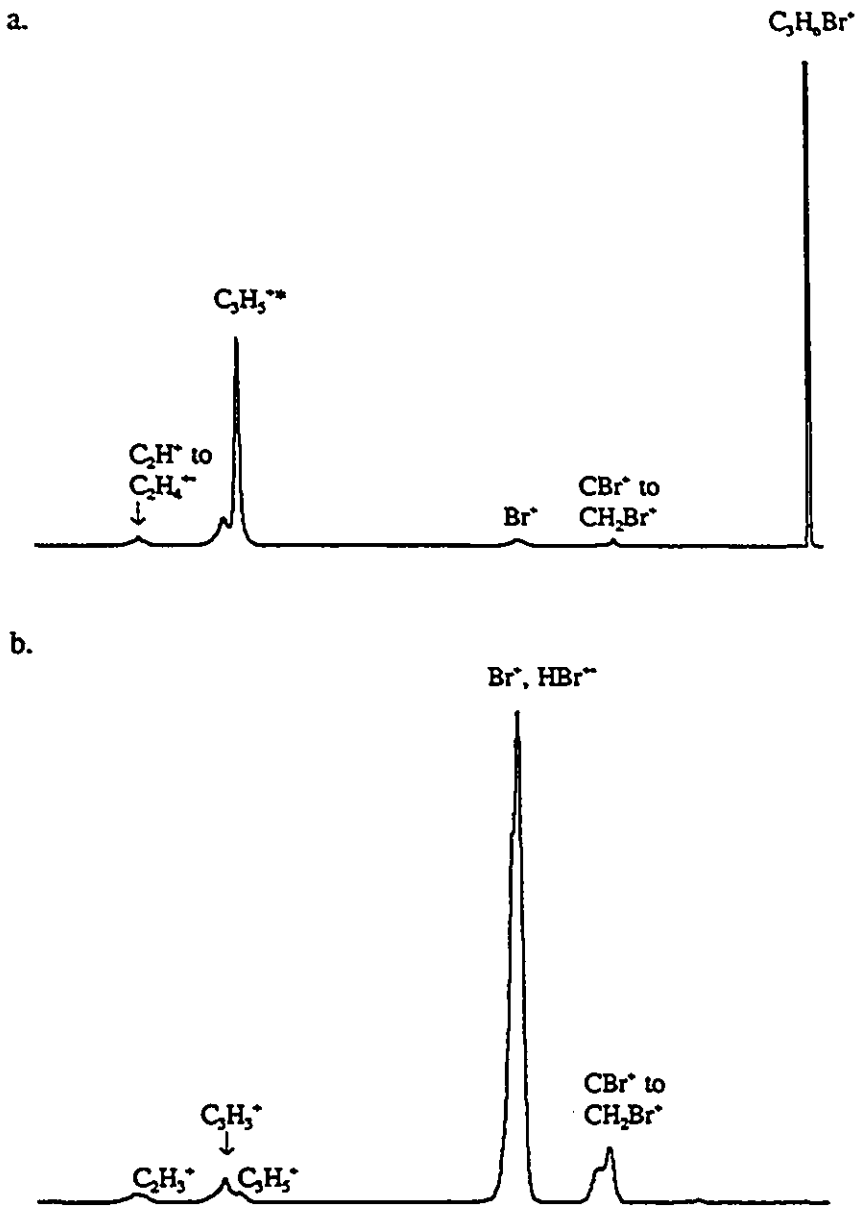

Figure 5.9 **The CID and NR mass spectra of $BrCH_2CH_2CH_2^+$**
a: CID mass spectrum
b: NR mass spectrum
* Including the MI contributions.

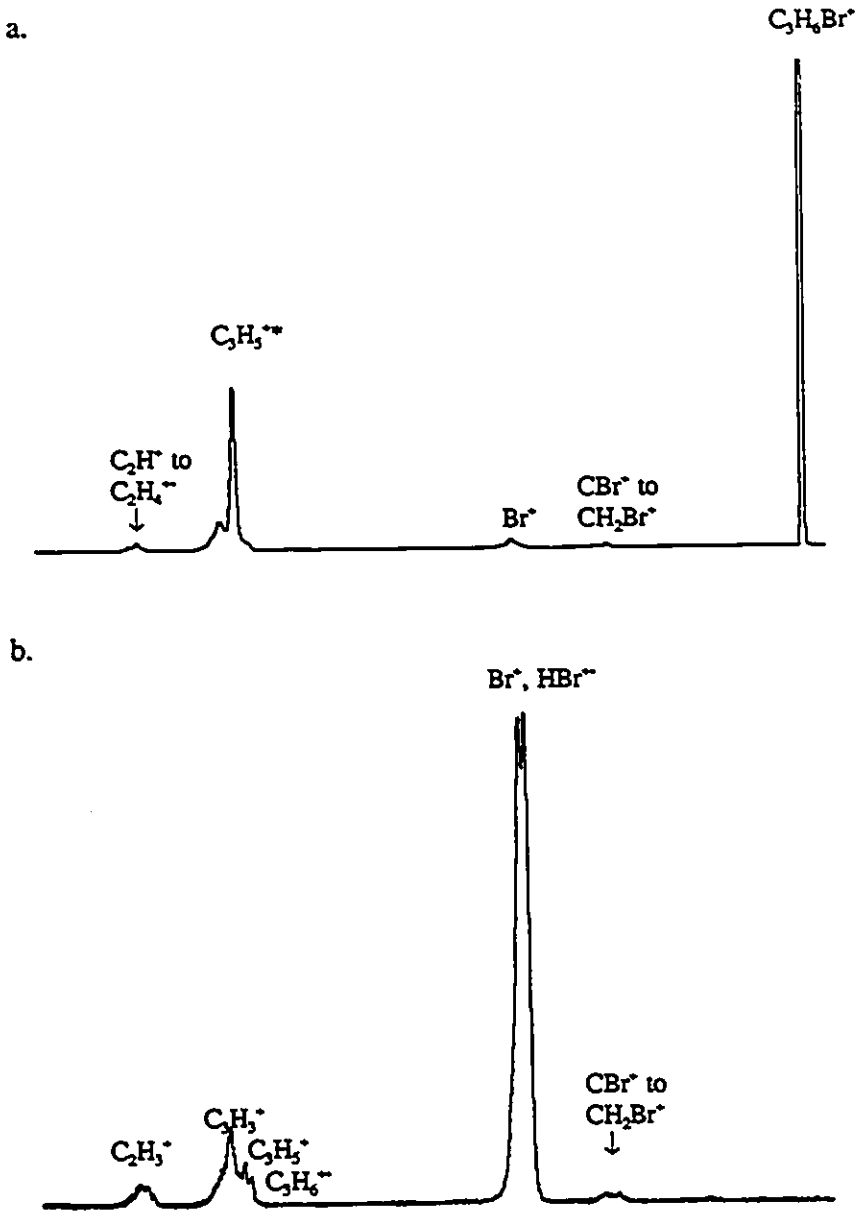

Figure 5.10 **The CID and NR mass spectra of $BrCH_2^+CHCH_3$**
a: CID mass spectrum
b: NR mass spectrum
* Including the MI contributions.

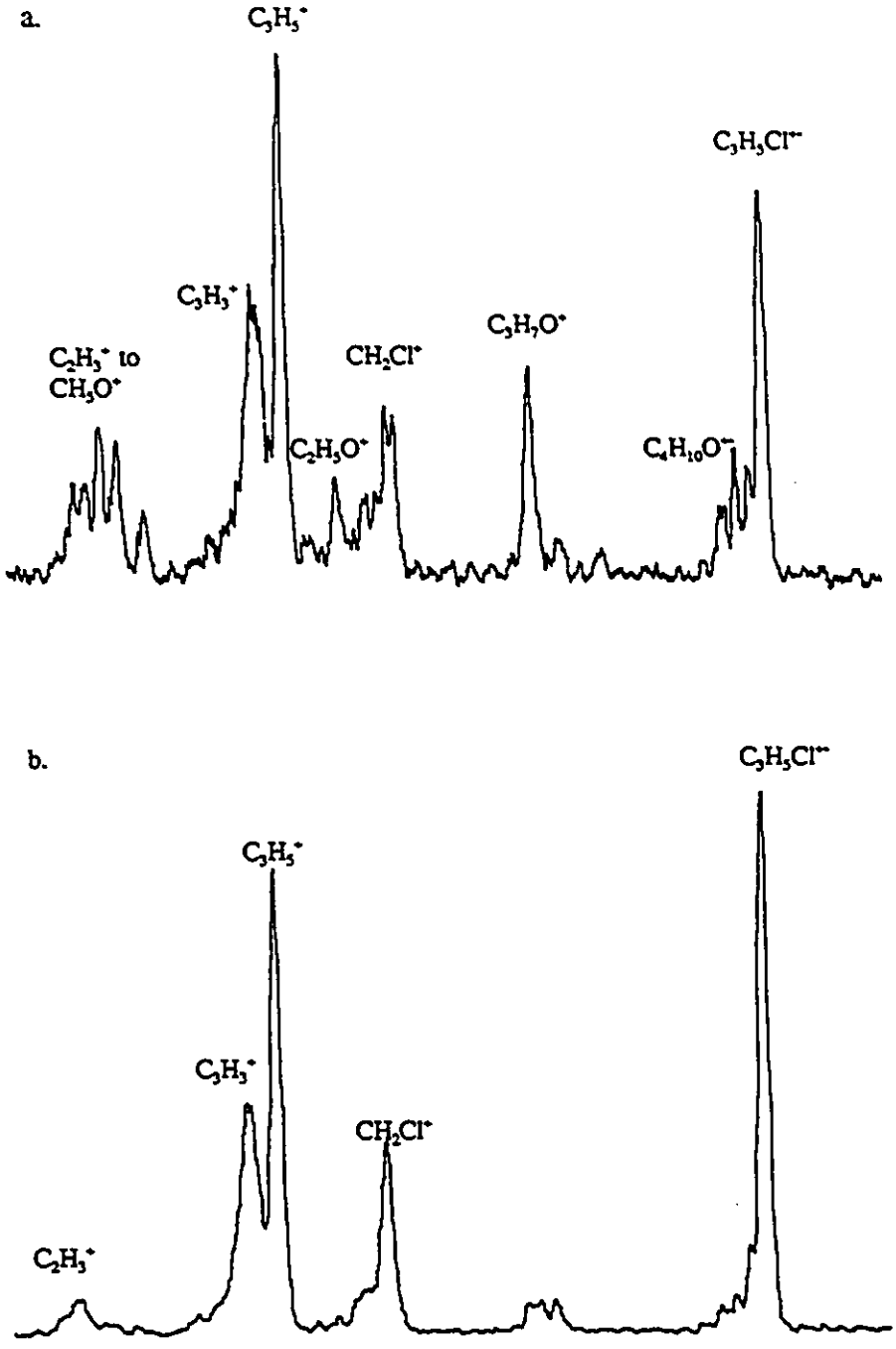

Figure 5.11 **CIDI mass spectra of adduct $(C_2H_5)_2O^{+}C_3H_6Cl$**
Precursors: a. $[ClCH_2CH_2CH_2Br^{\bullet}(C_2H_5)_2O]^{+\cdot}$-$Br^{\bullet}$
b. $[ClCH_2CHBrCH_3^{\bullet}(C_2H_5)_2O]^{+\cdot}$-$Br^{\bullet}$

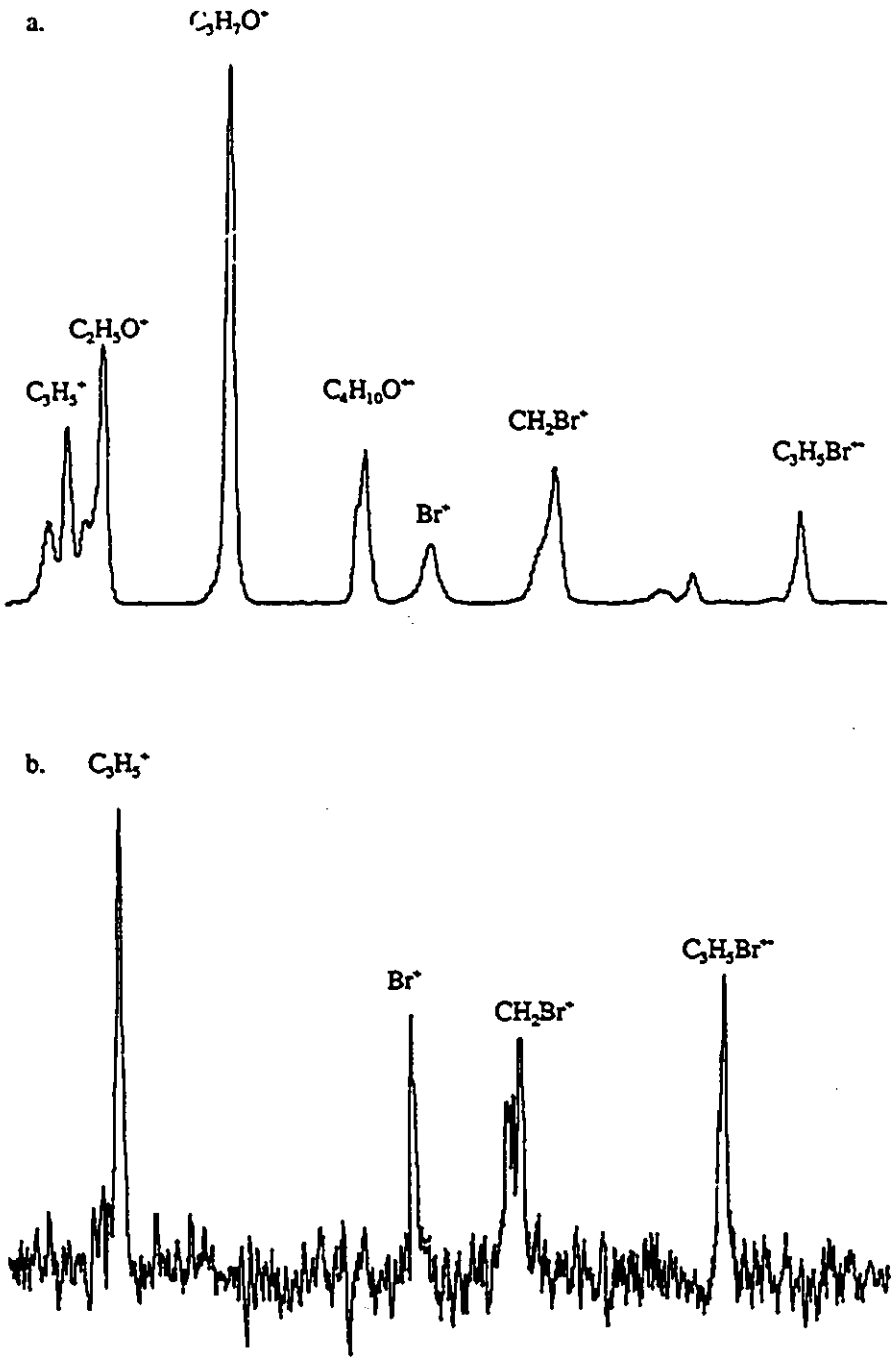

Figure 5.12 **CIDI mass spectra of $(C_2H_5)_2O^+C_3H_6Br$**
Precursors: a. $[BrCH_2CH_2CH_2Br\bullet(C_2H_5)_2O]^{+\bullet}$-$Br^\bullet$
b. $[BrCH_2CHBrCH_3\bullet(C_2H_5)_2O]^{+\bullet}$-$Br^\bullet$

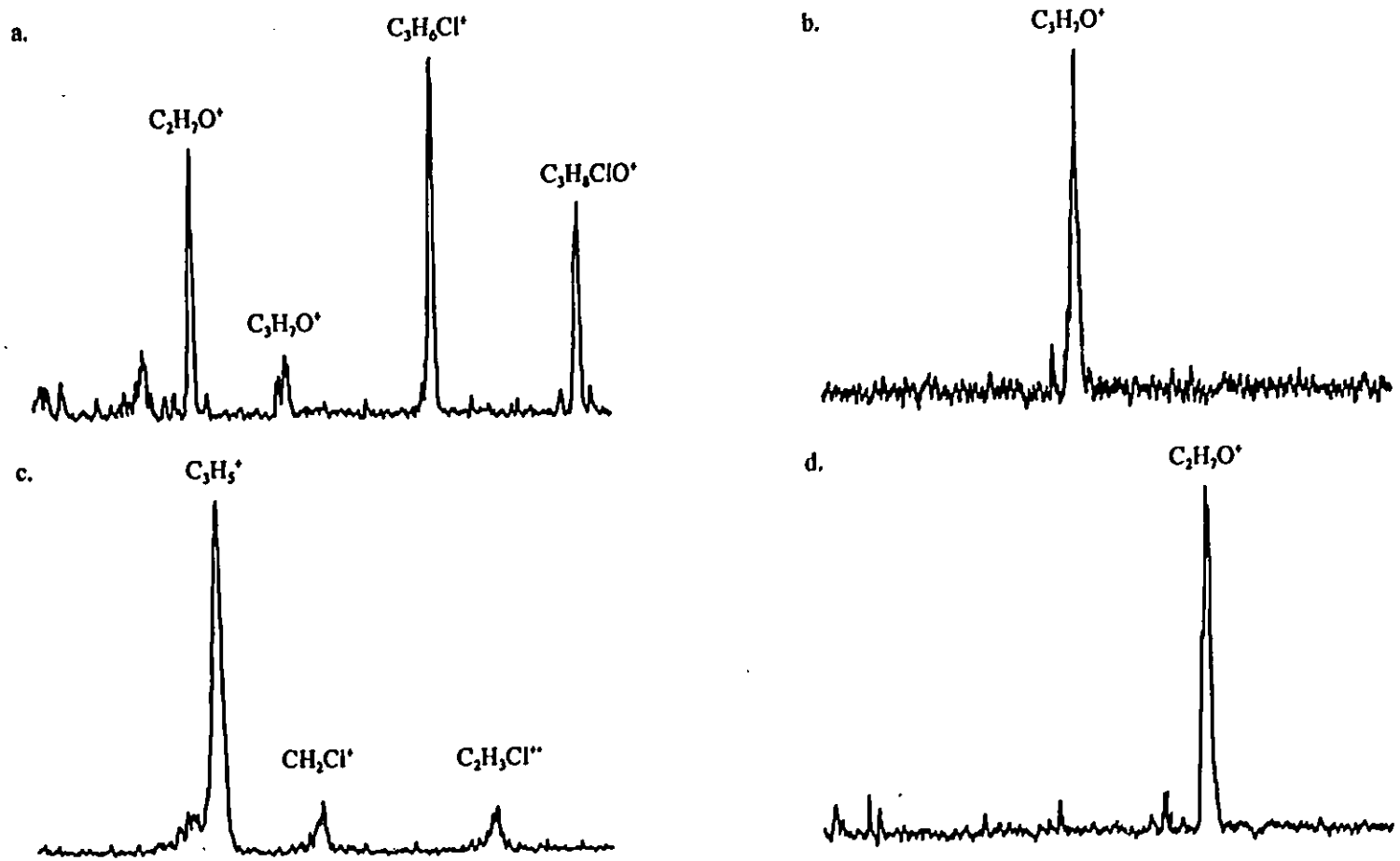

Figure 5.13 CID mass spectra of the daughter ions from $(C_2H_5)_2O^+CH_2CH_2CH_2Cl$ (m/z 151)

a. $C_5H_{12}OCl^+$ (C_2H_4 loss)
b. $C_5H_{13}O^+$ (C_2H_5Cl loss)
c. $C_3H_6Cl^+$ ($C_2H_5OC_2H_5$ loss)
d. $C_4H_{11}O^+$ (C_3H_5Cl loss)

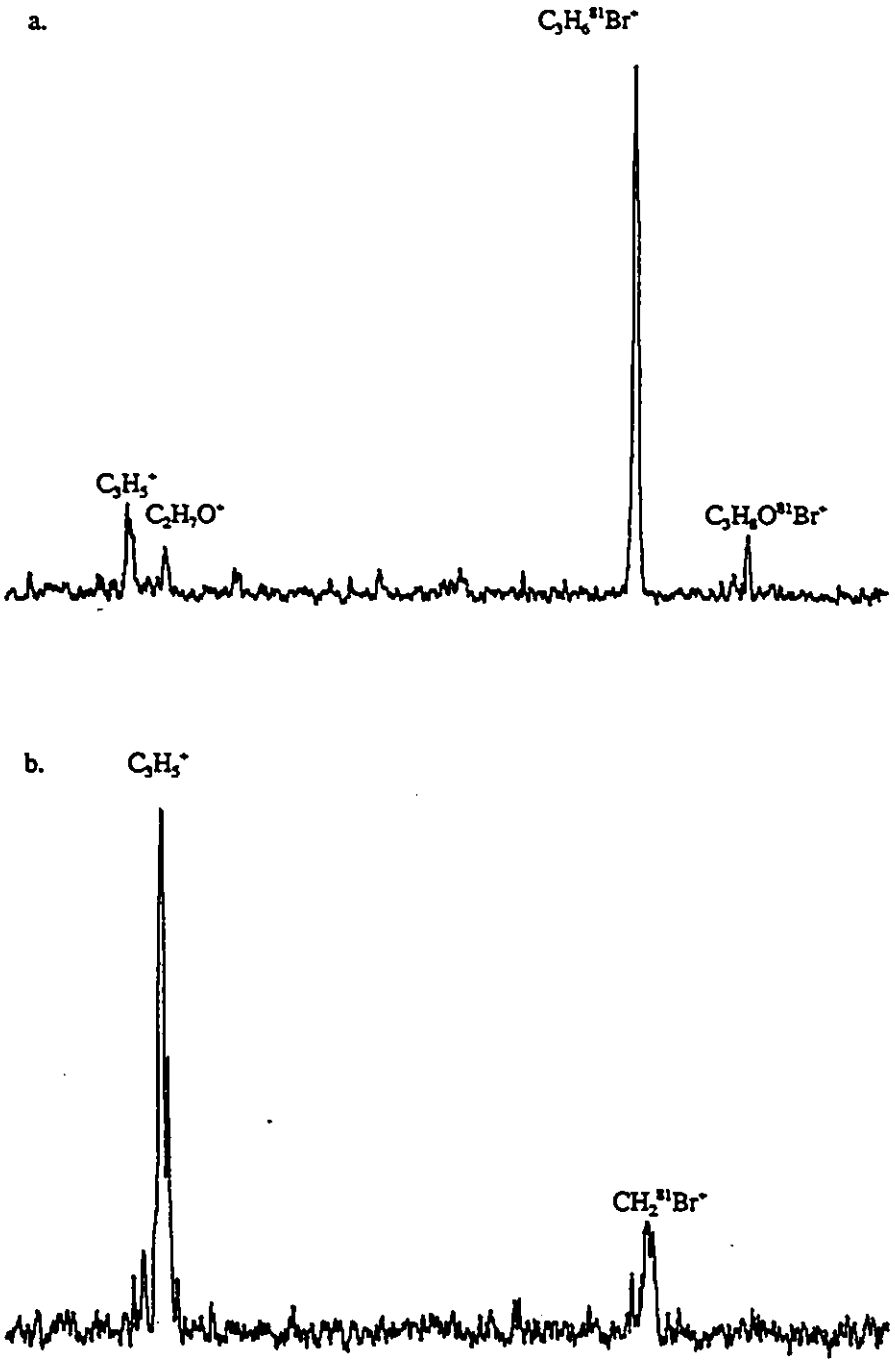

Figure 5.14 CID mass spectra of the daughter ions from $(C_2H_5)_2O^+CH_2CH_2CH_2^{81}Br$
a. $C_5H_{12}O^{81}Br^+$ (C_2H_4 loss) b. $C_3H_6^{81}Br^+$ ($C_2H_5OC_2H_5$ loss)

Chapter 6

Distonic radical cations

6.1 Introduction

The term "distonic ion" was introduced in 1984 by Radom et al[1] for ions with separated charge and radical sites that formally arise from the ionization of a zwitterion or a diradical. Greek letters were later proposed to indicate the relative location of the charge and radical sites. When using a conventional valence bond description, α-distonic ions have the charge and radical sites on adjacent atoms while two and three atoms separate the charge and radical sites in β- and γ-distonic ions, respectively. This method of identification is now widely accepted.[2]

A developing awareness that things were perhaps not quite that simple led to the appearance in the 1970's of scattered reports[3] describing stable gas-phase radical cations with structures that did not correspond to those of stable, neutral molecules. However, the current interest in the chemistry of these species seems to have been sparked by a number of papers appearing in 1981-1982 from different research groups, notably those of Holmes, Radom, Schwarz, and Terlouw.[4-6]

Distonic radical cations are of wide current interest for two reasons. First, many distonic ions are more stable than the isomeric conventional molecular ions. Small distonic ions, i.e. α-distonic ions, are especially stable and moreover are separated from their conventional isomers by quite large energy barriers. Thus a mutual interconversion between these distonic ions and the isomeric molecular ions is slow or does not occur at all. Secondly, distonic ions play an important role as the central intermediates and

products in the dissociation reactions of many ionized organic molecules, the best-known example being the McLafferty rearrangement of the molecular ions of carbonyl compounds.[2a,7] Further, it now seems likely that the gaseous, long-lived molecular ions of many organic compounds may exist as their distonic forms.[2] This is also true for the condensed phase: ESR studies indicate that stable distonic ions can be generated from many organic molecular ions in low-temperature freon matrices.[8] Furthermore, certain X- or γ-ray-irradiated amino acids have been shown to produce distonic ions in frozen matrices.[9] Thus, studies of distonic ions may lead to a better understanding of the biological consequences of ionizing radiation.

6.2 Results and discussion

In this Chapter the discussion of stable distonic radical cations is concentrated on their generation and characterization and the nature of these ions.

6.2.1 Generation and characterization of distonic radical cations

6.2.1.1 Generation of distonic radical cations

Distonic ions are generally formed from: (i) isomerization of a conventional radical cation; (ii) fragmentation of an isomerized molecular odd electron ion; and (iii) a bimolecular reaction between a distonic ion and a neutral molecule.

Isomerization of a conventional radical cation. When a heteroatom containing molecule is ionized, at first the heteroatom loses one electron from its lone-pair electrons and forms a conventional radical cation. If a hydrogen atom is available in the ion, the heteroatom may abstract this hydrogen to form a distonic ion.[7]

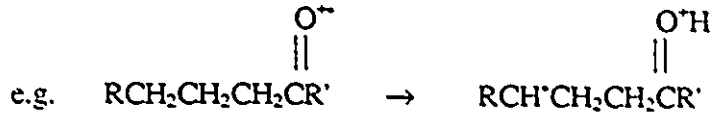

Even though most distonic ions were first proposed to arise from the isomerization of a conventional radical cation, the confirmation of the presence of such distonic ions is limited by the stability of the distonic ions. The distonic ion must be stable enough to produce distinguishable fragment products, different from those produced from the conventional radical cation. Otherwise it is difficult to confirm or prove the existence of the distonic ions.

Ring opening, or ring cleavage, of small cyclic radical cations is one mechanism expected to lead to stable distonic ions, such as the molecular ion of ethylene oxide (EO).[10]

The distonic ions thus produced are confirmed by their ability to transfer $CH_2^{+\bullet}$ to a molecule,[11] as well as by their characteristic CID mass spectra.

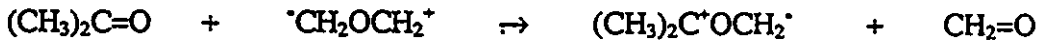

Fragmentation of an isomerized molecular ion.

The general method for the formation of a desired distonic ion involves a dissociative ionisation in which an appropriate rearrangement is followed by the elimination of a small stable molecule, such as CH_2O, CO_2, and CO.[12] For example, two newly observed distonic ions, $^{\bullet}CH_2CH_2C^{+}(OH)_2$ and $^{\bullet}CH_2CH_2OC^{+}(H)OH$ (Chapter 7)

were produced from the fragmentation of the following molecular ions.

$$CH_3OCH_2CH_2COOH^{+\bullet} \rightarrow {}^{\bullet}CH_2CH_2C^{+}(OH)_2 + CH_2O$$

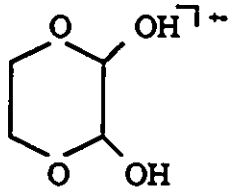

$$\rightarrow {}^{\bullet}CH_2CH_2OC^{+}HOH + HCOOH$$

Bimolecular reaction of a distonic ion with a neutral molecule.

Bimolecular reactions of distonic ions have been established either to produce another distonic ion or to be characteristic of the original distonic ion.[2] The novel ions generated this way include the first stable δ-distonic ion, ${}^{\bullet}CH_2CH_2CH_2CH_2CO^{+}$, an acyclic isomer of ionized cyclopentanone.[13]

$${}^{\bullet}CH_2CH_2CH_2CO^{+} + CH_2{=}C{=}O \rightarrow {}^{\bullet}CH_2CH_2CH_2CH_2CO^{+} + CO$$

6.2.1.2 Characterization of distonic radical cations

The presence of a distonic ion rather than a molecular ion of conventional structure can in some cases be demonstrated experimentally by exclusion; that is, by demonstrating that the properties of the ion in question are different from those of ions generated by direct ionization. Appearance energy (AE) measurements play an important role in the characterization of distonic radical cations. Heat of formation data are used in ion structure determination. If the Δ_fH^0 measured for an ion is different from that of a conventional counterpart the ion may have a distonic structure. Δ_fH° has been experimentally determined for several distonic ions by appearance energy (AE)

measurements.[14] A reliable $\Delta_f H^\circ$ value can be obtained if (i) the structure of the neutral product is known; (ii) the AE is accurately measured with well defined electron energies to limit the effect of the electron kinetic energy distribution.[15]

With a conventional double focusing mass spectrometer, most stable distonic ions can be distinguished from their conventional isomers by their structure characteristic fragmentations. The fragmentations of distonic ions are observed by metastable ion dissociation (MI), collision induced dissociation (CID), charge stripping (CS), collision induced dissociative ionization (CIDI) of the lost neutrals and neutralization-reionization (NR) mass spectrometries. Isotopically labelled precursors are used to provide additional evidence. CID is a powerful ion structural tool because high internal energies can be deposited in the ions upon collisional activation and the resultant direct bond cleavages being often favored over the slower and usually less informative rearrangement reactions. The CS mass spectrometry is more specifically used to characterize the distonic ions, since the radical site in a distonic ion may be readily ionized by collision.

NR mass spectrometry can provide valuable structure information in the characterisation of a distonic ion, because a distonic ion forms a diradical in the neutralization process, while the conventional counterpart does not. The dissociation of the diradical will produce a NR mass spectrum which is easily distinguishable from that of the conventional isomer.

Recently, examination of ion-molecule reactions with a Fourier-transform ion cyclotron resonance (FT-ICR) mass spectrometer has yielded information concerning the structures of low-energy ions. Differences in chemical reactivity may allow the distinction

of isomers that yield similar dissociation product distributions under CID conditions. However, the reactivity of an ion is strongly affected by its internal energy, especially when the ion in question has enough energy to isomerize. Thus the ion-molecule reactions approach to distonic ion characterization depends upon the condition that the ions must be generated with only small amounts of internal energy or that they are kinetically and internally relaxed without isomerisation prior to reaction.

High level ab initio molecular orbital theory studies have provided abundant information about an ion's bond lengths, bond angles, and charge distribution. Ab initio calculations have also been utilized in calculating heats of formation, as well as isomerization energy barriers. This kind of information is very useful to broaden our understanding of distonic ion chemistry.

6.2.2 Stable gas-phase distonic radical cations

To date over 50 distonic radical cations have been well characterized as stable gas-phase ionic species and more than 100 distonic ions have been proposed as the active intermediates involved in the dissociations of organic molecular radical cations. The generation and characterization of stable distonic radical cations will be discussed individually and shown briefly in Table 6.1.

6.2.2.1 Halogen-containing distonic radical cations

The distonic ions $^{\bullet}CH_2FH^+$ ($1^{+\bullet}$), $^{\bullet}CH_2ClH^+$ ($2^{+\bullet}$), and $^{\bullet}CH_2BrH^+$ ($3^{+\bullet}$) were produced from the fragmentation of $[XCH_2COOH]^{+\bullet}$ via CO_2 loss (X = F, Cl and Br).[12] These distonic ions were readily characterized by their distinctive CID mass spectra in

which the doubly charged $[CH_2XH]^{2+}$ cation is significantly stable, while for the conventional ion, CH_3X^{2+} has only marginal stability.[12] High level ab initio calculations have confirmed that these singly charged isomers are stable with respect to the high energy barrier between the distonic ions and the conventional isomers.[14] The heats of formation of $^{\bullet}CH_2XH^{+}$ ions have been measured to be 217±4 kcalmol^{-1}, 246±3 kcalmol^{-1}, and 237±3 kcalmol^{-1} for X = F, Cl and Br, respectively.[12] Thus $\mathbf{1}^{+\bullet}$ is 11 kcalmol^{-1} more stable than its conventional isomer $CH_3F^{+\bullet}$ (Δ_fH°, 228 kcalmol^{-1} [16]), $\mathbf{2}^{+\bullet}$ is 7 kcalmol^{-1} less stable than $CH_3Cl^{+\bullet}$ (Δ_fH°, 239 kcalmol^{-1} [16]), and $\mathbf{3}^{+\bullet}$ is 3 kcalmol^{-1} less stable than $CH_3Br^{+\bullet}$ (Δ_fH°, 234 kcalmol^{-1} [16]). The recently developed values from theoretical calculations are 230.8 kcalmol^{-1} for $\mathbf{1}^{+\bullet}$ and 251.0 kcalmol^{-1} for $\mathbf{2}^{+\bullet}$.[17] By the same calculations $\mathbf{1}^{+\bullet}$ is about 1 kcalmol^{-1} more stable than $CH_3F^{+\bullet}$ and $\mathbf{2}^{+\bullet}$ is 11 kcalmol^{-1} less stable than $CH_3Cl^{+\bullet}$. The theoretical calculations and the experimental measurements are in fair agreement for the heat of formation of $\mathbf{2}^{+\bullet}$ but not so for at the heat of formation of $\mathbf{1}^{+\bullet}$. If the energy difference between a distonic ion $^{\bullet}CH_2(CH_2)_nXH^{+}$ and its conventional isomer $CH_3(CH_2)_nX^{+\bullet}$ could be considered as the difference in the C-H bond strength and X-H bond strength, the extra stability of the distonic ion may account for the higher bond energy of X-H than C-H. From this point of view, one may expect that $\mathbf{1}^{+\bullet}$ should be more stable than $CH_3F^{+\bullet}$, since the H-F bond is stronger than a C-H bond. However, in an ionized species the bond strength may be different from the homolytic bond dissociation energy in the analogous neutral molecule.[18]

Three stable distonic ions, $^{\bullet}CH_2CH_2FH^{+}$ ($\mathbf{4}^{+\bullet}$), $^{\bullet}CH_2CH_2ClH^{+}$ ($\mathbf{5}^{+\bullet}$) and $^{\bullet}CH_2CH_2BrH^{+}$ ($\mathbf{6}^{+\bullet}$) have been generated from the fragmentations of $[XCH_2CH_2CH_2OH]^{+\bullet}$

(X = F, Cl and Br) via CH_2O loss.[19] The α-distonic isomers $CH_3{}^{\bullet}CHClH^+$ (**7**$^{\bullet\bullet}$) and $CH_3{}^{\bullet}CHBrH^+$ (**8**$^{\bullet\bullet}$) were also generated from $[CH_3CHXCOOH]^{\bullet\bullet}$ (X = Cl and Br) via CO_2 loss.[19,20] By CID mass spectrometry the distonic ions $^{\bullet}CH_2CH_2XH^+$ were characterized by the intense peaks at $CH_2^{\bullet\bullet}$, $C_2H_4^{\bullet\bullet}$ and $HX^{\bullet\bullet}$, whereas the $CH_3{}^{\bullet}CHXH^+$ isomers were characterized by the intense doubly charged ion peak $[CH_3CHXH]^{2+}$. In addition, a third type of distonic $C_2H_5X^{\bullet\bullet}$ isomer, $^{\bullet}CH_2Cl^+CH_3$ (**9**$^{\bullet\bullet}$) and $^{\bullet}CH_2Br^+CH_3$ (**10**$^{\bullet\bullet}$) were generated from $[XCH_2COOCH_3]^{\bullet\bullet}$ via CO_2 loss.[19,20] These distonic isomers showed pronounced dissociation via CH_3 loss.[19,20]

Ions **4**$^{\bullet\bullet}$ and **5**$^{\bullet\bullet}$ were found more stable than their conventional isomers. The heats of formation of these ions were indeed calculated to be 17.7 kcalmol^{-1} (X = F) and 3.1 kcalmol^{-1} (X = Cl) more stable than their corresponding conventional isomers.[21] However, the measured Δ_fH° values of $CH_3{}^{\bullet}CHClH^+$ (232 kcalmol^{-1}), $CH_3Cl^+CH_2{}^{\bullet}$ (242 kcalmol^{-1}), $CH_3{}^{\bullet}CHBrH^+$ (238 kcalmol^{-1}), and $CH_3Br^+CH_2{}^{\bullet}$ (253 kcalmol^{-1})[20] are all higher than those of the conventional isomers $C_2H_5X^{\bullet\bullet}$ ($C_2H_5Cl^{\bullet\bullet}$, 226 kcalmol^{-1} and $C_2H_5Br^{\bullet\bullet}$, 222 kcalmol^{-1})[16]. The difference between the heats of formation of $^{\bullet}CH_2CH_2ClH^+$ (**5**$^{\bullet\bullet}$) and $CH_3C^{\bullet}HClH^+$ (**7**$^{\bullet\bullet}$) may indicate the different C-H bond strengths in $CH_3CH_2ClH^+$. The hydrogen atom affinity (HA) values for even-electron ions have been thoroughly studied.[18]

$$\begin{array}{lll} RXH^+ \rightarrow & RX^{\bullet\bullet} + H^{\bullet} & \Delta Hr \\ HA\,[RX^{\bullet\bullet}] = \Delta Hr = & \Delta_fH^{\circ}\,[RX^{\bullet\bullet}] + \Delta_fH^{\circ}\,[H^{\bullet}] - \Delta_fH^{\circ}\,[RXH^+] & \end{array}$$

The HAs of **5**$^{\bullet\bullet}$ and **7**$^{\bullet\bullet}$ are thus estimated from the heats of formation of **5**$^{\bullet\bullet}$, **7**$^{\bullet\bullet}$, and $CH_3CH_2ClH^+$ (170 kcalmol^{-1} [16]) to be 105 kcalmol^{-1} and 114 kcalmol^{-1} for β-H and

α-H, respectively. It followed that the higher $\Delta_f H^\circ$ value of $7^{+\bullet}$ may result from the higher HA value at α- position. This probably results from the inductive effect of the -ClH group. The bond dissociation energies in CH_3CH_2Cl can be estimated from the heats of formation of CH_3CH_2Cl (-26.8 kcalmol^{-1} [16]), $^{\bullet}CH_2CH_2Cl$ (19.8 kcalmol^{-1} [22]) and $CH_3C^{\bullet}HCl$ (22.8 kcalmol^{-1} [22]); they are 101.7 kcalmol^{-1} and 98.2 kcalmol^{-1} for β-H and α-H, respectively. The two latter values are much closer than the HA values.

The higher $\Delta_f H^\circ$ value of $CH_3ClCH_2^{+\bullet}$ ($9^{+\bullet}$) is indicative of the weak C-Cl bond in the ion. The C-Br bond is also weak in ion $9^{+\bullet}$. This is expected and follows the same trend as the bond dissociation energy in the neutral counterparts.

6.2.2.2 Distonic isomers of alcohol radical cations, $^{\bullet}CH_2(CH_2)_nOH_2^+$.

The homologous distonic ions $^{\bullet}CH_2(CH_2)_nOH_2^+$ (n = 0 - 3) behave differently. The distonic ion $^{\bullet}CH_2OH_2^+$ ($11^{+\bullet}$) was produced from the fragmentation of several appropriate molecule radical cations[12]. In its CID mass spectrum $^{\bullet}CH_2OH_2^+$ was distinguished from $CH_3OH^{+\bullet}$ by an intense doubly charged ion peak at m/z 16.[4] Thus CS mass spectometry readily characterized this isomer.[4a] The heat of formation of $^{\bullet}CH_2OH_2^+$ was obtained by high level ab initio calculations to be 195±1 kcalmol^{-1},[17,23] which is in good agreement with that obtained from an AE measurement 195 ± 2 kcalmol^{-1}.[4a] Thus $11^{+\bullet}$ is 8 kcalmol^{-1} lower in energy than $CH_3OH^{+\bullet}$. The energy barrier for $^{\bullet}CH_2OH_2^+$ to isomerize to $CH_3OH^{+\bullet}$ was calculated to be 35±2 kcalmol^{-1}.[23,24]

The distonic ion $^{\bullet}CH_2CH_2OH_2^+$ ($12^{+\bullet}$) has also been produced from the fragmentation of the appropriate radical cations[6,25] and its MI and CID mass spectra were dominated by the dissociation process via H_2O loss. The very small kinetic energy release

value for this process was attributed to the involvement of a hydrogen-bridged water/ethene radical cation complex $[CH_2{=}CH{\bullet\bullet\bullet}H{\bullet\bullet\bullet}OH_2]^{+\bullet}$,[25,26] a proposal which was well supported by theoretical calculations.[25,27] The same calculations also predicted that the distonic ion $^{\bullet}CH_2CH_2OH_2^{+}$ is 7-10 kcalmol^{-1} more stable than the conventional isomer $CH_3CH_2OH^{+\bullet}$ and this is consistent with the experimental value (11 kcalmol^{-1}).[25] The bimolecular reactions of this distonic ion and its conventional isomer have been investigated in a Fourier transform ion cyclotron resonance mass spectrometer.[28] Strikingly different reactivity is observed for these two radical cations. The distonic ion undergoes thermoneutral exchange of a water molecule when reacted with ^2H- or ^{18}O-labeled water. Acetonitrile readily replaces water in this ion, as well. The ethanol radical cation predominantly reacts by proton transfer to all of these reagents.[28] Another distonic isomer is $CH_3{}^{\bullet}CHOH_2^{+}$ (**13**$^{+\bullet}$), which has been experimently observed[29] and theoretically calculated to be 6 kcalmol^{-1} more stable than $CH_3CH_2OH^{+\bullet}$.[25,27]

The distonic ion $^{\bullet}CH_2CH_2CH_2OH_2^{+}$ (**14**$^{+\bullet}$) is the reacting configuration for the H_2O loss from the propanol ion $CH_3CH_2CH_2OH^{+\bullet}$.[30,31] This distonic isomer has also been generated independently from the fragmentation of $[HOCH_2CH_2CH_2CH_2OH]^{+\bullet}$ via CH_2O loss.[30] The heat of formation of the ion was determined by an AE measurement to be 171±1 kcalmol^{-1}.[30] The theoretical prediction gave a value of 175 kcalmol^{-1}.[21] It has been confirmed by a deuterium-labelling experiment that the hydrogen transfer involved in the isomerization of $CH_3CH_2CH_2OH^{+\bullet}$ to $^{\bullet}CH_2CH_2CH_2OH_2^{+}$ is specifically from the methyl group.[30,31] The product ion from the dissociation of $^{\bullet}CH_2CH_2CH_2OH_2^{+}$ via H_2O loss has been confirmed to be cyclo-$C_3H_6^{+\bullet}$ by AE measurement[30] and by charge stripping

mass spectrometry. Thus the involvement of an ion-molecule complex [$\nabla^{+\bullet}$ OH_2] was proposed[31] and supported later by theoretical calculations.[32,33]

Competition between collision-activated isomerization and fragmentation of the distonic radical cations $^{\bullet}CH_2(CH_2)_nOH_2^+$ (n = 0 - 2) and their conventional counterparts ($CH_3(CH_2)_nOH^{+\bullet}$, n = 0 - 2) was examined under different experimental conditions in a triple quadrupole mass spectrometer and in a Paul-type quadrupole ion trap.[34] All the above pairs of isomers give structurally characteristic fragmentation products upon low-energy (eV) collision activation under single- and multiple-collision conditions in the triple quadrupole instrument. Fast direct bond cleavages dominate the fragmentation. Thus abundant even-electron ionic fragments are obtained for the conventional ions, while the distonic isomers yield prodominantly odd-electron ionic fragments. Further, the results suggest that the barrier between the ions $CH_3CH_2CH_2OH^{+\bullet}$ and $^{\bullet}CH_2CH_2CH_2OH_2^+$ is significantly lower than the barriers associated with the shorter chain homologues (n = 0 or 1).[34]

$^{\bullet}CH_2CH_2CH_2CH_2OH_2^+$ (**15**$^{+\bullet}$, formed by CH_2O loss from $HO(CH_2)_5OH^{+\bullet}$) showed very similar CID and NR mass spectra to its conventional isomer $CH_3CH_2CH_2CH_2OH^{+\bullet}$, suggesting their facile interconversion.[35] The heat of formation of ion **15**$^{+\bullet}$ has been measured in this laboratory to be 158 kcalmol^{-1}, being 8 kcalmol^{-1} lower than that of $CH_3(CH_2)_4OH^{+\bullet}$.

The distonic ion $^{\bullet}CH_2OCH_2CH_2OH_2^+$ (**16**$^{+\bullet}$) produced from the fragmentation of $[CH_3OCH_2OCH_2CH_2OH]^{+\bullet}$ via CH_2O loss was characterized by its MI and CID mass spectra.[36] The heat of formation of this distonic ion is not available yet.

6.2.2.3 Distonic isomers of ether radical cations

The smallest distonic isomer of ether radical cations is $^{\bullet}CH_2O^{+}(H)CH_3$ (**17**$^{\bullet\bullet}$), which was generated from the fragmentation of $[CH_3OCH_2COOH]^{+\bullet}$ via CO_2 loss.[29] This distonic ion was characterized by the absence of m/z 26 and m/z 27 in its CID mass spectrum. This indicates that the ion has no C-C bond. The major MI fragmentation produced m/z 31. The AE of this metastable peak led to an apparent Δ_fH° (m/z 31) = 201 kcalmol^{-1}, well above Δ_fH° ($^{+}CH_2OH$), 169 kcalmol^{-1} [37], and below Δ_fH° (CH_3O^{+}), 253 kcalmol^{-1} [38]. The daughter ion was thus confirmed to be $^{+}CH_2OH$. In contrast, loss of $CH_3^{\bullet}$ from $[CH_3OCH_3]^{+\bullet}$ produces an unstable $[CH_3O^{+}]$ ion which fragments into ^{+}CHO + H_2.[39] The heat of formation of $^{\bullet}CH_2O^{+}(H)CH_3$ has been calculated to be 186.5 kcalmol^{-1},[38] which is close to Δ_fH° ($CH_3OCH_3^{+\bullet}$), 187.2 kcalmol^{-1}.[16] The high energy barrier measured to be 53 kcalmol^{-1}, separates the two isomers and prevents their interconversion.[29]

Two distonic isomers, $^{\bullet}CH_2CH_2O^{+}(H)CH_3$ (**18**$^{\bullet\bullet}$) and $^{\bullet}CH_2O^{+}(H)CH_2CH_3$ (**19**$^{\bullet\bullet}$) were found to dissociate in a manner closely similar to that of ionized propan-1-ol.[40] The energy barriers for the isomerization of these ions have been established and the heat of formation of $^{\bullet}CH_2CH_2O^{+}(H)CH_3$ was measured to be 170±2 kcalmol^{-1}.[41]

The homologous distonic ion $^{\bullet}CH_2CH_2O^{+}(H)CH_2CH_3$ (**20**$^{\bullet\bullet}$) was generated by the fragmentation of $[CH_3CH_2OCH_2CH_2OCH_2CH_3]^{+\bullet}$ via CH_3CHO loss and found to have lower energy (Δ_fH^0 = 153 kcalmol^{-1})[41] than its conventional isomer $C_2H_5OC_2H_5^{+\bullet}$ (Δ_fH^0 = 159 kcalmol^{-1}).

$(CH_3)_2{}^{\bullet}CCH_2O^{+}(H)CH_3$ (**21**$^{+\bullet}$) is a distonic isomer of $C_5H_{12}O^{+\bullet}$ radical cations. It was formed from the rearrangement-dissociation of $[(CH_3)_2C(CH_2OH)CH_2OCH_3]^{+\bullet}$ via CH_2O loss[42] and its Δ_fH° was measured to be 6.5 kcalmol^{-1} lower in energy than that for its conventional isomer, $(CH_3)_3CCH_2OH^{+\bullet}$ (being 148 kcalmol^{-1}).[42] The latter isomer rearranges to $(CH_3)_2{}^{\bullet}CCH_2O^{+}(H)CH_3$ via the formation of a ion-radical complex $[(CH_3)_3C^{+}\ {}^{\bullet}CH_2OH]$, in which the radical can rotate, and so yielding the β-distonic ion $(CH_3)_2{}^{\bullet}CCH_2O^{+}(H)CH_3$.[43]

Another observed distonic isomer of $C_5H_{12}O^{+\bullet}$ ions is ${}^{\bullet}CH_2CH_2O^{+}(H)CH_2CH_2CH_3$ (**22**$^{+\bullet}$) generated from the fragmentation of 1-ethoxy-2-propoxyethane.[44] In its CID mass spectrum this ion yielded the same products as ionized 1-ethoxypropane ($CH_3CH_2OCH_2CH_2CH_3{}^{+\bullet}$), but with a different branching ratio.[44] This distonic ion was also observed to undergo competitive and successive long-distance H-transfer(1,4-H, 1,5- and 1,6-H shifts), whereas 1,2-H and 1,3-H shifts from a carbon atom to a radical site were not observed.[44]

The γ-distonic isomers of the ether molecule radical cations, $CH_3{}^{\bullet}CHCH_2CH(CH_3)O^{+}(H)CH_3$, $CH_3{}^{\bullet}CHCH_2CH(CH_3)O^{+}(H)CH2CH_3$, $\bullet CH2CH2CH(CH_3)O^{+}(H)CH_3$, $CH_3{}^{\bullet}CHCH_2CH_2O^{+}(H)CH_3$ and $CH_3{}^{\bullet}CHCH_2CH_2O^{+}(H)CH_2CH_3$ were generated by loss of neutral aldehydes form the appropriate diethers, according to the reasonable fragmentation mechanism depicted in Scheme 6.1.[45]

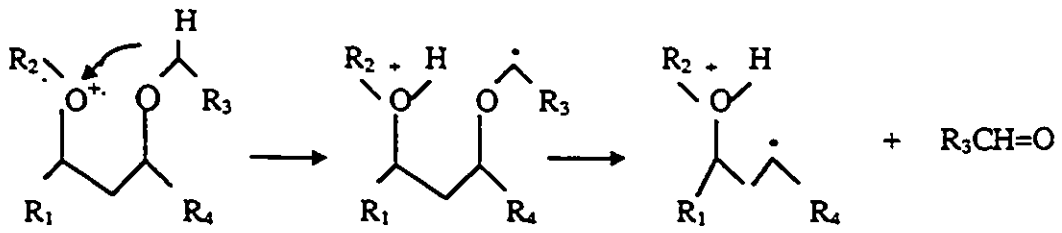

Scheme 6.1

These distonic radical cations have been studied by CID mass spectrometry and identified by their characteristic decomposition via alcohol loss.[45] However, no thermochemical data have been measured.

The δ-distonic oxonium ions $R_1{}^{\bullet}CHOCH_2CH_2O^{+}(H)R_2$ (R_1 = H, CH_3; R_2 = H, CH_3, CH_2CH_3) have been studied.[46] These δ-distonic ions are all derived from ionized $ROCH_2CH_2OR'$ (R, R' = H, CH_3, C_2H_5) and fragment, depending on R and R', by three reactions: the loss of an alcohol or a water molecule, the formation of a β-distonic ion $^{\bullet}CH_2CH_2O^{+}(H)R$ and a 1,4-H migration between carbon atoms.[46]

6.2.2.4 Distonic isomers of carbonyl compound radical cations

Intramolecular hydrogen atom transfer in a large number of aldehyde and ketone radical cations has been surmised to give rise to distonic isomers. However, unambiguous evidence for the stability of these ions has not been forthcoming, specially for high mass homologous distonic ions. One of the small distonic isomers among those $C_nH_{2n}O^{+\bullet}$ radical cations is $^{\bullet}CH_2CH_2CH=O^{+}H$ ($23^{+\bullet}$), which has been directly generated by the fragmentation of $[CH_3OCH_2CH_2CH=O]^{+\bullet}$ via CH_2O loss and characterized by MI and CID mass spectrometries.[47] The heat of formation derived from an AE measurement was 180.9 $kcalmol^{-1}$,[47] about 4 $kcalmol^{-1}$ [16] lower than that of $CH_3CH_2CHO^{+\bullet}$. However, it is

about 22 kcalmol^{-1} [16] higher in energy than the enol isomer $CH_3CH{=}CHOH^{+\bullet}$. This reveals that although a distonic ion can be stabilized by a higher X-H bond energy than C-H, an enol isomer may be the lowest energy species, stabilized by resonance stabilization.

The distonic ion $^{\bullet}CH_2CH_2C(=O^{+}H)CH_3$ (**24**$^{+\bullet}$) was generated from $CH_3COCH_2CH_2OCH_3$ by CH_2O loss.[58,59] The MI mass spectrum of **24**$^{+\bullet}$ is very similar to that of $CH_3C(OH)CHCH_3^{+\bullet}$, being distinguished only by the presence of a weak m/z 42 peak in the former spectrum. The CID mass spectra of **24**$^{+\bullet}$ and $CH_3C(OH)CHCH_3^{+\bullet}$ are also very similar, differing significantly only in the presence of a very weak m/z 58 in the spectrum of **24**$^{+\bullet}$. The weak m/z 58 in the CID mass spectrum of **24**$^{+\bullet}$ implies the presence of an exposed methylene in the collided ion. The heat of formation of **24**$^{+\bullet}$ was determined by an AE measurement to be 165 kcalmol^{-1}, indicating that the ion is not $CH_3C(OH)CHCH_3^{+\bullet}$ (Δ_fH°, 139 kcalmol^{-1} [16]). The distonic structure was therefore proposed.

The distonic ion **24**$^{+\bullet}$ combined with other distonic isomers, $CH_3{}^{\bullet}CHCH_2CH(=O^{+}H$ (**25**$^{+\bullet}$, Δ_fH = 164.9 kcalmol^{-1}) and $^{\bullet}CH_2CH(CH_3)CH(=O^{+}H)$ (**26**$^{+\bullet}$, Δ_fH = 153.9 kcalmol^{-1}), are believed to be important intermediates involved in the dissociation of $CH_3C(O)CH_2CH_3^{+\bullet}$ and $CH_3CH_2CH_2CHO^{+\bullet}$ radical cations.[48]

The homologous distonic isomers of $C_5H_{10}O^{+\bullet}$ and $C_6H_{12}O^{+\bullet}$ ions have been proposed to decompose at low energies in the same way as their conventional isomers and are all interconvertible with each other by three-, five- and six-membered ring hydrogen transfers and three membered ring skeletal rearrangements.[49,50]

Recent studies on the small ester molecular radical cations have shown unambiguously that these small ester molecular ions prefer to rearrange to their distonic isomers in the time scale of 10^{-5} s.[51-64] From double collision experiments on methyl formate ions, it was proposed that the non-decomposing ions have undergone rearrangement into the distonic isomer, $^{\bullet}CH_2OC^{+}HOH$ ($27^{+\bullet}$).[51] The proposal was supported by high level ab initio calculations,[52,53] which showed that first the methyl formate radical cation rearranges via a hydrogen 1,4-shift to the distonic ion, which in turn isomerizes to the hydrogen-bridged complex $[HC{=}O{\bullet\bullet\bullet}H{\bullet\bullet\bullet}O{=}CH_2]^{+\bullet}$.[53a] The calculations also showed that the distonic isomer lies 13.5 kcalmol^{-1} lower in energy than ionized methyl formate and the rearrangement of methyl formate radical cation to its distonic isomer requires 15.5 kcalmol^{-1}. Vertical ionization of methyl formate produces an ion lying 8.4 kcalmol^{-1} above ground state ionized methyl formate; consequently, rearrangement to the distonic ion only requires a further 1.4 kcalmol^{-1}. The calculations thus predict that ionization of methyl formate initially produces the σ state of the methyl formate radical cation which may rearrange with a small barrier to the distonic isomer $^{\bullet}CH_2OC^{+}HOH$.[53b]

$^{\bullet}CH_2CH_2OC^{+}HOH$ ($28^{+\bullet}$), the distonic isomer of ethyl formate radical cation has been generated directly from the fragmentation of 1,4-dioxane-2,3-diol molecule ions via HCOOH loss (Chapter 7). The MI, CID and NR mass spectrometric studies showed that this distonic isomer is the key intermediate involved in the dissociations of ethyl formate radical cations. The rearrangement of ethyl formate ion to this distonic ion was proposed earlier[54,55] but not substantiated. The heat of formation of this ion, derived from an AE

measurement was 137 kcalmol^{-1} (Chapter 7), which is 16 kcalmol^{-1} lower in energy than its conventional isomer $HCOOCH_2CH_3^{+\bullet}$ (Δ_fH = 153 kcalmol^{-1} [54]).

The distonic ion, $CH_3{}^{\bullet}CHCH_2OC^{+}HOH$ (**29**$^{+\bullet}$) was also proposed as an intermediate involved in the dissociation of the $HCOOCH_2CH_2CH_3^{+\bullet}$ radical cation.[56] The heat of formation of this distonic ion was estimated to be < 138 kcalmol^{-1}.[56]

The unimolecular chemistry of ionized methyl acetate has received attention anew,[57-62] when it was discoved that the $[H_3,C,O]^{\bullet}$ radicals formed together with CH_3CO^{+} chiefly have the $H_2C^{\bullet}OH$ structure rather than the expected methoxy radicals formed by a direct bond cleavage. The reacting configuration for formation of $H_2C^{\bullet}OH$ from ionized methyl acetate has been proposed to be the α-distonic ion $^{\bullet}CH_2OC^{+}(OH)CH_3$ (**30**$^{+\bullet}$).[61] Extensive deuterium-labelling experiments[58] on methyl acetate and its enol have led to the proposal that this distonic ion is the key intermediate, which accounts for the extensive, but incomplete, loss of positional identity of H and D atoms in the labeled isomers. The proposal was also confirmed by generation of the distonic ion from $[CH_3COOCH_2OCH_3]^{+\bullet}$ via CH_2O loss.[58] The heat of formation of $^{\bullet}CH_2OC^{+}(OH)CH_3$ was calculated (MP2/6-31G(d)//3-21G level) to be 127 kcalmol^{-1} [62], which is in good agreement with the experimentally measured value of 130±1 kcalmol^{-1}.[61] The key intermediate in the fragmentation has not been identified by experiment, but calculations[62] indicate that the H-bridged ion $[CH_3C^{\bullet}O\bullet\bullet\bullet H^{+}\bullet\bullet\bullet OCH_2]$ probably plays this role.

The homologous distonic ion $^{\bullet}CH_2CH_2C^{+}(OH)OCH_3$ (**31**$^{+\bullet}$) was also proposed to be involved in the dissociations of the $CH_3CH_2C(=O)OCH_3^{+\bullet}$ radical cation from the results of CID mass spectrometry.[61]

The distonic ion $^{\bullet}CH_2CH_2C^{+}(OH)_2$ ($32^{+\bullet}$) was proposed as an intermediate involved in the dissociation of ionized propanoic acid.[63] The experimental evidence showed (Chapter 7) that the ion $32^{+\bullet}$ was initially produced from $[CH_3OCH_2CH_2COOH]^{+\bullet}$ by loss of CH_2O, then quickly isomerized to the more stable isomer $CH_3CHC(OH)_2^{+\bullet}$. The CID mass spectrum of $32^{+\bullet}$ clearly showed CH_2 loss, which is absent in CID mass spectra of $CH_3CH_2COOH^{+\bullet}$ and $CH_3CHC(OH)_2^{+\bullet}$ (generated from $[CH_3CH_2CH(CH_3)COOH]^{+\bullet}$ by loss of C_2H_4).

The homologues $CH_3{}^{\bullet}CHCH_2C^{+}(OH)_2$ and $(CH_3)_2{}^{\bullet}CCH_2C^{+}(OH)_2$ were also proposed to be the intermediates involved in the dissociations of $CH_3CH_2CH_2COOH^{+\bullet}$ and $(CH_3)_2CHCH_2COOH^{+\bullet}$, respectively.[64]

6.2.2.5 Distonic ions as the isomers of cyclic radical cations

Several stable distonic ions which are the isomers of small cyclic radical cations, such as the molecular ions of ethylene oxide and cyclobutanone, have been well characterized by ion-molecule reactions.[2b] The distonic ion $^{\bullet}CH_2CH_2CH_2^{+}$ ($33^{+\bullet}$) is now believed to be formed by ring opening of internally excited, ionized cyclopropane.[65] This distonic ion has been calculated (MP2/6-31G*//UHF/6-31* level) to be 21.7 kcalmol^{-1} higher in energy than the cyclic cyclopropane radical cation.[66] An extensive experimental study[65] focusing on dissociation as well as bimolecular reactions of the cyclopropane radical cation showed that the low-energy radical cation is cyclic. Upon excitation, this ion isomerizes to the distonic radical cation, $^{\bullet}CH_2CH_2CH_2^{+}$,[65] and not to ionized propene as suggested earlier.[67]

The distonic ion $^{\bullet}CH_2OCH_2^+$ ($34^{+\bullet}$) is the acyclic isomer of ionised ethylene oxide. Ion $34^{+\bullet}$ was formed by electron ionization and subsequent ring opening of ethylene oxide or by loss of CH_2O from ionized 1,3-dioxolane.[3b] Ethylene carbonate loses CO_2 to give $^{\bullet}CH_2CH_2O^+$ which quickly isomerizes to $^{\bullet}CH_2OCH_2^+$. High level ab initio molecular orbital studies suggested[69] that the cleavage of the C-C bond of ionized ethylene oxide requires only 6.5 kcalmol^{-1} and yields an ion that is 20 kcalmol^{-1} lower in energy than the cyclic ethylene oxide radical cation, in agreement with experimental data.[2a] The ion $^{\bullet}CH_2OCH_2^+$ shows[70] $CH_2^{+\bullet}$ transfer when reacted with neutral reagents and to be facile for n-donor bases. This reaction has not been observed for other $C_2H_4O^{+\bullet}$ isomers.[3b]

The higher homologue of $^{\bullet}CH_2OCH_2^+$, the ion $^{\bullet}CH_2CH_2OCH_2^+$ ($35^{+\bullet}$), has also been studied. This ion is formed, for example, by the loss of formaldehyde from ionized 1,4-dioxane.[71] Ab initio molecular orbital theory calculations (RHF/4-31G//RHF/STO-3G) indicate[72] that $^{\bullet}CH_2CH_2OCH_2^+$ is 193 kcalmol^{-1}, in agreement with the AE measurement derived value of 194 kcalmol^{-1}.[71c] The ion $^{\bullet}CH_2CH_2OCH_2^+$ has been well characterized by CID[71] and NR[73] mass spectrometries. The studies of the bimolecular reactions of this distonic ion showed that the ion rapidly transfers ionized ethylene to neutral molecules such as CH_3COCH_3, CH_3COOH, NH_3 and CH_3CN, while the conventional counterpart, the ionized trimethylene oxide only reacts by electron transfer.[11,74] Abstraction of $CH_3S^{\bullet}$ from CH_3SSCH_3 by $35^{+\bullet}$ has been reported.[74] The fact that CH_3S abstraction was not observed for the conventional isomer or for the even-electron analog, $CH_3CH_2OCH_2^+$ has led to the suggestion that this reaction involves the

radical site in the distonic ion, and that bond-formation most likely occurs at the radical site.[74]

The distonic ion $^{\bullet}CH_2CH_2CO^{+}$ (36$^{+\bullet}$) is the acyclic isomer of ionised cyclopropanone. It was calculated to be the second most stable $C_3H_4O^{+\bullet}$ isomer.[75] Its heat of formation has been calculated to be 201.6 kcalmol^{-1} at the G2 level[75] and 197 kcalmol^{-1} at MP4/6-31G*/6-31G*+6-31G* ZPVE.[76]. The ion has been produced from fragmentation of the diketene radical cation via CO loss[76,77] or by loss of ethylene from ionized γ-butyrolactone.[78] The structure of this ion was deduced on the basis of its dissociation reactions.[76-78] The ion $^{\bullet}CH_2CH_2CO^{+}$ reacts with dimethyl disulfide through abstraction of a thiomethyl group and charge exchange.[79]

Ionization of cyclobutanone has been suggested to lead to the ring-opened distonic ion $^{\bullet}CH_2CH_2CH_2CO^{+}$ (37$^{+\bullet}$) on the basis of ab initio molecular orbital calculations (MP2/6-31G**//6-31G*+ZPVE) which indicate that the distonic structure is 18 kcalmol^{-1} lower in energy than the cyclic isomer.[80] Differences observed in the CID mass spectra and metastable ion dissociation of ionized cyclobutanone and other $C_4H_6O^{+\bullet}$ isomers provided further support for this proposal.[81] Comparison of the CID mass spectrum of the derivatized ion to those of reference ions, conclusively demonstrated that a stable γ-distonic ion is generated upon ionization of cyclobutanone.[82] While the majority of the bimolecular reactions of distonic ions seem to involve the charge site, the ring-opened cyclobutanone distonic radical cation shows different, radical-type behavior.[82] For example, the ion abstracts a hydrogen atom from acetone in a reaction that involves bond

formation at the radical site of $^{\bullet}CH_2CH_2CH_2CO^+$, as indicated by the CID mass spectra measured for the reaction product and for certain reference ions.[82]

Very recently the stable δ-distonic ion $^{\bullet}CH_2CH_2CH_2CH_2CO^+$ (**38**$^{\bullet\bullet}$) was observed from the ion-molecule reaction of $^{\bullet}CH_2CH_2CH_2CO^+$ (**37**$^{\bullet\bullet}$) with CH_2CO via CO loss.[13] Whereas the CID mass spectrum of ion **38**$^{\bullet\bullet}$ did not produce structurally informative data, the studies of its ion-molecule reaction showed that ion **38**$^{\bullet\bullet}$ abstracted $CH_3S^{\bullet}$ from CH_3SSCH_3.[13] The slower abstraction rate for **38**$^{\bullet\bullet}$ than for **37**$^{\bullet\bullet}$ has been rationalized on the basis that **37**$^{\bullet\bullet}$ can form a favorable six-membered transition state for the abstraction of $CH_3S^{\bullet}$ after addition of CH_3SSCH_3 to the charge site.[2d] The complete lack of electron-transfer reactions for the ion **38**$^{\bullet\bullet}$ demonstrates that this ion does not exist in equilibrium with any conventional $C_5H_8O^{\bullet\bullet}$ ion.[13]

6.2.2.6 Nitrogen-containing distonic radical cations

The well-described gas-phase distonic amine cation $^{\bullet}CH_2NH_3^+$ (**39**$^{\bullet\bullet}$) was generated by the loss of CH_2O from ionised ethanolamine.[12] The large differences between its CID mass spectrum and the CID mass spectrum of $CH_3NH_2^{\bullet\bullet}$, and the presence of an intense $^{\bullet}CH_2NH_3^{2+}$ ion, are similar to those observed in the $^{\bullet}CH_2OH_2^+$, $CH_3OH^{\bullet\bullet}$ system and clearly show that ion **39**$^{\bullet\bullet}$ is a stable species.[12] Ion **39**$^{\bullet\bullet}$ was characterized by the fragment $NH_3^{\bullet\bullet}$ in its NR mass spectrum, which is absent in the NR mass spectrum of $CH_3NH_2^{\bullet\bullet}$.[83] Recently, theoretical calculations (G2 level) showed the heat of formation of ion **39**$^{\bullet\bullet}$ (203.6 kcalmol^{-1}) is close to that of $CH_3NH_2^{\bullet\bullet}$ (204.7 kcalmol^{-1}).[17] The energy barrier between these two isomers was calculated to lie 42 kcalmol^{-1} above $^{\bullet}CH_2NH_3^+$.[14]

The MI and CID mass spectrometric studies on the distonic ion $^{\bullet}CH_2CH_2NH_3^+$ (**40**$^{+\bullet}$), generated by loss of CH_2=NH from $[H_2NCH_2CH_2CH_2NH_2]^{+\bullet}$, showed that this ion is markedly different from those of $CH_3CH_2NH_2^{+\bullet}$ and $CH_3NHCH_3^{+\bullet}$.[12,84] The NR mass spectrometric studies further confirmed that ion **40**$^{+\bullet}$ is distonic.[35] Ion **40**$^{+\bullet}$ was found (MP3/6-31G** ZPVE) as the most stable $C_2H_7N^{+\bullet}$ isomers (7.9 kcalmol^{-1} lower in energy than $CH_3CH_2NH_2^{+\bullet}$).[85]

Another $C_2H_7N^{+\bullet}$ distonic isomer has been identified as $CH_3{}^{\bullet}CHNH_3^+$ (**41**$^{+\bullet}$), formed from the fragmentation of $H_2NCH_2CH(CH_3)NH_2^{+\bullet}$ via CH_2=NH loss or from $HOCH_2CH(CH_3)NH_2^{+\bullet}$ by loss of CH_2O.[84] The ion **41**$^{+\bullet}$ was characterized by the presence of $CH_3{}^{\bullet}CHNH_3^{2+}$ in its CID mass spectrum and by deuterium-labelling experiments.[84] The heat of formation of **41**$^{+\bullet}$ has been determined by ab initio calculations carried out at the MP3/6-31G** ZPVE level to be 186.3 kcalmol^{-1}.[85] The two distonic isomers, **40**$^{+\bullet}$ and **41**$^{+\bullet}$ have similar Δ_fH° values and are well separated from their conventional isomers by high energy barriers (> 40 kcalmol^{-1}).[85]

The γ-distonic ion $^{\bullet}CH_2CH_2CH_2NH_3^+$ (**42**$^{+\bullet}$) was observed as an intermediate from ion-molecule reaction of ionised cyclopropane with NH_3.[86] Ion **42**$^{+\bullet}$ was characterized by decomposing to $CH_2NH_2^+$ and to another distonic species, $^{\bullet}CH_2NH_3^+$.[86] Stable $^{\bullet}CH_2CH_2CH_2NH_3^+$ was prepared from $H_2NCH_2CH_2CH_2CH_2NH_3^{+\bullet}$ by loss of CH_2=NH. Ion **42**$^{+\bullet}$ was also characterized by its NR mass spectrum which showed the fragment $NH_3^{+\bullet}$.[35] However, the CID mass spectrum of **42**$^{+\bullet}$ differed only slightly from that of the propylamine molecular ion.[35] Ab initio calculations confirm that **42**$^{+\bullet}$ should be a stable

species,[21,87] lying 6.7 kcalmol^{-1} [87] or 9.3 kcalmol^{-1} [21] lower in energy than ionised propylamine.

The higher homologous nitrogen-containing distonic ions, such as $^{\bullet}CH_2CH_2N^{+}H_2R$ [R = CH_3, C_2H_5, $CH_2CH_2CH_3$, $CH(CH_3)_2$, $CH_2CH_2CH_2CH_3$ and $C(CH_3)_3$], $CH_3{}^{\bullet}CRCH_2N^{+}H_3$ [R = H, and CH_3] and $^{\bullet}CH_2CR_1R_2CH_2N^{+}H_3$ [R_1, R_2 = H, CH_3] have been produced from the fragmentations of alkoxyalkylamine molecular ions, which react by loss of a neutral aldehyde or ketone.[88] The predominant fragmentation and isomerization processes shown in their CID mass spectra are (i) simple cleavage of a C-N bond with formation of alkene ions or alkene molecules, (ii) 1,2-migration of protonated amino groups, and (iii) formation of ammonium ions by elimination of alkenyl radicals. The hydrogen abstractions are generally reversible; in the presence of long alkyl groups, isomerization to amine molecular ions (and vice versa) can occur.

6.2.2.7 Sulphur-containing distonic radical cations

The distonic ion $^{\bullet}CH_2SH_2^{+}$ (**43**$^{\bullet\bullet}$) was generated from $[HOCH_2CH_2SH]^{\bullet\bullet}$ by loss of CH_2O.[12] The differences between the CID mass spectra of **43**$^{\bullet\bullet}$ and $CH_3SH^{\bullet\bullet}$ are not nearly so striking as for the oxy-analogues. Nevertheless, the enhanced charge stripping peak $[CH_2SH_2]^{2+}$ and the greater relative abundances of $H_2S^{\bullet\bullet}$ and $CH_2^{\bullet\bullet}$ are in keeping with the behavior of the distonic ion $^{\bullet}CH_2SH_2^{+}$.[12] The heat of formation of **43**$^{\bullet\bullet}$ is calculated (G2 level) to be 232.1 kcalmol^{-1}, being 18.7 kcalmol^{-1} higher in energy than $CH_3SH^{\bullet\bullet}$.[17] The experimentally obtained heat of formation of **43**$^{\bullet\bullet}$ was 223 kcalmol^{-1}.[12] The isomerization energy barrier between $^{\bullet}CH_2SH_2^{+}$ and $CH_3SH^{\bullet\bullet}$ was calculated to be

24.6 kcalmol^{-1} above $^{\bullet}CH_2SH_2^+$, slightly below the dissociation energy barriers.[14] This is consistent with the experimental observations.[12]

Another sulphur-containing distonic ion is $(CH_3)_2S^+$-$CH_2^{\bullet}$ (**44**$^{+\bullet}$), which was formed by the ion-molecule reaction of $^{\bullet}CH_2OCH_2^+$ + CH_3SCH_3 followed by CH_2O loss.[89] Ab initio MO calculations at the MP2/6-31G$^{\bullet}$//6-31G$^{\bullet}$ + ZPVE level suggest that the ion **44**$^{+\bullet}$ is 17.9 kcalmol^{-1} higher in energy than ionized ethyl methyl sulfide. However, this distonic ion is stable towards isomerization to the conventional structure: the two ions showed distinctly different reactivity in an FT-ICR mass spectrometer. This distonic radical cation possesses unique chemical reactivity in that its reactions are associated with the radical site. Most of these reactions involve a homolytic bond cleavage in the neutral molecule, resulting in abstraction of an atom or a radical by the ion. Hence ion **44**$^{+\bullet}$ can be described as an electrophilic radical with an inert charge site.[90]

6.2.3 The nature of distonic radical cations

6.2.3.1 The stability of distonic ions

The relative stability of distonic ions compared to their conventional isomers are shown in Table 6.2. Most O, N, F-containing distonic ions are more stable than their conventional isomers. If one viewed the distonic ions as being formed from a C-H bond cleavage in the conventional isomers followed by formation of an X-H bond (X = O, N, F, •••), then, the lower heats of formation of distonic ions compared to their conventional isomers may result from the difference between HAs for the C-H bond and X-H bond in the even-electron ions H-CRR'$(CH_2)_n$X-H$^+$. However, the $\Delta\Delta_fH$ values in Table 6.2 change from -20 kcalmol^{-1} to 31 kcalmol^{-1}, indicating a very wide range of BDEs and this

approach appears unsatisfactory. The HA of X-H in some oxygen-containing cations have been investigated.[18] In general, hydroxyl [O-H] HA values for the removal of a hydrogen atom from an aldehydic of ketonic carbonyl cation are not greatly different from the homolytic bond dissociation energies (BDE) of O-H, typically 104±1 kcalmol^{-1}.[91] In marked contrast, HA values for the ionized carbonyl groups are large indeed, generally exceeding the BDE in water, 119 kcalmol^{-1}.[91] For the nitrogen-containing cations, namely protonated amines, the HA values correspond closely to the BDE in NH_3, 107 kcalmol^{-1} [91] or are a little smaller. The H-CH_2 bond in oxygen-containing cations is significantly stronger than for any neutral counterparts. It follows that the H-C bond and X-H bond in H-CRR'$(CH_2)_n$X-H$^+$ may both be stronger than those in the neutral counterparts. Therefore, the stability of a distonic ion compared to that of the conventional isomer may not be directly estimated from the different C-H and X-H bond strengths. Alternatively, if one can assume that in a distonic ion the charge site and the radical site are independent, i.e. there is no significant interaction between the two sites, then the two sites may be considered individualy, as shown in Scheme 6.2.

$$\text{H-CRR'}(CH_2)_n\text{X} \xrightarrow{-H^\bullet} {}^\bullet\text{CRR'}(CH_2)_n\text{X} \xrightarrow{H^\bullet} {}^\bullet\text{CRR'}(CH_2)_n\text{XH}^+$$

R, R' = H, CH_3, C_2H_5, ••••
n = 0, 1, 2, ••••
X = F, Cl, Br, OR, C(=O)R, C(=O)OR, NRR', SR, ••••

Scheme 6.2

Thus, the heat of formation of a distonic ion can be estimated from the BDE in a neutral organic molecule (M) and the proton affinity (PA) of the molecule, as shown in Eq. 1.

$$\Delta_fH^\circ(D)_{est} = [\Delta_fH^\circ(M) + BDE(C\text{-}H) - \Delta_fH^\circ(H^\bullet)] + \Delta_fH^\circ(H^+) - PA(M)$$

$$= \Delta_fH^\circ(R^\bullet) + \Delta_fH^\circ(H^+) - PA(M) \qquad (1)$$

$\Delta_fH^\circ(R^\bullet)$ is the heat of formation of the organic radical produced from the C-H bond cleavage in an organic molecule. Most of $\Delta_fH^\circ(R^\bullet)$ values are from References 16 and 92. The other unknown $\Delta_fH^\circ(R^\bullet)$ values are estimated from BDE data, which for β- and γ- distonic ions are assumed as the BDE in ethane (100 kcalmol^{-1}).

The estimated heat of formation values of distonic ions are shown in Table 6.3. The estimation is based on the assumption that there is no charge-radical interaction in the distonic ions and so the difference between the estimated value, $\Delta_fH^\circ(D)_{est}$, and the measured (or calculated) value, $\Delta_fH^\circ(D)$, may indicate the presence of significant charge-radical interaction. The new difference values, $\Delta\Delta_fH$, are shown in Table 6.4.

It is noteworthy that the $\Delta\Delta_fH$ values of α-distonic ions are all close, being 14-18 kcalmol^{-1} except $^\bullet CH_2BrH^+$, the heat of formation of which may need further examination. It seems that the charge-radical interaction is not effected by the nature of the X group. This result also indicates that the BDE (C-H) adjacent to a protonated center in a cation is strengthened by about 16±2 kcalmol^{-1}.

The charge-radical interaction in a β-distonic ion is much less, with an average value of $\Delta\Delta_fH$ (Table 6.4) of about 4-5 kcalmol^{-1}, showing that the effect of the

protonated center on the β-position BDE (C-H) in a cation is significantly lower than for an α-distonic ion. The $\Delta\Delta_fH$ values for the β-distonic isomers of carbonyl containing molecular ions are similar to those of α-distonic ions, indicating some special charge distribution in those ions, i.e. the charge is located within the O-CR-OH group, or it is possibly a distonic ion such as $^{\bullet}CH_2O^{+}$=CROH.

The $\Delta\Delta_fH$ values of γ-distonic ions are not close to zero as might have been expected with the charge and radical sites further apart. Those Δ_fH°(D) values perhaps need further examination. The $\Delta\Delta_fH$ value of $^{\bullet}CH_2CH_2OC^{+}HOH$ (8 kcalmol^{-1}) is close to those of β-distonic ions. This may again result from the charge dislocation in the O-CH-OH group.

The nature of distonic radical cations can be further investigated by comparing the methylene ion affinity (MIA) and ethylene ion affinity (EIA) of some small molecules. The MIA and EIA are obtained from the Eq. 2.

$$CH_2^{+\bullet} \text{ (or } C_2H_4^{+\bullet}) + M \xrightarrow{\Delta Hr} {}^{\bullet}CH_2M^{+} \text{ (or } {}^{\bullet}CH_2CH_2M^{+})$$

$$\text{MIA (or EIA)} = -\Delta Hr$$

$$= \Delta_fH^{\circ}(CH_2^{+\bullet}, \text{ or } C_2H_4^{+\bullet}) + \Delta_fH^{\circ}(M) - \Delta_fH^{\circ}({}^{\bullet}CH_2M^{+}, \text{ or } {}^{\bullet}C_2H_4M^{+}) \qquad (2)$$

It is well known that for some small molecules the differences between methyl cation affinity (MCA) and ethyl cation affinity (ECA) are constant.[93] The difference values (Δ) shown in Table 6.5 give an average of 33 kcalmol^{-1} except for HF. The same property is also observed among the distonic ions, which are represented by their difference value between MIA and EIA. The difference values (Δ') shown in Table 6.6

give an average of 58 kcalmol^{-1} except for HF and HCl. By comparing Δ and Δ' values a common trend can be observed. The ECA values are lower than the MCA values, which is due to the CH_3 group in $C_2H_5^+$ having already stabilized the cation site. The EIA values are much lower than the MIA values, which reveals that the cation and radical are already separated in $C_2H_4^{+\bullet}$ compared to that in $CH_2^{+\bullet}$. This kind of stabilization is more effective than that of CH_3 substitution.

6.2.3.2 Isomerization of distonic ions

Both experimental and theoretical results indicated that the isomerization energy barrier between distonic ions and their conventional radical cations decreases with increasing size of the ion.[34,87]

The energy barriers between $CH_3(CH_2)_nNH_2^{+\bullet}$ and $^{\bullet}CH_2(CH_2)_nNH_3^+$ (n = 0, 1, 2) have been calculated at the MP2-6-31G* level,[87] as shown below.

			E (kcalmol^{-1})
$CH_3NH_2^{+\bullet}$	1,2 H - shift ⟶	$^{\bullet}CH_2NH_3^+$	41.8
$CH_3CH_2NH_2^{+\bullet}$	1,3 H - shift ⟶	$^{\bullet}CH_2CH_2NH_3^+$	34.4
$CH_3CH_2CH_2NH_2^{+\bullet}$	1,4 H - shift ⟶	$^{\bullet}CH_2CH_2CH_2NH_3^+$	16.2
$CH_3CH_2CH_2CH_2NH_2^{+\bullet}$	1,5 H - shift ⟶	$^{\bullet}CH_2CH_2CH_2CH_2NH_3^+$	4.3

The increasing ease of isomerization (hydrogen shift) is partly accounted for by the decreasing ring strain in the corresponding transition structures. The facile intramolecular rearrangements of larger molecular ions indicates that although the distonic ions may widely exist they will be difficult to characterize.

6.2.3.3 Bond cleavage in distonic ions

An examination of bond length change between distonic ions and their conventional isomers reveals that the bond length between the radical bearing carbon and its α-atom in a distonic ion is shorter than that in the corresponding conventional isomers (see Table 6.7), indicating a special interaction between the radical site and the neighbour group.

A detailed examination of the geometries in the isomers of CH_3CH_2OH, $CH_3CH_2OH_2^+$ $^{\bullet}CH_2CH_2OH$, and $^{\bullet}CH_2CH_2OH_2^+$ (Table 6.8) indicated that the α-bond shortening is also observed in the corresponding radicals. In contrast, the charge site makes its α-bond loose. This indicates that the radical site in a distonic ion is keeping the neighbour group close and the charge site is keeping the neighbour group apart. Thus the water loss is not observed from $^{\bullet}CH_2OH_2$, whereas water loss is dominant in the dissociations of $^{\bullet}CH_2CH_2OH_2^+$. The radical site in a distonic ion is probably more reactive than the charge center. It follows therefore that the common dissociation channel of distonic ions, i.e. the C-X bond cleavage (Scheme 6.3) is understandable.

$$^{\bullet}CH_2CH_2\text{-}XH^+ \rightarrow C_2H_4^{+\bullet} + XH$$
$$(X = OH, NH_2, F, Cl, \bullet\bullet\bullet\bullet)$$

Scheme 6.3

Moreover, the radical reactivity may trigger formation of a cyclic isomer.

$$^{\bullet}CH_2\text{-}CH_2\text{-}OH_2 \rightarrow [\ CH_2\text{-}CH_2\bullet\bullet\bullet OH_2\ ]^{+\bullet}$$

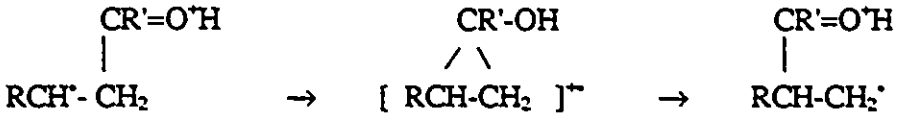

If the β-bond cleavage is indeed triggered by the radical reaction, this bond dissociation may be a rate-determining process. Thus an ion-neutral complex may be involved in the dissociation process. Indeed, the involvement of an ion-neutral complex in the dissociation of distonic ions has been proposed for many distonic ion systems.

6.2.3.4 Ring-strain in ionized molecules

Ring-strain (RS) values in many organic molecules are well documented.[94] Whether these values are comparable to the RS in the corresponding ionized molecules needs to be examined. From the available Δ_fH° values of distonic ions (Table 6.2) the RS energies of some molecular ions may be evaluated from the following equation:

$$\Delta_fH^\circ \text{ (Ring-opened distonic ion)} = \Delta_fH^\circ \text{ (Ring molecular ion)} - \text{RS}$$

Molecule	RS in molecule[94] (kcalmol^{-1})	RS in molecular ions (kcalmol^{-1})
Cyclopropane	27	-22
Oxirane	27	20
Oxetane	26	10
cyclopropanone	46	17

The values shown above indicate that the RS energy in a molecular ion is not consistent with that in neutral molecule. Ring-opening of a cyclopropane is even an endothermic process. Hence the ring-opening of a molecular ion to yield a distonic ion is not a simple ring-strain release process. Other factors may be in control, such as the resonance stabilities in both ring and ring-opened structures. Hence the relationship

between the heats of formation of a ring-opened distonic ion and its cyclic isomer is derived as follows:

$$\Delta_f H^\circ(\text{distonic ion}) = \Delta_f H^\circ(\text{Ring molecular ion}) - RS + R_1 - R_2$$

R_1: Resonance effect in the ring structure;
R_2: Resonance effect in the ring-opened structure

The R_1 can be estimated from the energy difference between $[CH_2CH_2CH_2]^{+\bullet}$ and [cyclopropane]$^{+\bullet}$, because there is no resonance effect in $[CH_2CH_2CH_2]^{+\bullet}$. If the resonance effect in these small cyclic molecular ions were taken to be the same, the resonance effect in the corresponding distonic ion could be estimated.

	$\Delta_f H^\circ$(Distonic ion)	$\Delta_f H^\circ$(Molecular ion)	RS	R_1	R_2
$[CH_2CH_2CH_2]^{+\bullet}$	262	240	27	49	0
$[CH_2OCH_2]^{+\bullet}$	211	231	27	(49)	42
$[CH_2CH_2OCH_2]^{+\bullet}$	194	204	26	(49)	33
$[CH_2CH_2CO]^{+\bullet}$	197	214	46	(49)	29

The above estimations result in a larger resonance effect in $[CH_2OCH_2]^{+\bullet}$ than $[CH_2CH_2OCH_2]^{+\bullet}$. This is consistent with that in the former the delocalization region is C-O-C, whereas in the latter the delocalization region is only O-CH_2. However, as the ring resonance effects are different in these molecular ions, we can only estimate the value of R_1+R_2. Theoretical calculations are required to make accurate evaluations.

6.3 Conclusion

44 stable distonic radical cations have been discussed. By analysis of the available thermochemical data the interaction of the radical site and the charge site was found to be 16±2 $kcalmol^{-1}$ in α-distonic ions or 3-4 $kcalmol^{-1}$ (average) in β-distonic ions. The examination of the bond length change in the distonic ions relative to their conventional isomers shows that the radical effect results in a shorter α-bond length and probably is responsible to the special bond cleavage in the distonic ions.

6.4 References

1. B. F. Yates, W. J. Bouma and L. Radom, J. Am. Chem. Soc., 106, 5805 (1984)

2. a: S. Hammerum, Mass Spectrom. Rev., 7, 123 (1986);

   b: K. M. Stirk, L. K. M. Kiminkinen and H. I. Kenttämaa, Chem. Rev., 92, 1649 (1992);

   c: H-F. Grützmacher, Int. J. Mass Spectrom. Ion Processes, 118/119, 825 (1992);

   d: H. I. Kenttämaa, Org. Mass Spectrom., 29, 1 (1994);

   e: References hereafter.

3. a: S. Billets, H. H. Jaffé and F. Kaplan, J. Am. Chem. Soc., 92, 6964 (1970)

   b: W. J. Bouma, J. K. MacLeod and L. Radom, J. Chem. Soc. Chem. Comm., 724 (1978)

4. See, for example, a: J. L. Holmes, F. P. Lossing, J. K. Terlouw and P. C. Burgers, J. Am. Chem. Soc., 104, 2931 (1982); b: W. J. Bouma, J. K. MacLeod and L. Radom, J. Am. Chem. Soc., 104, 2930 (1982)

5. H. Halim, B. Ciommer and H. Schwarz, Angew. Chem. Int. Ed. Engl., 21, 528 (1982)

6. J. K. Terlouw, W. Heerma and G. Dijkstra, Org. Mass Spectrom., 7, 326 (1981)

7. D. J. McAdoo, Org. Mass Spectrom., 23, 350 (1988)

8. M. C. R. Symons, Chem. Soc. Rev., 393 (1984)

9. L. Bonazzola, C. Iacona, J. P. Michaut and J. Roncin, J. Chem. Phys., 73, 4175 1980)

10. a: P. N. T. Van Velzen and W. J. Van der Hart, Chem. Phys. Lett., 83, 55 (1981); b: J. Rideout, M. C. R. Symons and B. W. Wren, J. Chem. Soc. Faraday Trans., I, 82, 167 (1986)

11. R. L. Smith, R. L. Franklin, K. M. Stirk and H. I. Kenttämaa, J Am. Chem. Soc., 115, 10348 (1993)

12. J. L. Holmes, F. P. Lossing, J. K. Terlouw and P. C. Burgers, Can J. Chem., 61, 2305 (1983)

13. R. L. Smith, L. J. Chyall, P. K. Chou and H. I. Kenttämaa, J Am. Chem. Soc., 116, 781 (1994)

14. References 4b, 12 and thereafter.

15. J. L. Holmes and F. P. Lossing, J. Am. Chem. Soc., 110, 7343 (1988)

16. J. Phys. Chem. Ref. Data, 17, (1988)

17. J. W. Gauld and L. Radom, J. Chem. Phys., 98, 777 (1994)

18. J. L. Holmes and F. P. Lossing, Int. J. Mass Spectrom. Ion Processes, 92, 111 (1991)

19. M. C. Blanchette, J. L. Holmes and F. P. Lossing, Org. Mass Spectrom., 22, 701 (1987)

20. J. L. Holmes, P. C. Burgers, J. K. Terlouw, H. Schwarz, B. Ciommer and H. Halim, Org. Mass Spectrom., 18, 208 (1983)

21. B. F. Yates, W. J. Bouma and L. Radom, Tetrahedron., 42, 6225 (1986)

22. J. L. Holmes and F. P. Lossing, J. Am. Chem. Soc., 110, 7343 (19880

23. N. L. Ma, B. J. Smith, J. A. Pople and L. Radom, J. Am. Chem. Soc., 113, 7903 (1991)

24. W. J. Bouma, R. H. Nobes and L. Radom, J. Am. Chem. Soc., 104, 2929 (1982)

25. R. Postma, P. J. A. Ruttink, B. Van Baar, J. K. Terlouw, J. L. Holmes and P. C. Burgers, Chem. Phys. Lett., 123, 409 (1986)

26. D. J. McAdoo and C. E. Hudson, Org. Mass Spectrom., 21, 779 (1986)

27. W. J. Bouma, R. H. Nobes and L. Radom, J. Am. Chem. Soc., 105, 1743 (1983)

28. K. G. Stirk and H. I. Kenttämaa, J. Phys. Chem., 96, 5272 (1992)

29. P. C. Burgers, J. L. Holmes, J. K. Terlouw and B. Van Baar, Org. Mass Spectrom., 20, 202 (1985)

30. J. L. Holmes, A. A. Mommers, J. E. Szulejko and J. K. Terlouw, J. Chem. Soc. Chem. Comm., 165 (1984)

31. R. D. Bowen, A. W. Colburn and P. J. Derrick, J. Am. Chem. Soc., 113, 1132 (1991)

32. J-D. Shao, T. Baer, J. C. Morrow and M. L. Fraser-Monteiro, J. Chem. Phys., 87, 5242 (1987)

33. C. E. Hudson, M. S. Ahmed, J. C. Traeger, C. S. Giam and D. J. McAdoo, Int. J. Mass Spectrom. Ion Pro., 113, 117 (1992)

34. V. H. Wysocki and H. I. Kenttämaa, J. Am. Chem. Soc., 112, 5110 (1990)

35. C. Wesdemiotis, P. O. Danis, R. Feng, J. Tso and F. W. McLafferty, J. Am. Chem. Soc., 107, 8059 (1985)

36. H. E. Audier, A. Milliet, D. Leblanc and T. H. Morton, J. Am. Chem. Soc., 114, 2020 (1992)

37. F. P. Lossing, J. Am. Chem. Soc., 99, 7526 (1977)

38. a: P. C. Burgers, J. L. Holmes, Org. Mass Spectrom., 19, 452 (1984)

b: W. J. Bouma, R. H. Nobes and L. Radom, Org. Mass Spectrom., 17, 315 (1982)

39. a: J. D. Dill, C. L. Fischer and F. W. McLafferty, J. Am. Chem. Soc., 101, 6531 (1979)

b: T. Nishimura, Q. Zha, P. R. Das, Y. Niwa and G. G. Meisels, Int. J. Mass Spectrom. Ion Proc., 113, 177 (1992)

40. D. J. McAdoo, M. S. Ahmed and C. E. Hudson, Int. J. Mass Spectrom. Ion Proc., 100, 579 (1990)

41. J. R. Cao, M. George and J. L. Holmes, Org. Mass Spectrom., 26, 481 (1991)

42. M. C. Bissonnette, M. George and J. L. Holmes, Int. J. Mass Spectrom. Ion Processes, 101, 309 (1990)

43. M. C. Bissonnette, M. George and J. L. Holmes, Org. Mass Spectrom., 25, 689 (1990)

44. A. Milliet, E. LeCarpentier and H. E. Audier, Org. Mass Spectrom., 29, 90 (1994)

45. A. Milliet and G. Sozzi, Org. Mass Spectrom., 25, 522 (1990)

46. A. Milliet, G. Sozzi and H. E. Audier, Org. Mass Spectrom., 27, 787 (1992)

47. D. J. McAdoo, C. E. Hudson and J. C. Traeger, Org. Mass Spectrom., 23, 764 (1988)

48. D. J. McAdoo and C. E. Hudson, Org. Mass Spectrom., 18, 11 (1983)

49. D. J. McAdoo, C. E. Hudson, F. W. McLafferty and T. E. Parks, Org. Mass Spectrom., 19, 353 (1984)

50. L. L. Griffin, K. Holden, C. E. Hudson and D. J. McAdoo, Org. Mass Spectrom., 21, 175 (1986)

51. S. Villeneuve and P. C. Burgers, Org. Mass Spectrom., 21, 733 (1986)

52. R. Flammang, M. Plisnier, G. Leroy, M. Sana, M. T. Nguyen and L. G. Vanquickenborne, Chem. Phys. Lett., 186, 393 (1991)

53. a: N. Heinrich, T. Drewello, P. C. Burgers, J. C. Morrow, J. Schmidt, W. Kulik, J. K. Terlouw and H. Schwarz, J. Am. Chem. Soc., 114, 3776 (1992); b: B. J. Smith, M. T. Nguyen and L. Radom, J. Am. Chem. Soc., 114, 1151 (1992)

54. Q. Zha, T. Nishimura and G. G. Meisels, Int. J. Mass Spectrom. Ion Proc., 120, 85 (1992)

55. C. E. Hudson and D. J. McAdoo, Org. Mass Spectrom., 27, 1384 (1992)

56. Q. Zha, R. N. Hayes, T. Nishimura, G. G. Meisels and M. L. Gross, J. Phys. Chem., 94, 1286 (1990)

57. P. C. Burgers, J. L. Holmes, A. A. Mommers, J. E. Szulejko and J. K. Terlouw, Org. Mass Spectrom., 19, 442 (1984)

58. C. Wesdemiotis, R. Csencsits and F. W. McLafferty, Org. Mass Spectrom., 20, 98 (1985)

59. J. L. Holmes and J. K. Terlouw, Org. Mass Spectrom., 21, 776 (1986)

60. a: C. Wesdemiotis, R. Feng, E. R. Williams and F. W. McLafferty, Org. Mass Spectrom., 21, 689 (1986); b: M. C. Blanchette, J. L. Holmes, C. E. C. A. Hop and A. A. Mommers, Org. Mass Spectrom., 23, 495 (1988)

61. P. C. Burgers, J. L. Holmes, C. E. C. A. Hop and J. K. Terlouw, Org. Mass Spectrom., 21, 549 (1986)

62. N. Heinrich, J. Schmidt, H. Schwarz and Y. Apeloig, J. Am. Chem. Soc., 109, 1317 (1987)

63. D. J. McAdoo and D. N. Witiak, Org. Mass Spectrom., 13, 499 (1978)

64. a: D. J. McAdoo, C. E. Hudson, J. J. Zwinselman and N. M. M. Nibbering, J. Chem. Soc. Perkin Trans., II, 1703 (1985); b: H. E. Audier and G. Sozzi, Org. Mass Spectrom., 19, 150 (1984)

65. T. M. Sack, D. L. Miller and M. L. Gross, J. Am. Chem. Soc., 107, 6795 (1985)

66. D. A. Hrovat, P. Du and W. T. Borden, Chem. Phys. Lett., 123, 337 (1986)

67. S. G. Lias and T. J. Buckley, Int. J. Mass Spectrom. Ion Proc., 56, 123 (1984)

68. B. C. Baumann and J. K. MacLeod, J. Am. Chem. Soc., 103, 6223 (1981)

69. R. H. Nobes, W. J. Bouma, J. K. MacLeod and L. Radom, Chem. Phys. Lett., 135, 78 (1987)

70. R. D. Rusli and H. Schwarz, Chem. Ber., 123, 535 (1990)

71. a: D. Wittneben and H. -F. Grützmacher, Int. J. Mass Spectrom. Ion Processes, 100, 545 (1990); b: R. C. Dunbar, F-S. Huang and S. J. Klippenstein, Int. J. Mass Spectrom. Ion Proc., 128, 21 (1993); c: M. L. Fraser-Monteiro, L. Fraser-Monteiro, J. J. Butler and T. Baer, J. Phys. Chem., 86, 739 (1982)

72. W. J. Bouma, J. K. MacLeod and L. Radom, J. Am. Chem. Soc., 102, 2246 (1980)

73. M. J. Polce and C. Wesdemiotis, J. Am. Chem. Soc., 115, 10849 (1993)

74. H. I. Kenttämaa, L. K. M. Kiminkinen, J. C. Orlowski and K. M. Stirk, Rapid Comm. Mass Spectrom., 6, 734 (1992)

75. M. L. McKee and L. Radom, Org. Mass Spectrom., 28, 1238 (1993)

76. F. Turecek, D. E. Drinkwater and F. W. McLafferty, J. Am. Chem. Soc., 113, 5950 (1991)

77. C. Dass, Rapid Comm. Mass Spectrom., 7, 95 (1993)

78. J. C. Traeger, C. E. Hudson and D. J. McAdoo, Org. Mass Spectrom., 24, 230 (1989)

79. K. M. Stirk, J. C. Orlowski, D. T. Leeck and H. I. Kenttämaa, J. Am. Chem. Soc., 114, 8604 (1992)

80. N. Heinrich, W. Koch, J. C. Morrow and H. Schwarz, J. Am. Chem. Soc., 110, 6332 (1988)

81. C. Dass and M. L. Gross, Org. Mass Spectrom., 25, 24 (1990)

82. K. M. Stirk and H. I. Kenttämaa, J. Am. Chem. Soc., 113, 5880 (1991)

83. C. Wesdemiotis, R. Feng, P. O. Danis, E. R. Williams and F. W. McLafferty, J. Am. Chem. Soc., 108, 5847 (1986)

84. S. Hammerum, D. Kuck and P. J. Derrick, Tetrahedron Lett., 25, 893 (1984)

85. B. F. Yates and L. Radom, Org. Mass Spectrom., 22, 430 (1987)

86. T. M. Sack, R. L. Cerny and M. L. Gross, J. Am. Chem. Soc., 107, 4562 (1985)

87. B. F. Yates and L. Radom, J. Am. Chem. Soc., 109, 2910 (1987)

88. T. Bjørnholm, S. Hammerum and D. Kück, J. Am. Chem. Soc., 110, 3862 (1988)

89. L. J. Chyall, M. H. C. Byrd and H. I. Kenttämaa, J. Am. Chem. Soc., 116, 10767 (1994)

90. R. L. Smith, L. J. Chyall, K. M. Stirk and H. I. Kenttämaa, Org. Mass Spectrom., 28, 1623 (1993)

91. D. F. McMillan and D. M. Golden, Ann. Rev. Phys. Chem., 33, 493 (1982)

92. J. L. Holmes, F. P. Lossing and P. M. Mayer, J. Am. Chem. Soc., 113, 9723 (1991)

93. D. V. Zagorevskii, S. P. Palii and J. L. Holmes, J. Am. Chem. Soc., Mass Spectrom., 5, 814 (1994)

94. S. W. Benson, *Thermochemical Kinetics*, 2nd. ed., John Wiley and Sons, Inc., 1976

Table 6.1 Generation and characterization of distonic radical cations

Distonic ion (D)	Generation			Characterization	References
$^{\cdot}CH_2FH^+$	$[FCH_2COOH]^{+\cdot}$	$\xrightarrow{-CO_2}$	$^{\cdot}CH_2FH^+$	CID, AE	12
$^{\cdot}CH_2ClH^+$	$[ClCH_2COOH]^{+\cdot}$	$\xrightarrow{-CO_2}$	$^{\cdot}CH_2ClH^+$	CID, AE	12
$^{\cdot}CH_2BrH^+$	$[BrCH_2COOH]^{+\cdot}$	$\xrightarrow{-CO_2}$	$^{\cdot}CH_2BrH^+$	CID, AE	12
$^{\cdot}CH_2CH_2FH^+$	$[FCH_2CH_2CH_2OH]^{+\cdot}$	$\xrightarrow{-CH_2O}$	$^{\cdot}CH_2CH_2FH^+$	MI,CID,NR	19
$^{\cdot}CH_2CH_2ClH^+$	$[ClCH_2CH_2CH_2OH]^{+\cdot}$	$\xrightarrow{-CH_2O}$	$^{\cdot}CH_2CH_2ClH^+$	MI,CID,CS,NR	19
$^{\cdot}CH_2CH_2BrH^+$	$[BrCH_2CH_2CH_2OH]^{+\cdot}$	$\xrightarrow{-CH_2O}$	$^{\cdot}CH_2CH_2BrH^+$	MI,CID,NR	19
$CH_3{}^{\cdot}CHClH^+$	$[CH_3CHClCOOH]^{+\cdot}$	$\xrightarrow{-CO_2}$	$CH_3{}^{\cdot}CHClH^+$	CID,CS,NR,AE	19,20
$CH_3{}^{\cdot}CHBrH^+$	$[CH_3CHBrCOOH]^{+\cdot}$	$\xrightarrow{-CO_2}$	$CH_3{}^{\cdot}CHBrH^+$	MI,CID,NR,AE	19,20
$^{\cdot}CH_2{}^+ClCH_3$	$[ClCH_2COOCH_3]^{+\cdot}$	$\xrightarrow{-CO_2}$	$CH_3{}^+ClCH_2{}^{\cdot}$	CID,CS,NR,AE	19
$^{\cdot}CH_2{}^+BrCH_3$	$[BrCH_2COOCH_3]^{+\cdot}$	$\xrightarrow{-CO_2}$	$CH_3{}^+BrCH_2{}^{\cdot}$	MI,CID,NR,AE	19
$^{\cdot}CH_2OH_2{}^+$	$[HOCH_2CH_2OH]^{+\cdot}$	$\xrightarrow{-CH_2O}$	$^{\cdot}CH_2OH_2{}^+$	CID,CS,CIDI,AE	4,12

Table 6.1 Generation and characterization of distonic radical cations, continues

Distonic ion (D)	Generation			Characterization	References
$^{\cdot}CH_2CH_2OH_2^+$	$[HOCH_2CH_2CH_2OH]^{+\cdot}$	$\xrightarrow{-CH_2O}$	$^{\cdot}CH_2CH_2OH_2^+$	MI,CID,AE	6,25
$CH_3{}^{\cdot}CHOH_2^+$	$[CH_3CH(OH)COOH]^{+\cdot}$	$\xrightarrow{-CO_2}$	$CH_3{}^{\cdot}CHOH_2^+$	MI,CID	28
$^{\cdot}CH_2CH_2CH_2OH_2^+$	$[HOCH_2CH_2CH_2CH_2OH]^{+\cdot}$	$\xrightarrow{-CH_2O}$	$^{\cdot}CH_2CH_2CH_2OH_2^+$	MI,CID,AE	30,31
$^{\cdot}CH_2CH_2CH_2CH_2OH_2^+$	$[HOCH_2CH_2CH_2CH_2CH_2OH]^{+\cdot}$	$\xrightarrow{-CH_2O}$	$^{\cdot}CH_2CH_2CH_2CH_2OH_2^+$	CID,NR	35
$^{\cdot}CH_2OCH_2CH_2OH_2^+$	$[CH_3OCH_2OCH_2CH_2OH]^{+\cdot}$	$\xrightarrow{-CH_2O}$	$^{\cdot}CH_2OCH_2CH_2OH_2^+$	MI,CID	36
$^{\cdot}CH_2O^+(H)CH_3$	$[CH_3OCH_2COOH]^{+\cdot}$	$\xrightarrow{-CO_2}$	$^{\cdot}CH_2O^+(H)CH_3$	CID	28,37
$^{\cdot}CH_2CH_2O^+(H)CH_3$	$[CH_3OCH_2CH_2OCH_3]^{+\cdot}$	$\xrightarrow{-CH_2O}$	$^{\cdot}CH_2CH_2O^+(H)CH_3$	MI,CID,AE	41
$^{\cdot}CH_2O^+(H)CH_2CH_3$	$[HOCH_2CH_2OCH_2CH_3]^{+\cdot}$	$\xrightarrow{-CH_2O}$	$^{\cdot}CH_2O^+(H)CH_2CH_3$	MI,CID	41
$^{\cdot}CH_2CH_2O^+(H)CH_2CH_3$	$[C_2H_5OCH_2CH_2OC_2H_5]^{+\cdot}$	$\xrightarrow{-CH_3CHO}$	$^{\cdot}CH_2CH_2O^+(H)CH_2CH_3$	MI,CID,AE	41
$(CH_3)_2{}^{\cdot}CCH_2O^+(H)CH_3$	$[(CH_3)_2C(CH_2OH)CH_2OCH_3]^{+\cdot}$	$\xrightarrow{-CH_2O}$	$(CH_3)_2{}^{\cdot}CCH_2O^+(H)CH_3$	MI,CID,AE	42,43
$^{\cdot}CH_2CH_2O^+(H)CH_2CH_2CH_3$	$[C_2H_5OCH_2CH_2OC_3H_7]^{+\cdot}$	$\xrightarrow{-CH_3CHO}$	$^{\cdot}CH_2CH_2O^+(H)CH_2CH_2CH_3$	MI,CID	45

Table 6.1 Generation and characterization of distonic radical cations, continues

Distonic ion (D)	Generation			Characterization	References
$^{\bullet}CH_2CH_2CH(=O^{+}H)$	$[CH_3OCH_2CH_2CHO]^{+\bullet}$	$\xrightarrow{-CH_3O}$	$^{\bullet}CH_2CH_2CH(=O^{+}H)$	MI,CID,AE	47
$CH_3{}^{\bullet}CHCH_2CH(=O^{+}H)$	$[CH_3CH_2CH_2CHO]^{+\bullet}$	$\rightarrow$	$CH_3{}^{\bullet}CHCH_2CH(=O^{+}H)$	MI,CID,AE	48
$^{\bullet}CH_2CH(CH_3)CH(=O^{+}H)$	$[CH_3CH(CH_3)CHO]^{+\bullet}$	$\rightarrow$	$^{\bullet}CH_2CH(CH_3)CH(=O^{+}H)$	MI,CID,AE	48
$^{\bullet}CH_2CH_2C(=O^{+}H)CH_3$	$[CH_3OCH_2CH_2COCH_3]^{+\bullet}$	$\xrightarrow{-CH_3O}$	$^{\bullet}CH_2CH_2C(=O^{+}H)CH_3$	MI,CID,AE	47
$^{\bullet}CH_2OC^{+}HOH$	$[HCOOCH_2CH(CH_3)_2]^{+\bullet}$	$\xrightarrow{-C_3H_6}$	$^{\bullet}CH_2OC^{+}HOH$	CID,NR	52
$^{\bullet}CH_2CH_2OC^{+}HOH$	[1,4-dioxane-2,3-diol]$^{+\bullet}$	$\xrightarrow{-HCOOH}$	$^{\bullet}CH_2CH_2OC^{+}HOH$	MI,CID,NR,AE	*
$CH_3{}^{\bullet}CHCH_2OC^{+}HOH$	$[HCOOCH_2CH_2CH_3]^{+\bullet}$	$\rightarrow$	$CH_3{}^{\bullet}CHCH_2OC^{+}HOH$	MI,CID,AE	56
$^{\bullet}CH_2OC^{+}(OH)CH_3$	$[CH_3COOCH_2OCH_3]^{+\bullet}$	$\xrightarrow{-CH_3O}$	$^{\bullet}CH_2OC^{+}(OH)CH_3$	MI,CID,AE	61
$^{\bullet}CH_2CH_2OC^{+}(OH)CH_3$	$[CH_3CH_2COOCH_3]^{+\bullet}$	$\rightarrow$	$^{\bullet}CH_2CH_2OC^{+}(OH)CH_3$	MI,CID,AE	61
$^{\bullet}CH_2CH_2C^{+}(OH)_2$	$[CH_3OCH_2CH_2COOH]^{+\bullet}$	$\rightarrow$	$^{\bullet}CH_2CH_2C^{+}(OH)_2$	MI,CID,NR	*
$^{\bullet}CH_2CH_2CH_2^{+}$	[cyclopropane]$^{+\bullet}$	$\rightarrow$	$^{\bullet}CH_2CH_2CH_2^{+}$	Bimole.	65
$^{\bullet}CH_2OCH_2^{+}$	[1,3-dioxolane]$^{+\bullet}$	$\xrightarrow{-CH_3O}$	$^{\bullet}CH_2OCH_2^{+}$	Bimole.	70
$^{\bullet}CH_2CH_2OCH_2^{+}$	[1,4-dioxane]$^{+\bullet}$	$\xrightarrow{-CH_3O}$	$^{\bullet}CH_2CH_2OCH_2^{+}$	CID,NR,Bimole.	71,73

Table 6.1 Generation and characterization of distonic radical cations, continues

Distonic ion (D)	Generation			Characterization	References
$^{\cdot}CH_2CH_2CO^{+}$	[γ-butyrolactone]$^{+\cdot}$	$\xrightarrow{-C_2H_4}$	$^{\cdot}CH_2CH_2CO^{+}$	Bimole.	76,77
$^{\cdot}CH_2CH_2CH_2CO^{+}$	[cyclobutanone]$^{+\cdot}$	$\rightarrow$	$^{\cdot}CH_2CH_2CH_2CO^{+}$	CID,Bimole.	81
$^{\cdot}CH_2CH_2CH_2CH_2CO^{+}$	$^{\cdot}CH_2CH_2CH_2O^{+} + CH_2CO$	$\xrightarrow{-CH_2O}$	$^{\cdot}CH_2CH_2CH_2CH_2CO^{+}$	CID,Bimole.	13
$^{\cdot}CH_2NH_3^{+}$	$[HOCH_2CH_2NH_2]^{+\cdot}$	$\xrightarrow{-CH_2O}$	$^{\cdot}CH_2NH_3^{+}$	CID,AE	12
$^{\cdot}CH_2CH_2NH_3^{+}$	$[H_2NCH_2CH_2CH_2NH_2]^{+\cdot}$	$\xrightarrow{-CH_2NH}$	$^{\cdot}CH_2CH_2NH_3^{+}$	CID,NR	12,84
$CH_3{}^{\cdot}CHNH_3^{+}$	$[H_2NCH(CH_3)CH_2NH_2]^{+\cdot}$	$\xrightarrow{-CH_2NH}$	$CH_3{}^{\cdot}CHNH_3^{+}$	CID,NR	84
$^{\cdot}CH_2CH_2CH_2NH_3^{+}$	$[H_2NCH_2CH_2CH_2CH_2NH_2]^{+\cdot}$	$\xrightarrow{-CH_2NH}$	$^{\cdot}CH_2CH_2CH_2NH_3^{+}$	CID,NR	35
$^{\cdot}CH_2SH_2^{+}$	$[HOCH_2CH_2SH]^{+\cdot}$	$\xrightarrow{-CH_2O}$	$^{\cdot}CH_2SH_2^{+}$	CID,AE	12
$(CH_3)_2S^{+}\text{-}CH_2^{\cdot}$	$^{\cdot}CH_2OCH_2^{+} + CH_3SCH_3$	$\xrightarrow{-CH_2O}$	$(CH_3)_2S^{+}\text{-}CH_2^{\cdot}$	Bimole.	89,90

Table 6.2 Heats of formation (kcalmol^{-1}) of distonic ions and their conventional isomers

Distonic Ions (D)	Δ_fH°(D)	Ref.	Conventional Ions (C)	Δ_fH°(C)	Ref.	$\Delta\Delta_fH$ (Δ_fH°(D)-Δ_fH°(C))
$^{\cdot}CH_2FH^+$	231	17	$CH_3F^{+\cdot}$	232	17	-1
$^{\cdot}CH_2CH_2FH^+$	187	21	$CH_3CH_2F^{+\cdot}$	205	16	-18
$^{\cdot}CH_2CH_2CH_2FH^+$	185	21	$CH_3CH_2CH_2F^{+\cdot}$	192	16	-7
$^{\cdot}CH_2ClH^+$	251	17	$CH_3Cl^{+\cdot}$	240	17	11
$^{\cdot}CH_2CH_2ClH^+$	223	21	$CH_3CH_2Cl^{+\cdot}$	226	16	-3
$CH_3{}^{\cdot}CHClH^+$	232	19				6
$CH_3{}^+ClCH_2{}^{\cdot}$	242	19				16
$^{\cdot}CH_2CH_2CH_2ClH^+$	219	21	$CH_3CH_2CH_2Cl^{+\cdot}$	218	16	1
$^{\cdot}CH_2BrH^+$	237	12	$CH_3Br^{+\cdot}$	234	16	3
$CH_3{}^{\cdot}CHBrH^+$	238	19	$CH_3CH_2Br^{+\cdot}$	222	16	16
$CH_3{}^+BrCH_2{}^{\cdot}$	253	19				31
$^{\cdot}CH_2OH_2^+$	195	17	$CH_3OH^{+\cdot}$	203	17	-8
$^{\cdot}CH_2CH_2OH_2^+$	176	21	$CH_3CH_2OH^{+\cdot}$	185	16	-9
$CH_3{}^{\cdot}CHOH_2^+$	179	27				-6
$^{\cdot}CH_2CH_2CH_2OH_2^+$	171	30	$CH_3CH_2CH_2OH^{+\cdot}$	175	16	-4
	175	21				0
$^{\cdot}CH_2CH_2CH_2CH_2OH_2^+$	158	*	$CH_3CH_2CH_2CH_2OH^{+\cdot}$	166	16	-8
$^{\cdot}CH_2O^+(H)CH_3$	186	38	$CH_3OCH_3^{+\cdot}$	187	16	-1
$^{\cdot}CH_2CH_2O^+(H)CH_3$	170	41	$CH_3CH_2OCH_3^{+\cdot}$	172	16	-2
$^{\cdot}CH_2CH_2O^+(H)CH_2CH_3$	153	41	$CH_3CH_2OCH_2CH_3^{+\cdot}$	159	16	-6
$(CH_3)_2C^{\cdot}CH_2O^+(H)CH_3$	142	42	$(CH_3)_3CCH_2OH^{+\cdot}$	148	16	-6
$^{\cdot}CH_2CH_2CH(=O^+H)$	181	47	$CH_3CH_2CHO^{+\cdot}$	185	16	-4
$^{\cdot}CH_2CH(CH_3)CH(=O^+H)$	154	48	$(CH_3)_2CHCHO^{+\cdot}$	172	16	-18
$CH_3{}^{\cdot}CHCH_2CH(=O^+H)$	165	48	$CH_3CH_2CH_2CHO^{+\cdot}$	177	16	-12
$^{\cdot}CH_2CH_2C(=O^+H)CH_3$	165	47	$CH_3CH_2COCH_3^{+\cdot}$	162	16	3

Table 6.2 Heats of formation (kcalmol^{-1}) of distonic ions and their conventional isomers, continues

Distonic Ions (D)	$\Delta_f H^\circ$(D)	Ref.	Conventional Ions (C)	$\Delta_f H^\circ$(C)	Ref.	$\Delta\Delta_f H$ ($\Delta_f H^\circ$(D)-$\Delta_f H^\circ$(C))
$^{\cdot}CH_2OC^{+}HOH$	151	53a	$HCOOCH_3^{+\cdot}$	164	16	-13
	156	52				-8
$^{\cdot}CH_2O^{+}(H)CHO$	173	53a				9
	184	52				20
$^{\cdot}CH_2CH_2OC^{+}HOH$	137	*	$HCOOCH_2CH_3^{+\cdot}$	153	16	-16
$^{\cdot}CH_2OC^{+}(OH)CH_3$	130	61	$CH_3COOCH_3^{+\cdot}$	139	16	-9
	127	62				-12
$^{\cdot}CH_2CH_2CH_2^{+}$	262	66	$cyclopropane^{+\cdot}$	240	16	22
$^{\cdot}CH_2OCH_2^{+}$	211	69	$ethylene\ oxide^{+\cdot}$	231	16	-20
$^{\cdot}CH_2CH_2OCH_2^{+}$	194	72	$trimethylene\ oxide^{+\cdot}$	204	16	-10
$^{\cdot}CH_2CH_2CO^{+}$	197	76	$cyclopropanone^{+\cdot}$	214	16	-17
$^{\cdot}CH_2CH_2CH_2CO^{+}$	176	80	$cyclobutanone^{+\cdot}$	194	16	-18
$^{\cdot}CH_2N^{+}H_3$	204	17	$CH_3NH_2^{+\cdot}$	205	17	-1
$^{\cdot}CH_2CH_2N^{+}H_3$	185	85	$CH_3CH_2NH_2^{+\cdot}$	193	16	-8
$CH_3{}^{\cdot}CHNH_3^{+}$	186	85				-7
$^{\cdot}CH_2CH_2CH_2N^{+}H_3$	177	21	$CH_3CH_2CH_2NH_2^{+\cdot}$	186	16	-9
$^{\cdot}CH_2SH_2^{+}$	232	17	$CH_3SH^{+\cdot}$	213	17	19
$(CH_3)_2S^{+}\text{-}CH_2^{\cdot}$	201	89	$CH_3CH_2SCH_3^{+\cdot}$	183	16	18

Table 6.3 Estimation of heats of formation of distonic radical cations, $(\Delta_f H^\circ(D))_{est}$ [1]

Molecule(M)	$\Delta_f H^\circ(M)$	$\Delta_f H^\circ(R)$	BDE(C-H)[2]	PA(M)	Distonic ion (D)	$\Delta_f H^\circ(D)_{est}$
CH_3F	-59	-8	103	145	$^{\cdot}CH_2FH^+$	213
CH_3CH_2F	-63		(100)	165	$^{\cdot}CH_2CH_2FH^+$	186
$CH_3CH_2CH_2F$	-68		(100)	(165)	$^{\cdot}CH_2CH_2CH_2FH^+$	181
CH_3Cl	-20	31	103	163	$^{\cdot}CH_2ClH^+$	234
CH_3CH_2Cl	-27		(100)	169	$^{\cdot}CH_2CH_2ClH^+$	218
		19[3]		169	$CH_3{}^{\cdot}CHClH^+$	216
$CH_3CH_2CH_2Cl$	-32		(100)	(169)	$^{\cdot}CH_2CH_2CH_2ClH^+$	213
CH_3Br	-9.1	42	103	166	$^{\cdot}CH_2BrH^+$	242
CH_3CH_2Br	-15	27[3]		171	$CH_3{}^{\cdot}CHBrH^+$	222
CH_3OH	-48	-6.2	94	182	$^{\cdot}CH_2OH_2^+$	178
CH_3CH_2OH	-56	-13.5[4]		188	$^{\cdot}CH_2CH_2OH_2^+$	165
CH_3CH_2OH	-56	-14.5[4]		188	$CH_3{}^{\cdot}CHOH_2^+$	163
$CH_3CH_2CH_2OH$	-61	-16[4]		191	$^{\cdot}CH_2CH_2CH_2OH_2^+$	159
CH_3OCH_3	-44	-3	93	192	$^{\cdot}CH_2O^+(H)CH_3$	171
$CH_3CH_2OCH_3$	-52		(100)	196	$^{\cdot}CH_2CH_2O^+(H)CH_3$	166
$CH_3CH_2OC_2H_5$	-60		(100)	200	$^{\cdot}CH_2CH_2O^+(H)C_2H_5$	153
CH_3CH_2CHO	-45		(100)	190	$^{\cdot}CH_2CH_2CH(=O^+H)$	179
$CH_3CH_2CH_2CHO$	-50		(100)	192	$CH_3{}^{\cdot}CHCH_2CH(=O^+H)$	172
$(CH_3)_2CHCHO$	-52		(100)	193	$^{\cdot}CH_2CH(CH_3)CH(=O^+H)$	169
$CH_3CH_2COCH_3$	-58		(100)	200	$^{\cdot}CH_2CH_2C(=O^+H)CH_3$	156
$HCOOCH_3$	-85		(97)	188	$^{\cdot}CH_2OC^+HOH$	138
CH_3COOCH_3	-98	-57.5[4]		198	$^{\cdot}CH_2OC^+(OH)CH_3$	111
$HCOOCH_2CH_3$	-92		(100)	193	$^{\cdot}CH_2CH_2OC^+HOH$	129
CH_3NH_2	-5.5	38	96	214	$^{\cdot}CH_2NH_3^+$	190
$CH_3CH_2NH_2$	-11		(100)	217	$^{\cdot}CH_2CH_2NH_3^+$	185
CH_3NHCH_3	-4.4	30		221	$^{\cdot}CH_2N^+H_2CH_3$	175

1. Values are from Reference 16, except indicated.
2. From estimations.
3. From reference 22.
4. Values are from Reference 92.

Table 6.4 Comparison of observed heats of formation of distonic ions with estimated values

Distonic ion (D)	$\Delta H_f^\circ(D)$	$\Delta H_f^\circ(D)_{est}$	$\Delta\Delta H_f = \Delta H_f^\circ(D) - \Delta H_f^\circ(D)_{est}$
α-distonic ions			
$^\bullet CH_2FH^+$	231	213	18
$^\bullet CH_2ClH^+$	251	234	17
$CH_3{}^\bullet CHClH^+$	232	216	16
$CH_3{}^\bullet CHBrH^+$	238	222	16
$^\bullet CH_2OH_2^+$	196	178	18
$CH_3{}^\bullet CHOH_2^+$	179	163	16
$^\bullet CH_2O^+(H)CH_3$	186	171	15
$^\bullet CH_2NH_3^+$	204	190	14
$^\bullet CH_2{}^+NH_2CH_3$	191	175	16
β-distonic ions			
$^\bullet CH_2CH_2FH^+$	187	186	1
$^\bullet CH_2CH_2ClH^+$	223	218	5
$^\bullet CH_2CH_2OH_2^+$	176	165	11
$^\bullet CH_2CH_2O^+(H)CH_3$	170	166	4
$^\bullet CH_2CH_2NH_3^+$	185	185	0
$^\bullet CH_2CH_2O^+(H)C_2H_5$	153	153	0
β-distonic isomers of carbonyl molecular ions			
$^\bullet CH_2OC^+HOH$	156	138	18
$^\bullet CH_2OC^+(OH)CH_3$	127	111	16
γ-distonic ions			
$^\bullet CH_2CH_2CH_2FH^+$	185	181	4
$^\bullet CH_2CH_2CH_2ClH^+$	219	213	6
$^\bullet CH_2CH_2CH_2OH_2^+$	172	159	13
$^\bullet CH_2CH_2CH_2NH_3^+$	177	179	-2
γ-distonic isomers of carbonyl molecular ions			
$^\bullet CH_2CH_2OC^+HOH$	137	129	8
$^\bullet CH_2CH_2CH(=O^+H)$	181	179	2
$CH_3{}^\bullet CHCH_2CH(=O^+H)$	165	172	-7
$^\bullet CH_2CH(CH_3)CH(=O^+H)$	154	169	-15
$^\bullet CH_2CH_2C(=O^+H)CH_3$	165	156	9

Table 6.5 The methyl cation affinity (MCA) and ethyl cation affinity (ECA) of some small molecules, in kcalmol^{-1} [1]

Molecule (M)	$\Delta_f H^\circ$ (M)	$\Delta_f H^\circ$ (CH_3M^+)	MCA (M)	$\Delta_f H^\circ$ ($C_2H_5M^+$)	ECA (M)	Δ
HF	-65	162	34	138	13	(21)
HCl	-22	183	56	170	24	32
HBr	-9	191	61	180	27	34
H_2O	-58	136	67	121	37	30
CH_3OH	-48	130	83	118	50	33
HCOOH	-90.5	92	78	80	46	32
CH_3COOH	-103	69	89	59	54	35
NH_3	-11	146	104	137	68	36
CH_3NH_2	-5.5	141	114	132	78	36
H_2S	-5	173	83	164	47	36
					Average	33

1. All values from reference 16.

Table 6.6 The methylene ion affinity (MIA) and ethylene ion affinity (EIA) of some small molecules, in kcalmol^{-1}

Molecule(M)	MIA(M)	EIA(M)	Δ'
HF	35	3	(32)
HCl	58	10	(48)
H_2O	78	22	56
CH_3OH	97	37	60
HCOOH	84	27	57
CH_2CO (Δ_fH°,-11)	123	67	56
CH_2O (Δ_fH°,-26)	94	35	59
NH_3	116	59	57

Table 6.7 The bond length change in distonic radical cations

Molecular ion	Bond length (Å)	Distonic ion	Bond length (Å)	Ref.
$[FCH_2\text{-}CH_3]^{+\bullet}$	2.020	$HF^{+}CH_2\text{-}CH_2^{\bullet}$	1.404	21
$[ClCH_2\text{-}CH_3]^{+\bullet}$	1.938	$HCl^{+}CH_2\text{-}CH_2^{\bullet}$	1.401	21
$[HOCH_2\text{-}H]^{+\bullet}$	1.097	$H_2O^{+}CH^{\bullet}\text{-}H$	1.079	23
$[CH_3O\text{-}CH_3]^{+\bullet}$	1.500	$CH_3O^{+}(H)\text{-}CH_2^{\bullet}$	1.446	27
$[HCOO\text{-}CH_3]^{+\bullet}$	1.492	$HC^{+}(OH)O\text{-}CH_2^{\bullet}$	1.411	53b
	1.491		1.417	53a
$[CH_3OC(=O)\text{-}CH_3]^{+\bullet}$	1.490	$CH_3OC^{+}(OH)\text{-}CH_2^{\bullet}$	1.440	62
$[HOCH_2\text{-}CH_3]^{+\bullet}$	2.013	$H_2O^{+}CH_2\text{-}CH_2^{\bullet}$	1.461	27
	1.952		1.470	21
$[HOCH_2\text{-}CH_3]^{+\bullet}$	2.013	$H_2O^{+}CH^{\bullet}\text{-}CH_3$	1.479	27
$[CH_3CH_2\text{-}OH]^{+\bullet}$	1.301	$^{\bullet}CH_2CH_2\text{-}OH_2^{+}$	1.652	27
$[CH_3CH_2\text{-}OH]^{+\bullet}$	1.301	$CH_3CH^{\bullet}\text{-}OH_2^{+}$	1.517	27
$[H_2NCH_2\text{-}CH_3]^{+\bullet}$	1.539	$H_3N^{+}CH_2\text{-}CH_2^{\bullet}$	1.489	21
$[H_2NCH_2CH_2\text{-}CH_3]^{+\bullet}$	1.531	$H_3N^{+}CH_2CH_2\text{-}CH_2^{\bullet}$	1.503	87

Table 6.8 The bond lengths in C_2H_5OH, $C_2H_5OH_2^+$, $C_2H_4OH^\bullet$ and $C_2H_4OH_2^{+\bullet}$ [1]

	CH_3CH_2OH	$CH_3CH_2OH_2^+$	$CH_3C^\bullet HOH$	$CH_3C^\bullet HOH_2^+$	$^\bullet CH_2CH_2OH$	$^\bullet CH_2CH_2OH_2^+$
C_1-H	1.092	1.090	1.100	1.098	1.082	1.081
C_2-H	1.099	1.088	1.090	1.083	1.105	1.088
C-C	1.512	1.498	1.486	1.472	1.484	1.459
C-O	1.428	1.547	1.382	1.500	1.429	1.607
O-H	0.971	0.987	0.971	0.989	0.971	0.987

1. Unpublished values from Dr. L. Radom; at MP2//G-31G* level.

Chapter 7

$C_3H_6O_2^{+\bullet}$ radical cations

7.1 Introduction

A particular interest in $C_3H_6O_2^{+\bullet}$ isomers was evoked by the observation that the majority of low-energy molecular ions of methyl acetate lost $^{\bullet}CH_2OH$ rather than $CH_3O^{\bullet}$ in the formation of the acetyl cation, CH_3CO^+. The key experiment was the collision-induced dissociative ionization of the free-radical products from metastable methyl acetate molecular ions.[1] The dissociation process was proposed[2,3] to involve a distonic isomer $CH_3C^+(OH)OCH_2^{\bullet}$ (2), which in turn isomerizes to a hydrogen-bridged radical cation $[CH_3C{=}O{\bullet\bullet\bullet}H{\bullet\bullet\bullet}O{=}CH_2]^{+\bullet}$ (3) followed by direct hydrogen bond cleavage to the products:

$$\underset{\textbf{(1)}}{CH_3COOCH_3^{+\bullet}} \rightarrow \underset{\textbf{(2)}}{CH_3C^+(OH)OCH_2^{\bullet}}$$

$$\downarrow$$

$$\underset{\textbf{(3a)}}{[CH_3C{=}O{\bullet\bullet\bullet}H{\bullet\bullet\bullet}O{=}CH_2]^{+\bullet}} \rightarrow CH_3CO^+ + {}^{\bullet}CH_2OH$$

Scheme 7.1

The involvement of the O••H••O bridged isomer **3a** in the gas-phase ion chemistry of ionized acetol, $CH_3C(=O)CH_2OH^{+\bullet}$ (4) has been considered recently.[4] The MS/MS/MS experiments on D-labeled acetol isotopomers and ab initio MO calculations led to the proposal that ions **4** dissociated to $CH_3CHOH^+ + CHO^{\bullet}$ via a C••H••O bridged

isomer **3b** instead of the O••H••O bridged isomer **3a**. Although **3b** is ~ 11 kcalmol^{-1} higher in energy than **3a**,[3] it was readily formed from the ion-neutral complex $[CH_3C(=O)^+ \bullet\bullet\bullet HOCH_2^\bullet]$ (**4a**), which was found by the calculations to be accessible from ion **4**. Thus the most satisfactory pathway was suggested as the following:

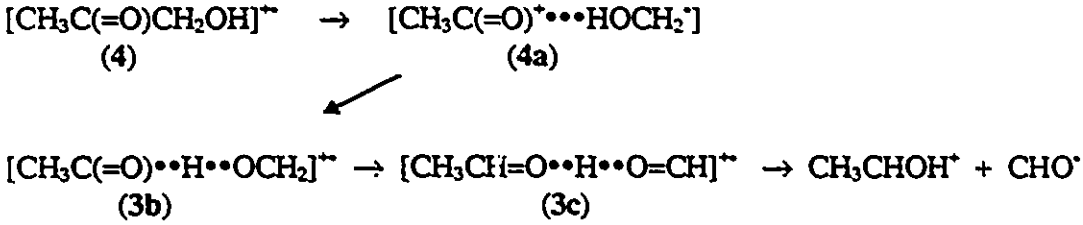

Scheme 7.2

These thorough studies on $CH_3COOCH_3^{+\bullet}$ and $CH_3COCH_2OH^{+\bullet}$ indicated that both distonic isomers and hydrogen-bridged isomers are all actively involved in these $C_3H_6O_2^{+\bullet}$ systems.

Ionized ethyl formate (**5**) displays characteristics quite different from isomers **1** and **4** in its unimolecular dissociation processes. The important fragmentation in the MI mass spectrum of **5** is H_2O loss, which lost its priority in the CID mass spectrum of **5**, being exceeded by the intensity of the $C_2H_4^{+\bullet}$ ion (HCOOH loss).[5] The different decay rate constants observed for the formation of $C_2H_4^{+\bullet}$ and $C_3H_4O^{+\bullet}$ (H_2O loss) indicates two separate, prior isomerization processes.[6] The intermediate involved in the formation of $C_2H_4^{+\bullet}$ was assigned to a distonic ion $^\bullet CH_2CH_2OC^+HOH$ (**6**), which was formed from ion **5** via a McLafferty rearrangement. The other intermediate, responsible for the formation of $C_3H_4O^{+\bullet}$ was first suggested to be $CH_3CHC(OH)_2^{+\bullet}$ (**7**). The examination of the structure of $C_3H_4O^{+\bullet}$, however, showed that it most likely was $^\bullet CH_2CH_2CO^+$, rather than

$CH_3CHCO^{+\bullet}$ which is known to be produced from $CH_3CHC(OH)_2^{+\bullet}$ (7). Hence it was proposed that the fragmentation to $^{\bullet}CH_2CH_2CO^{+}$ also came from the distonic ion 6.[5] Some more complicated isomerization steps, which remain unknown, may be involved in this dissociation process.

The direct generation and detailed characterization of the distonic ion $^{\bullet}CH_2CH_2OC^{+}HOH$ (6) will be shown in this Chapter. Moreover, the characterization of ion 7 and its distonic isomer $^{\bullet}CH_2CH_2C^{+}(OH)_2$ (8) which has been produced for the first time, will be also discussed.

7.2 Experimental

The metastable ion (MI), the collision-induced dissociation (CID) and the neutral-reionization (NR) mass spectra were obtained with the VG ZAB-3F mass spectrometer. Appearance energy (AE) values were measured with the KRATOS MS 902 mass spectrometer. The CID and NR mass spectra (8-keV ions) were obtained in the second field-free region (2ffr) of the ZAB-3F using He to effect collision-induced dissociation or using O_2 to effect reionization (main beam transmission 80%) and Xe for neutralization. The structure of the products of spontaneous or collision-induced dissociation of ions in the 2ffr was probed by obtaining their CID mass spectra in the third field-free region (3ffr) using O_2 as the collision gas. All compounds used were commercially available (Aldrich) and purified where necessary. Deuteration of the hydroxyl groups in 1,4-dioxane-2,3-diol and $CH_3OCH_2CH_2COOH$ was achieved by dissolving a small amount of sample in D_2O, after which water was removed; this was repeated three times.

7.3 Results and discussion

7.3.1 Generation of $C_3H_6O_2^{+\bullet}$ isomers

The distonic ion $^{\bullet}CH_2CH_2OC^{+}HOH$ was produced directly from the fragmentation of ionized 1,4-dioxane-2,3-diol (A) via HCOOH loss.

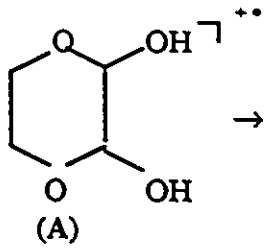

(A)

$$\rightarrow \quad {}^{\bullet}CH_2CH_2OC^{+}HOH \; (6) \; + \; HCOOH \qquad (1)$$

As discussed in Chapter 6, a cyclic molecular ion may well fragment to a distonic ion via loss of a small molecule. Indeed ion **6** (m/z 74) is dominant in the MI and CID mass spectra of A. The kinetic energy release ($T_{0.5}$) in the metastable dissociation of A via HCOOH loss is 19 meV, likely indicating that no reverse energy barrier was involved. It is possible that the ion A first isomerized to an acyclic intermediate (by breaking the C2-C3 bond) which then dissociated directly to ion **6** by HCOOH loss.

The appearance energy (AE) of ion **6** measured from the metastable dissociation of A was 9.26 ± 0.1 eV, leading to the heat of formation of **6** as 137 kcalmol^{-1}. The heat of formation of HCOOH is -90.5 kcalmol^{-1} [7] and the heat of formation of 1,4-dioxane-2,3-diol is estimated by the additivity rule[8] to be -167 kcalmol^{-1}. Thus ion **6** is 16 kcalmol^{-1} more stable than ionized ethyl formate (Δ_fH° = 153 kcalmol^{-1} [7]). This result is expected, as the distonic isomers of ester molecular ions are commonly more stable than their conventional isomers. For instance, $^{\bullet}CH_2OC^{+}(OH)CH_3$ (Δ_fH° = 127 kcalmol^{-1} [2b]) is lower

in energy than $CH_3COOCH_3^{+\bullet}$ (Δ_fH° = 139 kcalmol^{-1} [7]), but so stable as the enol ion $^{\bullet}CH_2C^{+}(OH)OCH_3$, Δ_fH° = 114 kcalmol^{-1}.[7]

The enol isomer of ionized propanoic acid $CH_3CHC(OH)_2^{+\bullet}$ (7) was generated from the fragmentation of $CH_3CH_2CH(CH_3)COOH^{+\bullet}$ (**B**) via C_2H_4 loss or from the dissociation of $CH_3CH(COOH)_2^{+\bullet}$ (**C**) via CO_2 loss.

$$\underset{\textbf{(B)}}{CH_3CH_2CH(CH_3)COOH^{+\bullet}} \rightarrow \underset{\textbf{(7)}}{CH_3CHC(OH)_2^{+\bullet}} + C_2H_4 \qquad (2)$$

$$\underset{\textbf{(C)}}{CH_3CH(COOH)_2^{+\bullet}} \rightarrow \underset{\textbf{(7)}}{CH_3CHC(OH)_2^{+\bullet}} + CO_2 \qquad (3)$$

Both reactions 2 and 3 are rearrangement-fragmentation processes. Ion 7 is the second most intense peak in the MI and CID mass spectra of **B**, which preferably dissociated via $CH_3^{\bullet}$ loss. The possible product ion by $CH_3^{\bullet}$ (Δ_fH°, 34.8 kcalmol^{-1} [7]) loss is $CH_3CHCHC(OH)_2^{+}$ (Δ_fH°, 78 kcalmol^{-1} [7]). This dissociation process is slightly less endothermic than dissociation to $CH_3CHC(OH)_2^{+\bullet}$ (Δ_fH°, 104 kcalmol^{-1} [7]) via C_2H_4 (Δ_fH°, 12.5 kcalmol^{-1} [7]) loss. The $T_{0.5}$ value in the metastable dissociation of **B** for C_2H_4 loss was measured to be 6.2 meV, indicating that no reverse energy barrier was involved. It is thus suggested that $CH_3CH_2CH(CH_3)C\dot{O}OH^{+\bullet}$ (**B**) rapidly isomerizes to a distonic isomer $CH_3C^{\bullet}HCH(CH_3)C^{+}(OH)_2$ (**B'**) via a 1,4-hydrogen shift. Ion **B'** is the precursor which dissociates to both $CH_3CHC(OH)_2^{+\bullet}$ (7) and $CH_3CHCHC(OH)_2^{+}$.

The MI dissociation of $CH_3CH(COOH)_2^{+\bullet}$ (**C**) to ion 7 via CO_2 loss (reaction 3) showed a $T_{0.5}$ value of 721 meV, which may result from a significant reverse energy barrier for dissociation or a high isomerization energy barrier for **C** to isomerize to a more

stable isomer. The intensity of m/z 74 increased 73% in the CID mass spectrum of C, indicating it is sensitive to collisional activation. The process is thus believed to involve a transition state higher in energy than that for $CH_3CHC(OH)_2^{+\bullet}$ + CO_2, i.e.

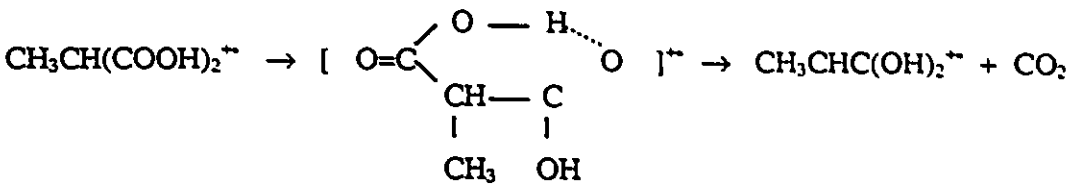

Scheme 7.3

The distonic ion $^{\bullet}CH_2CH_2C^{+}(OH)_2$ (8) was produced from the fragmentation of ionized 3-methoxy-propanoic acid via CH_2O loss.

$$\underset{\textbf{(D)}}{CH_3OCH_2CH_2COOH^{+\bullet}} \rightarrow \underset{\textbf{(8)}}{^{\bullet}CH_2CH_2C^{+}(OH)_2} + CH_2O \qquad (4)$$

Ion 8 was dominant in the MI and CID mass spectra of ion D. That the intensity of ion 8 (m/z 74) was not increased by introducing collision gas to the 2ffr indicates that this dissociation process may involve a stable intermediate. Moreover, the kinetic energy release ($T_{0.5}$ 13 meV) was not affected by the collisional activation either, indicating that the isomerization energy barrier to the stable intermediate may lie close to the dissociation energy barrier. This intermediate is most likely $^{\bullet}CH_2OCH_2CH_2C^{+}(OH)_2$ (D') which is accessible by a 1,6-hydrogen shift from ion D.

7.3.2 Characterization of $C_3H_6O_2^{+\bullet}$ distonic isomers 6 and 8

The distonic isomers can be characterized by their MI and CID mass spectrometries. However, if the isomerization energy barrier between the distonic ion and

its conventional isomer is below the lowest energy requirement for dissociation, the distonic ion may not be distinguishable by MI mass spectrometry but may show some specific dissociations in its CID mass spectrum.

7.3.2.1 $^{\bullet}CH_2CH_2OC^{+}HOH$, **6**

The distinguishing characteristic of this distonic isomer was the intense peak at m/z 28 in its MI mass spectrum (Table 7.1) compared to that in the MI mass spectrum of $HCOOCH_2CH_3^{+\bullet}$ (**9**). The m/z 28 daughter ion was confirmed by the fragments of m/z 25 - m/z 27 in its CID mass spectrum to be $C_2H_4^{+\bullet}$. The similar small KER ($T_{0.5}$) values 2-3 meV, for this dissociation of metastable **6** and **9** indicates that both isomers probably have the same dissociation energy barrier. It was suggested[5] that isomer **9** isomerized to **6** via a McLafferty rearrangement followed by dissociation to $C_2H_4^{+\bullet}$ via HCOOH loss. The domination of $C_2H_4^{+\bullet}$ in the MI and CID mass spectra (Tables 7.1 and 7.2) of the directly generated **6** confirmed this suggestion. Whereas in the CID mass spectra of both **6** and **9** the intensities of $C_2H_4^{+\bullet}$ increased, the increase in the CID mass spectrum of **6** was greater, in keeping with it being a direct bond cleavage. It was noticible that the other dissociations of metastable **6** other than HCOOH loss, showed different sensitivities to collisional activation, indicating that they are involved in some other isomerization processes. These will be discussed in the following section. Thus distonic isomer **6** is the reacting configuration by which ion **9** loses HCOOH.

Another distinguishing characteristic of **6** was the doubly charged ion $C_3H_6O_2^{2+}$ in its CID mass spectrum. There was no doubly charged ion peak in the CID mass spectrum of **9**. This characteristic further confirms **6** as a distonic ion. In general, distonic ions show

doubly charged peaks in their CID mass spectra more often than their conventional isomers.[9]

In the MI dissociations of $C_3H_6O_2^{+\bullet}$ isomers (Table 7.1) only **6** showed a fragment at m/z 45 (CHO loss). This daughter ion was confirmed by the ratio of m/z 19 to m/z 43 in its CID mass spectrum to be $CH_2CHOH_2^+$,[10] see Figure 1. Moreover, in the MI mass spectrum of $^{\bullet}CH_2CH_2OC^+HOD$, produced from 1,4-dioxane-2,3-diol-d_2 by HCOOD loss, the ratio of m/z 45 (CDO loss) to m/z 46 (CHO loss) was 12 (Table 7.3), indicating that the hydroxyl group is likely involved in CHO loss. It is therefore proposed that a hydrogen-bridged species $[CH_2CH_2O{\bullet\bullet\bullet}H{\bullet\bullet\bullet}OCH]^{+\bullet}$ may lead to the CHO loss.

7.3.2.2 $^{\bullet}CH_2CH_2C^+(OH)_2$, **8**

The MI mass spectrum of **8** was the same as those of $CH_3CHC^+(OH)_2$ (**7**) and $CH_3CH_2COOH^{+\bullet}$ (**10**), see Table 7.1. The only characteristic of **8** was the presence of the fragment $C_2H_4O_2^{+\bullet}$ in its CID mass spectrum (Table 7.2). The fragments of $C_2H_2O^{+\bullet}$ (H_2O loss) and CHO_2^+ (CH_3 loss) in the CID mass spectrum of this $C_2H_4O_2^{+\bullet}$ daughter ion (Figure 7.2) confirmed that it is $CH_2C(OH)_2^{+\bullet}$.[11] Thus the structure of **8** is indeed $^{\bullet}CH_2CH_2C^+(OH)_2$, which fragments to $CH_2C(OH)_2^{+\bullet}$ by CH_2 loss. The $C_2H_4O_2^{+\bullet}$ peak in the CID mass spectrum of **8** generated from metastable $CH_3OCH_2CH_2COOH^{+\bullet}$ via CH_2O loss was more intense (Figure 7.3) than that of the ion source generated species, indicating that ion **8** having a lower internal energy (MI generated), shows stronger structure characteristics than those with higher internal energy (ion source generated). Thus the ion source generated ions **8** most likely (at least in part) isomerize to the more stable isomer **7** (Δ_fH°, 104 kcalmol^{-1} [7]). The heat of formation of **8** can be estimated from a

thermochemical cycle (Eq. 1) to be 115 kcalmol^{-1} by taking PA(CH_3CH_3COOH) = 192 kcalmol^{-1}, BDE(H-CH_2CH_2COOH) = 100 kcalmol^{-1} and Δ_fH°(CH_3CH_2COOH) = -107 kcalmol^{-1}.[7]

$$\Delta_fH^\circ (8) = [\Delta_fH^\circ (P) + BDE(C\text{-}H) - \Delta_fH^\circ (H)] + \Delta_fH^\circ (H^+) - PA (P) \quad \text{Eq. 1}$$

$$P = CH_3CH_2COOH$$

The MI dissociations of **7**, **8** and **10** by H_2O loss had closely similar $T_{0.5}$ values, 87-91 meV, indicating that the three isomers have a common dissociation barrier. The dissociation energy barrier for **10** dissociating by H_2O loss has been measured to be 144.4 kcalmol^{-1}, from its appearance energy of 10.9 eV.[12] Thus the isomerization barrier between **7**, **8** and **10** is below 144.4 kcalmol^{-1}, as shown in the energy diagram (Figure 7.4).

7.3.3 Isomerization-dissociation processes of $C_3H_6O_2^{+\bullet}$ isomers

The $C_3H_6O_2^{+\bullet}$ isomers, **6**, **7** and **8** together with ionized ethyl formate, $HCOOCH_2CH_3^{+\bullet}$ (**9**) and ionized propanoic acid, $CH_3CH_2COOH^{+\bullet}$ (**10**) were characterized by MI, CID, CIDI and NR mass spectrometries. The MI and CID mass spectra of those $C_3H_6O_2^{+\bullet}$ isomers are summarized in Tables 7.1 and 7.2, respectively.

According to the relative intensities in their MI and CID mass spectra, the $C_3H_6O_2^{+\bullet}$ isomers **6**, **7**, **8**, **9** and **10** can be divided into two groups. The first group includes $HCOOCH_2CH_3^{+\bullet}$ (**9**) and its γ-distonic isomer $^{\bullet}CH_2CH_2OC^{+}HOH$ (**6**). The second group includes $CH_3CH_2COOH^{+\bullet}$ (**10**), its enol isomer $CH_3CHC(OH)_2^{+\bullet}$ (**7**) and its β-

distonic isomer $^{\bullet}CH_2CH_2C^{+}(OH)_2$ (8). The significant difference between the two groups is the fragmentation by HCOOH loss for **9** and **6**.

7.3.3.1 Dissociation by HCOOH loss

The dissociation by HCOOH loss was only observed in the MI mass spectra of the first group (Table 7.1). The kinetic energy release of this process was very small ($T_{0.5}$, 2-3 meV). Moreover, the intensity of $C_2H_4^{+\bullet}$ in the MI mass spectrum of **6** was much higher than that in the MI mass spectrum of **9**, indicating that **6** is the direct precursor for $C_2H_4^{+\bullet}$ + HCOOH. This was further confirmed by the CID mass spectrum of **6**, in which $C_2H_4^{+\bullet}$ was predominant (Table 7.2). As discussed above ion **6** is 16 kcalmol^{-1} lower in energy than ion **9**. The latter may thus easily isomerize to the former via a McLafferty rearrangement.

$$\underset{\mathbf{6}}{[\,CH_2CH_2OCH\,]^{+\bullet}} \rightarrow \underset{\mathbf{9}}{{}^{\bullet}CH_2CH_2OC^{+}H} \rightarrow CH_2CH_2^{+\bullet} + HCOOH \qquad (5)$$

The MI mass spectrum of $^{\bullet}CH_2CH_2OC^{+}HOD$ (Table 7.3) showed little H/D mixing in the HCOOH loss. In the CID mass spectrum of $^{\bullet}CH_2CH_2OC^{+}HOD$ the ratio of m/z 28 ($C_2H_4^{+\bullet}$) to m/z 29 (most $C_2H_3D^{+\bullet}$) was about 1, indicating a great extent of H/D mixing during collisional activation. Thus the barrier for a hydrogen shift in **9** must be higher than that for the CH_2CH_2–O bond cleavage. It is noteworthy that the C-O bond cleavage in $^{\bullet}CH_2CH_2OC^{+}HOH$ produces ionized ethene. The charge is retained on the alkyl group. Even in the CID mass spectra of **6** and **9** the $CH_2O_2^{+\bullet}$ ion was absent. However, in the

CID mass spectra of the second group of ions, i.e. **7**, **8** and **9**, $CH_2O_2^{+\bullet}$ was observed, indicating that the charge was retained on the carbonyl group.

7.3.3.2 Dissociation by H_2O loss

The isomers in the first group showed $C_3H_4O^{+\bullet}$ as the most intense peak in their MI mass spectra. The structure of this $C_3H_4O^{+\bullet}$ daughter ion was examined by being transmitted to the 3ffr, where its CID mass spectrum was produced, as shown in Table 7.4. The base peak of m/z 28 in the CID mass spectra of $C_3H_4O^{+\bullet}$ is due to CO loss, it being 80 kcalmol^{-1} less endothermic than C_2H_4 loss. The heats of formation of CO, $CO^{+\bullet}$, C_2H_4, and $C_2H_4^{+\bullet}$ are -26 kcalmol^{-1}, 296.7 kcalmol^{-1}, 12.5 kcalmol^{-1} and 254.8 kcalmol^{-1}, respectively. The fragment ion m/z 42 in the CID mass spectra of the $C_3H_4O^{+\bullet}$ daughter ions from isomers **6** and **9** clearly indicated the presence of a terminal methylene group and therefore the structure $^{\bullet}CH_2CH_2CO^{+}$ was assigned to it. The base peak of m/z 28 in the CID mass spectra of $C_3H_4O^{+\bullet}$ daughter ions from isomers **7**, **8** and **10** also result from CO loss. The weak peak at m/z 41 and the absence of m/z 42, indicates the structure $CH_3CHCO^{+\bullet}$.

The $C_3H_6O_2^{+\bullet}$ isomers in the second group dissociate to $CH_3CHCO^{+\bullet}$ by H_2O loss with the same kinetic energy release ($T_{0.5}$, 87-91 meV), indicating that the same intermediate ion was involved. It has been calculated[13] that the dissociation of $CH_3COOH^{+\bullet}$ (**I**) to $CH_2CO^{+\bullet}$ by H_2O loss involves the stable intermediate $^{\bullet}CH_2C(=O)OH_2^{+}$ (**II**). The isomerization is a stepwise process, i.e. **I** first isomerizes to $CH_2C(OH)_2^{+\bullet}$ (**III**), which is 20 kcalmol^{-1} lower in energy than **I**. Ion **III** then isomerizes to **II** with an energy barrier of 52 kcalmol^{-1}. Ion **II** has been experimentally observed and

characterized.[14] By analogy, $CH_3CHC(=O)OH_2^{+\bullet}$ (**11**) may be the intermediate involved in the dissociation of $CH_3CHC(OH)_2^{+\bullet}$ (**7**), $CH_2CH_2C(OH)_2^{+\bullet}$ (**8**) and $CH_3CH_2COOH^{+\bullet}$ (**10**) to $CH_3CHCO^{+\bullet} + H_2O$. Ions **8** and **10** may readily isomerize to ion **7**, since **7** is 26 kcalmol^{-1} more stable than **10**[7] and about 11 kcalmol^{-1} more stable than **8**. Isomer **10** may isomerize to **8** by a simple 1,4-hydrogen shift. Such a five-membered ring H-transfer has been found to compete with the McLafferty rearrangement in ionized carbonyl compounds.[15] Thus the isomerization of **10** to **8** may require only a small energy barrier. The isomerization energy barrier between **7** and **8** can be estimated from that for the 1,2-hydrogen shift between $CH_3CHCO^{+\bullet}$ and $^{\bullet}CH_2CH_2CO^{+}$, which was calculated to be 25.5 kcalmol^{-1} (G2 procedure).[16] The isomerization process is shown in Figure 7.4.

The MI mass spectrum of $^{\bullet}CH_2CH_2C^{+}(OH)OD$ produced from dissociation of $CH_3OCH_2CH_2COOD^{+\bullet}$ via CH_2O loss showed that the ratio of HDO loss to H_2O loss is about 0.41, which is less than the statistical value of 0.5 and so indicating incomplete H/D mixing before water loss. The intermediate **11** is most likely involved in this dissociation process, as shown in Scheme 7.4.

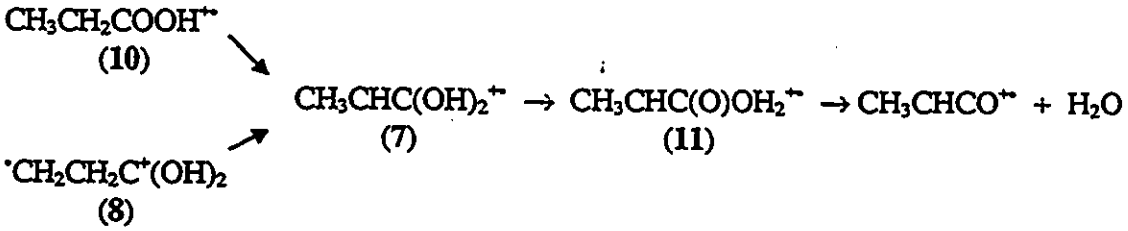

Scheme 7.4

The dissociation by H_2O loss of the $C_3H_6O_2^{+\bullet}$ isomers in the first group, $^{\bullet}CH_2CH_2C^{+}HOH$ (**6**) and $HCOOCH_2CH_3^{+\bullet}$ (**9**), is more complicated. The two isomers

gave the same kinetic energy release ($T_{0.5}$, 37 meV) in this dissociation process (Table 7.1), indicating that they isomerize to the same intermediate before dissociation. As the daughter ion $C_3H_4O^{+\bullet}$ was confirmed to be $^{\bullet}CH_2CH_2CO^+$, the question is how isomers **6** and **9** produce this fragment ion. Is the C-O bond cleavage and the C-C bond formation a stepwise or a concerted process?

By analogy with the isomers in the second group, the precursor ion structure for $^{\bullet}CH_2CH_2CO^{+\bullet}$ may well be $^{\bullet}CH_2CH_2C(O)OH_2^+$, which may arise from $[H_2C(\bullet\bullet\bullet O)\text{-}CHOH]^{+\bullet}$ (**12**). Hudson and McAdoo suggested that the immediate product from H_2O loss is $CH_2CH_2OC^{+\bullet}$, higher in energy than $CH_2CH_2CO^{+\bullet}$, and which might readily collapse to the latter. If it were the case, the reacting configuration for H_2O loss would be $^{\bullet}CH_2CH_2OC^+HOH$ (**6**). The water loss would be encouraged by collisional activation as was the dissociation of **6** to $CH_2CH_2^{+\bullet}$ by HCOOH loss. However, the water loss was very insensitive to collisional activation, indicating that another intermediate is likely involved. Moreover, the MI mass spectrum of $^{\bullet}CH_2CH_2OC^+HOD$ showed little H/D mixing in HCOOH loss. However, the ratio of $C_3H_4O^{+\bullet}$ (HDO loss) to $C_3H_3DO^{+\bullet}$ (H_2O loss) was 0.75 (statistical = 0.5), indicating some extent of H/D mixing in the water loss process. This result supports the proposal that the H_2O loss involves an intermediate other than isomer **6**.

An examination of the metastable ion dissociations of several ester radical cations showed that only ionized ethyl esters dissociate by H_2O loss. Ionized methyl or propyl esters do not do so.

Ionized alkyl ester	Distonic isomers	H_2O loss in MI mass spectrum
$HCOOCH_3^{+\cdot}$	$HCO(OH)OCH_2^{+\cdot}$	No
$HCOOCH_2CH_3^{+\cdot}$	$HCO(OH)OCH_2CH_2^{+\cdot}$	Yes
$HCOOCH_2CH_2CH_3^{+\cdot}$	$HCO(OH)OC_3H_6^{+\cdot}$	No
$CH_3COOCH_3^{+\cdot}$	$CH_3C(OH)OCH_2^{+\cdot}$	No
$CH_3COOCH_2CH_3^{+\cdot}$	$CH_3C(OH)OCH_2CH_2^{+\cdot}$ *	Yes
$CH_3COOCH_2CH_2CH_3^{+\cdot}$	$CH_3C(OH)OC_3H_6^{+\cdot}$	No
$CH_3CH_2COOCH_3^{+\cdot}$	$CH_3CH_2C(OH)OCH_2^{+\cdot}$	No
$CH_3CH_2COOCH_2CH_3^{+\cdot}$	$CH_3CH_2C(OH)OCH_2CH_2^{+\cdot}$	Yes

(* The distonic isomer involved in the dissociation of $CH_3COOCH_2CH_3^{+\cdot}$ was suggested[171] to be CH_2=C(OH)$OCH_2CH_3^{+\cdot}$. However, the latter may readily isomerize to $CH_3C(OH)OCH_2CH_2^{+\cdot}$ via a McLafferty rearrangement.)

Thus ionized esters may well have a common behaviour for H_2O loss,which likely involves a species such as [$H_2C^{\bullet\bullet\bullet}O$ / $H_2C^{\bullet\bullet\bullet}C(R)OH$] $^{+\cdot}$ (12', R = H, CH_3, C_2H_5). It may be formed from an incomplete O-C bond cleavage. The dissociation process is possibly under thermodynamic control, because the hydrogen lost, whether from R or from the ethyl group depends upon which product ion has lower energy.

$C_nH_{2n-2}O^{+\cdot}$ [1]	$\Delta_fH^\circ(C_nH_{2n-2}O^{+\cdot})$, kcalmol^{-1}
$\underline{CH_2CH_2CO^{+\cdot}}$	195
$CH_2CHCHO^{+\cdot}$	215
$\underline{CH_2CHCOCH_3^{+\cdot}}$	189
$CH_2CH_2COCH_2^{+\cdot}$	219
$\underline{CH_2CHCOCH_2CH_3^{+\cdot}}$	186
$CH_2CH_2COCHCH_3^{+\cdot}$	>194[2]

(1. The $C_nH_{2n-2}O^{+\cdot}$ ions underlined are the product ions.
2. Estimated from methyl substitution on $^{\cdot}CH_2CH_2OCH_2^{+}$, the value of the methyl substitution effect was assumed to be the same as for $CH_3CH_2^{+} + CH_3^{\cdot} \rightarrow CH_3C^{+}HCH_3 + H^{\cdot}$)

We propose that the O-C bond cleavage in isomer **6** and C-C bond formation to form intermediate **12** are most likely completed before the H_2O loss. Note that the ionized methyl esters, $[RC(OH)\text{-}OCH_2]^{+\bullet}$ only showed C-O bond cleavage and the ionized propyl esters, $[RC(OH)O\text{-}C_3H_6]^{+\bullet}$ only showed complete O-C bond cleavage without the formation of a C-C bond. Therefore the C-C bond formation in ionized ethyl esters may result from the incomplete O-C bond cleavage, followed rapidly by hydrogen abstraction leading to H_2O loss. The dissociation process for **6** and **9** by H_2O loss is shown in Scheme 7.5.

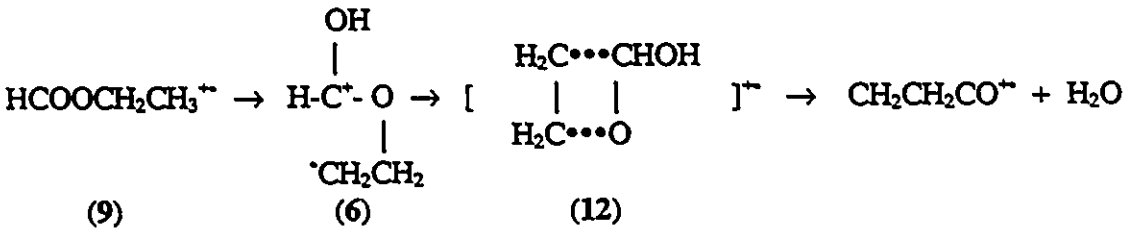

(9) (6) (12)

Scheme 7.5

The appearance energy of $C_3H_4O^{+\bullet}$ from **9** has been measured to be 10.73 eV, corresponding to an energy barrier at 155.4 kcalmol^{-1}. This is 2.4 kcalmol^{-1} above the energy of **9** (Δ_fH° = 153 kcalmol^{-1} [7]), indicating that the isomer **9** only lies in a shallow well on the potential energy surface of $C_3H_6O_2^{+\bullet}$ isomers, as shown in Figure 7.5. The isomer **6** being 16 kcalmol^{-1} lower in energy than **9**, sits in a relatively deep well in the potential energy surface. By contrast, the species **12** may lie in only a shallow well, because the water loss process lost its priority in collisional activation decompositions, indicating a lower density of states for intermediate **12** relative to more stable isomers.

7.3.3.3 Dissociation by H loss

Dissociation by H loss was dominant in the MI and CID mass spectra of 7, 8 and 10 and also produced the second most intense peak in the MI mass spectra of 6 and 9 (Tables 7.1 and 7.2). However in the CID mass spectra of 6 and 9, the peak at m/z 73 was only from metastable ions. The structure of the $C_3H_5O_2^+$ daughter ions were characterized by their CID mass spectra, which were all identical to that of $CH_2CHC(OH)_2^+$ produced from $CH_2CHCOOH + H^+$ (Table 7.5). The absence of m/z 43 in these CID mass spectra indicates that neither $CH_3CHCOOH^+$ nor $CH_2CH_2COOH^+$ was produced.[18]

The dissociations of 7, 8 and 10 by H loss may be straightforward. The precursor is possibly either $CH_3CHC(OH)_2^{+\bullet}$ (7) or $^{\bullet}CH_2CH_2C^+(OH)_2$ (8). Ion 7 is the most stable $C_3H_6O_2^{+\bullet}$ isomer and so its direct dissociation processes should be sensitive to collisional activation. Indeed the CID mass spectra of these three isomers all showed an intense peak at $C_3H_5O_2^+$, even after the substraction of MI contributions.

The CID mass spectrum of $^{\bullet}CH_2CH_2C^+(OH)OD$ produced from $CH_3OCH_2CH_2COOD^{+\bullet}$ via CH_2O loss, showed a ratio of D loss to H loss of about 0.09 (Table 7.4), indicating either a large isotope effect or that the H loss is almost wholly from the ethylene group with very little H shift between it and the C(OH)(OD) group. It has been observed[19] that the ratio of D loss to H loss in the MI decompositions of deuterium labelled 8 and 10 was about 0.04, indicating that H/D exchange between the α- and β-carbons in these isotopmers was rapid and that between the ethylene group and the carbonyl group was slow.

The dissociation of isomers **6** and **9** by H loss was very insensitive to collisional activation, the $C_3H_5O_2^+$ peak in their CID mass spectra being totally from metastable ions. Hence the dissociating species must be an intermediate which is higher in energy than **6**, but which lies in a well. One possibility is that the hydrogen shift in the intermediate **12** may lead to isomer **8**, $^{\bullet}CH_2CH_2C^+(OH)_2$, which dissociated to $CH_2CHC(OH)_2^+$ and $H^{\bullet}$. .

$$\mathbf{6} \rightarrow \mathbf{12} \rightarrow {}^{\bullet}CH_2CH_2C^+(OH)_2\ (\mathbf{8}) \rightarrow CH_2CHC(OH)_2^+ + H^{\bullet}$$

Scheme 7.6

The MI and CID mass spectra of $^{\bullet}CH_2CH_2OC^+HOD$ produced from 1,4-dioxane-2,3-diol-d_2 via $CHDO_2$ loss, showed a ratio of D loss to H loss of about 0.61 (Table 7.3), indicating a strong isotope effect preferred for D loss. Note that in the MI dissociations of $^{\bullet}CH_2CH_2OC^+HOD$, the HCOOH loss showed little H/D mixing, while the H_2O or H loss showed a certain extent of H/D mixing, indicating that the reactions involved different intermediates.

Whereas the H loss from $^{\bullet}CH_2CH_2C^+(OH)_2$ (**8**) did not show H/D mixing, the H loss from $^{\bullet}CH_2CH_2OC^+HOH$ (**9**) showed extensive H/D mixing; the latter involves more complex isomerization steps. Moreover, in the CID mass spectra of **7**, **8** and **10** the presence of m/z 55, which was not observed in the CID mass spectra of **6** and **9**, indicated a sequential dissociation from $C_3H_5O_2^+$ by H_2O loss. This further confirmed that the H loss from **6** and **9** is a slower process, involving several isomerization steps.

7.3.3.4 Dissociation by CO_2 loss

Another common fragment in the MI mass spectra of these $C_3H_6O_2^{+\bullet}$ isomers is m/z 30, $C_2H_6^{+\bullet}$. The fragments at m/z 24 - m/z 29 in the CID mass spectrum of this daughter ion confirmed that it was $C_2H_6^{+\bullet}$. The fragment at m/z 31 in the MI mass spectra of $^{\bullet}CH_2CH_2OC^{+}HOD$ and $^{\bullet}CH_2CH_2C^{+}(OH)OD$ (Table 7.3) further confirmed this structure.

$$C_3H_6O_2^{+\bullet} \rightarrow C_2H_6^{+\bullet} + CO_2 \qquad (6)$$

Studies[18] on the $C_3H_5O_2^{+}$ isomers have revealed that the dissociating configuration of $C_3H_5O_2^{+}$ ions by CO_2 loss was $CH_3CH_2OCO^{+}$, which metastably dissociates to $C_2H_5^{+}$ by CO_2 loss with a $T_{0.5}$ of ≤ 0.5 meV. In contrast the $T_{0.5}$ values for loss of CO_2 from other $C_3H_5O_2^{+}$ isomers $\overset{\text{!}}{\underbrace{CH_2CH_2OC^{+}OH}}$, $^{+}CH_2CH_2COOH$, $CH_3C^{+}HCOOH$, and $HOCH_2CH_2CO^{+}$ (30 - 35 meV), are much larger than that for loss of CO_2 from $CH_3CH_2OCO^{+}$, indicating that an energy barrier exists for interconversion. In the system of $C_3H_6O_2^{+\bullet}$ isomers, the analogous isomer cannot be directly obtained. However, a complex intermediate such as $[CH_3CH_2\bullet\bullet\bullet H\bullet\bullet\bullet OCO]^{+\bullet}$ may be achieved from **9** and **10**. The $T_{0.5}$ values of **9** and **10** are a little smaller than those of **6**, **7** and **8** (Table 7.1) indicating that the above may well be the structure leading to direct CO_2 loss.

7.3.3.5 Dissociation by CO loss

The dissociation channel by CO loss is only observed in the MI mass spectra of isomers **6** and **9**. The structure of the $C_2H_6O^{+\bullet}$ daughter ion was investigated by its CID mass spectrum performed in the 3ffr (Figure 7.6a). The intense peak at m/z 28 rather than

m/z 29 indicated that the structure was $CH_2CH_2OH_2^{+\bullet}$.[20] The fragment at m/z 46 in the CID mass spectra of **7**, **8** and **10** is $CH_2O_2^{+\bullet}$ which was confirmed by the presence of major fragments at m/z 29 and m/z 45 in its CID mass spectrum (Figure 7.6b).

One possible pathway for **6** and **9** to fragment to $CH_2CH_2OH_2^{+\bullet}$ is via a hydrogen bridged complex $[CH_2CH_2O(H)\bullet\bullet\bullet H\bullet\bullet\bullet CO]^{+\bullet}$ (**13**) which may be formed from an intermediate such as $^{\bullet}CH_2CH_2O(H)^{+}CHO$ (**14**). The proposed mechanism for CO loss is shown below:

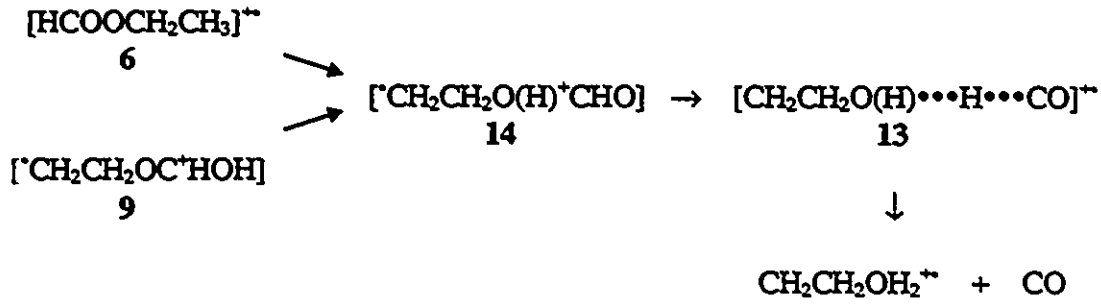

Scheme 7.7

It has been observed that at low temperature (77K) $^{\bullet}CD_2CH_2OC^{+}HOD$ radicals (presumably formed by isomerization of $CD_3CH_2OCHO^{+\bullet}$) rearrange to $^{\bullet}CH_2CD_2OC^{+}HOD$,[21] suggesting a shift of oxygen between the carbons. Thus the isomerization from **6** to **14** may be energetically accessible. The energy for the isomerization-dissociation of $HCOOCH_3^{+\bullet}$ (**IV**) by CO loss has been calculated (MP3/6-31G$^{+\bullet}$//6-31G* + ZPVE).[22] The isomerization energy barrier between **IV** and $^{\bullet}CH_2O^{+}(H)CHO$ (**V**) lies 44.4 kcalmol^{-1} above **IV**, but the energy barrier between $^{\bullet}CH_2OC^{+}HOH$ (**VI**) and **V** is 51.8 kcalmol^{-1} above **IV**. Ion **V** isomerizes to a hydrogen bridged complex $[CH_2O(H)\bullet\bullet\bullet H\bullet\bullet\bullet CO]^{+\bullet}$ followed by its dissociation to $CH_2OH_2^{+\bullet}$ +

CO. In the system **6** and **9** the isomerization energy barriers may be lower than for the analogous ions IV and VI, because the energy barriers for hydrogen shift from alkyl carbon to a heteroatom will decrease with increase of size of the chain in the alkyl group. For example, the isomerization energy barrier between $CH_3(CH_2)_nNH_2^{+\bullet}$ and $^{\bullet}CH_2(CH_2)_nNH_3^{+}$ decreases as n increases.[23]

7.3.4 The NR mass spectra of $C_3H_6O_2^{+\bullet}$ isomers

The NR mass spectra of isomers $\mathbf{6}^{+\bullet}$ and $\mathbf{9}^{+\bullet}$ (Figure 7a,b) were different from the CID mass spectrum of $\mathbf{9}^{+\bullet}$ (Figure 7c). The major peaks in their NR mass spectra were m/z 46 and m/z 29, which are most likely from the collision induced dissociations accompanying neutralization with Xe.

$$\mathbf{6}^{+\bullet},\ \mathbf{9}^{+\bullet} \xrightarrow{Xe} C_2H_4^{+\bullet} + CH_2O_2 \xrightarrow{Deflect} CH_2O_2 \xrightarrow{O_2} CH_2O_2^{+\bullet} \rightarrow CHO_2^{+}, CHO^{+} \qquad (7)$$

$$\xrightarrow{Xe} CHO_2^{+} + C_2H_5^{\bullet} \xrightarrow{Deflect} C_2H_5^{\bullet} \xrightarrow{O_2} C_2H_5^{+} \rightarrow C_2H_3^{+}, \bullet\bullet\bullet \qquad (8)$$

Dissociation to $C_2H_4^{+\bullet}$ + CH_2O_2 was predominant over CHO_2^{+} + $C_2H_5^{\bullet}$ in the collision induced dissociations (CID). However, $C_2H_5^{\bullet}$ has a lower ionization energy (IE, 8.13 eV[7]) than CH_2O_2 (11.33 eV[7]) and so is significant in the NR process. The small peaks at m/z 18 and m/z 17 in the NR mass spectra of $\mathbf{6}^{+\bullet}$ and $\mathbf{9}^{+\bullet}$ were also produced from the CID during the neutralization process.

$$\mathbf{6}^{+\bullet},\ \mathbf{9}^{+\bullet} \xrightarrow{Xe} C_3H_4O^{+\bullet} + H_2O \xrightarrow{Deflect} H_2O \xrightarrow{O_2} H_2O^{+\bullet} \qquad (9)$$

H_2O loss was only a minor process in the CID of $\mathbf{6}^{+\bullet}$ and $\mathbf{9}^{+\bullet}$ (most of the intensity is the contribution of MI dissociation) and the IE of H_2O is very high (12.61 eV). Hence fragments m/z 18 and m/z 17 were the weakest peaks in the NR mass spectra of the two isomers. The weak recovery signal of m/z 74 in the NR mass spectrum of $\mathbf{9}^{+\bullet}$ indicated that a small amount of $\mathbf{9}^{+\bullet}$, without isomerization to $\mathbf{6}^{+\bullet}$, survived the neutralization process. The peaks at m/z 55-56 are derived from the dissociations of reionized $\mathbf{9}^{+\bullet}$. Thus the neutral counterpart of $\mathbf{9}^{+\bullet}$, most likely [CH_3CH_2OCHO], is stable, whereas the neutral counterpart of $\mathbf{6}^{+\bullet}$ is unstable. The higher ratio of m/z 28 to m/z 27 in the NR mass spectra of $\mathbf{6}^{+\bullet}$ and $\mathbf{9}^{+\bullet}$ may indicate that some neutral C_2H_4 is produced in the dissociation of neutral $C_3H_6O_2$, followed by reionization with O_2.

$$\mathbf{6}^{+\bullet} \xrightarrow{Xe} {}^{\bullet}CH_2CH_2OC^{+}HOH \xrightarrow{Deflect} C_2H_4 + CH_2O_2 \xrightarrow{O_2} C_2H_4^{+\bullet} + CH_2O_2^{+\bullet} \qquad (10)$$

In contrast to $\mathbf{6}^{+\bullet}$, the NR mass spectrum of $\mathbf{7}^{+\bullet}$ showed a good recovery signal at m/z 74 (Figure 7.8a). Moreover, the NR mass spectrum of $\mathbf{7}^{+\bullet}$ was similar to its CID mass spectrum (Figure 7.8b), indicating that the neutral counterpart of $\mathbf{7}^{+\bullet}$ was quite stable.

$$\mathbf{7}^{+\bullet} \xrightarrow{Xe} CH_3CHC(OH)_2 \xrightarrow{O_2} CH_3CHC(OH)_2^{+\bullet} \qquad (11)$$

In the NR mass spectra of $\mathbf{8}^{+\bullet}$ and $\mathbf{10}^{+\bullet}$ (Figure 7.8c,d) the smaller recovery signals and intense peaks at m/z 44 and m/z 28, which were the major peaks in their CIDI mass

spectra, indicated that these $C_3H_6O_2^{+\bullet}$ isomers undergo significant collision induced dissociation as well as neutralization when collided with Xe.

7.4 Conclusions

Five $C_3H_6O_2^{+\bullet}$ isomers have been characterized by MI, CID and NR mass spectrometries. Dissociation mechanisms were proposed from the identification of daughter ion structures. The involvement of unusual intermediates has been proposed. The stablility of neutral $CH_3CHC(OH)_2$ (1,1-dihydroxy prop-1-ene) in the gas phase has been confirmed by NR mass spectrometry.

7.5 References

1. J. K. Terlouw, J. L. Holmes and P. C. Burgers, Int. J. Mass Spectrom. Ion Processes, 66, 239 (1985)
2. P. C. Burgers, J. L. Holmes, C. E. C. A. Hop and J. K. Terlouw, Org. Mass Spectrom., 21, 549 (1986)
3. N. Heinrich, J. Schmidt, H. Schwarz and Y. Apeloig, J. Am. Chem. Soc., 109, 1317 (1987)
4. M. George, C. A. Kingsmill, D. Suh, J. K. Terlouw and J. L. Holmes, J. Am. Chem. Soc., 116, 7807 (1994)
5. C. E. Hudson and D. J. McAdoo, Org. Mass Spectrom., 27, 1384 (1992)
6. Q. Zha, T. Nishimura and G. G. Meisels, Int. J. Mass Spectrom. Ion Processes, 120, 85 (1992)
7. S. G. Lias, J. E. Bartmess, J. F. Liebman, J. L. Holmes, R. D. Levin, and W. G. Mallard, J. Phys. Chem. Ref. Data, 17, No 1, 1988
8. S. W. Benson, *Thermochemical Kinetics*, 2nd. ed., John Wiley and Sons, New York, 1976
9. J. L. Holmes, F. P. Lossing, J. K. Terlouw and P. C, Burgers, Can. J. Chem., 61, 2305 (1983)
10. P. C. Burgers, J. K. Terlouw and J. L. Holmes, 369 (1982)
11. J. L. Holmes and F. P. Lossing, J. Am. Chem. Soc., 102, 3732 (1980)
12. R. Arakawa, Bull Chem. Soc. Jpn., 63, 754 (1990)
13. N. Heinrich and H. Schwarz, Int. J. Mass Spectrom. Ion Processes, 79, 295 (1987)

14. J. K. Terlouw, C. G. de Koster, W. Heerma, J. L. Holmes and P. C. Burgers, Org. Mass Spectrom., 18, 223 (1983)

15. D. J. McAdoo, Org. Mass Spectrom., 23, 350 91988)

16. M. L. McKee and L. Radom, Org. Mass Spectrom., 28, 1238 (1993)

17. a: J. L. Holmes, P. C. Burgers and J. K. Terlouw, Can. J. Chem., 59, 1805 (1981)

b: L. Fraser-Monteiro, M. L. Fraser-Monteiro, J. J. Butler and T. Baer, J. Phys. Chem., 86, 752 (1982)

18. D. Suh, C. A. Kingsmill, P. J. A. Ruttink, J. K. Terlouw and P. C. Burgers, Org. Mass Spectrom., 28, 1270 (1993)

19. D. J. McAdoo and D. N. Witiak, , Org. Mass Spectrom., 13, 499 (1978)

20. a: J. K. Terlouw, W. Heerma and G. Dijkstra, Org. Mass Spectrom, 17, 326 (1981)

b: P. C. Burgers, J. L. Holmes, J. K. Terlouw and B. Van Baar, Org. Mass Spectrom, 20, 202 (1985)

21. M. D. Sevilla, D. Becker, C. L. Sevilla and S. Swarts, J. Phys. Chem., 89, 633 (1985)

22. N. Heinrich, T. Drewello, P. C. Burgers, J. L. Morrow, J. Schwidt, W. Kulik, J. K. Terlouw and H. Schwarz, J. Am. Chem. Soc., 114, 3776 (1992)

23. B. F. Yates and L. Radom, J. Am. Chem. Soc., 109, 2910 (1987)

Table 7.1 MI mass spectra of $C_3H_6O_2^{+\bullet}$ isomers[1]

Fragments	$^{\bullet}CH_2CH_2OC^{+}HOH$ **6**	$HCOOCH_2CH_3^{+\bullet}$ **9**	$CH_3CHC(OH)_2^{+\bullet}$ **7**	$^{\bullet}CH_2CH_2C^{+}(OH)_2$ **8**	$CH_3CH_2COOH^{+\bullet}$ **10**
$CH_2CHC(OH)_2^{+} + H$	100 (146)	100 (137)	100 (124)	100 (118)	100 (117)
$^{\bullet}CH_2CH_2CO^{+} + H_2O$	100 (37)	98 (37)	-	-	-
$CH_3CHCO^{+\bullet} + H_2O$	-	-	38 (87)	33 (91)	35 (88)
$^{\bullet}CH_2CH_2OH_2^{+} + CO$	6 (50)	5 (48)	-	-	-
$C_2H_5O^{+} + HCO$	3 (8)	-	-	-	-
$C_2H_6^{+\bullet} + CO_2$	16 (37)	17 (33)	6 (49)	6 (46)	5 (26)
$C_2H_4^{+\bullet} + HCOOH$	55 (2)	6 (3)	-	-	-

1. Relative intensities (%). Values in parentheses are kinetic energy releases ($T_{0.5}$) in meV.

Table 7.2 CID mass spectra of $C_3H_6O_2^{+\bullet}$ isomers[1]

Fragments	$^{\bullet}CH_2CH_2OC^{+}HOH$ (6)	$HCOOCH_2CH_3^{+\bullet}$ (9)	$CH_3CHC(OH)_2^{+\bullet}$ (7)	$^{\bullet}CH_2CH_2C^{+}(OH)_2$ (8)	$CH_3CH_2COOH^{+\bullet}$ (10)
$C_3H_5O_2^{+}$	16	100	100	100	100
$C_2H_4O_2^{+\bullet}$	-	-	-	3	-
$C_3H_4O^{+\bullet}$	16	100	45	51	47
$C_3H_3O^{+}$	-	-	21	19	17
$CH_3O_2^{+}$	11	10	4	5	4
$CH_2O_2^{+}$, $C_2H_6O^{+\bullet}$	3	6	15	17	14
CHO_2^{+}, $C_2H_5O^{+}$	8	10	46	60	44
$C_3H_6O_2^{2+}$	1	-	4	3	3
CH_3O^{+}	3	2	7	7	6
$C_2H_6^{+\bullet}$	5	18	27	28	22
$C_2H_5^{+}$, HCO^{+}	11	8	35	30	28
$C_2H_4^{+\bullet}$, $CO^{+\bullet}$	100	99	44	41	38
$C_2H_3^{+}$	14	8	59	55	48
$C_2H_2^{+\bullet}$	6	6	29	24	22

1. Relative intensities (%).

Table 7.3 MI and CID mass spectra of $C_3H_5DO_2^{+\bullet}$ [1]

Neutral loss	$^{\bullet}CH_2CH_2C^{+}(OH)OD$ [2] MI	CID	$^{\bullet}CH_2CH_2C^{+}HOD$ [3] MI	CID	Statistic
H	0.92	0.92	0.62	0.61	0.83
D	0.08	0.08	0.38	0.39	0.17
H_2O	0.71	0.60	0.57	0.55	0.67
HDO	0.29	0.40	0.43	0.45	0.33
CHO	-	-	0.07	- [4]	0.83
CDO	-	-	0.93	- [4]	0.17
CH_2O_2	-	-	0.10	0.48	0.67
$CHDO_2$	-	-	0.90	0.52	0.33

1. Relative intensity (%).
2. Generated from $CH_3OCH_2CH_2COOD^{+\bullet}$ by CH_2O loss.
3. Generated from $DO\overline{CHOCH_2CH_2O}CHOD^{+\bullet}$ by $CHDO_2$ loss.
4. Overlapped by $C_2H_5^{\bullet}$ and $C_2H_4D^{\bullet}$ losses.

Table 7.4 CID mass spectra of $C_3H_4O^{+\bullet}$ daughter ions[1]

m/z	Parent ions				
	$^{\cdot}CH_2CH_2OC^{+}HOH$ (6)	$HCOOCH_2CH_3^{+\bullet}$ (9)	$CH_3CHC(OH)_2^{+\bullet}$ (7)	$^{\cdot}CH_2CH_2C^{+}(OH)_2$ (8)	$CH_3CH_2COOH^{+\bullet}$ (10)
55	17	15	27	26	22
42	5	4	-	-	-
41	5	5	12	15	13
28	100	100	100	100	100
27	25	27	55	59	65
26	15	15	31	29	36

1. Relative intensities (%).

Table 7.5 CID mass spectra of $C_3H_5O_2^{+\bullet}$ daughter ions[1]

m/z	Parent ions					
	$^{\bullet}CH_2CH_2OC^{+}HOH$ (6)	$HCOOCH_2CH_3^{+\bullet}$ (9)	$CH3CHC(OH)_2^{+\bullet}$ (7)	$^{\bullet}CH_2CH_2C^{+}(OH)_2$ (8)	$CH_3CH_2COOH^{+\bullet}$ (10)	$CH_2CHCOOH+H^{+}$
72	56	62	56	79	47	42
55	100	100	100	100	100	100
53	16	22	18	26	16	12
46	33	30	25	26	22	28
45	61	68	68	65	61	75
73^{2+}	19	18	12	13	16	12
31	8	6	5	9	4	6
29	17	19	19	18	19	22
28	25	16	19	16	14	16
27	58	58	62	72	55	68
26	20	28	23	26	24	19

1. Relative intensities (%); He is the target gas.
2. From self protonation of $CH_2CHCOOH$; ^{13}C interferences were subtracted.

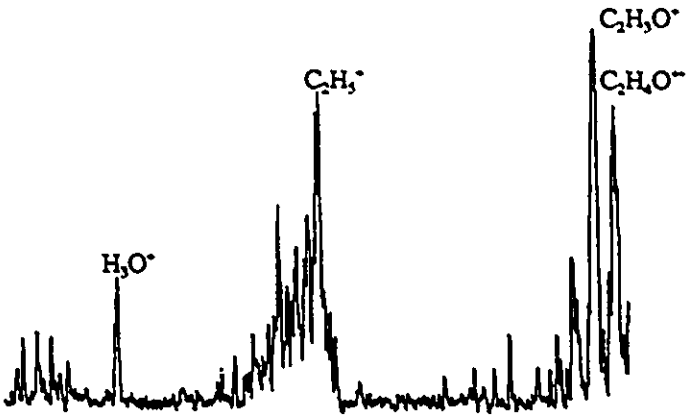

Figure 7.1 CID mass spectrum of $C_2H_5O^+$ daughter ions

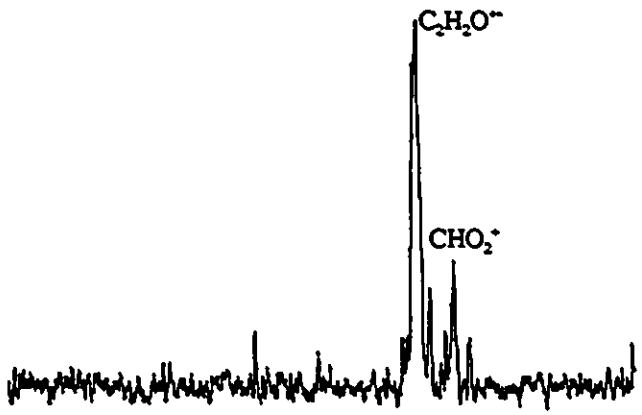

Figure 7.2 CID mass spectrum of $C_2H_4O_2^{+\cdot}$ daughter ions

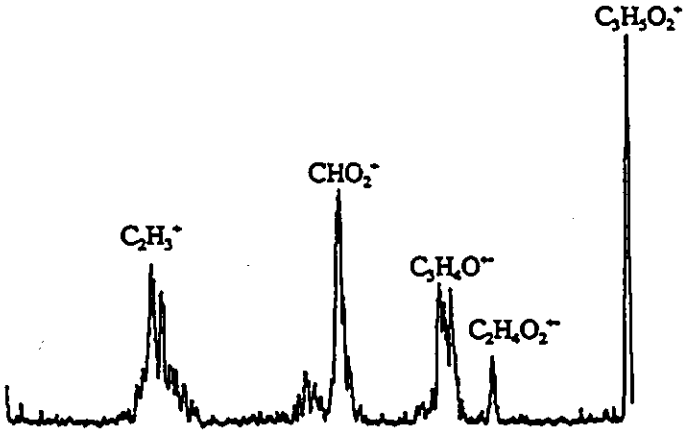

Figure 7.3 CID mass spectrum of $^{\cdot}CH_2CH_2C^+(OH)_2$ from metastable $[CH_3OCH_2CH_2COOH]^{+\cdot}$ by CH_2O loss

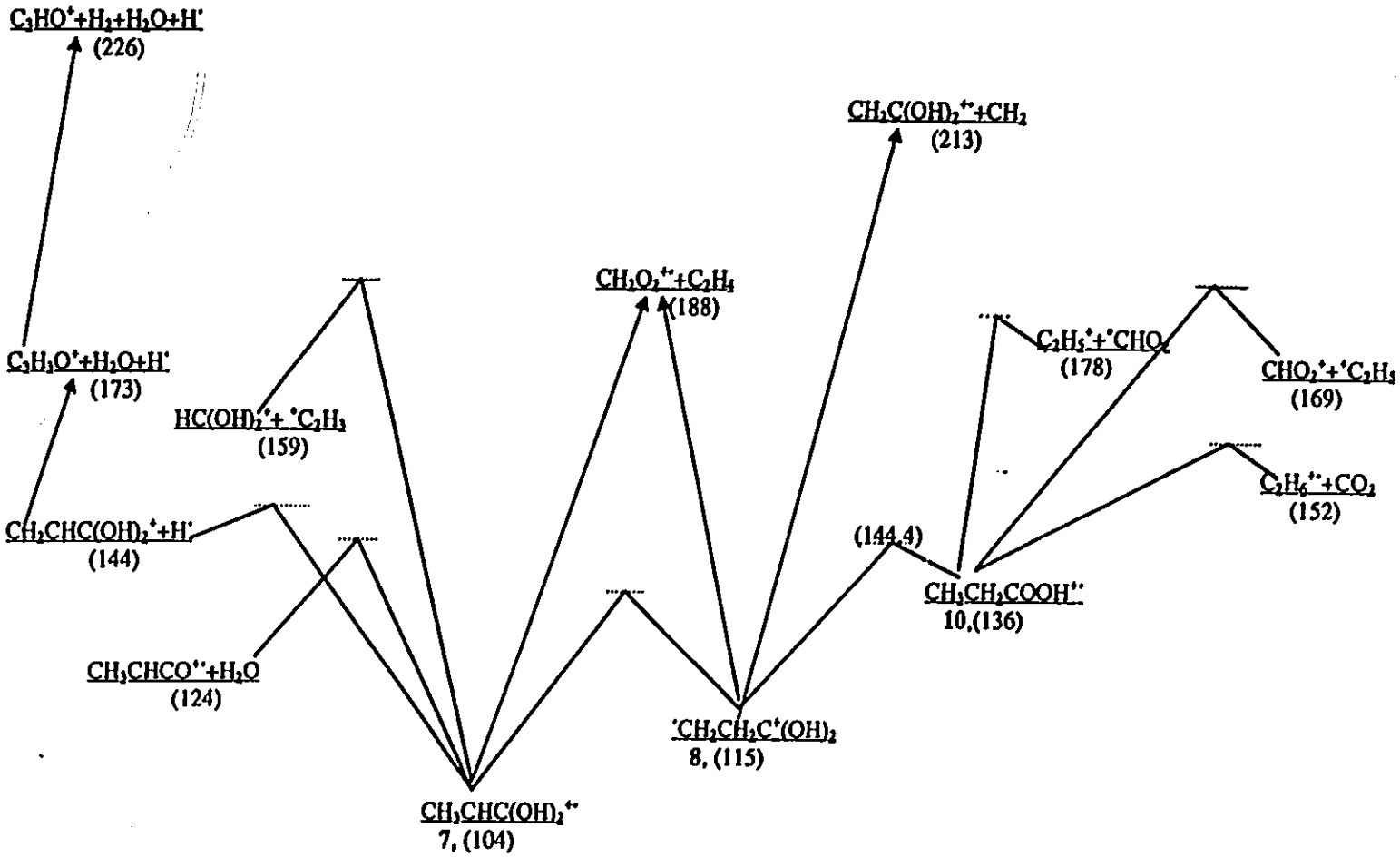

Figure 7.4 Energy diagram (in kcalmol^{-1}) for the isomerization-dissociations of $CH_3CHC(OH)_2^{+\bullet}$ **(7)**, $^{\bullet}CH_2CH_2C^{+}(OH)_2$ **(8)** and $CH_3CH_2COOH^{+\bullet}$ **(10)**

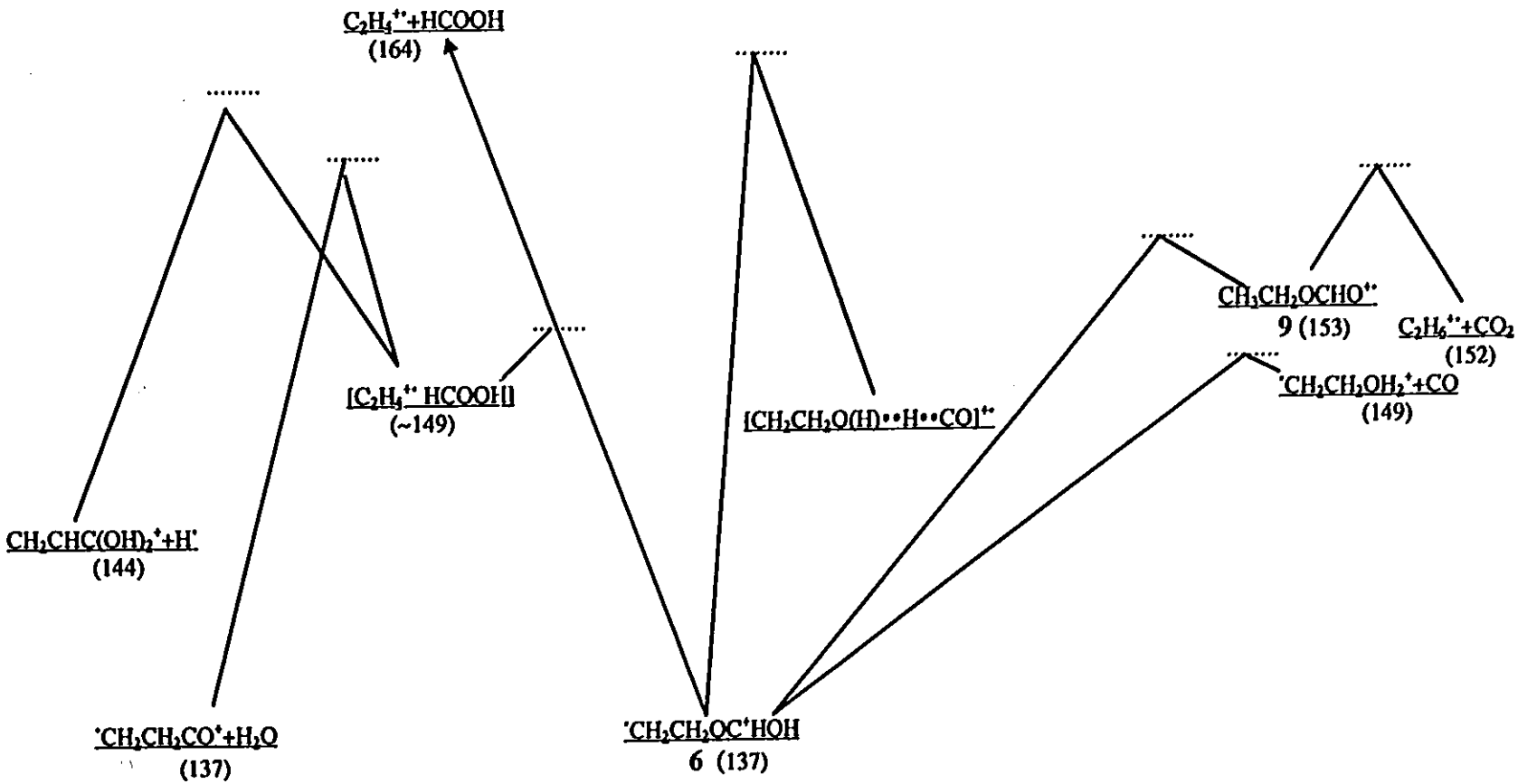

Figure 7.5 Energy diagram for the isomerization-dissociations of $^{\bullet}CH_2CH_2OC^{+}HOH$ (**6**) and $CH_3CH_2OCHO^{+\bullet}$ (**9**) (kcalmol^{-1}).

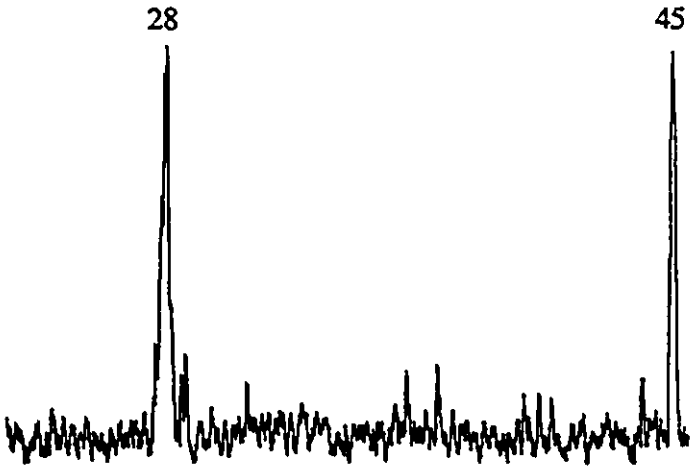

Figure 7.6a CID mass spectrum of $C_2H_6O^{+\bullet}$ daughter ion from $^{\bullet}CH_2CH_2C^{+}(OH)_2$ **(8)**

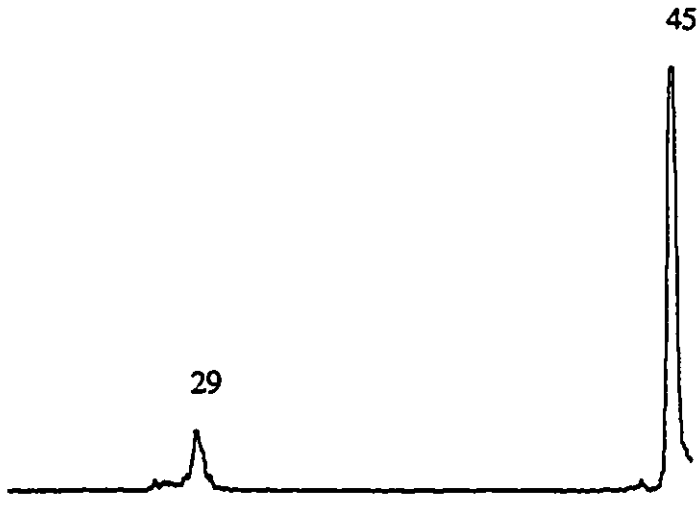

Figure 7.6b CID mass spectrum of $CH_2O_2^{+\bullet}$ daughter ion from $^{\bullet}CH_2CH_2OC^{+}H(OH)$ **(6)**

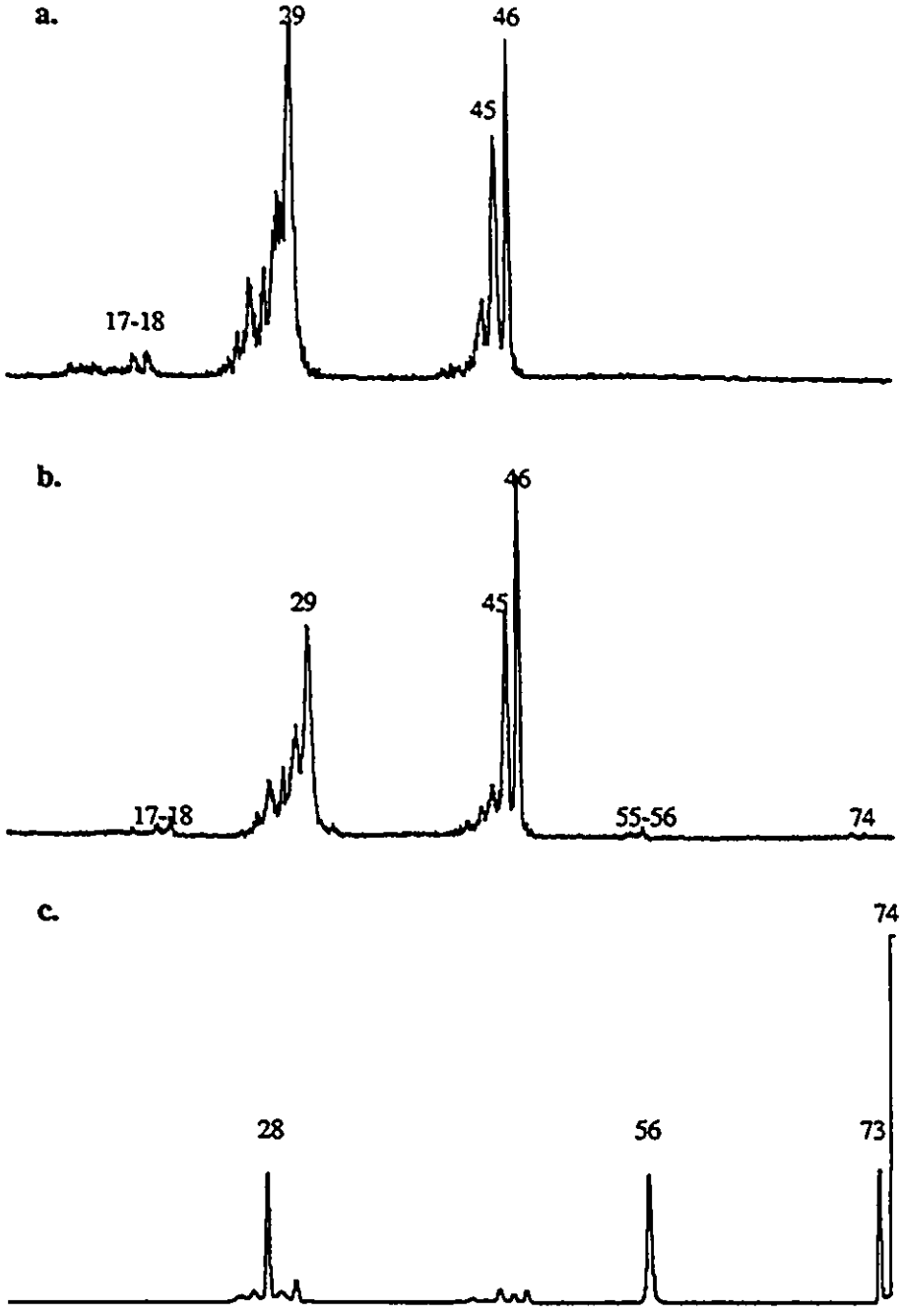

Figure 7.7 **CID and NR mass spectra of 6 and 9**
a: NRMS of $^{\bullet}CH_2CH_2OC^{+}HOH$ (6), Xe/O_2
b: NRMS of $HCOOCH_2CH_3^{+\bullet}$ (9), Xe/O_2
c: CIDMS of $HCOOCH_2CH_3^{+\bullet}$ (9), He

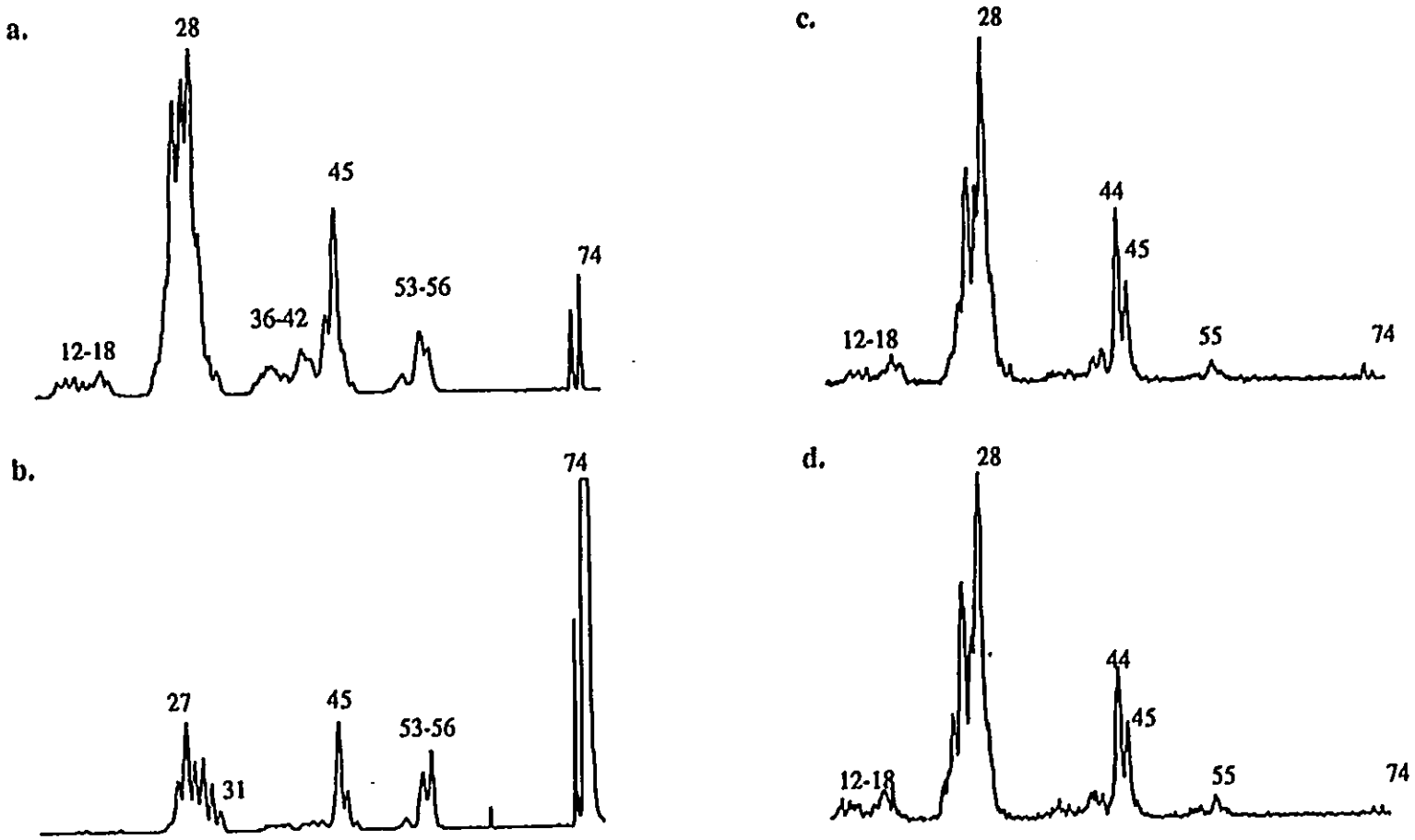

Figure 7.8 CID and NR mass spectra of 7, 8 and 10

a: NRMS of $CH_3CHC^+(OH)_2$ (7), Xe/O_2

b: CIDMS of $CH_3CHC^+(OH)_2$ (7), Xe/O_2

c: NRMS of $^{\cdot}CH_2CH_2C^+(OH)_2$ (8), Xe/O_2

d: NRMS of $CH_3CH_2COOH^{+\cdot}$ (10), Xe/O_2